INVESTIGATION OF WATERHAMMER PROBLEMS IN ÇAMLIDERE DAM - İVEDİK WATER TREATMENT PLANT PIPELINE AT VARIOUS HYDRAULIC CONDITIONS

A THESIS SUBMITTED TO
THE GRADUATE SCHOOL OF NATURAL AND APPLIED SCIENCES
OF
MIDDLE EAST TECHNICAL UNIVERSITY

BY

EMRE SAKABAŞ

IN PARTIAL FULFILLMENT OF THE REQUIREMENTS
FOR
THE DEGREE OF MASTER OF SCIENCE
IN
CIVIL ENGINEERING

FEBRUARY 2012

Approval of the thesis:

INVESTIGATION OF WATERHAMMER PROBLEMS IN ÇAMLIDERE DAM - İVEDİK WATER TREATMENT PLANT PIPELINE AT VARIOUS HYDRAULIC CONDITIONS

submitted by **EMRE SAKABAŞ** in partial fulfillment of the requirements for the degree of **Master of Science in Civil Engineering Department, Middle East Technical University** by,

Prof. Dr. Canan Özgen _____
Dean, Graduate School of **Natural and Applied Science**

Prof. Dr. Güney Özcebe _____
Head of Department, **Civil Engineering**

Assoc. Prof. Dr. Zafer Bozkuş _____
Supervisor, **Civil Engineering Dept., METU**

Examining Committee Members:

Prof. Dr. İsmail Aydın _____
Civil Engineering Dept., METU

Assoc. Prof. Dr. Zafer Bozkuş _____
Civil Engineering Dept., METU

Assoc. Prof. Dr. Nuri Merzi _____
Civil Engineering Dept., METU

Assist. Prof. Dr. Mete Köken _____
Civil Engineering Dept., METU

Dr. Kutay Çelebioğlu _____
Su-Ener Müh. ve Enerji Hiz. San. Ltd. Şti.

Date: **08.02.2012**

I hereby declare that all information in this document has been obtained and presented in accordance with academic rules and ethical conduct. I also declare that, as required by these rules and conduct, I have fully cited and referenced all material and results that are not original to this work.

Name, Last name : Emre SAKABAŞ

Signature :

ABSTRACT

INVESTIGATION OF WATERHAMMER PROBLEMS IN ÇAMLIDERE DAM - İVEDİK WATER TREATMENT PLANT PIPELINE AT VARIOUS HYDRAULIC CONDITIONS

Sakabaş, Emre

M.Sc., Department of Civil Engineering

Supervisor: Assoc. Prof. Dr. Zafer Bozkuş

February 2012, 189 pages

Çamlıdere Dam supplies significant portion of the potable water demand of the City of Ankara. Consequently, it is very important that the pipelines extending over 60 km between the dam and the treatment plant at İvedik operate continuously. At present, two composite parallel lines are in operation and construction of a third line is considered for the future. It is the aim of this study to investigate the water hammer problems to be expected under various scenarios and also suggest the safe operation conditions for the system. Water hammer analyses of the pipeline are carried out by computer software named HAMMER. This software employs the Method of Characteristics (MoC) which is a widely used mathematical procedure in solving the non-linear differential equations caused by unsteady flow. Within this theses work, existing tunnels, prestressed concrete and steel pipes, third steel pipeline which is planned to be constructed in the future and existing, and future-planned valves are modeled and calibration of the model is implemented. A plenty of scenarios and valve closure principles are

constituted in order to specify steady-state conditions and additional water hammer pressures generated by several excitations through the pipeline. Results of these scenarios are compared with previous works conducted on the pipeline system and the most unfavorable ones among those are determined. Then, appropriate closure durations are identified and suggested for pipe fracture safety valves and the flow control valves at İvedik in order not to cause excessive pressures in the system.

Keywords: Pipeline, water hammer, safe operation conditions

ÖZ

ÇAMLIDERE BARAJI - İVEDİK SU ARITMA TESİSİ BORU HATTINDA ÇEŞİTLİ KOŞULLARDA SU DARBESİ PROBLEMLERİNİN ARAŞTIRILMASI

Sakabaş, Emre
Yüksek Lisans, İnşaat Mühendisliği Bölümü
Tez Yöneticisi: Doç. Dr. Zafer Bozkuş

Şubat 2012, 189 sayfa

Çamlıdere Barajı Ankara şehrinin içme suyu gereksiniminin önemli bir kısmını karşılayan bir barajdır. Dolayısı ile barajla İvedik arıtma tesisi arasındaki 60 km'yi aşan boru hatlarının kesintisiz olarak işletmede olması çok önemlidir. Halen, iki kompozit paralel boru hattı işletmede olup, gelecekte üçüncü hattın inşası düşünülmektedir. Bu çalışmanın amacı çeşitli senaryolar altında sistemdeki su darbesi problemlerini araştırmak ve ayrıca güvenli işletme koşullarını önermektir. Hattın su darbesi analizleri HAMMER isimli bir bilgisayar programı aracılığıyla gerçekleştirilmiştir. Bu programda, zamanla değişen akımların oluşturduğu doğrusal olmayan diferansiyel denklemlerin çözülmesinde yaygın kullanımı olan Karakteristikler Metodu adı verilen matematiksel bir yöntem kullanılmaktadır. Bu tez çalışması içerisinde hattaki mevcut tüneller, öngermeli beton ve çelik borular, gelecekte yapılması planlanan üçüncü çelik boru hattı ile hat üzerinde yerleştirilmiş ve yerleştirilecek vanalar modellenmiş ve modelin kalibrasyonu yapılmıştır. Hat boyunca; zamandan bağımsız akım koşullarının ve bazı tahriklerin oluşturduğu ilave su darbesi basınçlarının belirlenmesi için birçok

senaryo ve vana kapanma prensibi oluşturulmuştur. Bu senaryolardan çıkan sonuçlar hat üzerinde yürütülen geçmiş çalışmalarla karşılaştırılmış ve aralarındaki en olumsuz durumlar tespit edilmiştir. Daha sonra, hat kırılma emniyet vanaları ile İvedikte kullanılan akım kontrol vanaları için sistemde aşırı basınçlara neden olmayacak kapanma süreleri belirlenmiş ve önerilmiştir.

Anahtar Kelimeler: Boru hattı, su darbesi, güvenli işletme koşulları

To My Family…

ACKNOWLEDGEMENTS

I would like to express my deepest gratitude to my supervisor Assoc. Prof. Dr. Zafer Bozkuş for his excellent supervision, guidance, encouragement and endless patience throughout my study.

My workmates and my boss Mustafa Çobanoğlu showed an everlasting patience during my graduate education. I am very grateful to them all for their invaluable respect.

I appreciate the help of my colleague Ezgi Köker in helping me while establishing the software used in this study.

I also want to thank my special friends Ömür, Özerk and especially Eren from the bottom of my heart due to their moral support until today.

And most importantly, very special thanks are due to my beloved parents for supporting and encouraging me when I was worn out. I got spoilt due to their infinite tolerance.

TABLE OF CONTENTS

LIST OF TABLES

TABLES

LIST OF FIGURES

FIGURES

NOMENCLATURE

A	Cross-sectional area of pipe, [m^2]
A_V	Effective valve area, [m^2]
a	Wave propagation velocity through the fluid, [m/s]
C_D	Discharge coefficient
D	Pipe diameter, [m]
E	Modulus of elasticity of pipe material, [N/m^2]
e	Wall thickness of pipe, [m]
F	Force, [N]
f	Darcy-Weisbach friction factor
g	Gravitational acceleration, [m/s^2]
H	Pressure head in the pipe in steady state flow, [m]
h_f	Major (Friction) loss, [m]
h_m	Minor (Local) loss, [m]
K	Bulk modulus of elasticity of fluid, [N/m^2]
L	Length of the pipe, [m]
P	Pressure, [N/m^2]
Q	Discharge, [m^3/s]
Re	Reynolds number

n	Manning roughness coefficient
$\vec{n}$	Unit vector normal to area element
t	Time, [s]
T_C	Closure time, [s]
V	Velocity, [m/s]
V_0	Initial velocity, [m/s]
ΔA	Change in the cross-sectional area of due to water hammer, [m^2]
ΔH	Change in the pressure head in the transient conditions, [m]
ΔP	Change in the pressure in the transient conditions, [N/m^2]
Δs	The length of pipe extension due to water hammer, [m]
ΔV	Change in the flow velocity in the transient conditions, [m/s]
$\Delta \rho$	Change in density of fluid due to water hammer, [kg/m^3]
$\forall$	Volume, [m^3]
γ	Specific weight of fluid, [N/m^3]
ϵ	Roughness height, [mm]
$\emptyset$	Diameter
ρ	Density of fluid, [kg/m^3]
μ	Poisson's ratio
τ	Dimensionless valve opening
τ_w	Wall shear stress, [N/m^2]
ν	Liquid kinematic viscosity, [m^2/s]

ABBREVIATIONS

ASKİ	General Directorate of Water and Sewer Works of Ankara
C.S.	Control Surface
C.V.	Control Volume
DSİ	General Directorate of State Hydraulic Works
D/S	Downstream
Elev.	Elevation
Eqn.	Equation
EPS	Extended Period Simulation
Fig.	Figure
HGL	Hydraulic Grade Line
IWTP	İvedik Water Treatment Plant
LJ	Larner-Johnson
Max.	Maximum
Min.	Minimum
MoC	Method of Characteristics
OPM	Obermeyer Project Management
PCP	Prestressed Concrete Pipe

PFSV	Pipe Fracture Safety Valve
Res.	Reservoir
Scn.	Scenario
U/S	Upstream
WSE	Water Surface Elevation
WTP	Water Treatment Plant

CHAPTER 1

INTRODUCTION

1.1 Rationale for the Study

The main goal while utilizing any kind of reservoir like large dams, head ponds or even a small tank is to supply municipal, industrial and/or agricultural water needs of people. For such hydraulic projects, transmission of stored water continuously and sufficiently to demand locations without any problem is very crucial in terms of meeting the requirements and therefore, should be the leading design criterion. In order to provide continuous and safe operation conditions, behavior of liquid to be transferred should be considered by analyzing it under different hydraulic environments.

In the light of abovementioned necessities, motivation and focus of this study is to investigate the water hammer problems to be expected through the existing pipelines and the third one, that is planned to be constructed when the future projections are taken into consideration, between Çamlıdere Dam, which supplies greater portion of potable water demand of Ankara, and water treatment plant at İvedik under various scenarios and thereby to light the way for a stable, safe and continuous system.

1.2 Specific Objectives of the Present Study

The objective of present study, mainly, is to investigate existing pipelines and future planned third pipeline between Çamlıdere Dam and İvedik Water Treatment Plant (IWTP) which work properly under dynamic loads due to transient motion caused by various excitations on the system.

Achieving the main goal, some specific questions should be asked which guide this study:

- What are the initial and boundary conditions of the Çamlıdere Dam – IWTP pipeline system?
- What is the transient motion generated by unsteady boundary conditions?
- Which scenarios are going to be appropriate to examine the transient motions through the pipeline?
- What are the magnitudes of the dynamic loads generated due to unsteady boundary conditions?
- What are the effects and contributions of obtaining dynamic loads under various scenarios to operate the pipeline in safe and continuous manner? In other words, how are these analyses results enlighten us about the present study?

In order to answer these questions, an appropriate mathematical model should be constituted and the system should be analyzed by a relevant numerical technique which reflects the behavior of water transmitted exactly under different

excitations. Therefore, the results of analyses obtained are going to guide the suggestions on operating the transmission line safely and continuously in order to prevent such pipeline damages illustrated in Figure 1.1.

(a)

(b)

Figure 1.1 Pipeline damages along Çamlıdere – IWTP in 2000 (Bozkuş, 2008)

1.3 Scope of the Present Study

This study is composed of three parts in order to come up with the most appropriate system at the end, in terms of meeting the dynamic loads generated by transient motion.

First part consists of examining the existing two pipelines between Çamlıdere Dam and İvedik water treatment plant and defining the overall system by integrating the third line. Initial and boundary conditions are specified, an appropriate mathematical model and numerical technique are selected.

In the second part, dynamic loads generated due to various excitations to the system are analyzed by the help of an advanced numerical simulator, HAMMER, (explained in detail in CHAPTER 4) which uses selected numerical technique.

Finally in the third part, analyses are evaluated and discussed, and the study is concluded with the suggestions toward the analyses results for the safe and continuous operation conditions of existing and future planned pipelines.

CHAPTER 2

LITERATURE REVIEW

2.1 Introduction

The objective of this study is to figure out and make suggestions in order to overcome the excessive dynamic loads due to hydraulic transients through Çamlıdere Dam – IWTP pipeline.

Time dependent variations in boundary conditions give way to tremendous velocity and pressure changes along the pipeline. In the following topics, a literature review is shared out that guides this study for understanding the logic of unsteady or transient flow and existing Çamlıdere Dam – IWTP pipeline system which is going to be examined under water hammer effects.

2.2 Transient Flow in Pipelines

Having satisfactory knowledge about the "unsteady flow" that underlies this study is a necessity in terms of examining and evaluating the results of time dependent variations in pipeline systems together with the normal operation conditions.

As is known, the basic definition of steady flow is that the rate of change of quantities of interest namely velocity ($\partial V/\partial t$), pressure ($\partial P/\partial t$), fluid density ($\partial \rho/\partial t$), and cross – section, which may vary at any point along the path, do not depend on time.

Although, slight variations in velocity and pressure can be observed in real life applications, flow is considered as steady since the average values of those are constant.

However, in unsteady flow, the conditions at any point differ with time due to some excitations on the system and the terms transient flow or water hammer are used to describe unsteady pipe flow of fluids, interchangeably.

Investigation of the propagation of sound waves in air, the propagation of waves in shallow water and the flow of blood in arteries promoted the fluid transient phenomenon. Newton's efforts on the propagation of sound waves, Lagrange's analysis on the flow of compressible and incompressible fluids and Euler's derivations on differential equation for wave propagation can be defined as the origin of unsteady flow. On the other hand, Young's investigations on the propagation of pressure in pipes for incompressible fluid must not be ruled out (Chaudhry, 1987).

Early studies on unsteady flow or water hammer were performed in late 1800's by Joukowsky (1904) who is accepted as one of the most important contributors to the phenomenon. Water hammer can be defined as a transient event that leads to large pressure variations resulting from abrupt changes in flow rate. After a plenty of experiments on pipes, Joukowsky came up with the concept that the pressure wave speed in a pipeline depends on the elasticity of water and the circumferential stiffness of the pipe material. Joukowsky equation, $\Delta P = -\rho a \Delta V$, relates the pressure change to the pressure wave speed and the change in velocity (Potter & Wiggert, 2002) where ρ is fluid density, a is pressure wave speed and ΔV is change in velocity.

In other words, the pressure wave speed decreases if the pipe material is relatively elastic and this reduction is governed by the size and elastic properties of pipe material and the external constraints. In order to be able to derive a wave speed equation regarding the pipe material, Joukowsky made some assumptions for the sake of simplicity;

- Pressure is uniform across the cross section.
- Mass of pipe material is neglected.
- The axial and bending stresses in the pipe wall are neglected.
- The radial inertia of liquid is neglected.

In early 1900's, Allievi developed a new theory of water hammer neglecting the convective term in the momentum equation. He introduced dimensionless parameters in order to define interrelation between pipe material and fluid, and valve behavior. In addition, he produced charts for pressure rise and drop at a valve section due to uniform closure (Ghidaoui, Zhao, Duncan, & Axworthy, 2005).

Unsteady flow and water hammer phenomenon have been studied broadly later by Parmakian (1955) Wylie and Streeter (1978) and Chaudhry (1987) who have outlined several analytical solutions of transient motion under various boundary conditions in their textbooks.

While establishing dimensional and non-dimensional parameters for flow velocity and transient pressure, Parmakian (1955) used elastic water column theory and came up with graphical methods in order to perform water hammer analyses.

Wylie and Streeter (1978) derived an unsteady momentum equation and continuity equation for a fixed control volume in a pipe section. They took into

account the support conditions of pipes in terms of elongation regarding Poisson's ratio effect and considered axial and radial stress-strain relations during a transient event in order to establish wave speed equations.

Chaudry (1987), furthermore, considered elastic pipe and compressible fluid in his derivations. He also employed continuity and momentum equations for a fixed control volume resulting in equations consisting of some variables namely area, velocity and fluid density. Then he promoted pressure and flow rate as variables by eliminating area term. Therefore, he came up with a definition of wave speed including strain related pressure terms by rearranging previously derived continuity and momentum equations. He observed the effect of pipe material on pressure wave speed in order to enhance wave speed equation.

In recent years many scientists have focused on unsteady flow to develop new numerical techniques for solving the basic equations of the water hammer phenomenon since the common concern is to overcome the large pressure variations during transient motion in order to protect the relevant system components. One of the most significant causes of pressure rise is that of the closure of a valve or a gate. Although the most damaging pressure peaks are caused by rapid flow stoppage, water hammer can frequently occur with more gradual flow changes, especially in long pipe lines (Bozkuş, 1991).

2.3 Çamlıdere Dam - İvedik Water Treatment Plant Pipeline

In order to establish the system description of the present study, another survey is needed about Çamlıdere Dam and water conveyance line between dam and İvedik WTP, and fortunately, sufficient number of studies, projects and documents are available for a reliable definition.

About the conveyance line, there are successive studies attained by which the history of dam and pipeline system can be outlined. The first one is a preliminary

report (KİSKA Komandit Şti, 1977) about the pipeline under construction between Çamlıdere Dam and İvedik WTP. This preliminary report initially gives general information about pipeline like types and lengths of pipes, which are going to be detailed in proceeding chapters and then defines the service. This study aims to understand the hydraulic behavior of pipeline system and determine the maximum pressures generated, pipe discharges and pressure surge taking the various hydraulic scenarios into account. Furthermore, it covers alternative suggestions about necessary control valves against overloading of pipeline, determinations of their closure times, and calculation of tunnel and pipe diameters. This study provided basis for initial conditions of a final study.

Considering the preliminary results of abovementioned report as inputs, Obermeyer Project Management (OPM) (1978) finalized the study by illustrating detailed calculations, designs and suggestions for each item through the pipeline. For example, pressure rises of each pipe segment, pipe fracture safety devices, valve closure durations, and intake structures etc.

Basmacı (1996) published a report on hydraulic calculation of Çamlıdere Dam-IWTP transmission line. This report covers minor and major loss calculations along pipeline. In addition, hydraulics features and schemes of needle valves at IWTP entrance were given and head losses across those were calculated.

Bozkuş (1996) conducted a study on investigation of pipeline and the pressure reduction gate at the intake structure of Çamlıdere Dam under various hydraulic conditions. This study defines the characteristics of pipeline system, head losses and steady-state discharges for different reservoir elevations regarding the head losses defined previously by Basmacı (1996). Furthermore, function of pressure reduction gate, discharge rating curves for partial openings etc. were illustrated clearly.

In parallel with the previous studies, the work reported by Yüksel Project (2004) gives further information about the water conveyance line and takes stock of the operation problems from past to present.

Extending across the previous studies, this study has revealed the inefficient operation of both pipelines for the duration of their services and therefore, intended to investigate pipeline system, prepare the operation guidelines for various alternatives, determine the short and long run precautions in order to operate the system in a safe manner, perform investments, rehabilitation reports, additional constructions, maintenance, repair and fixture replacement and estimation of services.

In the section 1.1 of Yüksel Project's report (2004) (Aim and Scope of the Project), system has been defined which sets an example. Moreover, dam information and hydrological data, tunnel and pipe materials, lengths, diameters, geographical positions, treatment plant capacities have been denoted which catalyzes this study. In the section 3.4.7, water hammer calculations, evaluation criteria of precautions and results have been shared with the flow charts of scenarios emphasized on.

Additionally, regarding this study, inessentiality of third pipeline on those days' conditions has been explained by supporting with reasons and appropriate construction time has been suggested.

The latest study on Çamlıdere Dam – İvedik Water Treatment Plant pipeline is done by Bozkuş (2008) by composing aforementioned studies and the final reports concluded by him in 1996 and in 2006. Referring to the previous studies on pipeline, water hammer analyses of pipeline under various operation scenarios have been performed by using method of characteristics.

System has been defined once again, hydraulic losses have been identified, the mathematical model has been constructed for water hammer analyses and

scenarios have been defined. Finally the study has been concluded by recommending appropriate closure durations (see Figure 2.1) for pipe fracture safety devices through the pipeline which are going to be operated automatically in case of emergency, in order not to cause excessive pressures and failures (Bozkuş, 2008).

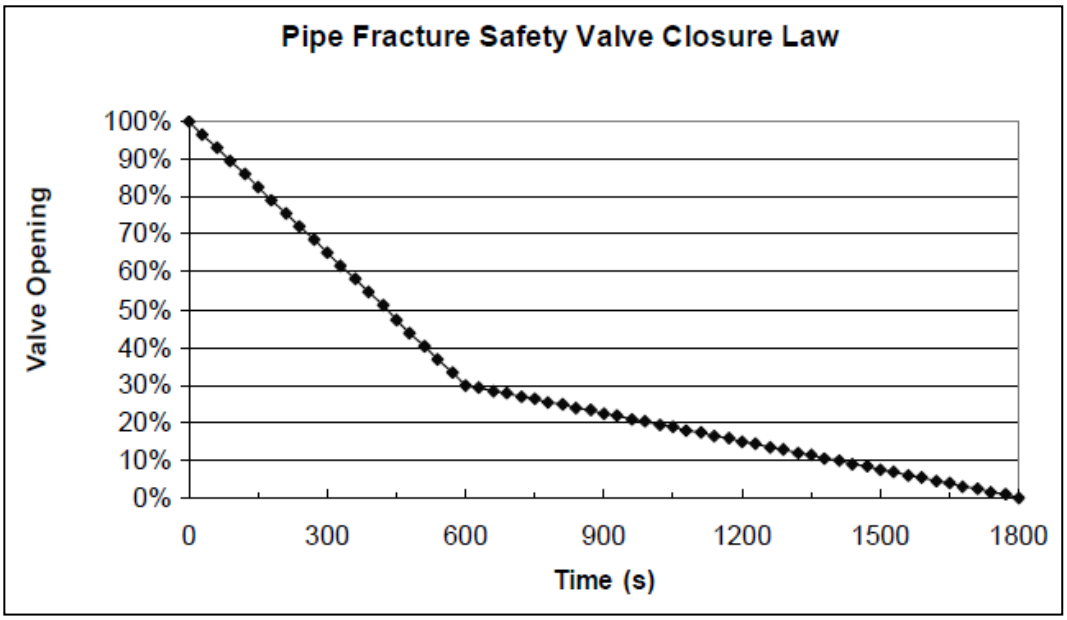

Figure 2.1 Pipe fracture safety valve closure law (Bozkuş, 2008)

CHAPTER 3

HYDRAULIC TRANSIENTS IN PIPELINE SYSTEMS

3.1 Transient Flow

The transient flow, as the name implies, is a transition between two steady state flow conditions. Every transient flow appears as a reaction of fluid to several changes in the hydraulic conditions controlling the fluid and in the surrounding environment. Transient flow can be grouped into two categories in general:

The first one is *quasi-steady flow*. During this type of flow, discharges and pressures vary so gradually with time that the flow can be considered as steady over short time intervals. Draining of a large tank is a typical example for quasi-steady flow.

The other transient flow type is *true transient flow*. Fluid inertia and/or elastic properties of pipe and fluid are taken into account for this type of flow. If only fluid inertia is considered for true transient, the flow is named as *rigid-column flow*. *Water hammer*, on the other hand, is such a true transient in which both fluid inertia, elasticity of pipe and compressibility of fluid are considered together for an accurate approach.

3.2 Water Hammer

Water hammer known as a hydraulic transient during which the velocities in a steady-state pipe system differ so rapidly and this rapid change results in a high pressure surge. As well as it is more complex than a rigid-column analysis, water hammer reflects the real behavior of the flow more accurately since the elastic properties of the pipe material and liquid are taken into account.

There are several effects that trigger water hammer (Bozkuş, 2009), such as;

- Valve operations
- Starting or stopping pumps or turbines
- Emergency shutdowns
- Fluctuating reservoir level
- Waves on a reservoir
- Vibration of impellers or guide vanes in pumps or turbines
- Vibration of valves

Figure 3.1 illustrates a reservoir, pipeline and valve system in steady state condition with velocity V, and piezometric head H throughout the pipe (Frictionless flow). A sudden closure of the valve will cause a transient motion in the pipe and force fluid velocity to zero. This gives way to an abrupt increase of head at valve section by an amount $\Delta H = aV/g$, where a is pressure wave speed and g gravitational acceleration, which reduces the momentum of the moving fluid to zero. The pressure head propagates upstream at a speed a and reaches to reservoir in L/a seconds after closure of valve. At that moment velocity in the pipe becomes zero and pressure becomes $H + \Delta H$ throughout the pipe. The pipe is

enlarged and the fluid is compressed. Propagation of pressure wave process continues to evolve with time (Larock, Jeppson, & Watters, 1999).

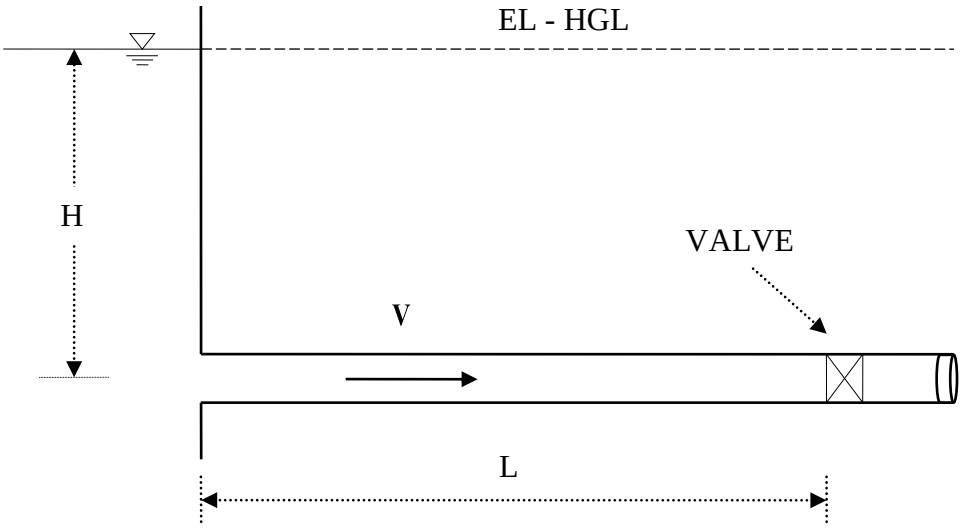

Figure 3.1 Steady-state flow from reservoir without friction

At time $2L/a$ after closure, pressure inside the pipe returns its steady-state value at the beginning of the motion. In other words, pressure head drops an amount ΔH. However, direction of velocity is reversed. By the time $3L/a$, negative pressure wave reaches reservoir and velocity inside the pipe becomes zero. However, due to non-equilibrium between pressure head at the reservoir and reservoir head, fluid starts to move inside the pipe with velocity V again. At time $4L/a$ the pressure wave reaches the valve and variables return their steady-state value in the very beginning. Figures 3.2 - 3.5 show the movement of pressure wave in the pipe for different time intervals in an exaggerated way. Especially, the area change is exaggerated to emphasize it.

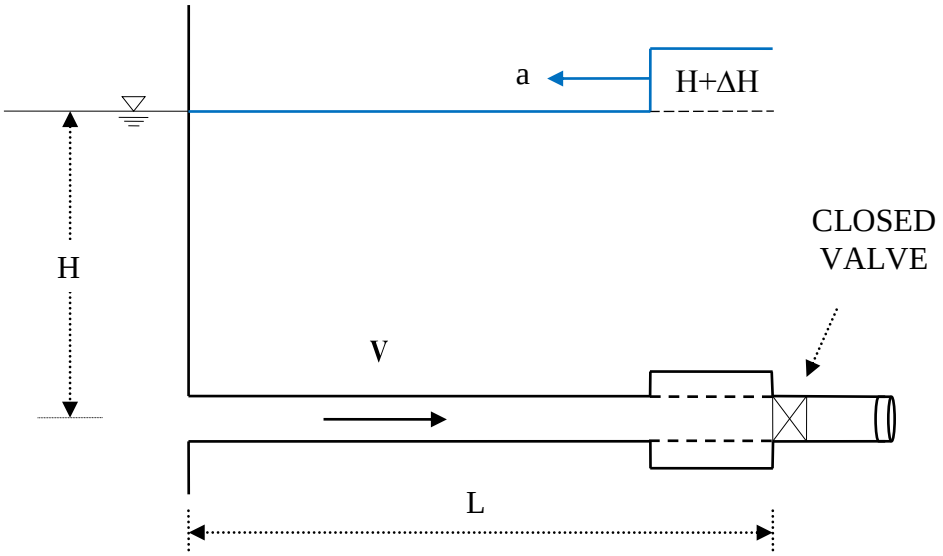

(a) t < L/a

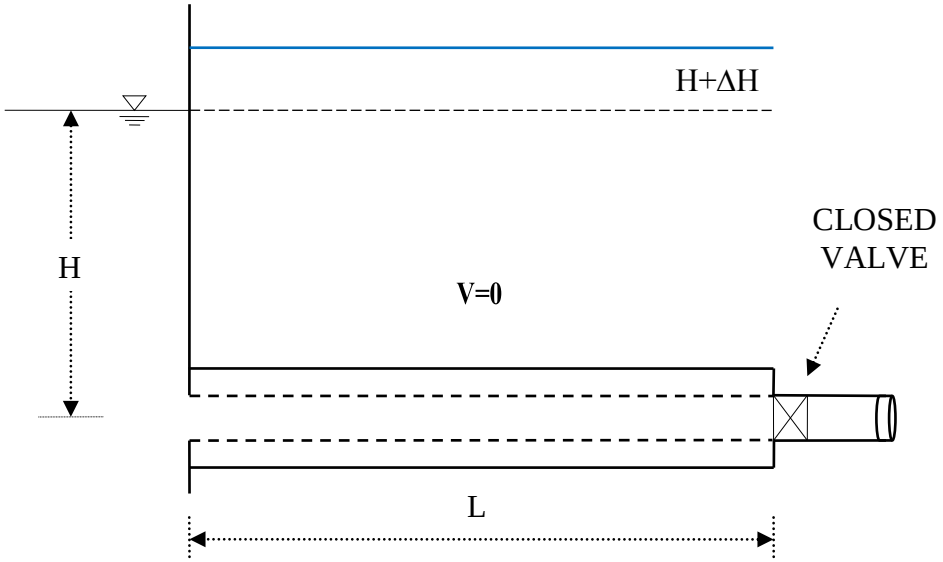

(b) t = L/a

Figure 3.2 Evolution of pressure wave at (a) t < L/a and (b) t = L/a

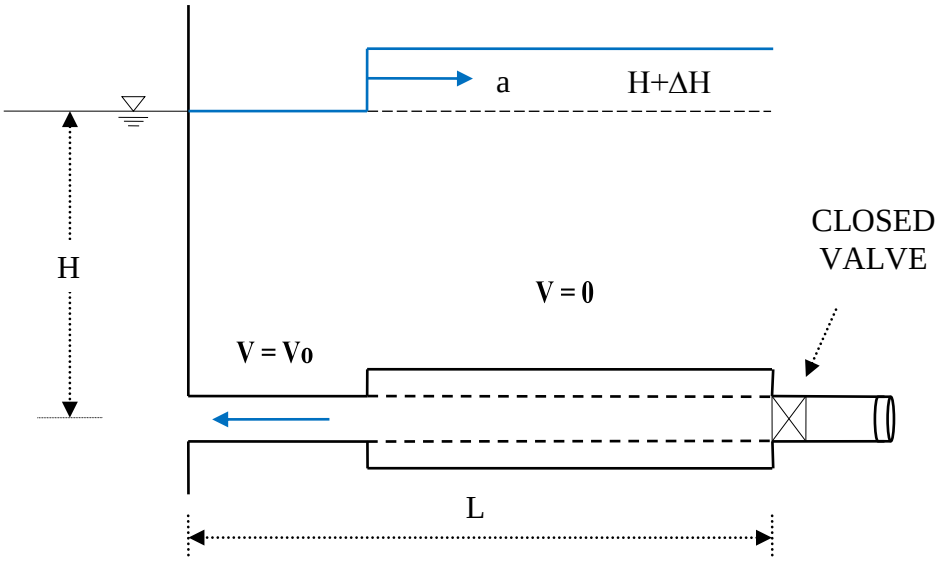

(c) L/a < t < 2L/a

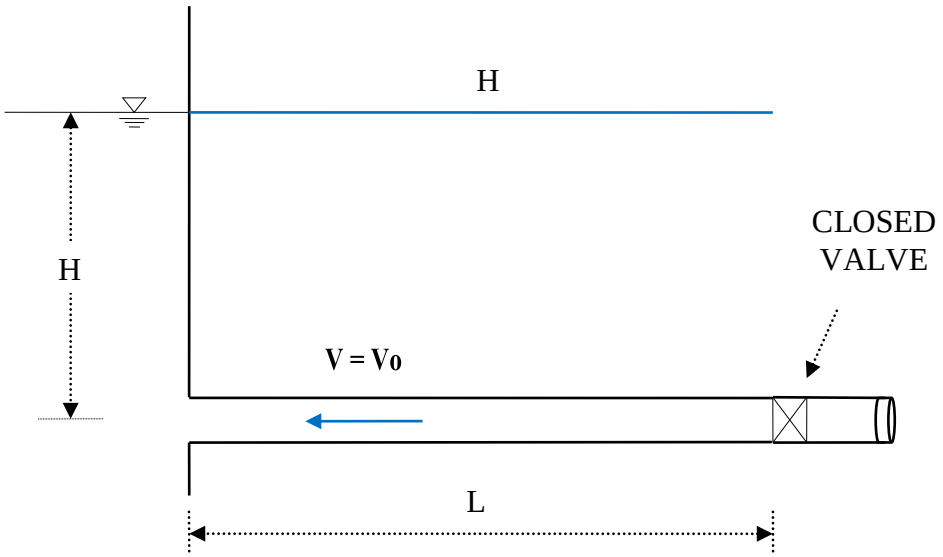

(d) t = 2L/a

Figure 3.3 Evolution of pressure wave at (c) L/a < t < 2L/a and (d) t = 2L/a

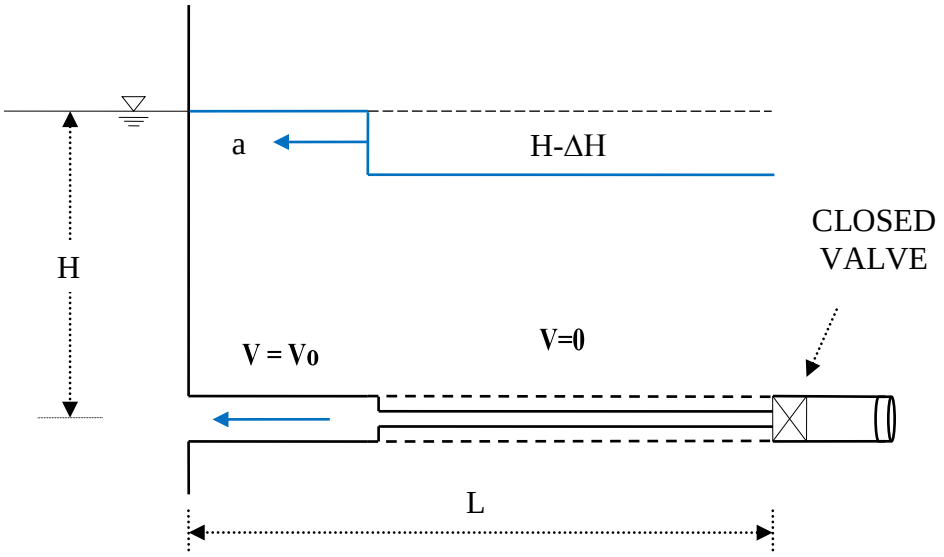

(e) 2L/a < t < 3L/a

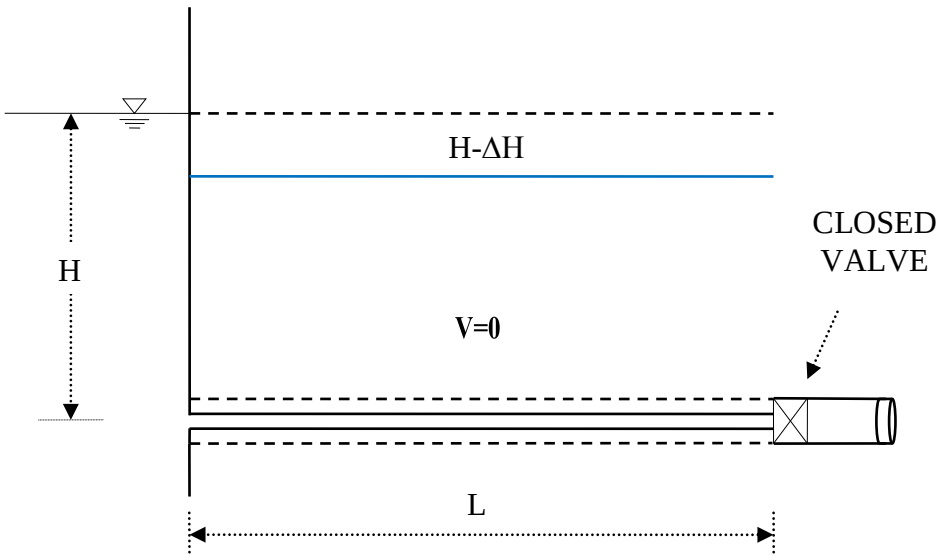

(f) t = 3L/a

Figure 3.4 Evolution of pressure wave at (e) 2L/a < t < 3L/a and (f) t = 3L/a

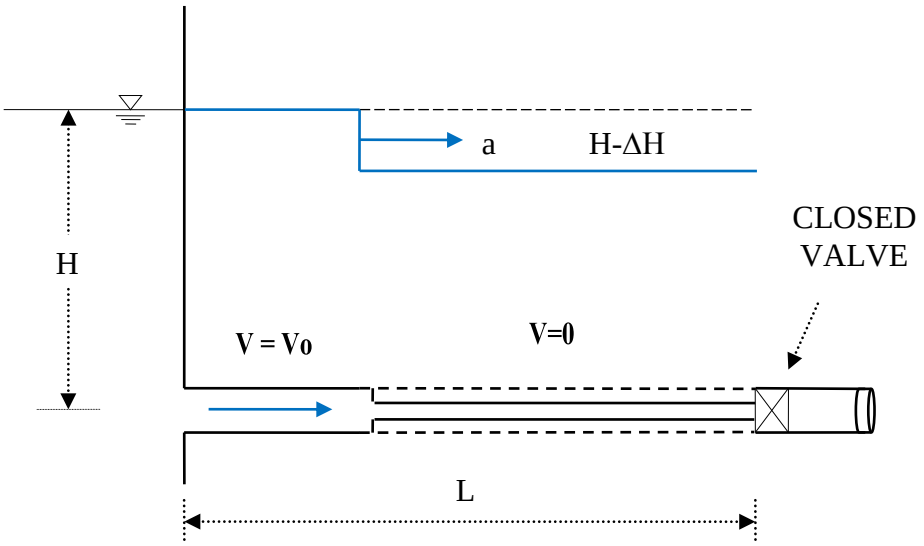

(g) 3L/a < t < 4L/a

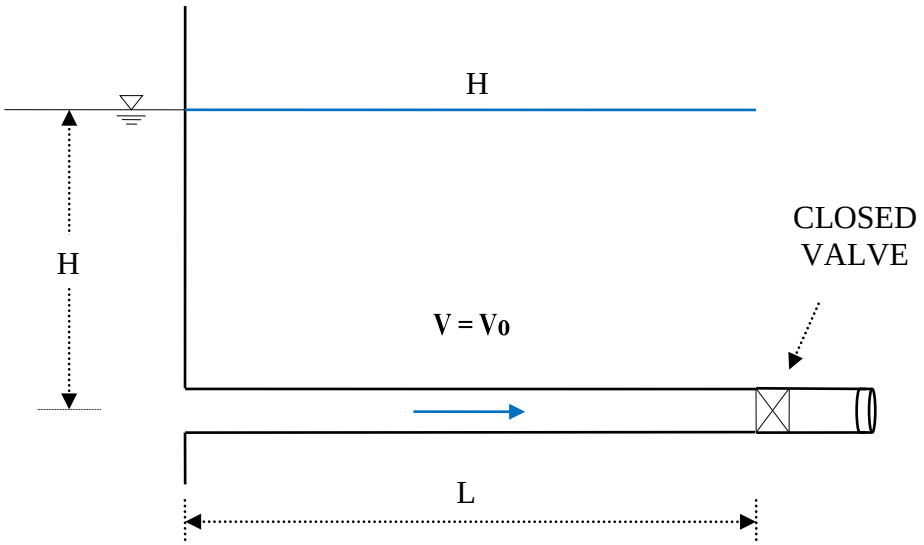

(h) t = 4L/a

Figure 3.5 Evolution of pressure wave at (g) 3L/a < t < 4L/a and (h) t = 4L/a

3.2.1 Derivation of Wave Speed Equation

In order to derive pressure wave propagation equations, transient action must be initiated by exciting a control volume at a section of a pipe. Describing a sudden valve closure case at the downstream, the continuity and momentum equations are applied to the control volume shown in Figure 3.6. Applying the momentum equation to control volume, the pressure wave propagates to upstream with an absolute speed of $a - V_0$ where V_0 is the initial velocity. The head difference ΔH at the valve section is accompanied by a velocity difference ΔV. The momentum equation through the direction of flow in a control volume is just equal to the time rate of change of momentum within the control volume plus the net efflux of momentum from the control volume.

Mathematical expression for momentum equation is,

$$\frac{\partial}{\partial t}\int_{c.v.} \rho\vec{V}\, d\forall + \int_{c.s.} \vec{V}(\rho\,\vec{V}\cdot\vec{n})\, dA = \sum \vec{F} \tag{3.1}$$

On the other hand it can be expressed as,

$$-\gamma\Delta H A = \rho A(a - V_0)\Delta V + \rho A(V_0 + \Delta V)^2 - \rho A V_0^2 \tag{3.2}$$

By neglecting the term ΔV^2 which is a very small quantity and $V_0/a \ll 1$, Eqn. (3.2) becomes

$$\Delta H = -\frac{a\Delta V}{g}\left(1 + \frac{V_0}{a}\right) \approx -\frac{a\Delta V}{g} \tag{3.3}$$

For completely stopped flow, $\Delta V = -V_0$, and therefore, $\Delta H = aV_0/g$.

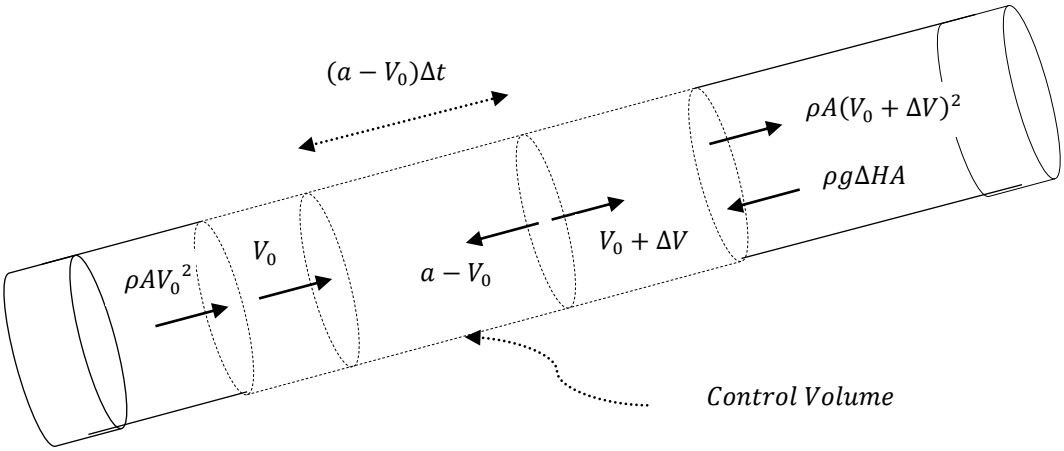

Figure 3.6 Unsteady flow control volume for momentum analysis

In order to determine the magnitude of wave speed a, the continuity equation accompanies Eqn.(3.3). If the valve at downstream of pipe is closed suddenly, pipe elongates in length Δs depending on the support condition (see Figure 3.7). Since the fluid takes that distance in L/a seconds, velocity at the valve becomes $\Delta V = \Delta s/L - V_0$. The pipe accommodates the mass entering the pipe, that is $\rho A V_0 L/a$, by increasing its cross-sectional area, by filling extra volume due to extension Δs, and by compressing the fluid due to higher pressure during L/a seconds after the closure of valve.

$$\rho A V_0 \frac{L}{A} = \rho L \Delta A + \rho A \Delta s + L A \Delta \rho \tag{3.4}$$

In order to eliminate V_0, $\Delta V = \Delta s/L - V_0$ is used, then Eqn.(3.4) simplifies to

$$-\frac{\Delta V}{a} = \frac{\Delta A}{A} + \frac{\Delta \rho}{\rho} \tag{3.5}$$

and to eliminate ΔV, Eqn.(3.3) is used. Therefore,

$$a^2 = \frac{g \Delta H}{\Delta A/A + \Delta \rho/\rho} \tag{3.6}$$

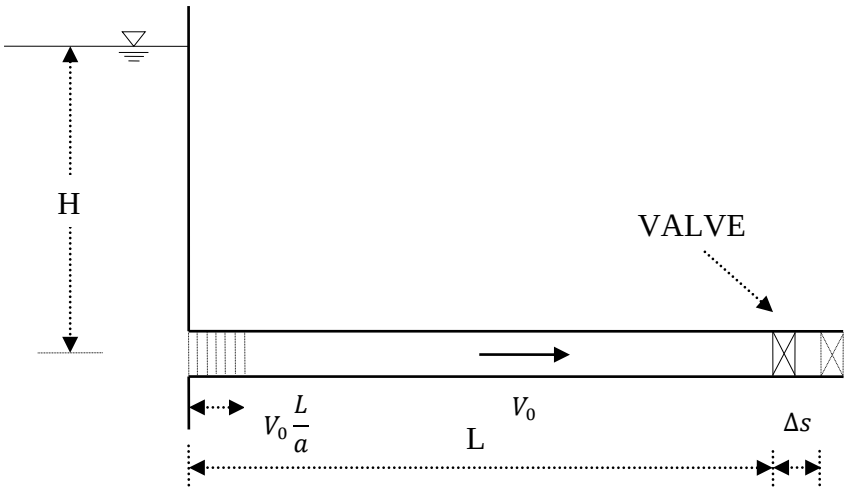

Figure 3.7 Simple sketch for a sudden valve closure

The bulk modulus of elasticity of the fluid, K, is defined as,

$$K = \frac{\Delta P}{\frac{\Delta \rho}{\rho}} = -\frac{\Delta P}{\frac{\Delta \forall}{\forall}} \tag{3.7}$$

Rearranging Eqn. (3.6) by using Eqn. (3.7) will yield to

$$a^2 = \frac{K/\rho}{1 + (K/A)(\Delta A/\Delta P)} \tag{3.8}$$

Circumferential tensile stress and strain relations on the pipe wall finally bring us to general form of wave speed equation:

$$a = \frac{\sqrt{K/\rho}}{\sqrt{1 + [(K/E)(D/e)]c_1}} \tag{3.9}$$

where c_1 is a constant that accounts for the support conditions of pipe:

$c_1 = 1 - 0.5\mu$ If pipe is anchored at the upstream end only

$c_1 = 1 - \mu^2$ If pipe is anchored against axial movement

$c_1 = 1$ If pipe sections are anchored with expansion joints

where μ is the Poisson's ratio of pipe material.

3.3 Differential Equations for Transient Flow

3.3.1 Continuity Equation

Continuity equation (Eqn. 3.10) is derived from the conservation of mass equation and the first term of the equation defines the time rate of change of mass inside the control volume shown in Figure 3.8 and the other defines the net flux across the entire control surface sections.

Several assumptions made for deriving continuity equation are listed below:

- Control volume is fixed,
- Fluid is single-phased liquid and slightly compressible,
- Conduit is elastic and prismatic,
- Flow and wave motions are one-dimensional, i.e. planar,

$$\frac{\partial}{\partial t}\int_{c.v.} \rho \, d\forall + \int_{c.s.} \rho \, \vec{V} \cdot \vec{n} \, dA = 0 \qquad (3.10)$$

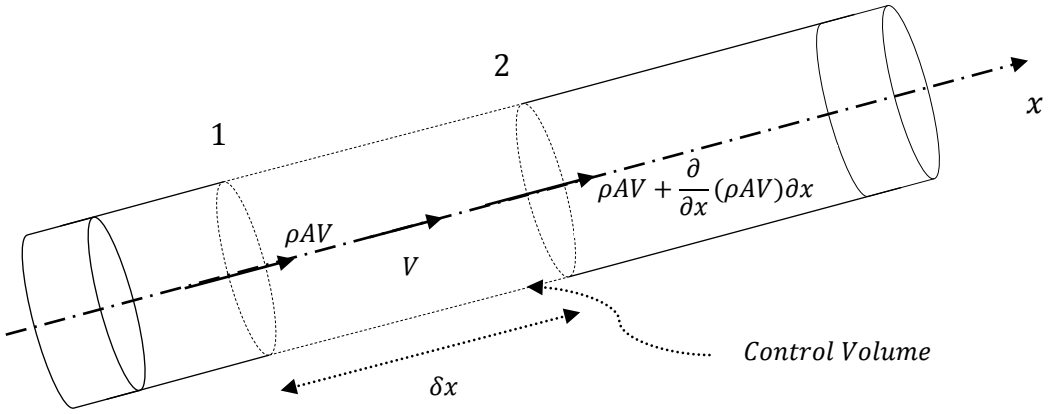

Figure 3.8 Control volume for continuity equation

Assuming ρ is constant inside the control volume,

$$\frac{\partial}{\partial t}(\rho A)\delta x + \left[\rho AV + \frac{\partial}{\partial x}(\rho AV)\delta x\right] - \rho AV = 0 \tag{3.11}$$

Dividing Eqn. (3.11) by δx, it becomes

$$\frac{\partial}{\partial t}(\rho A) + \frac{\partial}{\partial x}(\rho AV) = 0 \tag{3.12}$$

Differentiating Eqn. (3.12) by parts and substituting the expressions in definition of bulk modulus of elasticity given in Eqn. (3.7), will yield to

$$\left(\frac{1}{K} + \frac{D}{Ee}\right)\left(\frac{\partial P}{\partial t} + V\frac{\partial P}{\partial x}\right) + \frac{\partial V}{\partial x} = 0 \tag{3.13}$$

Finally, substituting Eqn. (3.8) into Eqn. (3.13) and simplifying the resulting equation give the equation below which is the general form of continuity equation;

$$\frac{\partial P}{\partial t} + V\frac{\partial P}{\partial x} + \rho a^2 \frac{\partial V}{\partial x} = 0 \tag{3.14}$$

3.3.2 Conservation of Momentum (Equations of Motion)

Momentum equation (Eqn. 3.15) in the direction of flow for a fixed control volume shown in Figure 3.9 can be written as follows,

$$\sum \vec{F_x} = \frac{\partial}{\partial t}\int_{c.v.} \rho \vec{V}\, d\forall + \sum_{c.s.} \rho V_{ix}(\vec{V_i} \cdot \vec{n_i}) A_i \tag{3.15}$$

The first term is the resultant force;

$$\sum F_x = PA - \left[PA + \frac{\partial}{\partial x}(PA)\delta x\right] - \tau_w \pi D \delta x - \rho g A \sin\theta\, \delta x \tag{3.16}$$

The second term is the time rate of change of momentum inside the control volume;

$$\frac{\partial}{\partial t}\int_{c.v.} \rho \vec{V}\, d\forall = \frac{\partial}{\partial t}(\rho V A)\delta x \tag{3.17}$$

Finally the third term is the momentum flux through the sections 1 and 2;

$$\sum_{c.s.} \rho V_{ix}(\vec{V_i} \cdot \vec{n_i}) A_i = \rho V^2 A + \frac{\partial}{\partial x}(\rho V^2 A)\delta x - \rho V^2 A = \frac{\partial}{\partial x}(\rho V^2 A)\delta x \tag{3.18}$$

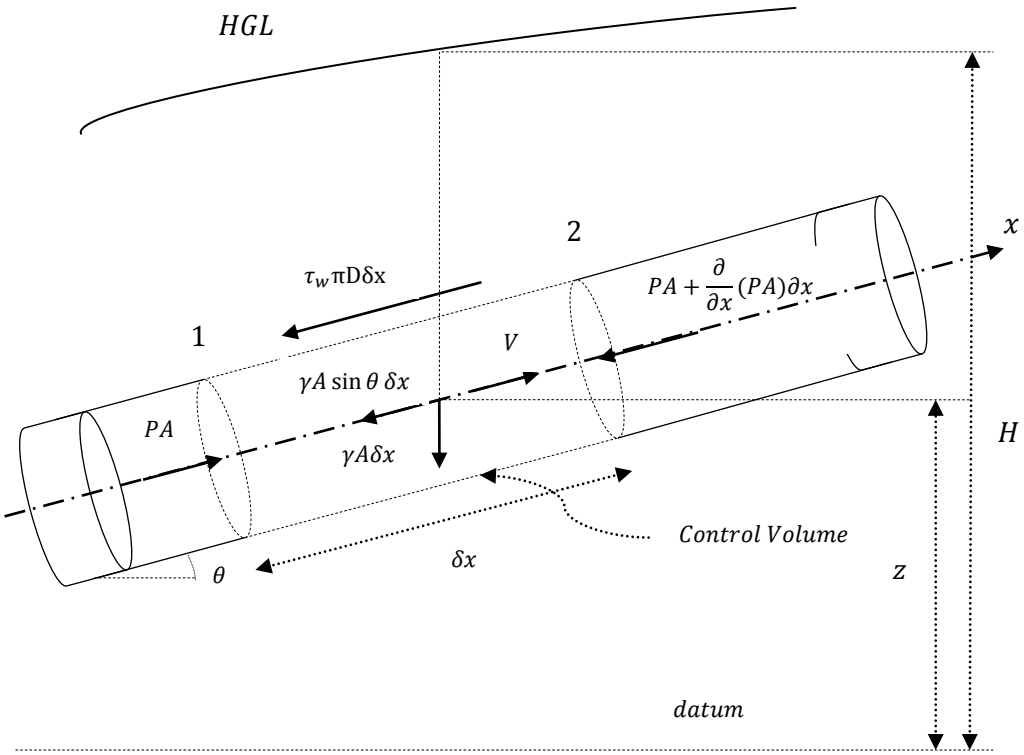

Figure 3.9 Control volume for momentum equation

Therefore;

$$-\left(A\frac{\partial P}{\partial x} + \tau_w \pi D + \rho g A \sin\theta\right)\delta x = \frac{\partial}{\partial t}(\rho V A)\delta x + \frac{\partial}{\partial x}(\rho V^2 A)\delta x \qquad (3.19)$$

δx terms cancel each other and after expanding the right side of Eqn. (3.19),

$$\frac{\partial}{\partial t}(\rho V A) + \frac{\partial}{\partial x}(\rho V^2 A) = V\underbrace{\left[\frac{\partial}{\partial t}(\rho A) + \frac{\partial}{\partial x}(\rho V A)\right]}_{Continuity\ Equation=0} + \rho A\left(\frac{\partial V}{\partial t} + V\frac{\partial V}{\partial x}\right) \qquad (3.20)$$

Dividing each term by ρA and employing $A = \pi D^2/4$, Eqn. (3.20) can be rearranged and written as,

$$\frac{1}{\rho}\frac{\partial P}{\partial x} + \frac{\partial V}{\partial t} + V\frac{\partial V}{\partial x} + \left(\frac{4\tau_w}{\rho D} + g\sin\theta\right) = 0 \tag{3.21}$$

which is the momentum equation.

3.4 Solution by the Method of Characteristics

3.4.1 Characteristics and Compatibility Equations

In previous sections two non-linear partial differential equations, namely the continuity and momentum equations, are derived. These equations having the dependent variables pressure, $P(x,t)$, and velocity, $V(x,t)$, and the independent variables distance along the pipeline, x, and time, t, can be transformed into four ordinary differential equations by using the method of characteristics to come up with numerically.

$$\underbrace{\frac{\partial P}{\partial t} + V\frac{\partial P}{\partial x} + \rho a^2\frac{\partial V}{\partial x} = 0}_{Continuity\ Equation} \tag{3.22}$$

$$\underbrace{\frac{1}{\rho}\frac{\partial P}{\partial x} + \frac{\partial V}{\partial t} + V\frac{\partial V}{\partial x} + \left(\frac{4\tau_w}{\rho D} + g\sin\theta\right) = 0}_{Momentum\ Equation} \tag{3.23}$$

Let say

$$\left(\frac{4\tau_w}{\rho D} + g\sin\theta\right) = F = F(V) \tag{3.24}$$

Then

$$L_1 = \frac{\partial P}{\partial t} + V\frac{\partial P}{\partial x} + \rho a^2 \frac{\partial V}{\partial x} = 0 \tag{3.25}$$

$$L_2 = \frac{1}{\rho}\frac{\partial P}{\partial x} + \frac{\partial V}{\partial t} + V\frac{\partial V}{\partial x} + F = 0 \tag{3.26}$$

$$L_1 + \lambda L_2 = 0 \tag{3.27}$$

where λ is a multiplier.

$$\frac{\partial P}{\partial t} + V\frac{\partial P}{\partial x} + \rho a^2 \frac{\partial V}{\partial x} + \lambda\left(\frac{1}{\rho}\frac{\partial P}{\partial x} + \frac{\partial V}{\partial t} + V\frac{\partial V}{\partial x} + F\right) = 0 \tag{3.28}$$

$$\left[\frac{\partial P}{\partial t} + \left(V + \frac{\lambda}{\rho}\right)\frac{\partial P}{\partial x}\right] + \lambda\left[\frac{\partial V}{\partial t} + \left(V + \frac{\rho a^2}{\lambda}\right)\frac{\partial V}{\partial x}\right] + \lambda F = 0 \tag{3.29}$$

Refreshing memories from calculus for $\varphi(x,t)$,

$$\frac{d\varphi}{dt} = \frac{\partial \varphi}{\partial t} + \frac{\partial \varphi}{\partial x}\frac{dx}{dt} \tag{3.30}$$

Therefore,

$$\frac{\partial P}{\partial t} + \left(V + \frac{\lambda}{\rho}\right)\frac{\partial P}{\partial x} = \frac{dP}{dt} \qquad where\ V + \frac{\lambda}{\rho} = \frac{dx}{dt} \tag{3.31}$$

and similarly

$$\frac{\partial V}{\partial t} + \left(V + \frac{\rho a^2}{\lambda}\right)\frac{\partial V}{\partial x} = \frac{dV}{dt} \quad where\ V + \frac{\rho a^2}{\lambda} = \frac{dx}{dt} \tag{3.32}$$

Eqn. (3.27) becomes

$$\frac{dP}{dt} + \lambda \frac{d\lambda}{dt} + \lambda F = 0 \tag{3.33}$$

and

$$\frac{dx}{dt} = \left(V + \frac{\lambda}{\rho}\right) = \left(V + \frac{\rho a^2}{\lambda}\right) \tag{3.34}$$

Solving above equation for λ;

$$\frac{\lambda}{\rho} = \frac{\rho a^2}{\lambda} \Longrightarrow \lambda^2 = \rho^2 a^2 \Longrightarrow \lambda = \pm \rho a \tag{3.35}$$

$$\frac{dx}{dt} = V \pm a \tag{3.36}$$

Since $V \ll a$, therefore Eqn. (3.36) yields to

$$\frac{dx}{dt} \cong \pm a \tag{3.37}$$

which is called characteristic equation and the compatibility equations are expressed as follows:

$$\left\{\frac{1}{\rho}\frac{dP}{dt} + a\frac{dV}{dt} + aF = 0 \quad where \quad \frac{dx}{dt} = +a \qquad \rightarrow C^+\right\} \tag{3.38}$$

$$\left\{\frac{1}{\rho}\frac{dP}{dt} - a\frac{dV}{dt} - aF = 0 \quad where \quad \frac{dx}{dt} = -a \qquad \rightarrow C^-\right\} \tag{3.39}$$

Figure 3.10 is a simple sketch of time-space domain consisting characteristics lines on which the compatibility equations are valid.

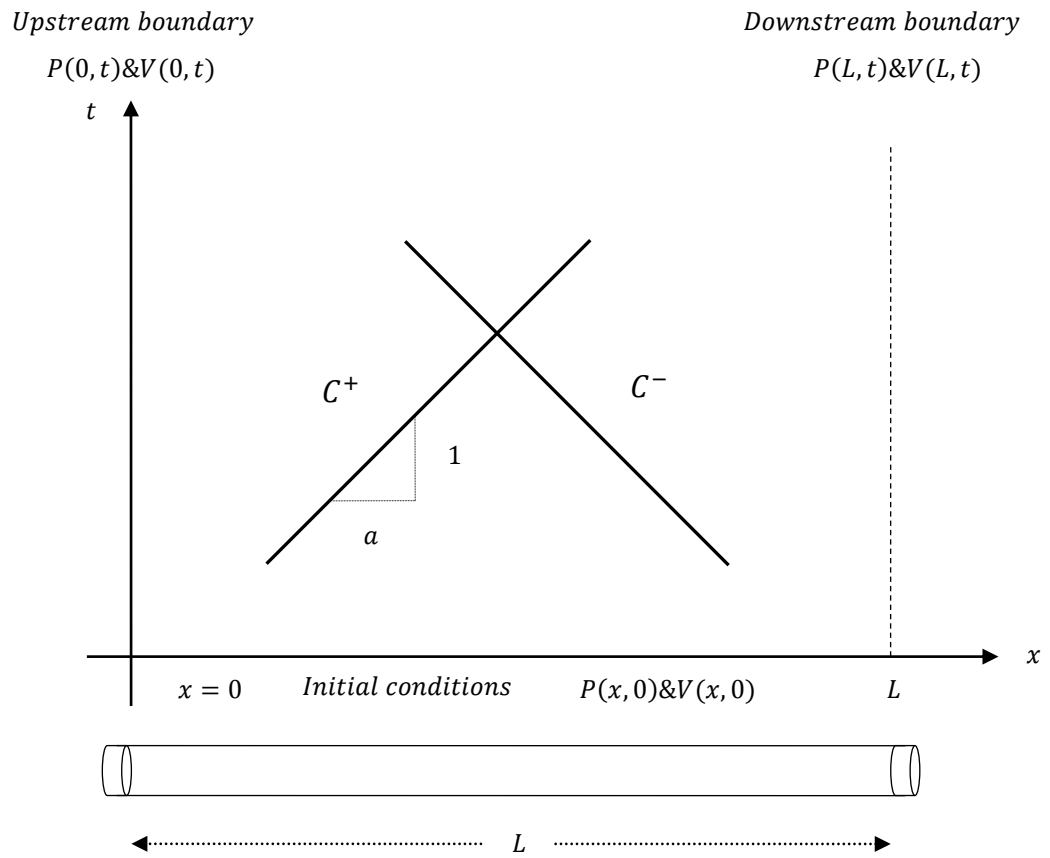

Figure 3.10 Time-space domain for solving compatibility equations

3.5 Finite Difference Equations

The characteristics and compatibility equations are derived in preceding section by using the method of characteristics which are needed to be integrated along

respective characteristic directions within the solution domain shown in Figure 3.11;

$$C^+: \quad \frac{1}{\rho a} dP + dV + Fdt = 0 \quad ; \quad dx = +adt \tag{3.40}$$

$$C^-: \quad \frac{1}{\rho a} dP - dV - Fdt = 0 \quad ; \quad dx = -adt \tag{3.41}$$

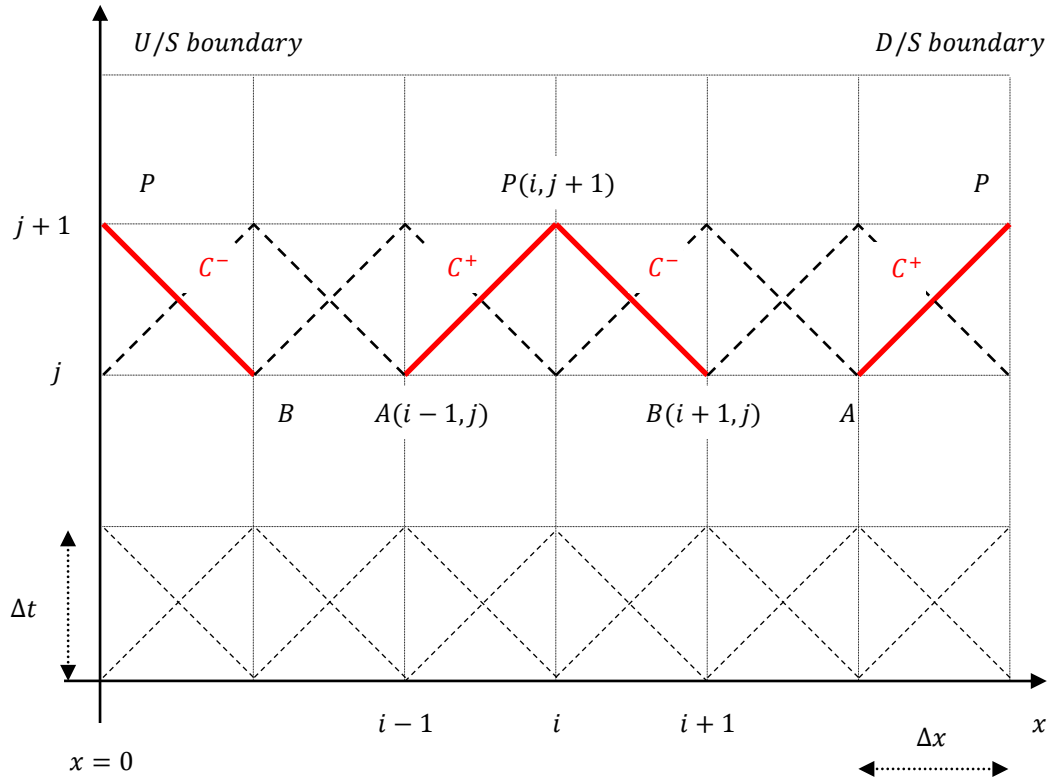

Figure 3.11 Characteristic grid of solution domain

Figure 3.11 above is a space-time (x-t) plane for undefined pressure, P, and velocity, V, which are unique variables at any point P. Intersection of the characteristic lines C^+ and C^- drawn through point P with x-axis are points A

and B respectively for which P and V values are set as an initial condition or computed and they guide to determine P and V values at point P.

$$C^+: \quad \int_A^P \frac{1}{\rho a} dP + \int_A^P dV + \int_A^P F dt = 0 \quad ; \quad \int_A^P dx = \int_A^P a dt \tag{3.42}$$

$$C^-: \quad -\int_B^P \frac{1}{\rho a} dP + \int_B^P dV + \int_B^P F dt = 0 \quad ; \quad \int_B^P dx = -\int_B^P a dt \tag{3.43}$$

$$C^+: \quad \frac{1}{\rho a}(P_P - P_A) + (V_P - V_A) + \int_A^P F dt = 0 \quad ; \quad \Delta x = a\Delta t \tag{3.44}$$

$$C^-: \quad -\frac{1}{\rho a}(P_P - P_B) + (V_P - V_B) + \int_B^P F dt = 0 \quad ; \quad \Delta x = -a\Delta t \tag{3.45}$$

Assuming "quasi-steady" friction;

$$\frac{4\tau_w}{\rho D} = f\frac{V|V|}{2D} \quad where \quad \tau_w = \frac{1}{8} f \rho V|V|$$

Eqn. (3.24) becomes

$$\int_A^B F dt = \int_A^B \left(g \sin\theta + f\frac{V|V|}{2D} \right) dt = g \sin\theta \Delta t + \frac{f}{2D} \int_A^B V|V| dt \tag{3.46}$$

Euler approximation (1st order):

$$\int_A^B V|V|dt \cong V_A|V_A|\Delta t \tag{3.47}$$

Characteristics equations becomes

$$C^+: \quad \int_{t_A}^{t_P} Fdt \approx g\sin\theta\Delta t + \frac{f}{2D}V_A|V_A|\Delta t = G_A \tag{3.48}$$

$$C^-: \quad \int_{t_B}^{t_P} Fdt \approx g\sin\theta\Delta t + \frac{f}{2D}V_B|V_B|\Delta t = G_B \tag{3.49}$$

$$C^+: \quad (P_P - P_A) + \rho a(V_P - V_A) + \rho a G_A = 0 \tag{3.50}$$

$$C^-: \quad -(P_P - P_B) + \rho a(V_P - V_B) + \rho a G_B = 0 \tag{3.51}$$

Adding above equations to solve for V_P and subtracting them to solve for P_P results in

$$V_P = \frac{1}{2}\left[(V_A + V_B) + \frac{1}{\rho a}(P_A - P_B) - (G_A - G_B)\right] \tag{3.52}$$

$$P_P = \frac{1}{2}\left[(P_A + P_B) + \frac{(V_A - V_B)}{\rho a} - \rho a(G_A + G_B)\right] \tag{3.53}$$

Equations derived in terms of pressure head H and velocity V for C^+ and C^- respectively are as follows (Wylie & Streeter, 1978);

Compatibility equations:

$$C^+: \quad \frac{g}{a}\frac{dH}{dt} + \frac{dV}{dt} + \frac{fV|V|}{2D} \tag{3.54}$$

$$C^-: \quad -\frac{g}{a}\frac{dH}{dt} + \frac{dV}{dt} + \frac{fV|V|}{2D} \tag{3.55}$$

Characteristics equations:

$$C^+: \quad \frac{dx}{dt} = +a, \tag{3.56}$$

$$C^-: \quad \frac{dx}{dt} = -a, \tag{3.57}$$

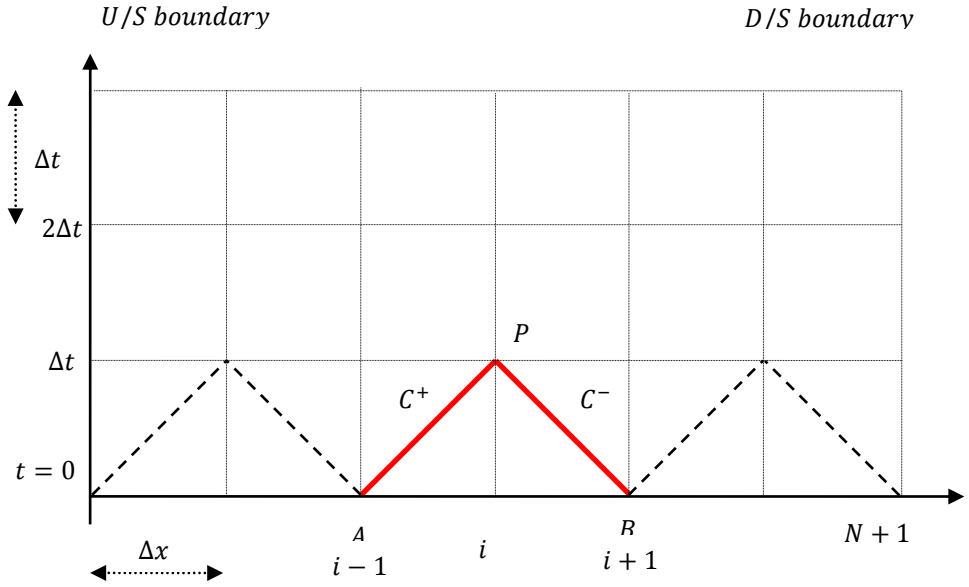

Figure 3.12 (x-t) Grid for solution of single pipe problems

Figure 3.12 is the illustration of a pipeline divided into N equal reaches each Δx in length. Positively sloped diagonal line AP (C^+) demonstrates Eqn. (3.56) by computing a time step $\Delta t = \Delta x/a$ (Courant condition). Regarding initially known V and H values at point A, Eqn. (3.54) can be integrated along line AP and, thusly, be written based on unknown variables V and H at point P. Similarly, integration of Eqn. (3.55) along line BP (C^-), which is the reflection of Eqn. (3.57) on grid, yields to another equation with variables known at B and unknown at P. Solving both equations simultaneously corresponds to conditions at point P. C^+ equation may be represented in terms of discharge Q in lieu of velocity V by employing area of the pipe and multiplying it by $a(dt/g) = dx/g$ ends up with Eqn. (3.58)

$$\int_{H_A}^{H_P} dH + \frac{a}{gA}\int_{Q_A}^{Q_P} dQ + \frac{f}{2gDA^2}\int_{X_A}^{X_P} Q|Q|dx = 0 \tag{3.58}$$

Then the integration of the Eqn. (3.58) results in

$$H_P - H_A + \frac{a}{gA}(Q_P - Q_A) + \frac{f\Delta x}{2gDA^2}Q_A|Q_A| = 0 \tag{3.59}$$

Similar procedure as for C^-;

$$H_P - H_B - \frac{a}{gA}(Q_P - Q_B) - \frac{f\Delta x}{2gDA^2}Q_B|Q_B| = 0 \tag{3.60}$$

Above algebraic equations by which the transient propagation of piezometric head, H, and discharge, Q, are described, can be rearranged as shown below:

$$C^+: \quad H_P = H_A - B(Q_P - Q_A) - RQ_A|Q_A| \tag{3.61}$$

$$C^-: \quad H_P = H_B + B(Q_P - Q_B) + RQ_B|Q_B| \tag{3.62}$$

$$where \qquad B = \frac{a}{gA} \qquad and \qquad R = \frac{f\Delta x}{2gDA^2}$$

In case of the steady-state condition the flows are $Q_A = Q_P = Q_B$ and friction head loss $Q_A|Q_A|$. The solution of a transient problem starts with steady-state initial conditions H and Q which are known at time zero and proceeds with computing head and discharge values at each grid point in solution domain throughout the specified time interval.

Eqn.s (3.61) and (3.62) are simply written as

$$C^+: \quad H_{P_i} = C_P - BQ_{P_i} \tag{3.63}$$

$$C^-: \quad H_{P_i} = C_M + BQ_{P_i} \tag{3.64}$$

and

$$H_{P_i} = \frac{(C_P + C_M)}{2} \tag{3.65}$$

where C_P and C_M are known or predefined constants and can be written as,

$$C_P: \quad H_{i-1} + BQ_{i-1} - RQ_{i-1}|Q_{i-1}| \tag{3.66}$$

$$C_M: \quad H_{i+1} - BQ_{i+1} + RQ_{i+1}|Q_{i+1}| \tag{3.67}$$

3.6 Boundary Conditions

Either end of a single pipe accommodates only one compatibility equation. While Eqn. (3.64) holds along C^- characteristic line at upstream end, Eqn. (3.63) stands for C^+ line at downstream end of pipe shown in Figure 3.13.

Aforementioned linear equations in terms of Q_P and H_P transfer the entire behavior and response of the fluid to the regarding boundary throughout the transient event. Auxiliary equations or relations are necessary for both cases to identify Q_P and H_P (Bozkuş, 2009). Each boundary condition solved independently from others conveys the regarding information at boundaries to the points at interior regions.

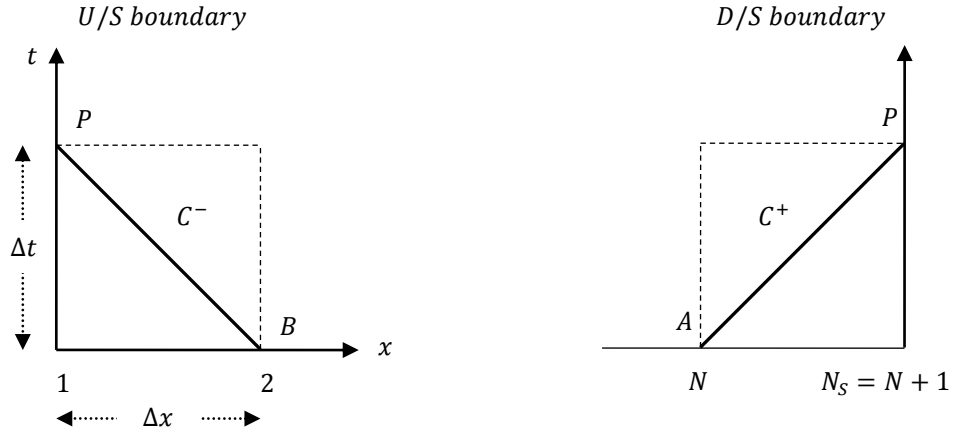

(a) (b)

Figure 3.13 Characteristic lines at (a) U/S and (b) D/S boundary

3.6.1 Reservoir at Upstream End with Specified Elevation

In case of a large reservoir at the upstream of a pipeline system, variations in reservoir elevation due to transient motion can be neglected, that is, HGL is constant. This boundary condition corresponds to a constant head at starting node (point 1) of pipeline during transient event which is designated by following equation.

$$H_{P_1} = H_R \tag{3.68}$$

where H_R is reservoir head. And the discharge at point 1 can be obtained by solving Eqn. (3.64) directly,

$$Q_{P_1} = \frac{(H_{P_1} - C_M)}{B} \tag{3.69}$$

3.6.2 Reservoir at Upstream End with Specified Variable Head

If there is a large reservoir located at upstream end of a pipeline which has a fluctuating surface elevation in a known manner, let say a sine wave, head and discharge at starting node become;

$$H_{P_1} = H_R + \Delta H \sin \omega t \tag{3.70}$$

and

$$Q_{P_1} = \frac{(H_{P_1} - C_M)}{B} \tag{3.71}$$

respectively, where

ΔH : Amplitude of the sine wave

ω : Circular frequency

3.6.3 Discharge as a Specified Function of Time at Upstream End

Eqn. (3.72) expresses the flow through a positive displacement pump located at upstream end of a pipeline explicitly as a function of time.

$$Q_{P_1} = Q_0 + \Delta Q|\sin \omega t| \tag{3.72}$$

Thus, direct application of Eqn. (3.64) with known Q_{P1} at any instant brings one to find H_{P1} at each time step.

3.6.4 Pump at U/S End with Head-Discharge Curve Specified

A constant speed centrifugal pump supplying flow from a suction reservoir can be operated at the U/S end. Using reservoir surface elevation as a reference datum for HGL and defining the pump characteristics curve, the boundary condition equation becomes

$$H_{P_1} = Q_{P_1}\left(a_1 + a_2 Q_{P_1}\right) \tag{3.73}$$

in which H_S is shut-off head and a_1 and a_2 are constants constituting pump characteristics curve. Simultaneous solution of Eqn.s (3.64) and (3.73) results in

$$Q_{P_1} = \frac{1}{2a_2}\left(B - a_1 - \sqrt{(B - a_1)^2 + 4a_2(C_M - H_S)}\right) \tag{3.74}$$

and value of Q_{P1} obtained from above equation is used in either Eqn. (3.64) or Eqn. (3.73) to determine H_{P1}.

3.6.5 Dead End at the Downstream End of Pipe

A dead end at the downstream corresponds to zero flow, that is,

$$Q_{P_{NS}} = 0 \tag{3.75}$$

Therefore, $H_{P_{NS}}$ can be determined by using either Eqn. (3.61) or Eqn. (3.63).

3.6.6 Valve at the Downstream End of Pipe

In case of a valve at D/S end of a pipeline (see Figure 3.14), the orifice equation can be utilized for

$$Q_0 = (C_d A_V)_0 \sqrt{2gH_0} \tag{3.76}$$

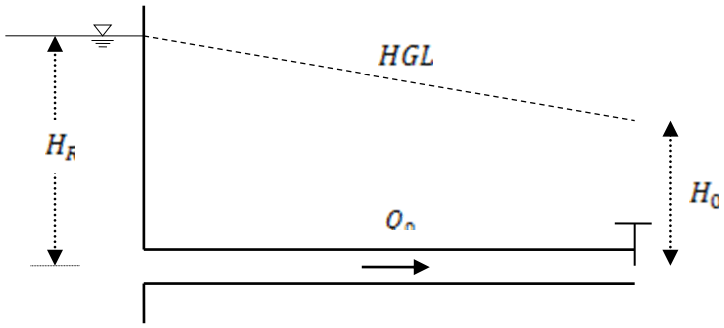

Figure 3.14 Simple sketch of valve at downstream end of a pipe

In which C_d is the discharge coefficient and, A_V is effective valve area and H_0 is steady state head loss across the valve. General expression for discharge passing through a valve can be written as follows;

$$Q_P = (C_d A_V)\sqrt{2g\Delta H} \tag{3.77}$$

where ΔH represents the instantaneous drop in HGL across the valve.

Dividing instantaneous discharge to steady-state one results in

$$\frac{Q_P}{Q_0} = \frac{(C_d A_V)}{(C_d A_V)_0} \sqrt{\frac{\Delta H}{H_0}} \tag{3.78}$$

and thus,

$$Q_P = \frac{Q_0}{\sqrt{H_0}} \tau \sqrt{\Delta H} \tag{3.79}$$

where τ is namely dimensionless valve opening

$$\tau = \frac{(C_d A_V)}{(C_d A_V)_0} \tag{3.80}$$

- If $\tau = 0$, valve is closed, $Q = 0$
- If $\tau = 1$, steady state or initial condition is ensured
- If $0 < \tau < 1$ valve is being closed
- If $\tau > 1$ valve is opening further

Simultaneous solution of Eqn.s (3.79) and (3.63) ends up with

$$Q_{P_{NS}} = -BC_V + \sqrt{(BC_V)^2 + 2C_P C_V} \tag{3.81}$$

$$C_V = \frac{(Q_0 \tau)^2}{2H_0} \tag{3.82}$$

for downstream boundary condition.

Similarly, boundary condition equation for orifice at the downstream end can be defined by referring $\tau = 1$.

3.6.7 Reservoir at the Downstream End with Constant Head

Boundary condition equation in terms of head at the last node of a pipeline ends with a constant head reservoir is defined by

$$H_{P_{NS}} = H_{R_{D/S}} \tag{3.83}$$

3.6.8 Internal Valve

In case of a valve located at an intermediate section of a pipeline, the orifice equation must be utilized at that node simultaneously for each pipe end. Therefore, the orifice equation for positive flow and negative flow with steady state head loss H_0 across valve can be written as

$$Q_{P_{2,1}} = Q_{P_{1,NS}} = \pm \frac{Q_0 \tau}{\sqrt{H_0}} \sqrt{H_{P_{1,NS}} - H_{P_{2,1}}} \tag{3.84}$$

respectively and combining Eqn. (3.84) with Eqn.s (3.63) and (3.64) for pipes 1 and 2 results in following boundary condition equation:

$$Q_{P_{2,1}} = \mp C_V (B_1 + B_2) \pm \sqrt{{C_V}^2 (B_1 + B_2)^2 \pm 2 C_V \left(C_{P_1} - C_{M_2}\right)} \tag{3.85}$$

3.6.9 Series Pipe Junctions

The boundary condition equation of a junction of pipes in series with different physical properties, such as roughness and/or diameter etc., can be defined in terms of common hydraulic conditions at that junction, that is, the application of continuity equation and using same pressure head (neglecting local loss) bring two equations for the junction.

$$Q_{P_{1,NS}} = Q_{P_{2,1}} \tag{3.86}$$

and

$$H_{P_{1,NS}} = H_{P_{2,1}} \tag{3.87}$$

and simultaneous solution of above equations with Eqn.s (3.63) and (3.64) ends up with

$$Q_{P_{2,1}} = \frac{C_{P_1} - C_{M_2}}{B_1 + B_2} \tag{3.88}$$

3.6.10 Branching Pipes

Similar procedure in terms of common hydraulic conditions can be utilized for a branching junction consisting of incoming and outgoing pipes sharing same node. Assuming equal pressure head and flow (the continuity principle) values at junction at which any number of pipes, let say 2 incoming and 2 outgoing, connected, C^+ compatibility equation designates incoming pipes while C^- covers outgoing ones.

$$H_P = H_{P_{1,NS}} = H_{P_{2,NS}} = H_{P_{3,1}} = H_{P_{4,1}} \tag{3.89}$$

$$Q_{P_{1,NS}} = -\frac{H_P}{B_1} + \frac{C_{P_1}}{B_1}$$

$$Q_{P_{2,NS}} = -\frac{H_P}{B_2} + \frac{C_{P_2}}{B_2}$$

$$-Q_{P_{1,NS}} = -\frac{H_P}{B_3} + \frac{C_{M_3}}{B_3}$$

$$-Q_{P_{1,NS}} = -\frac{H_P}{B_4} + \frac{C_{M_4}}{B_4}$$

and

$$H_P = \frac{\frac{C_{P_1}}{B_1} + \frac{C_{P_2}}{B_2} + \frac{C_{M_3}}{B_3} + \frac{C_{M_4}}{B_4}}{\sum \frac{1}{B}} \tag{3.90}$$

3.6.11 Surge Tanks

Surge tanks are basically open top reservoirs extending up to HGL with different sizes and shapes. Boundary condition equation in case of a simple surge tank located on a pipeline (see Figure 3.15) can be derived as follows;

$$C^+ for\ end\ node\ of\ pipe\ i, \qquad H_{P_i} = C_P - BQ_{P_i} \tag{3.91}$$

$$C^- for\ starting\ node\ of\ pipe\ i+1, \qquad H_{P_i} = C_M + BQ_{P_i} \tag{3.92}$$

Satisfying continuity principle for the intersection point of two pipes and the surge tank, the discharge is noted as,

$$Q_{P_{i,n+1}} = Q_{P_{1+1,1}} + Q_{P_{Surge\ tank}} \tag{3.93}$$

where $Q_{P_{Surge\ tank}}$ is the discharge through the surge tank,

and the head balance is;

$$H_{P_{i,n+1}} = H_{P_{i+1,1}} = Z_P \tag{3.94}$$

in which Z and Z_P are the elevation of liquid column in the surge tank at start and end of time interval respectively.

Therefore, equation of the liquid surface elevation for time interval Δt, preferably small enough, becomes

$$Z_P = Z + \frac{\Delta t}{2A_S}(Q_{PS} + Q_s) \tag{3.95}$$

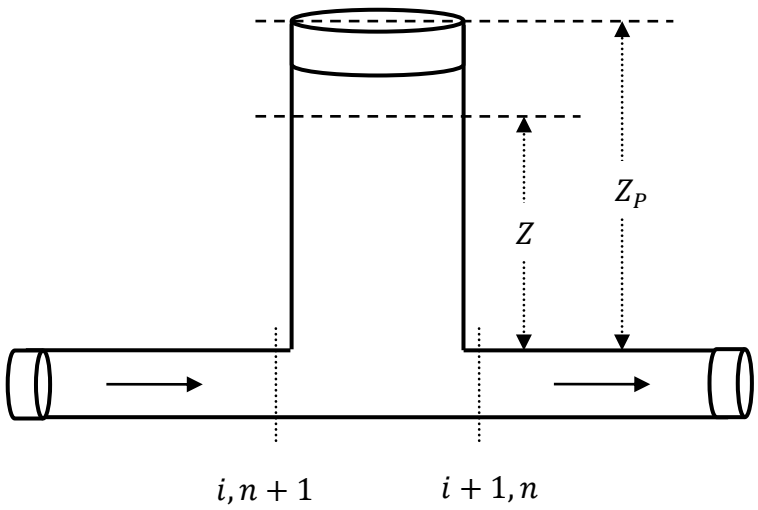

Figure 3.15 Schematic illustration of a surge tank located on a pipeline

where is cross-sectional area of surge tank, and Q_{PS} and Q_S are discharges at the end and start of the time interval.

CHAPTER 4

COMPUTER PROGRAM UTILIZED FOR ANALYSES

4.1 General Overview

An accurate modeling of a safe and economic hydraulic system in terms of transient analysis requires more than a handmade calculation. Considering the significance of generating fast solutions for recent engineering studies as well as safety and economy, it is inevitable to take advantage of reliable software to solve complex equations derived from a hydraulic system in a short time regarding several boundary conditions and various scenarios. A number of computer softwares which use the Method of Characteristics (MoC) for solution of complex transient flow equations are developed up to the present in order to simulate hydraulic systems numerically. In this regard, the investigation of the water hammer problems to be expected under various scenarios and suggestions for safe operation conditions of Çamlıdere Dam – İvedik WTP pipeline system is performed by HAMMER transient analysis and modeling software.

4.2 Modeling and Computational Features of the Software

HAMMER is an advanced numerical simulator for several hydraulic structures such as hydropower plants, pumping systems or piping networks which are supposed to experience transient phenomena or water hammer frequently. It allows designers for creating safe and economical surge control systems in quick and professional manner to prevent destructive pipe and equipment damages (Bentley HAMMER V8i User's Guide, 2010).

The software is capable of computing both steady-state operation conditions and extended period simulation (EPS) in order to establish initial conditions for transient results along the pipes and at junctions by using MoC which has been described as the most reliable algorithm for hydraulic transient flow analysis.

The operating behavior of the system at a specific node in time is determined by steady-state analyses instantaneously. EPS, on the other hand, simulates the variation of the system attributes over time. While the steady-state solution demonstrates the capability of the system to meet a certain average demand, EPS reflects the ability of the system whether it is supposed to provide acceptable levels of service over a long period.

Prior to run steady state analysis and computing initial conditions, the program gives chance to check modeling or data errors by *validate* command and, thus, a notification window appears and lists errors with warning messages to fix if there is any.

HAMMER uses MoC by default for solution of the transient equations induced by Newtonian fluids which corresponds to compressible fluids and elastic pipe wall. Rigid column theory, which is a simpler method assuming incompressible fluid and rigid pipe, is a solution option but not to be set as default.

The transient analysis is performed by *compute* command after specifying initial conditions manually or by allowing the software to compute them automatically. In addition to the information required for a steady-state analysis and predefined boundary conditions for tools by HAMMER, hydraulic transient simulation desires;

- Pipe characteristics to figure out the wave speed
- Vapor pressure of the fluid
- Pump and motor inertia of the pump
- Pump and/or turbine characteristics
- Valve characteristics and operation strategies
- The characteristics of surge-protection equipment

It is possible to import a model automatically from a data source such as EPA Net or CAD drawings as well as creating your own model. Program is also fully compatible with WaterCAD and WaterGEMS that the data files imported from these programs can directly be opened in HAMMER, or vice versa, without conversion, translation or data loss. Moreover, identification of the components with their real appearances can be supported by importing pictures as background layers behind the model (Bentley HAMMER, 2011).

To speed up defining inputs and simplify the evaluation of results, Flex tables (see Figure 4.1) are brought into use which allows for sorting, filtering and global editing of inputs and outputs. While it accommodates ready to use data for hydraulic calculations, such as minor loss coefficients for valves or friction coefficients for pipes, HAMMER enables users to create their own engineering libraries in order to enter information once for hydraulic elements and store it to use many times. The software also provides opportunity to use recommended time steps or to define it yourself.

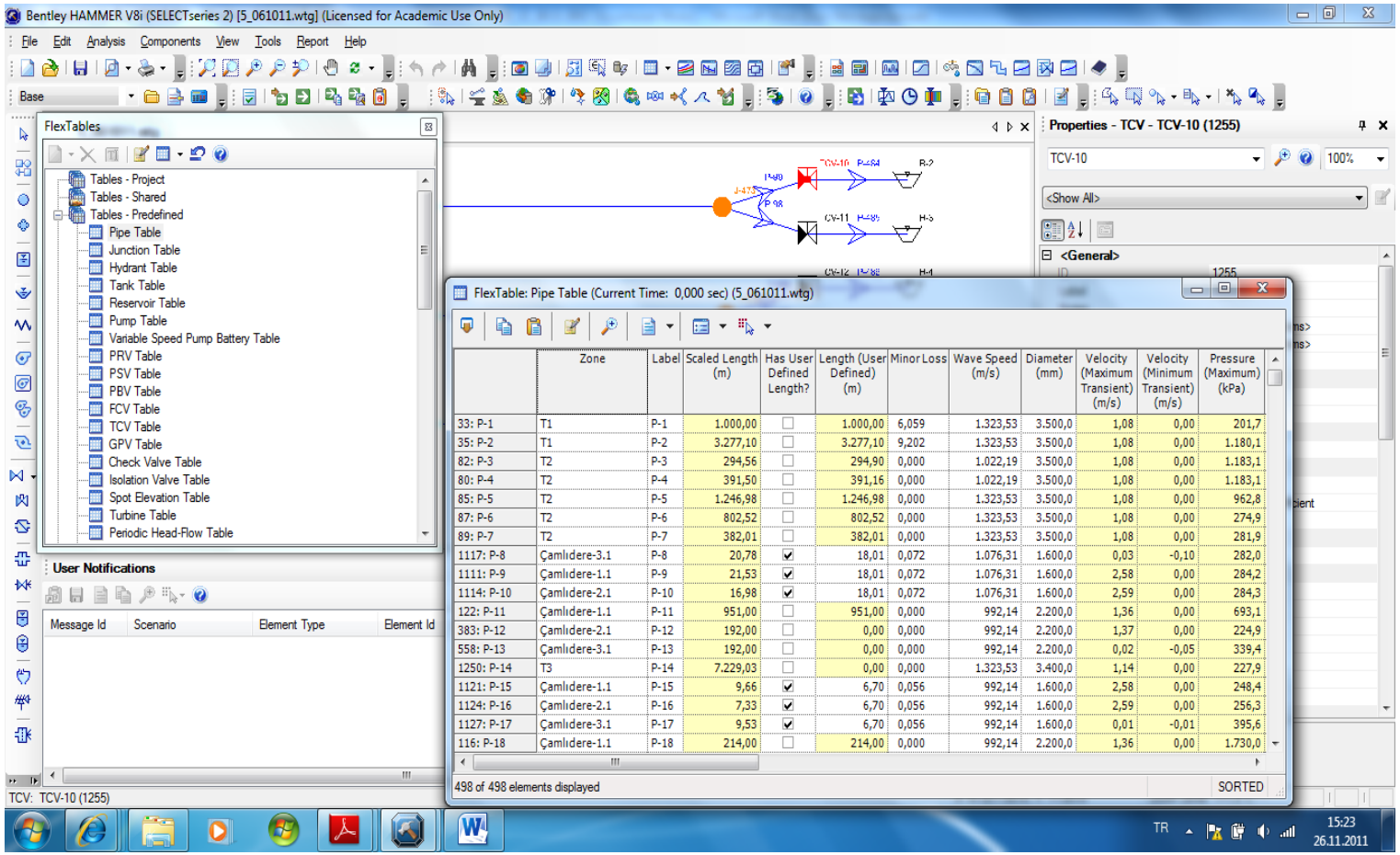

	Zone	Label	Scaled Length (m)	Has User Defined Length?	Length (User Defined) (m)	Minor Loss	Wave Speed (m/s)	Diameter (mm)	Velocity (Maximum Transient) (m/s)	Velocity (Minimum Transient) (m/s)	Pressure (Maximum) (kPa)
33: P-1	T1	P-1	1.000,00	☐	1.000,00	6,059	1.323,53	3.500,0	1,08	0,00	201,7
35: P-2	T1	P-2	3.277,10	☐	3.277,10	9,202	1.323,53	3.500,0	1,08	0,00	1.180,1
82: P-3	T2	P-3	294,56	☐	294,90	0,000	1.022,19	3.500,0	1,08	0,00	1.183,1
80: P-4	T2	P-4	391,50	☐	391,16	0,000	1.022,19	3.500,0	1,08	0,00	1.183,1
85: P-5	T2	P-5	1.246,98	☐	1.246,98	0,000	1.323,53	3.500,0	1,08	0,00	962,8
87: P-6	T2	P-6	802,52	☐	802,52	0,000	1.323,53	3.500,0	1,08	0,00	274,9
89: P-7	T2	P-7	382,01	☐	382,01	0,000	1.323,53	3.500,0	1,08	0,00	281,9
1117: P-8	Çamlıdere-3.1	P-8	20,78	☑	18,01	0,072	1.076,31	1.600,0	0,03	-0,10	282,0
1111: P-9	Çamlıdere-1.1	P-9	21,53	☑	18,01	0,072	1.076,31	1.600,0	2,58	0,00	284,2
1114: P-10	Çamlıdere-2.1	P-10	16,98	☑	18,01	0,072	1.076,31	1.600,0	2,59	0,00	284,3
122: P-11	Çamlıdere-1.1	P-11	951,00	☐	951,00	0,000	992,14	2.200,0	1,36	0,00	693,1
383: P-12	Çamlıdere-2.1	P-12	192,00	☐	0,00	0,000	992,14	2.200,0	1,37	0,00	224,9
558: P-13	Çamlıdere-3.1	P-13	192,00	☐	0,00	0,000	992,14	2.200,0	0,02	-0,05	339,4
1250: P-14	T3	P-14	7.229,03	☐	0,00	0,000	1.323,53	3.400,0	1,14	0,00	227,9
1121: P-15	Çamlıdere-1.1	P-15	9,66	☑	6,70	0,056	992,14	1.600,0	2,58	0,00	248,4
1124: P-16	Çamlıdere-2.1	P-16	7,33	☑	6,70	0,056	992,14	1.600,0	2,59	0,00	256,3
1127: P-17	Çamlıdere-3.1	P-17	9,53	☑	6,70	0,056	992,14	1.600,0	0,01	-0,01	395,6
116: P-18	Çamlıdere-1.1	P-18	214,00	☐	214,00	0,000	992,14	2.200,0	1,36	0,00	1.730,0

Figure 4.1 Flex tables

A plenty of hydraulic devices shown in Figure (4.2) can be selected by designer in order to create desired piping system schematically or scaled on drawing pane and perform numerous operating scenarios. The devices used for establishing Çamlıdere Dam-İvedik WTP pipeline system can be listed as follows;

- *Reservoir* is selected for Çamlıdere Dam at the very beginning and aeration pool inside İvedik WTP at the end of the system. Water surface elevations, which are the start and end of steady-state HGL, and, inlet and outlet elevations are defined respectively.

- *Pipe* is selected for the tunnels and pipelines. Also the bifurcation and trifurcation structures are composed of pipes. The program needs basic information, namely, diameter, length, friction factor, minor loss coefficient along pipe and wave speed in order to initiate an analysis. The wave speed of a pipe element which is a must for transient analysis can be either defined manually or computed by the *wave speed calculator* command.

- *Junction* is the connection of two pipes which have different properties and/or changes in direction. Designer is supposed to specify the elevation of the junction only. This command can also be utilized for creating a wye.

- *Throttle Control Valves* are selected as the flow control devices during analysis. There exist needle valves at İvedik WTP inlet and butterfly valves at the start and end of tunnels as pipe fracture safety devices for maintenance and storage purposes. For this type of valves, the elevation of valve, diameter, and discharge coefficient are necessary data that must be defined.

Calculation options, which is the design criteria of the system in a manner, can be defined in terms of steady-state (or EPS) and transient solvers. Initially steady-state friction method must be defined for steady-state solver. Activation of demand and roughness adjustments, display of status messages of elements, calculation flags, time step convergence messages and calculation times are defined within calculation options. Additionally, physical properties of liquid transmitted are specified in this manager. Similarly, selection of transient friction method is the fundamental criterion for transient solver. There are four options for transient friction method, namely steady, quasi-steady, unsteady, and unsteady-Vitkovski. Detailed reporting options can be specified in this field also. The content, range and size of transient analysis reports can be adjusted. The transient solver also covers both time step interval, either defined manually or recommended by program automatically, and entire run duration time. For the sake of simplicity a global wave speed for pipes can be assigned instead of assigning for each pipe. The vapor pressure of liquid to observe vaporization and vapor pockets is defined manually or can be selected from engineering libraries.

In addition to abovementioned ones, user can assign several devices according to the scope of the design. A *turbine* for a hydropower plant or a *pump* for a discharge line and different surge control devices like *air valve* can be selected in order to achieve the goal.

The user can confirm capability of the penstock and flow control devices under steady-state operation or transient pressure rise due to load acceptance and load rejection operations or during emergency shutdowns. Similar verification is possible for discharge lines and pumps.

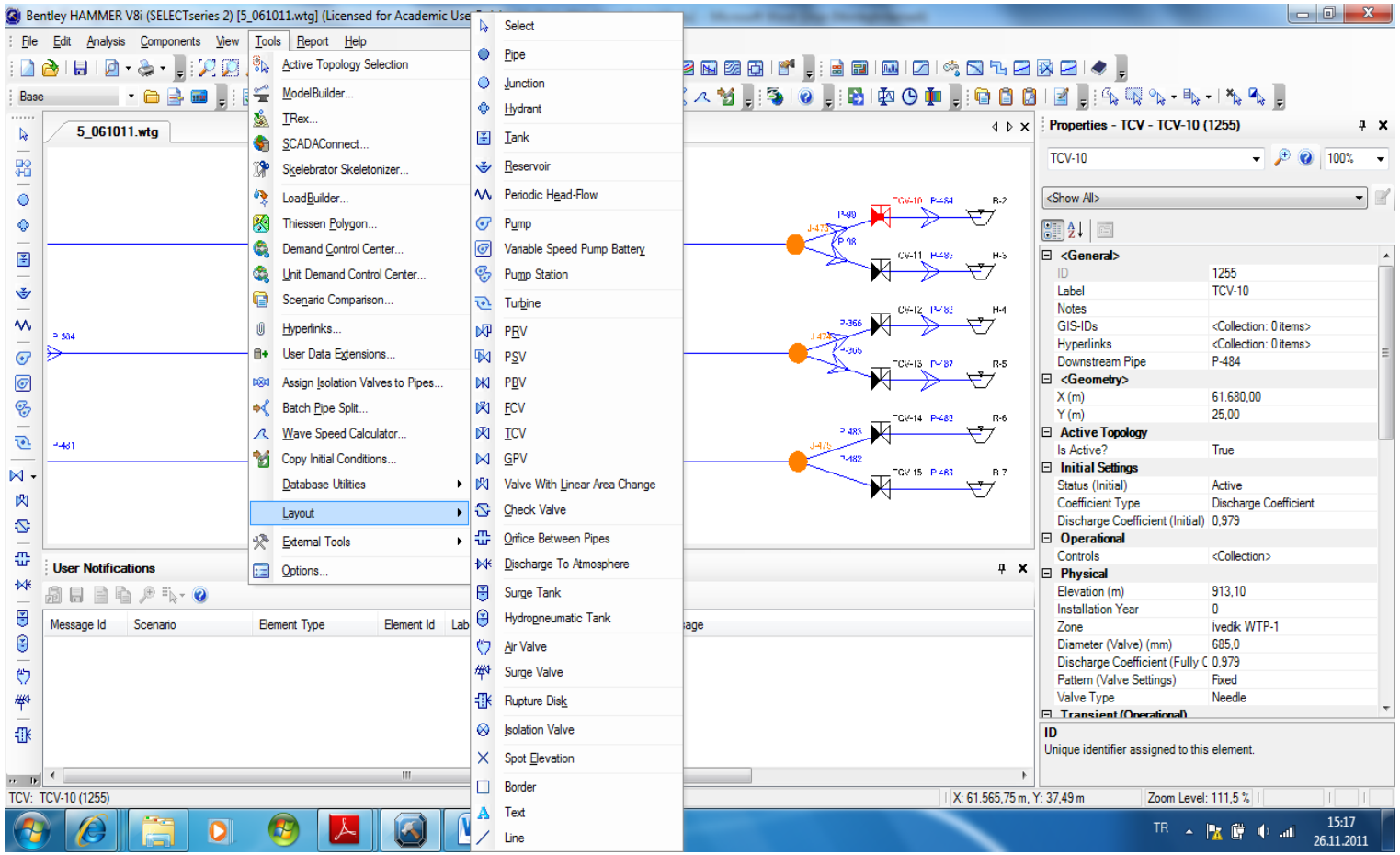

Figure 4.2 Tools for modeling on main window

Furthermore, the software is capable of computing the magnitude and direction of transient forces exerted on a pipe automatically for each time step which can be activated within transient solver. The results can be analyzed with graphs and integrated into structural analysis programs to investigate the structural ability of piping system.

After modeling the system by appropriate devices and adequate data, the software accurately simulates the transient phenomena ranging from a slow surge to a rapid transient motion and let user to come up with the suitable surge control strategy.

4.3 Creating and Editing Scenarios

HAMMER contains a scenario control manager in order to observe different operation and calculation options concurrently. This tool enables designer to create unlimited number of scenarios consisting of all the input data, calculation options, results and notes associated with a set of calculations and designer can modify, compute and review the design under those conditions accordingly (Bentley HAMMER V8i User's Guide, 2010). The user can switch between scenarios and compare variations among different operating options in a short time.

A scenario unifies a set of *alternatives* containing physical, operational, transient options etc. that hold categorized input data together for a particular element of the system as well as calculation options. Performing computations to observe the effects of alternatives on the system, for example trying different diameters for a set of pipe, the best one for the system can be preferred permanently. Besides, it is possible to assign an alternative to different scenarios independently.

4.4 Presentation of Results and Reporting Features

As well as performing accurate analysis, any software is supposed to demonstrate results understandably. For this reason, HAMMER can generate several types of graphs or animations and reports to illustrate results at specific points selected or profiles created before running the program. It is possible to get results for entire system; however, depending on the content of model, output files can be very large in size.

As soon as a transient analysis finished, *transient calculation summary* appears on main screen where designer can see the calculation summary, initial conditions, and extreme heads and pressures. After this global check, detailed graphical or tabular results and reports can be attained. Going a step further, *Transient results viewer* dialog under *analysis* command shows detailed results for created profiles and for time histories of selected points in terms of graphs containing hydraulic grade, flow, air/vapor volume, transient force etc. output.

Some examples of graphical and visual illustrations treated above are;

- HGL profile: It is possible to create profiles along pipeline for graphical illustration of results. Steady-state HGL can be plotted and the maximum and minimum transient pressures can be marked along the main path.

- Time-History: Time-dependent alterations in transient flow and pressure can be plotted and the volume of vapor or air at specified point can be displayed.

- Animations: The system can be animated to observe how system variables alter over time following a power failure and transient pressure stabilizes after a while. Program synchronizes and animates every path and history on the screen simultaneously.

- Color mapping: This option helps user to clarify problematic regions with color maps of maximum or minimum transient pressures, flow or air/vapor volume. *Transient thematic viewer* dialog colorizes hydraulic elements in selected range in accordance with their calculated values for a specified attribute.

HAMMER is also capable of creating *reports* which are printable contents regarding the physical features of model and analysis results. Inputs, graphs, animations, color maps etc. can be transferred in a report in words and numbers.

CHAPTER 5

ÇAMLIDERE DAM – İVEDİK WTP PIPELINE SYSTEM

5.1 Introduction

Çamlıdere Dam-İvedik WTP pipeline system plays an important role in terms of supplying the potable water demand of Ankara while it has been projected that 66% of the drinking water need for the city will be provided by Çamlıdere Dam in year 2027 (Bozkuş, 1996).

Although the master plan projections require 3 pipelines, Çamlıdere Dam – IWTP pipeline system has been composed of two composite pipelines yet (Çamlıdere 1 & Çamlıdere 2) extending over 60 km between dam and treatment plant which include hydraulic devices for operation and maintenance purposes. Nevertheless, increasing potable water consumption of city due to population growth makes the construction of third pipeline unavoidable in the future.

As a result, considering the aforementioned importance of the pipeline system for the city of Ankara and, moreover, recognizing that such a pipeline system can experience transient events frequently, it is crucial to operate the system in a continuous and safe manner.

In this regard, this chapter is dedicated to describe the pipeline system in detail physically with existing and future planned hydraulic components, investigate water hammer problems expected under various scenarios by the help of methods and software narrated in previous chapters, and illustrate results of analyses to come up with suggestions for the safe operation conditions.

5.2 Description of the Pipeline System

5.2.1 Çamlıdere Dam

Çamlıdere Dam, which is located 63 km northwest of Ankara on Bayındır Creek, is a rock fill dam with 753 km^2 drainage area and it was constructed between 1976 and 1985. The thalweg and crest elevations of the dam are 900 m and 1,002 m respectively. Although the mean annual flow at dam location is $171x10^6$ m^3, reservoir volume is around $1.3x10^9$ m^3. The reason for this huge difference is the water derivation project planned for the future from Gerede Basin (Işıklı Water Supply Project) to Çamlıdere Dam. Appendix A illustrates the planning works on Işıklı derivation project. Recent studies on this project illustrates that the amount of this derivation will be around $230x10^6$ m^3 annually (Yüksel Proje Uluslararası A.Ş., 2004). Therefore, the additional volume will result in variation of water surface elevation of Çamlıdere Dam between 960.00 – 998.70 m. The minimum water level is supposed to drop 942.00 m. in case of emergency.

Currently, the raw water stored in dam reservoir is transmitted to İvedik WTP by two existing pipelines (Çamlıdere 1 & Çamlıdere 2) exceeding 60 km and distributed to the city as potable water after treatment processes. Figure 5.1 shows the simple layout of Çamlıdere Dam – IWTP pipeline system. Also Appendix B shows the layout of the dams and pipelines that supply potable water to the city of Ankara.

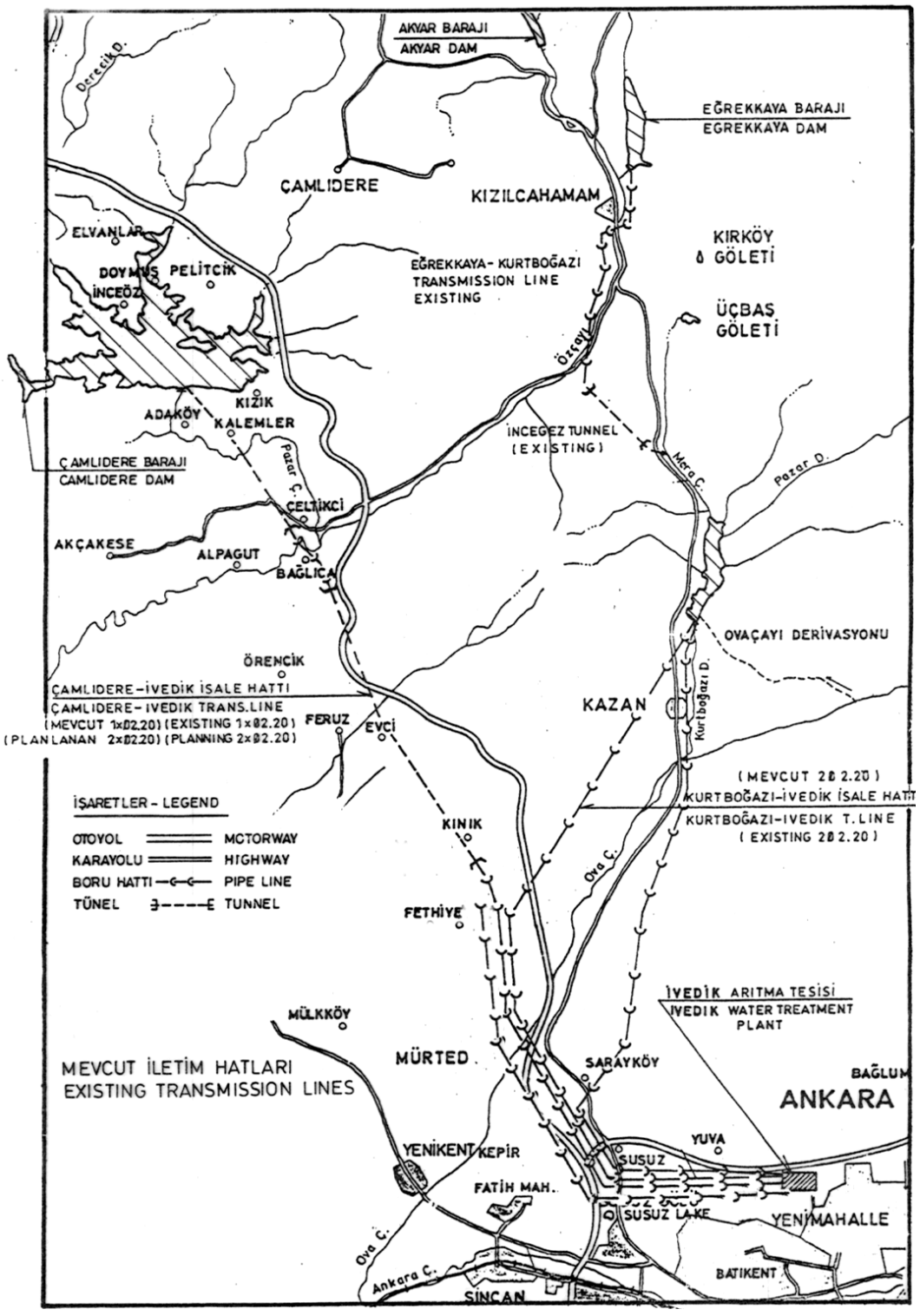

Figure 5.1 Simple layout of Çamlıdere Dam – IWTP pipeline (Bozkuş, 2008)

5.2.2 Intake Structure

During the construction stage of Çamlıdere Dam, OPM (1978) performed a hydraulic consultancy and came up with a final report covering;

- The maximum pressure surges that the pipeline can experience,
- The maximum discharges through the pipeline,
- The safety protections through the pipeline,
- Design of the water intake structure.

The water intake is a tower type structure including two independent vertical shafts. One of these shafts (Shaft A) is used to take water into pipeline and the other (Shaft B) is operated for pressure dissipation purposes. Regarding the variation of water surface elevations of Çamlıdere Dam between 942.00 and 998.70 m and length of the pipelines, the intake tower was designed to maintain water level at 960.00 m, which had been described as the minimum water surface elevation at operation, in order to prevent irrelevant dimensions of tunnels and pipes due to large pressures and for ease of operation. However, considering excess pressures and operational failures, entire pipeline system is designed and constructed regarding 970.00 m static water level (Yüksel Proje Uluslararası A.Ş., 2004). As a result, it is necessary to maintain water level at 960.00 m even if the reservoir level exceeds 960.00 m. Besides, the structure is designed to take water 10 – 15 m below the surface level considering water quality problems caused by taking water from bottom inlet since there is 56 m elevation difference between maximum and minimum water levels.

Four gates (Gates No. 5, 6, 7 and 8), operated by crane, are equipped at 955 m, 965 m, 975 m and 985 m in water intake shaft (Shaft A) to make it possible to

obtain water from different elevations in accordance with the reservoir level. There also exists a gate (Gate 3) at the bottom inlet to benefit from dead volume while minimum reservoir level is experienced.

Shaft B, on the other hand, aims to transfer water from shaft A to pipeline at a maximum level of 960 m even if the reservoir level exceeds 960 m. In order to provide this, there is a hydraulic pressure reduction gate (Gate 4) between two shafts which was designed to be operated at partial openings in accordance with regulation of the level of the pressure reduction and desired discharges through the pipeline. For reservoir level between 955 – 965 m, a hydraulic gate (Gate 2) located between two shafts connects them each other. When the reservoir level drops below 955 m, the water is taken directly by opening Gate 3 at the bottom inlet. Finally, the hydraulic Gate 1 is located between shaft B and pipeline entrance. Appendix C shows the plan and sections views of Çamlıdere Dam intake tower.

5.2.3 Pipelines

The water conveyance line, which has a composite structure, consists of two tunnels in series one with diameter of 3.50 m and length of 7,100 m, another with 3.40 m diameter and 16,312 m length, prestressed concrete pipes (PCP) and steel pipes between tunnels and İvedik WTP with 2.20 m diameter. Also, there exist plenty of hydraulic devices equipped through the line. Figure 5.2 shows the profile of pipeline system.

Starting point of the existing conveyance line is the intake tower connected with T1 tunnel which is 3.50 m in diameter. The tunnel reaches Bayındır Creek valley near Alicin region at station 4+277 km and passes the creek with 295 m long steel pipes in 3.50 m diameter. At the end of the year 1987, 2.20 m diameter steel pipe has been adapted inside the tunnel due to leakage and subsidence of ground.

Therefore, in order to compensate the reduction of area at pipeline section, two more 2.20 m diameter steel pipes were connected to the tunnel from both sides and connected to 3500 mm diameter steel pipe at the end of the tunnel (Yüksel Proje Uluslararası A.Ş., 2004).

T2 tunnel, following T1 tunnel, is also 3500 mm in diameter with total length of 2,823 m. It starts at station 4+572 km. and ends at 7+395 km near Çeltikçi Village. At the exit of T2 tunnel, a trifurcation structure (see Figure (5.3)) is adapted that reduces diameter from Ø3500 mm to 3 no.s of Ø1600 mm. Ø1600 mm butterfly valves are equipped as pipe fracture safety devices (see Appendix D) on each pipe and then the diameter is enlarged to Ø2200 mm by a conical expansion part.

According to the master plan, it was planned to construct 3 pipelines between Çamlıdere Dam and İvedik WTP, and so, the first pipeline (Çamlıdere 1), which was composed of prestressed concrete pipes was constructed by DSİ and taken into operation in 1987. However, in accordance with the information obtained from the authorities during a visit to İvedik WTP in 22.08.2011, PCPs between T2 and T3 tunnels were replaced with steel pipes within the operation period until today. The second pipeline (Çamlıdere 2), on the other hand, was constructed completely with Ø2200 mm steel pipes by ASKİ and taken into operation in 2003.

After the exit of T2 tunnel, two pipelines pass Hamam Creek and Çamlıdere 1 and 2 pipelines reach T3 (Kınık) tunnel at station 14+201.14 km. Diameters of pipes are reduced to Ø1600 mm by conical contractions at trifurcation structure. Ø1600 mm diameter pipe fracture safety valves are also equipped at this location for maintenance and storage purposes. Then, the pipes are connected to Ø3400 mm steel pipe

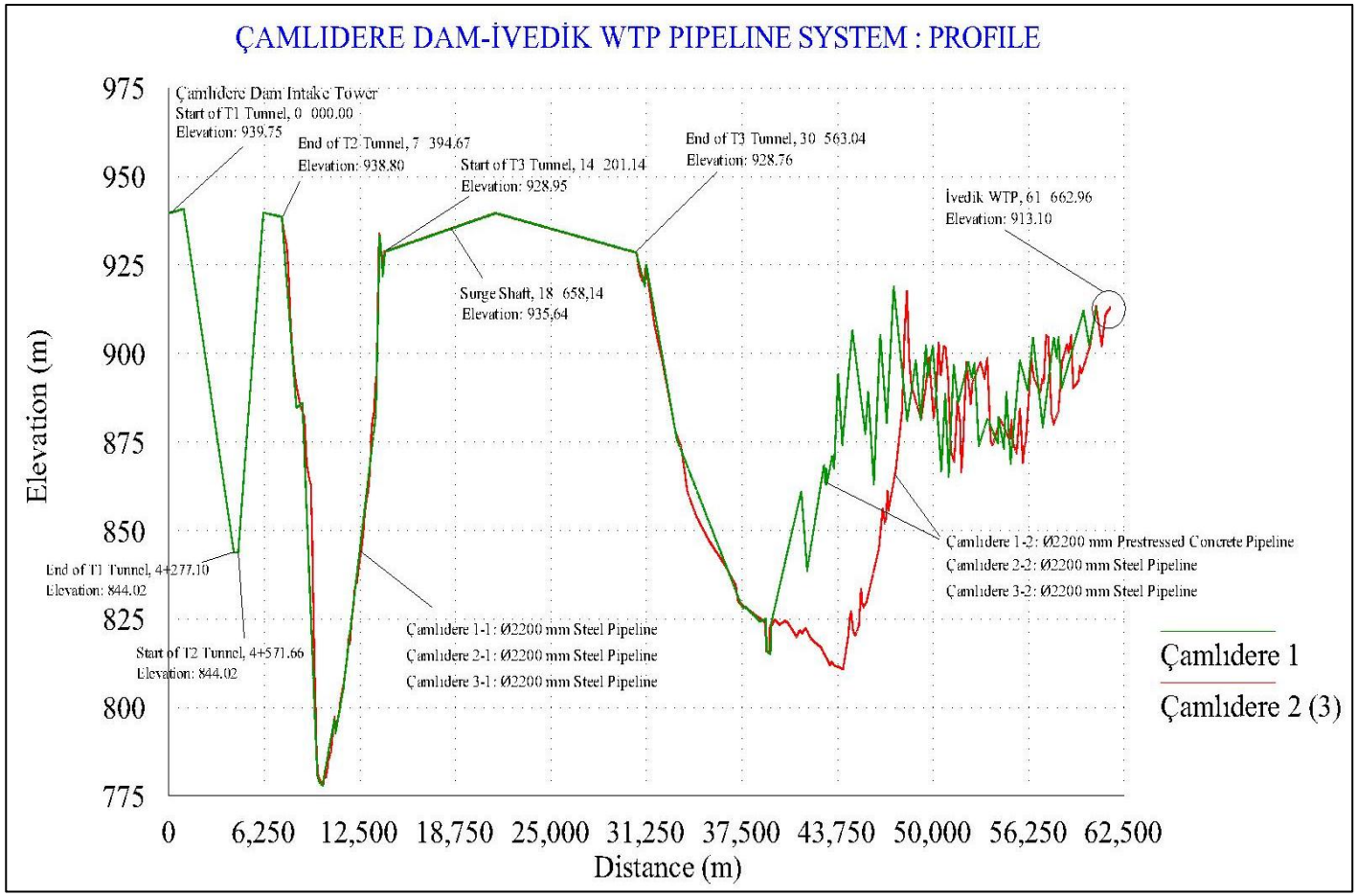

Figure 5.2 Çamlıdere Dam – IWTP pipeline system profile

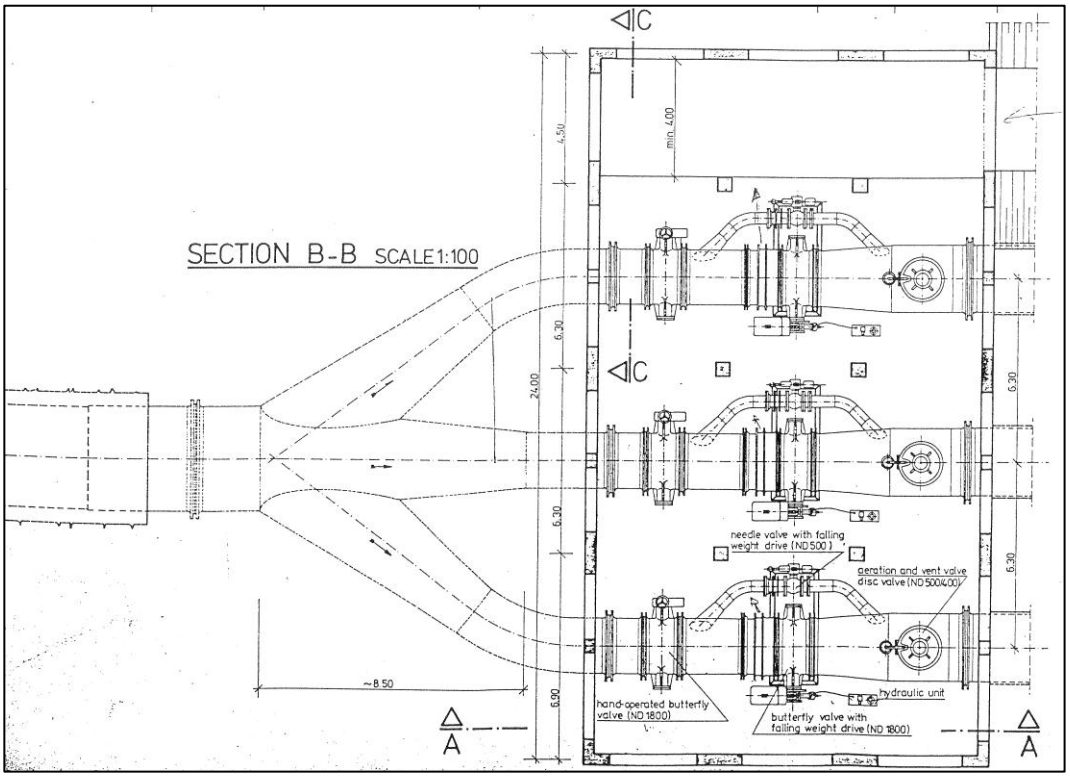

Figure 5.3 Trifurcation structure (Obermeyer Project Management, 1978)

T3 (Kınık) tunnel is 16,386 m long and 3400 mm in diameter. There is a 6 m diameter surge shaft 4,457 m after the start (18+658.14 km), and at the end of the tunnel, another steel trifurcation structure connects Ø3400 mm tunnel and three numbers of Ø1600 mm steel transition pipes. These pipes are also equipped with butterfly valves, and after these valves, the diameter is widened to Ø2200 mm again. Two existing lines constructed parallel to each other pass Ova Creek at station 60+740 km and 61+553 km respectively and enter İvedik WTP.

Finally, at the entrance of WTP, each line is divided into two branches with Ø1600 mm diameter by a steel bifurcation structure. The flow passing through the pipelines is controlled by two Larner-Johnson type needle valves for each line with dimensions of 1000x685x1000 mm. Figure 5.4 simply illustrates the inlet structure with Larner-Johnson (LJ) valves at İvedik WTP (see Appendix E for

pictures of İvedik WTP inlet structure). Entire pipeline system, apart from T3 tunnel, was designed regarding 970 m head. T3 tunnel, on the other hand, is able to handle 980 m head (Yüksel Proje Uluslararası A.Ş., 2004).

In addition to the existing components of the system, a third steel pipeline parallel to Çamlıdere 2 with Ø2200 mm diameter have been planned to be constructed for the future projections. For this reason, there exist trifurcations instead of bifurcations and third pipe fracture safety valves equipped at the start and end of tunnels. Also there exists a connection point at İvedik WTP for third pipeline. Details of pipelines and HAMMER inputs are given in Appendix F.

Table 5.1 Pipeline characteristics

Pipe Segment		Diameter (mm)	Length (m)	Material
T1 Tunnel		3,500	4,277	Conc,
T2 Tunnel		3,500	2,823	Conc,
Between T2-T3 Tunnels	Çamlıdere 1	2,200	6,807	Steel
	Çamlıdere 2	2,200	6,807	Steel
	Çamlıdere 3	2,200	6,807	Steel
T3 Tunnel		3,400	16,386	Conc,
Between T3 Tunnel – İvedik	Çamlıdere 1	2,200	30,178	PCP
	Çamlıdere 2	2,200	31,282	Steel
	Çamlıdere 3	2,200	31,282	Steel

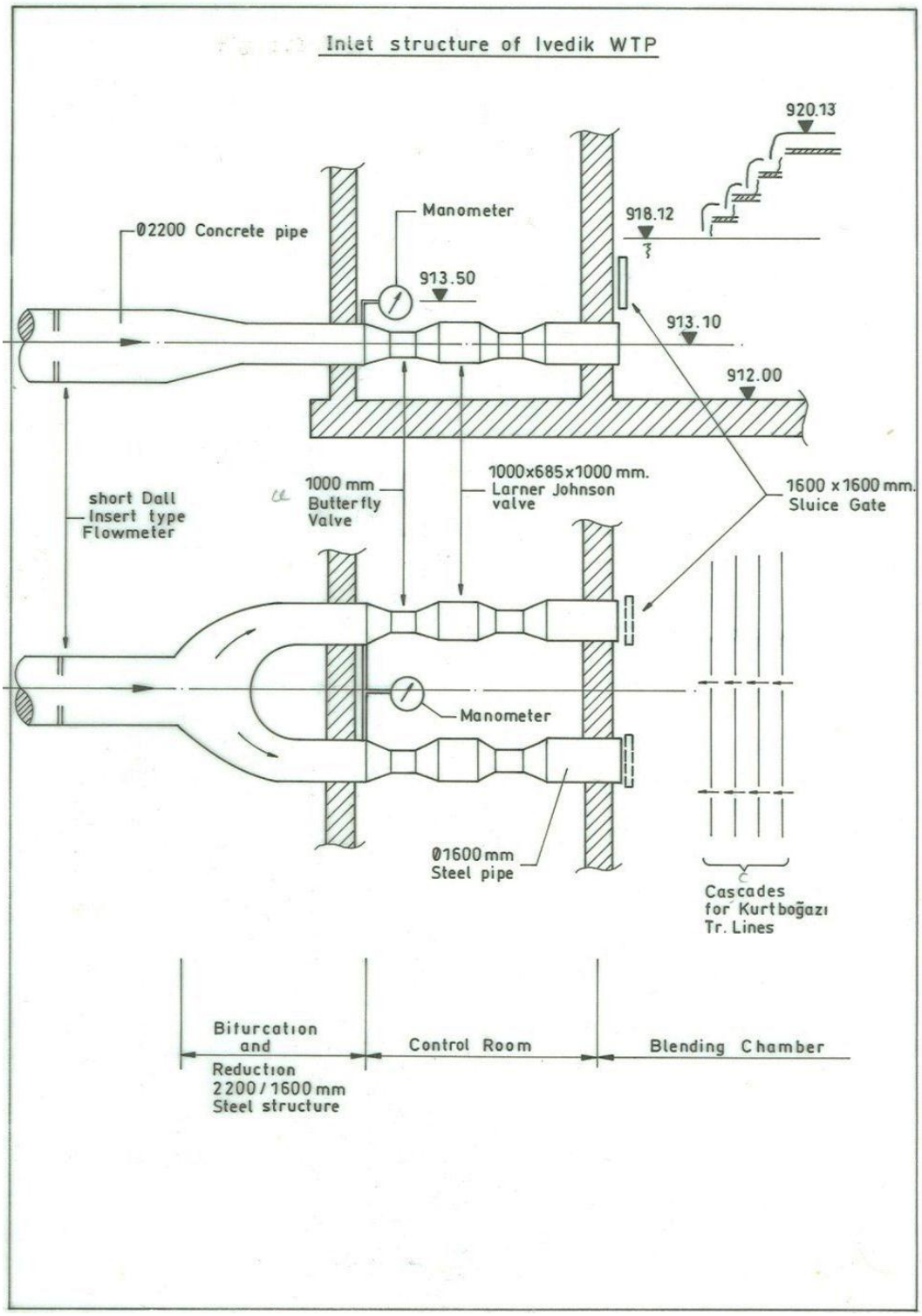

Figure 5.4 Simple sketch of inlet structure at IWTP (Bozkuş, 2008)

5.3 Hydraulic Losses

The hydraulic losses throughout the pipeline system can be examined in terms of major (friction) losses and minor (local) losses. Although, friction losses govern the entire head loss calculations due to the length of pipeline extending over 60 km, minor losses especially those of needle valves at the entrance of İvedik WTP cannot be ignored.

During steady – state and transient analyses, Darcy – Weisbach formula is set as a global friction method and friction losses are calculated by Eqn. 5.1 :

$$h_f = f\frac{L}{D}\frac{V^2}{2g} = \frac{8fL}{g\pi^2 D^5}Q^2 \tag{5.1}$$

It should be noted that Darcy – Weisbach friction coefficient, f, depends on relative roughness, ϵ/D, and Reynolds number ($Re = VD/\nu$). Within the previous works conducted on Çamlıdere Dam – İvedik WTP pipeline system, various friction coefficient values were selected for analyses. Darcy – Weisbach friction factor, f, was selected 0.012 for tunnels and 0.0125 for pipes which corresponds to $0.20\,mm$ roughness height during the analyses performed by OPM (1978). However, considering the passing years, these values considered very optimistic for analyses conducted by Bozkuş (1996) and were needed to be replaced with more realistic ones.

Bozkuş (1996) used $f = 0.012$ for Ø2200 mm steel pipes which corresponds to $0.25\,mm$ roughness height and $f = 0.0152$ for Ø2200 mm PCPs which corresponds to $0.70\,mm$ roughness height. For tunnels, various combinations of Manning roughness coefficient, n, have been tested for steady state analyses and $n = 0.014$ was selected for the transient computations performed by Bozkuş (2006). This value was described as the most accurate (Bozkuş, 2006) depending

on the comparison of flow computations by Yüksel Project (2004). Then, Manning roughness coefficient was converted into friction factor, f, and ended up with;

For T1 and T2 tunnels; $n = 0.014$; $D = 3500\,mm$; $f = 0.0239$

For T3 tunnel ; $n = 0.014$; $D = 3400\,mm$; $f = 0.0241$

The analyses performed in this study, on the other hand, only require roughness height values in order to calculate friction losses. Roughness heights for steel pipes and PCPs are defined $0.25\,mm$ and $0.70\,mm$ respectively. Besides, roughness height, ϵ, values for tunnels are converted from corresponding f values defined above by using Swamee-Jain equation given below:

$$f = \frac{1.325}{\left[\ln\left(0.27\left(\frac{\epsilon}{D}\right) + \frac{5.74}{Re^{0.9}}\right)\right]^2} \tag{5.2}$$

Therefore a general roughness height determined for tunnels in this study becomes,

$\epsilon = 7.42\,mm.$

Minor losses considered in this study are listed as follows:

- Entrance losses due to intake structure,
- Losses at the outlet of T1 tunnel due to contractions, expansions and bends,

- Losses due to trifurcation structures, contractions and expansions at this sections,
- Pipe fracture safety valve (Butterfly valves) losses,
- Exit losses at İvedik WTP,
- Larner-Johnson needle valve losses.

Minor loss expressions as a function in transmission line and hydraulic structures were calculated previously by Basmacı (1996) for each operating option and summarized on the table below:

Table 5.2 Minor loss expressions through the pipeline (Basmacı, 1996)

Item	Single Pipe	Double Pipe	Triple Pipe
	λQ^2		
Head loss at intake structure	$0.003336 Q^2$	$0.013344 Q^2$	$0.030024 Q^2$
Head loss at outlet of T1 tunnel due to reduction of pipe diameter	$0.005067 Q^2$	$0.020268 Q^2$	$0.045603 Q^2$
Head loss at flowmeter and bifurcation steel structure from Ø2200 to 1600 mm	$0.005877 Q^2$	$0.005877 Q^2$	$0.005877 Q^2$
Head loss at İvedik WTP inlet before LJ valve	$0.005312 Q^2$	$0.005312 Q^2$	$0.005312 Q^2$
Head loss at İvedik WTP inlet after LJ valve	$0.011039 Q^2$	$0.011039 Q^2$	$0.011039 Q^2$

In addition to minor losses listed above, head losses at Larner-Johnson needle valve, shown in Figure 5.5, were calculated in that study as follows:

Main formula for LJ valve for each line was taken as;

$$\frac{Q}{2} = C_D A\sqrt{2gH} \tag{5.3}$$

where

$Q/2$: Discharge passing through LJ valves (half of the flow), [m^3/s]

A : Area of valve throat, [m^2]

C_D : Coefficient of discharge for full opening, $C_D = 0.60$

H : Head at upstream of LJ valve, [m]

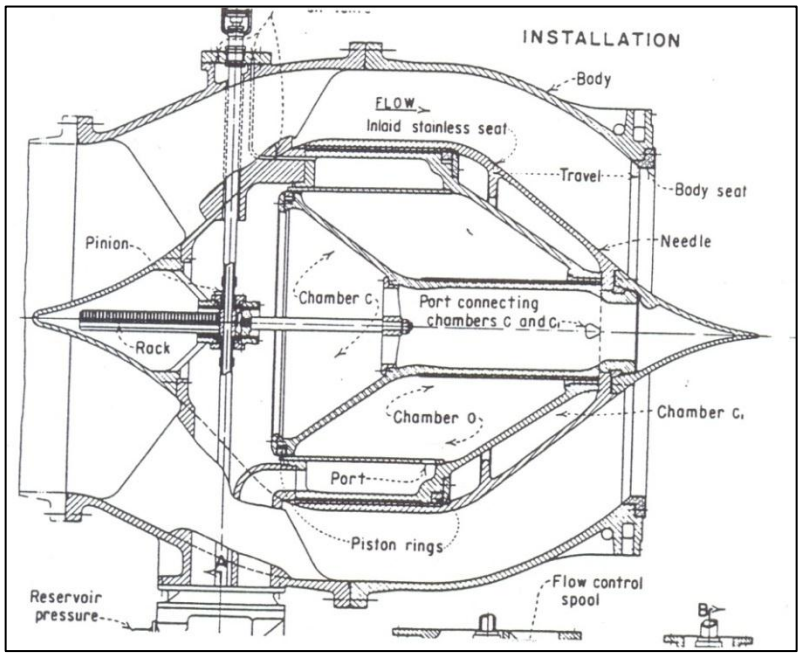

Figure 5.5 Larner – Johnson needle valve (Basmacı, 1996)

Therefore, solution for head loss in LJ valve to allow a definite discharge becomes;

$$H = \frac{Q^2}{4A^2{C_D}^2 2g} \tag{5.4}$$

Diameter of the LJ valve is 685 mm and, therefore, area of the valve throat is

$$A = \frac{\pi D^2}{4} = \frac{\pi(0.685)^2}{4} = 0.368529\ m^2$$

Finally, resultant head loss term at LJ valve has been denoted as,

$$H = 0.260613\ Q^2 \tag{5.5}$$

In order to perform an analysis by HAMMER, abovementioned head loss equations need to be converted into head loss coefficients and assigned to related pipes and hydraulic devices in the model. In other words, model should be calibrated by calculating corresponding head loss coefficients.

General term for minor loss is;

$$h_m = K\frac{V^2}{2g} = K\frac{Q^2}{2gA^2} \tag{5.6}$$

where K is minor loss coefficient.

$H = h_m$

and therefore,

$$\lambda\, Q^2 = K\frac{Q^2}{2gA^2} \tag{5.7}$$

By canceling squares of discharges and rearranging terms, head loss coefficient, K, can be written as;

$$K = \lambda\, 2g\, A^2 \tag{5.8}$$

As a result, converted head loss coefficient by using Eqn. 5.8 can be listed as follows;

Table 5.3 Converted minor loss coefficient

Item	Minor loss coefficient, K
Head loss at intake structure	6.059
Head loss at outlet of T1 tunnel due to reduction of pipe diameter	9.202
Head loss at flowmeter and bifurcation steel structure from Ø2200 to 1600 mm	1.666
Head loss at İvedik WTP inlet before LJ valve	1.506
Head loss at İvedik WTP inlet after LJ valve	0.219

Minor loss coefficients above are assigned to related pipes in the model. Additionally, head loss coefficient for pipe fracture safety valves (butterfly valves) is set to 0.20 for fully open initial condition (Thorley, 2004) and Figure 5.6 shows the head loss coefficients assigned in the analysis model for different

spindle movements of butterfly valves ranging from Ø1200 mm to Ø1800 mm in diameter.

Nevertheless, discharge coefficient value for HAMMER differs from the conventional C_D value. Although discharge equation is written as,

$$Q = C_D A \sqrt{2gH} \tag{5.9}$$

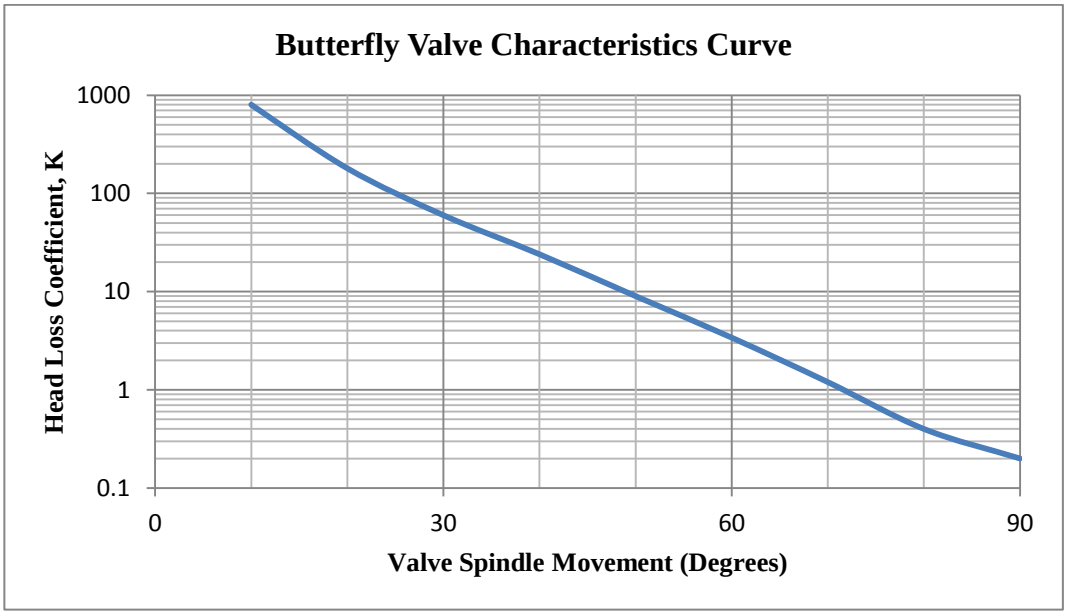

Figure 5.6 Butterfly valve head loss coefficient curve (Thorley, 2004).

Discharge coefficient term in HAMMER is,

$$C_V = C_D A \sqrt{2g} \tag{5.10}$$

and thus discharge equation becomes,

$$Q = C_V \sqrt{H} \tag{5.11}$$

Solving Eqn. 5.10 for discharge coefficient that HAMMER requires results in

$$C_V = 0.368529\ (0.60)\ \sqrt{2g} = 0.979$$

which is assigned to LJ valves in the model for fully open initial condition. Table 5.4 shows valve characteristics input of LJ valves for different openings and Figure 5.7 shows the characteristics curve of LJ valves:

Table 5.4 Valve characteristics of LJ needle valves (Basmacı, 1996)

Valve opening (%)	Discharge Coefficient, C_D	Relative Discharge Coefficient (%)
0	0	0
10	0.100	16.67
20	0.190	31.67
30	0.265	44.17
40	0.330	55.00
50	0.388	64.67
60	0.440	73.33
70	0.487	81.17
80	0.528	88.00
90	0.565	94.17
100	0.600	100.00

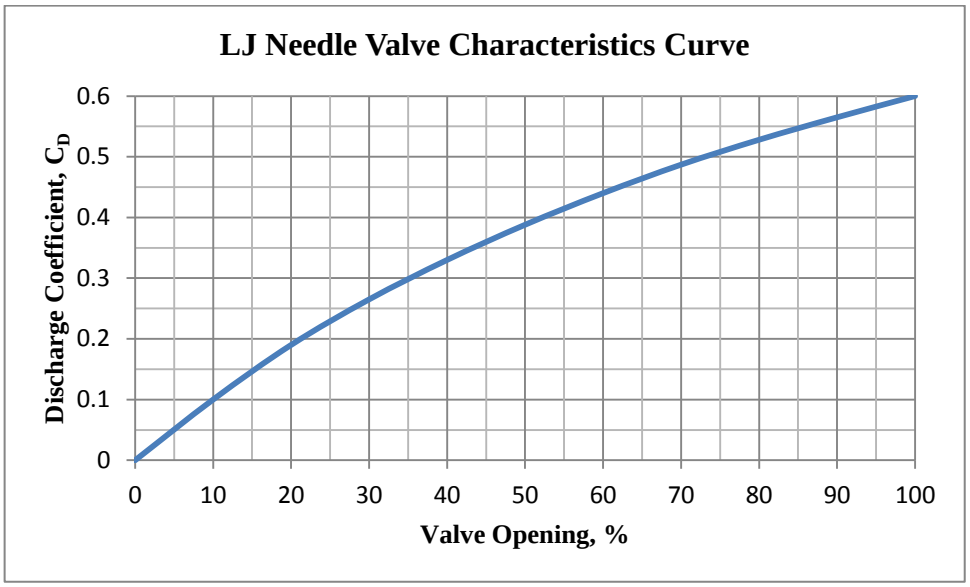

Figure 5.7 LJ needle valve discharge coefficient curve (Basmacı, 1996)

5.4 Computation of Steady-State Discharges

Steady – state discharges passing through Çamlıdere Dam-İvedik WTP pipeline were first calculated by OPM (1978) and concluded as 7.35 m^3/s for single line, 14.5 m^3/s for double line and 21 m^3/s for triple line. The points here that should be taken into consideration are that the water surface elevation in the reservoir while calculating the discharges was taken as 970 m and Darcy – Weisbach friction factor for tunnels and pipes were taken 0.012 and 0.0125 respectively. On the other hand, the friction factors used in discharge computations were suggested to be larger than those of OPM in another study conducted by Bozkuş (1996). Additionally, Bozkuş (2006) came up with that the water surface elevation inside shaft B of intake structure must be 960 m and never be allowed to exceed 965 m which is the maximum allowable water surface elevation for safety of pipeline

system, since the pipeline was designed in accordance with the maximum head of 970 m (Yüksel Proje Uluslararası A.Ş., 2004). Thereby, the discharge values obtained in Bozkuş's study were lower than those of OPM.

A comprehensive study conducted by Yüksel Project (2004) demonstrates discharges as 5.90 m^3/s, 11.20 m^3/s and 14.50 m^3/s respectively for single, double and triple lines for 965 m water surface elevation. Results obtained by Yüksel Project (2004) and Bozkuş (1996) for same water surface elevations seem close. Fortunately, after calibration of analysis model, steady-state discharges computed in this study in a range of 945 – 970 m WSE at intake structure exhibit approximate values comparing with those of Yüksel Project (2004) and Bozkuş (1996). The results of steady-state discharge computations are listed and compared with previous works in Table 5.5.

Table 5.5 Comparison of steady – state discharges

WSE at Intake	WSE at İvedik	Single Pipeline (Çamlıdere 1)				Double Pipeline (Çamlıdere 1+2)				Triple Pipeline (Çamlıdere 1+2+3)			
Z1 (m)	Z2 (m)	Q (m^3/s)				Q (m^3/s)				Q (m^3/s)			
		OPM (1978)	Bozkuş (1996)	Yüksel (2004)	Sakabaş (2011)	OPM (1978)	Bozkuş (1996)	Yüksel (2004)	Sakabaş (2011)	OPM (1978)	Bozkuş (1996)	Yüksel (2004)	Sakabaş (2011)
945.00	918.12	-	4.57	3.90	4.56	-	8.28	6.40	8.30	-	10.89	7.50	10.79
946.00	918.12	-	4.66	-	4.65	-	8.43	-	8.46	-	11.09	-	10.99
947.00	918.12	-	4.74	-	4.73	-	8.58	-	8.61	-	11.29	-	11.18
948.00	918.12	-	4.82	-	4.81	-	8.73	-	8.76	-	11.49	-	11.38
949.00	918.12	-	4.90	-	4.89	-	8.88	-	8.91	-	11.68	-	11.57
950.00	918.12	-	4.98	4.50	4.97	-	9.02	8.60	9.05	-	11.86	10.50	11.76
951.00	918.12	-	5.06	-	5.05	-	9.16	-	9.19	-	12.05	-	11.94
952.00	918.12	-	5.13	-	5.13	-	9.30	-	9.33	-	12.23	-	12.12
953.00	918.12	-	5.21	-	5.20	-	9.43	-	9.47	-	12.41	-	12.30
954.00	918.12	-	5.28	-	5.28	-	9.57	-	9.61	-	12.59	-	12.48
955.00	918.12	-	5.36	5.00	5.35	-	9.70	9.50	9.74	-	12.76	12.35	12.65
956.00	918.12	-	5.43	-	5.42	-	9.83	-	9.87	-	12.93	-	12.82
957.00	918.12	-	5.50	-	5.49	-	9.96	-	10.00	-	13.10	-	12.99

Table 5.5 cont.'d

WSE at Intake	WSE at İvedik	Single Pipeline (Çamlıdere 1)				Double Pipeline (Çamlıdere 1+2)				Triple Pipeline (Çamlıdere 1+2+3)			
Z1 (m)	Z2 (m)	Q (m^3/s)				Q (m^3/s)				Q (m^3/s)			
		OPM (1978)	Bozkuş (1996)	Yüksel (2004)	Sakabaş (2011)	OPM (1978)	Bozkuş (1996)	Yüksel (2004)	Sakabaş (2011)	OPM (1978)	Bozkuş (1996)	Yüksel (2004)	Sakabaş (2011)
958.00	918.12	-	5.57	-	5.57	-	10.09	-	10.13	-	13.27	-	13.16
959.00	918.12	-	5.64	-	5.64	-	10.21	-	10.26	-	13.43	-	13.33
960.00	918.12	-	5.71	5.50	5.70	-	10.34	10.40	10.39	-	13.60	13.50	13.49
961.00	918.12	-	5.78	-	5.77	-	10.46	-	10.51	-	13.76	-	13.65
962.00	918.12	-	5.84	-	5.84	-	10.58	-	10.63	-	13.92	-	13.81
963.00	918.12	-	5.91	-	5.91	-	10.70	-	10.75	-	14.08	-	13.97
964.00	918.12	-	5.98	-	5.97	-	10.82	-	10.87	-	14.23	-	14.12
965.00	918.12	-	6.04	5.90	6.04	-	10.94	11.20	10.99	-	14.39	14.50	14.28
966.00	918.12	-	6.10	-	6.10	-	11.05	-	11.11	-	14.54	-	14.43
967.00	918.12	-	6.17	-	6.17	-	11.17	-	11.23	-	14.69	-	14.58
968.00	918.12	-	6.23	-	6.23	-	11.28	-	11.34	-	14.84	-	14.73
969.00	918.12	-	6.29	-	6.29	-	11.39	-	11.46	-	14.99	-	14.88
970.00	918.12	7.35	6.35	-	6.35	14.50	11.51	-	11.57	21.00	15.13	-	15.03

5.5 Pressure Wave Speed and Characteristic Time

The wave speeds for T1, T2 and T3 tunnels and Ø2200 pipes are selected in accordance with the study conducted by Bozkuş (2006) and the others are calculated by using *wave speed calculator* tool of the software.

Table 5.6 Wave Speed Along Pipeline

Pipe	Diameter (mm)	Material	Wave Speed, a (m/s)
T1 Tunnel	3,500	Concrete	1,230.00
Alicin Cross between T1-T2	3,500	Steel	1,033.64
T2 Tunnel	3,500	Concrete	1,230.00
T3 Tunnel	3,400	Concrete	1,240.00
Çamlıdere 1-2-3	2,200	PCP	1,280.00
	2,200	Steel	1,198.00
Trifurcations	1,600	Steel	1,076.31

In order to satisfy courant condition ($\Delta t = \Delta x/a$), characteristic time is calculated considering the shortest pipe and wave speed correspond to it. The shortest pipe is 6.70 m steel branch of trifurcation structure and wave speed defined for this pipe is 1,076.31 m/s. Therefore, the maximum characteristic time along pipeline is;

$$\Delta t = \frac{6{,}70}{1{,}076.31} = 0.0062\ s$$

However, 0.005 s assigned to analysis model in order to follow results at every 1 second easily.

5.6 Scenarios Used in Transient Analyses

The transient scenarios used in this study are selected considering the studies carried out by Yüksel Project (2004) and Bozkuş (2006) in order to compare the results by HAMMER. 10 operation alternatives are selected for water hammer analyses including the future planned third pipeline and the numbering of alternatives is designated as those of Yüksel Project (2004) and Bozkuş's study (2006) to compare results easily. These operation alternatives are repeated for different valve closure principles demonstrated in Appendix G regarding mainly WSE of 960 m at intake structure since the WSE must be retained around this level and never be allowed to exceed 965 m (Yüksel Proje Uluslararası A.Ş., 2004). It must be noted that the pipeline system is designed in accordance with the 970 m pressure head. Also water surface elevations of 965 m and 970 m are carried out for single, double and triple pipeline operation alternatives in order to investigate system in an overloading case. Additionally, closure of the Larner – Johnson valves from 45% partial opening is observed to investigate pressure rises in a partial opening case.

10 operation alternatives considered in this study are listed as follows:

1. Çamlıdere 1
2. Çamlıdere 2
3. Çamlıdere 1+2
4. Çamlıdere 1+2+3
7. Çamlıdere 2 between T2-T3 — Çamlıdere 2+3 between T3-WTP
8. Çamlıdere 1+2 between T2-T3 — Çamlıdere 1+2+3 between T3-WTP
9. Çamlıdere 1+2 between T2-T3 — Çamlıdere 1 between T3-WTP
10. Çamlıdere 1+2 between T2-T3 — Çamlıdere 2 between T3-WTP
11. Çamlıdere 1+2+3 between T2-T3 — Çamlıdere 1+2 between T3-WTP
12. Çamlıdere 1+2+3 between T2-T3 — Çamlıdere 2+3 between T3-WTP

5.7 Results of Water Hammer Analyses

The results of water hammer analyses in this study are given in Tables from 5.7 to 5.15. Tables consist of 5 main columns. 1st column represents the number of analysis and some of them are divided into two rows in order to compare the common results computed by Bozkuş (2006). 2nd column represents the scenario ran for that analysis. 3rd column corresponds to the valve closure principle applied for simulation of the transient event in the governing scenario. 4th column which is divided into three parts illustrates the start and end node of analysis and initial conditions of those. Finally, the 5th column illustrates the peak pressure head due to water hammer computed at end node for governing analysis.

5.7.1 Analysis No. 1 – 10: WSE of 960 m & 30 min. Valve Closure

These analyses are performed considering 30 minutes of closure duration suggested by Yüksel Project (2004) for LJ needle valves at İvedik WTP. Scenario names are to be inspired from those of Bozkuş's study (2006) in order to compare them easily. For example, scenario "B1-30" gives the water hammer results of Çamlıdere 1 pipeline. To explain, "B" stands for "Base" analyses in which the valve operations are implemented at İvedik WTP while "1" stands for the operation alternative listed in section 5.4.2, and "30" represents the valve closure duration in minutes. Governing valve closure principle for analyses 1 – 10 is "VALVE30" and the details of that are given in Appendix G. Similarly, "B3-30" represents the 30 minutes of closure duration for Larner-Johnson needle valves at the end of Çamlıdere 1 and Çamlıdere 2 pipelines reaching İvedik WTP. Table 5.7 Results of water hammer analyses (1)shows the results of analyses 1-10 in a tabular form.

Table 5.7 Results of water hammer analyses (1)

Analysis No.		Scenario	Valve Closure Principle	Initial Conditions			Results at IWTP
				Res. WSE (m)	HGL at IWTP (m)	Q (m^3/s)	Peak HGL Elev. (m)
1.	*Bozkuş*	B1-30	VALVE30	*960.20*	*926.10*	*5.50*	*966.56*
	Sakabaş			960.20	926.67	5.72	965.39
2.	*Bozkuş*	B2-30	VALVE30	*960.12*	*926.10*	*6.50*	*967.83*
	Sakabaş			960.12	927.42	5.97	965.41
3.	*Bozkuş*	B3-30	VALVE30	*960.10*	*926.40*	*10.40*	*967.85*
	Sakabaş			960.10	925.57	10.40	966.53
4.	Sakabaş	B4-30	VALVE30	960.00	923.05	13.49	967.54
5.	Sakabaş	B7-30	VALVE30	960.00	923.73	9.27	967.23
6.	Sakabaş	B8-30	VALVE30	960.00	923.13	12.92	967.99
7.	*Bozkuş*	B9-30	VALVE30	*960.31*	*926.20*	*6.00*	*967.23*
	Sakabaş			960.31	927.52	6.00	965.11
8.	*Bozkuş*	B10-30	VALVE30	*960.75*	*926.30*	*7.05*	*969.11*
	Sakabaş			960.75	928.57	6.32	965.71
9.	Sakabaş	B11-30	VALVE30	960.00	925.98	10.68	966.13
10.	Sakabaş	B12-30	VALVE30	960.00	925.84	10.87	966.14

5.7.2 Analysis No. 11 – 20: WSE of 960 m & 45 min. Valve Closure

These analyses are repeated for same operation alternatives. The only difference for these analyses is the 45 minutes valve closure duration for LJ needle valves at İvedik WTP. This duration was declared by the technical staff at İvedik WTP as the governing closure principle for LJ valves in a technical visit in 22.08.2011. Also Bozkuş (2006) considered this duration in his computations. The results of

these analyses are compared with those of previous analyses to discuss (see Table 5.8).

Table 5.8 Results of water hammer analyses (2)

Analysis No.		Scenario	Valve Closure Principle	Initial Conditions			Results at IWTP
				Res. WSE (m)	HGL at IWTP (m)	Q (m^3/s)	Peak HGL Elev. (m)
11.	*Bozkuş*	B1-45	VALVE45	*960.20*	*926.10*	*5.50*	*962.24*
	Sakabaş			960.20	926.67	5.72	965.73
12.	*Bozkuş*	B2-45	VALVE45	*960.12*	*926.10*	*6.50*	*962.66*
	Sakabaş			960.12	927.42	5.97	965.73
13.	*Bozkuş*	B3-45	VALVE45	*960.10*	*926.40*	*10.40*	*962.68*
	Sakabaş			960.10	925.57	10.40	966.94
14.	Sakabaş	B4-45	VALVE45	960.00	923.59	13.49	968.00
15.	Sakabaş	B7-45	VALVE45	960.00	923.73	9.27	967.65
16.	Sakabaş	B8-45	VALVE45	960.00	923.13	12.92	968.49
17.	*Bozkuş*	B9-45	VALVE45	*960.31*	*926.20*	*6.00*	*962.33*
	Sakabaş			960.31	927.52	6.00	965.41
18.	*Bozkuş*	B10-45	VALVE45	*960.75*	*926.30*	*7.05*	*963.17*
	Sakabaş			960.75	928.57	6.32	966.00
19.	Sakabaş	B11-45	VALVE45	960.00	925.98	10.68	966.50
20.	Sakabaş	B12-45	VALVE45	960.00	925.84	10.87	966.50

5.7.3 Analysis No. 21 – 30: WSE of 960 m & 6.5 min. Valve Closure

These analyses are performed to investigate the amount of pressure rises under a fast closure, caused by an operation failure, of LJ needle valves at İvedik WTP and the results are given in Table 5.10. The importance of investigating fast closure is to observe pressure rises whether they are in a range that the system can handle in terms of strength and, if these are beyond acceptable values (970 m pressure head), to suggest a closure principle for pipe fracture safety valves in order to protect remaining system. Minimum closure duration for LJ needle valves is obtained from the specs of manufacturer as 6.5 minutes and, therefore, "VALVE6.5" (see Appendix G) shows the linear closure of valves in 6.5 minutes.

Table 5.9 Results of water hammer analyses (3)

Analysis No.		Scenario	Valve Closure Principle	Initial Conditions			Results at IWTP
				Res. WSE (m)	HGL at IWTP (m)	Q (m^3/s)	Peak HGL Elev. (m)
21.	Sakabaş	B1-6.5	VALVE6.5	960.20	926.67	5.72	1,068.03
22.	Sakabaş	B2-6.5	VALVE6.5	960.12	927.42	5.97	1,068.44
23.	Sakabaş	B3-6.5	VALVE6.5	960.10	924.81	10.40	1,074.16
24.	Sakabaş	B4-6.5	VALVE6.5	960.00	923.05	13.49	1,068.40
25.	Sakabaş	B7-6.5	VALVE6.5	960.00	923.73	9.27	1,063.94
26.	Sakabaş	B8-6.5	VALVE6.5	960.00	923.13	12.92	1,065.47
27.	Sakabaş	B9-6.5	VALVE6.5	960.31	927.52	6.00	1,066.16
28.	Sakabaş	B10-6.5	VALVE6.5	960.75	928.57	6.32	1,068.19
29.	Sakabaş	B11-6.5	VALVE6.5	960.00	925.18	10.68	1,074.18
30.	Sakabaş	B12-6.5	VALVE6.5	960.00	925.84	10.87	1,073.54

5.7.4 Analysis No. 31 – 60: WSE of 960 m & Closure of PFSV's

The scenarios designated by "U" in Tables 5.10, 5.11 and 5.12 are performed in order to observe the pressure rises due to the closure of pipe fracture safety valves (PFSV) separately in case of a failure along pipeline. These valves are located at the end of T2 tunnel and at the entrance and end of T3 tunnel. In order to perform these analyses, *discharge to atmosphere tool* is utilized at İvedik WTP to simulate pipe fracture since the discharge does not reach LJ valves. "T3C" represents end of T3 tunnel while "T3G" and "T2C" stand for entrance of T3 tunnel and end of T2 tunnel respectively.

The closure duration for valves is selected as 30 minutes which is previously observed and suggested as a safe operation condition by Bozkuş (2006) for single and double pipelines. In these analyses, peak pressures caused by 30 minutes closure duration for PFSV's is compared with those of Bozkuş's study (2006) and checked for third pipeline. the valve closure principle for PFSV's is "FAST3". In this principle, 70% closure is implemented in 600 s and remaining 30% closure is completed in 1200 s (see Appendix G).

Table 5.10 Results of water hammer analyses (4)

Analysis No.		Scenario	Valve Closure Principle	Initial Conditions			Results at the End of T3
				Res. WSE (m)	HGL at the End of T3 (m)	Q (m^3/s)	Peak HGL Elev. (m)
31.	*Bozkuş*	U1-T3C	FAST3	*960.00*	*950.12*	*5.50*	*962.18*
	Sakabaş			960.00	948.17	6.77	963.23
32.	*Bozkuş*	U2-T3C	FAST3	*960.00*	*948.54*	*6.50*	*962.47*
	Sakabaş			960.00	946.83	7.16	962.93
33.	Sakabaş	U3-T3C	FAST3	960.00	938.99	12.07	963.67
34.	Sakabaş	U4-T3C	FAST3	960.00	931.21	15.29	964.89
35.	Sakabaş	U7-T3C	FAST3	960.00	931.59	10.55	964.50
36.	Sakabaş	U8-T3C	FAST3	960.00	929.52	14.55	965.31
37.	*Bozkuş*	U9-T3C	FAST3	*960.00*	*954.30*	*6.00*	*962.37*
	Sakabaş			960.00	952.52	7.18	963.32
38.	*Bozkuş*	U10-T3C	FAST3	*960.00*	*952.32*	*7.05*	*962.63*
	Sakabaş			960.00	951.51	7.65	963.64
39.	Sakabaş	U11-T3C	FAST3	960.00	940.77	12.48	963.92
40.	Sakabaş	U12-T3C	FAST3	960,00	939,94	12.75	964.05

Table 5.11 Results of water hammer analyses (5)

Analysis No.		Scenario	Valve Closure Principle	Initial Conditions			Results at the Start of T3
				Res. WSE (m)	HGL at the Start of T3 (m)	Q (m^3/s)	Peak HGL Elev. (m)
41.	*Bozkuş*	U1-T3G	FAST3	*960.00*	*951.93*	*5.50*	*961.30*
	Sakabaş			960.00	951.45	6.77	961.06
42.	*Bozkuş*	U2-T3G	FAST3	*960.00*	*951.02*	*6.50*	*961.38*
	Sakabaş			960.00	950.51	7.16	961.07
43.	Sakabaş	U3-T3G	FAST3	960.00	949.40	12.07	961.40
44.	Sakabaş	U4-T3G	FAST3	960.00	947.91	15.29	961.74
45.	Sakabaş	U7-T3G	FAST3	960.00	939.55	10.55	961.08
46.	Sakabaş	U8-T3G	FAST3	960.00	944.65	14.55	961.41
47.	*Bozkuş*	U9-T3G	FAST3	*960.00*	*956.43*	*6.00*	*961.35*
	Sakabaş			960.00	956.21	7.18	961.40
48.	*Bozkuş*	U10-T3G	FAST3	*960.00*	*955.19*	*7.05*	*961.48*
	Sakabaş			960.00	955.70	7.65	961.40
49.	Sakabaş	U11-T3G	FAST3	960.00	951.91	12.48	961.74
50.	Sakabaş	U12-T3G	FAST3	960.00	951.56	12.75	961.74

Table 5.12 Results of water hammer analyses (6)

Analysis No.		Scenario	Valve Closure Principle	Initial Conditions			Results at the End of T2
				Res. WSE (m)	HGL at the End of T2 (m)	Q (m^3/s)	Peak HGL Elev. (m)
51.	*Bozkuş*	U1-T2C	FAST3	*960.00*	*958.58*	*5.50*	*960.65*
	Sakabaş			960.00	958.40	6.77	960.34
52.	*Bozkuş*	U2-T2C	FAST3	*960.00*	*958.07*	*6.50*	*960.64*
	Sakabaş			960.00	958.21	7.16	960.86
53.	Sakabaş	U3-T2C	FAST3	960.00	954.92	12.07	960.63
54.	Sakabaş	U4-T2C	FAST3	960.00	951.86	15.29	960.95
55.	Sakabaş	U7-T2C	FAST3	960.00	956.12	10.55	960.91
56.	Sakabaş	U8-T2C	FAST3	960.00	952.63	14.55	960.63
57.	*Bozkuş*	U9-T2C	FAST3	*960.00*	*958.33*	*6.00*	*960.65*
	Sakabaş			960.00	958.20	7.18	960.63
58.	*Bozkuş*	U10-T2C	FAST3	*960.00*	*957.75*	*7.05*	*960.61*
	Sakabaş			960.00	957.96	7.65	960.64
59.	Sakabaş	U11-T2C	FAST3	960.00	954.57	12.48	960.95
60.	Sakabaş	U12-T2C	FAST3	960.00	954.34	12.75	960.95

5.7.5 Analysis No. 61 – 64: WSE of 965 m & 45 min. Valve Closure

These four analyses denoted by "W" are performed to investigate peak pressure heads at İvedik WTP for single, double and triple pipelines under 965 m water surface elevation at intake structure which was defined as the maximum level that should not be exceeded for safe operation conditions. For this reason, "VALVE45" is assigned as closure principle of LJ valves in terms of reflecting the actual case and the results of analyses are given in Table 5.13.

Table 5.13 Results of water hammer analyses (7)

Analysis No.		Scenario	Valve Closure Principle	Initial Conditions			Results at IWTP
				Res. WSE (m)	HGL at IWTP (m)	Q (m^3/s)	Peak HGL Elev. (m)
61.	Sakabaş	W1-45	VALVE45	965.00	927.65	6.04	970.78
62.	Sakabaş	W2-45	VALVE45	965.00	928.52	6.31	970.91
63.	Sakabaş	W3-45	VALVE45	965.00	926.45	10.99	972.17
64.	Sakabaş	W4-45	VALVE45	965.00	924.25	14.28	973.44

5.7.6 Analysis No. 65 – 69: WSE of 970 m & 45 min. Valve Closure

Additionally, these five analyses denoted by "X" are performed to investigate peak pressure heads at İvedik WTP for single, double and triple pipelines under WSE of 970 m at intake structure which was performed by OPM in 1978 for a single pipeline. Analysis No. 65 is the comparison of 33 minutes valve closure duration (VALVE33) suggested by OPM (1978) for a single pipeline. In this principle, 80% of the valve is closed in 720 seconds and closure of remaining 20% is completed in 1260 seconds. Remaining analyses are performed considering "VALVE45" closure principle of LJ valves in terms of reflecting the actual case and results are given in Table 5.14.

Table 5.14 Results of water hammer analyses (8)

Analysis No.		Scenario	Valve Closure Principle	Initial Conditions			Results at IWTP
				Res. WSE (m)	HGL at IWTP (m)	Q (m^3/s)	Peak HGL Elev. (m)
65.	OPM	X1-33	VALVE33	970.00	928.07	7.35	976.21
	Sakabaş			970.00	928.67	6.35	975.11
66.	Sakabaş	X1-45	VALVE45	970.00	928.67	6.35	976.00
67.	Sakabaş	X2-45	VALVE45	970.00	929.64	6.64	976.11
68.	Sakabaş	X3-45	VALVE45	970.00	927.35	11.57	977.43
69.	Sakabaş	X4-45	VALVE45	970.00	924.91	15.03	978.86

5.7.7 Analysis No. 70 – 73: WSE of 960 m & 45% Partial Opening

These four analyses denoted by "P_{45}" are performed to investigate peak pressure heads along Çamlıdere 1 and Çamlıdere 2 (3) pipelines resulted from closure of LJ valves at İvedik WTP from 45% partial opening under WSE of 960 m at intake structure which was defined as the maximum level that should not be exceeded for safe operation conditions. Here, "P_{45}" stands for 45% partial opening. Currently, 2700 seconds (45 min.) closure duration is utilized for LJ valves to close them from fully open case. However, in these analyses, 55% of the valves are assumed to be closed in 1065 seconds linearly and remaining 45% of the valve opening is assumed to be closed in 1635 seconds (~27 min.) in two stages regarding "VALVE45" closure principle. The valve opening reduces from 45% to 22.5 % in 435 seconds and from 22.5% to 0% in 1200 seconds. For this reason, "VALVE27" is assigned as closure principle of LJ valves in terms of reflecting the actual case.

Table 5.15 Results of water hammer analyses (9)

Analysis No.		Scenario	Valve Closure Principle	Initial Conditions			Results at IWTP
				Res. WSE (m)	HGL at IWTP (m)	Q (m^3/s)	Peak HGL Elev. (m)
70.	Hammer	P_{45}1-27	VALVE27	960.00	935.46	4.88	965.35
71.	Hammer	P_{45}2-27	VALVE27	960.00	936.57	5.04	965.54
72.	Hammer	P_{45}9-27	VALVE27	960.00	936.67	5.05	964.89
73.	Hammer	P_{45}10-27	VALVE27	960.00	937.93	5.22	965.06

5.8 Discussion of Water Hammer Analyses Results

Valve operations along the Çamlıdere Dam – İvedik WTP pipeline system are the most important fact in terms of triggering the excessive pressure rises or water hammer. Therefore, valve closure principle and duration govern the amount of pressure rise in corresponding analysis.

Water hammer analyses 1-10 are performed in order to investigate pipeline system under 30 minutes closure duration of Larner-Johnson needle valves at İvedik WTP, which was suggested by Yüksel Project (2004). This closure duration is also performed by Bozkuş (2006) for single and double pipelines. In this study, results of common analyses are compared with previous works and new results are observed including third pipeline.

"VALVE30" principle, which is two phase closure duration, governs these analyses. 80% of valve closes in 700 s and closure of remaining 20% is completed in 1100 s.

Analyses results illustrate that 30 minutes closure duration causes approximately 40 m pressure head rise at IWTP. While the piezometric head is around 965-966 m for single and double lines, this value rises up to 967.50 m when the combinations of third pipeline are taken into account. For example, peak HGL elevations are 965.39 m (ΔH=38.72 m) for single pipeline (B1-30), 966.53 m (ΔH=40.96 m) for double pipelines (B3-30) and 967.54 m (ΔH=44.49 m) for triple pipelines (B4-30). Figure 5.8 demonstrates the evolution of HGL at İvedik WTP for single, double and triple lines within 2000 s. At the end of the first phase (700^{th} s) all pipelines experience first peak piezometric head and the maximum HGL is reached at complete closure (1800^{th} s). After completion of closure pressure wave starts to oscillate.

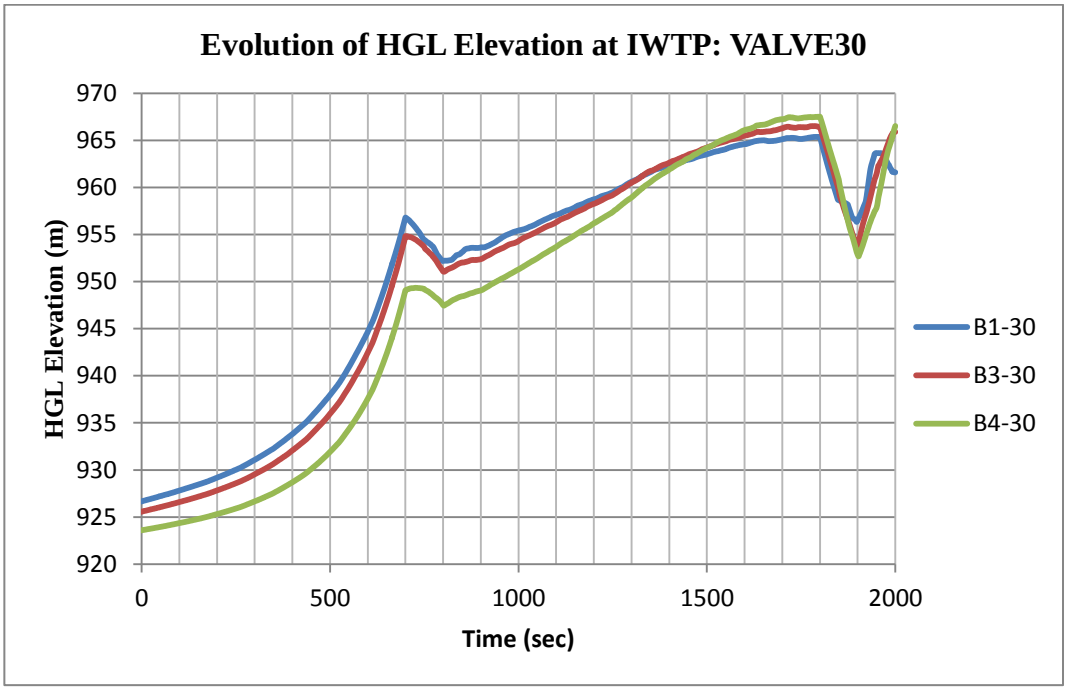

Figure 5.8 Comparison of HGL elevations for "VALVE30" closure

The maximum HGL elevation value for these analyses is observed under scenario B4-30 at the end of Çamlıdere 1 pipeline. Figure 5.9 shows the maximum and minimum HGL elevations reached along Çamlıdere 1 profile. Also, Figure 5.10 illustrates the flow and HGL time – history of İvedik-1 node at the end of Çamlıdere 1 pipeline under scenario B4-30. Evaluating the common scenarios performed by Bozkuş (2006) previously, it can be observed that the peak piezometric heads computed at the end of pipelines for scenarios B1-30, B2-30 and B3-30 are close to each other. On the other hand, peak HGL elevations computed for scenarios B9-30 and B10-30 are lower than those of computed by Bozkuş (2006). For instance, the peak HGL elevations computed by Sakabaş and Bozkuş for scenario B9-30 are 965.23 m and 967.23 m respectively. The reason for that can be explained in terms of accuracy of models since the characteristic time for computations is defined as 0.005 seconds while it is defined 6 seconds by Bozkuş (2006).

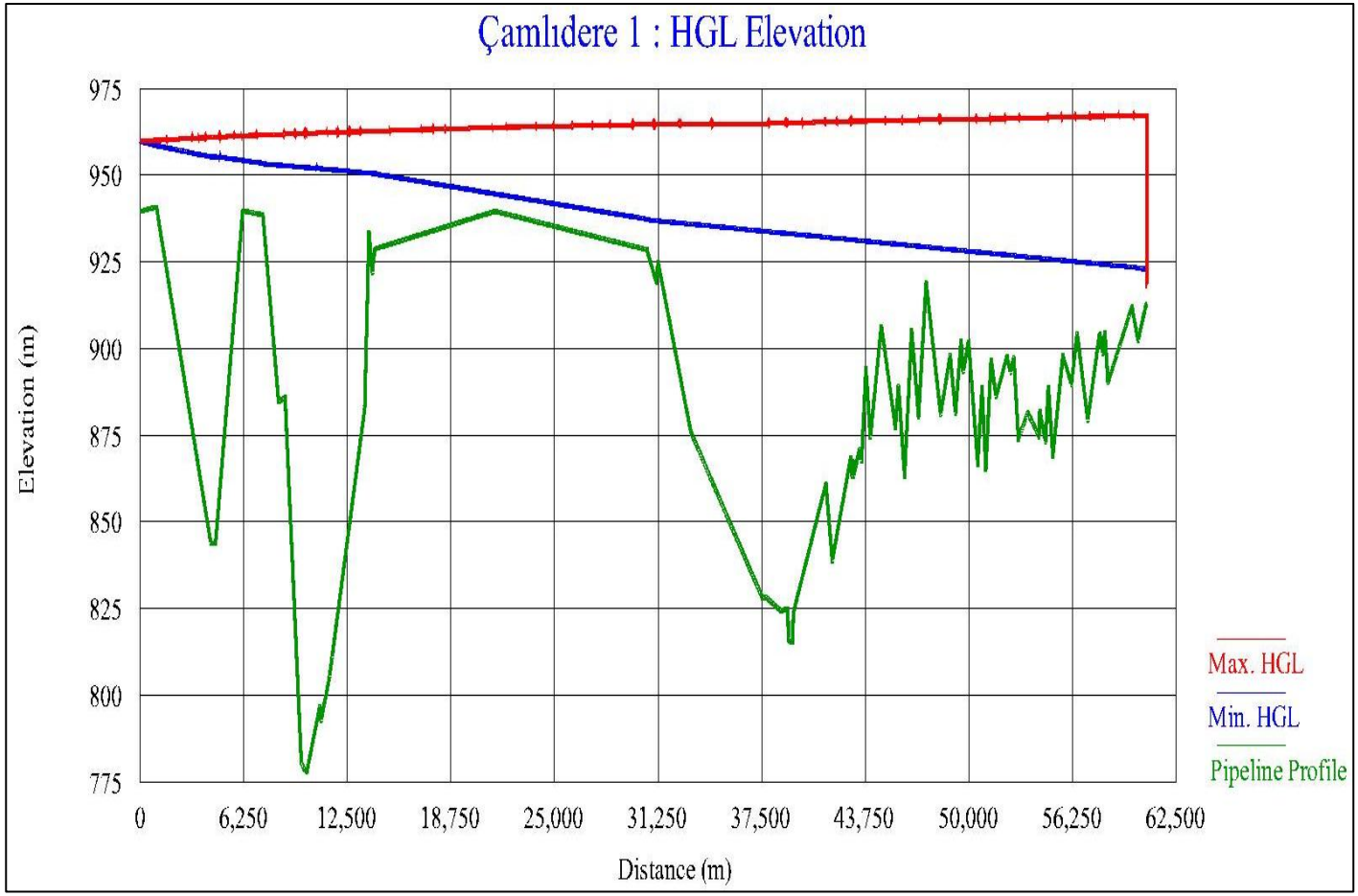

Figure 5.9 Max. and min. HGL envelopes of Çamlıdere 1 (Scn.: B4-30)

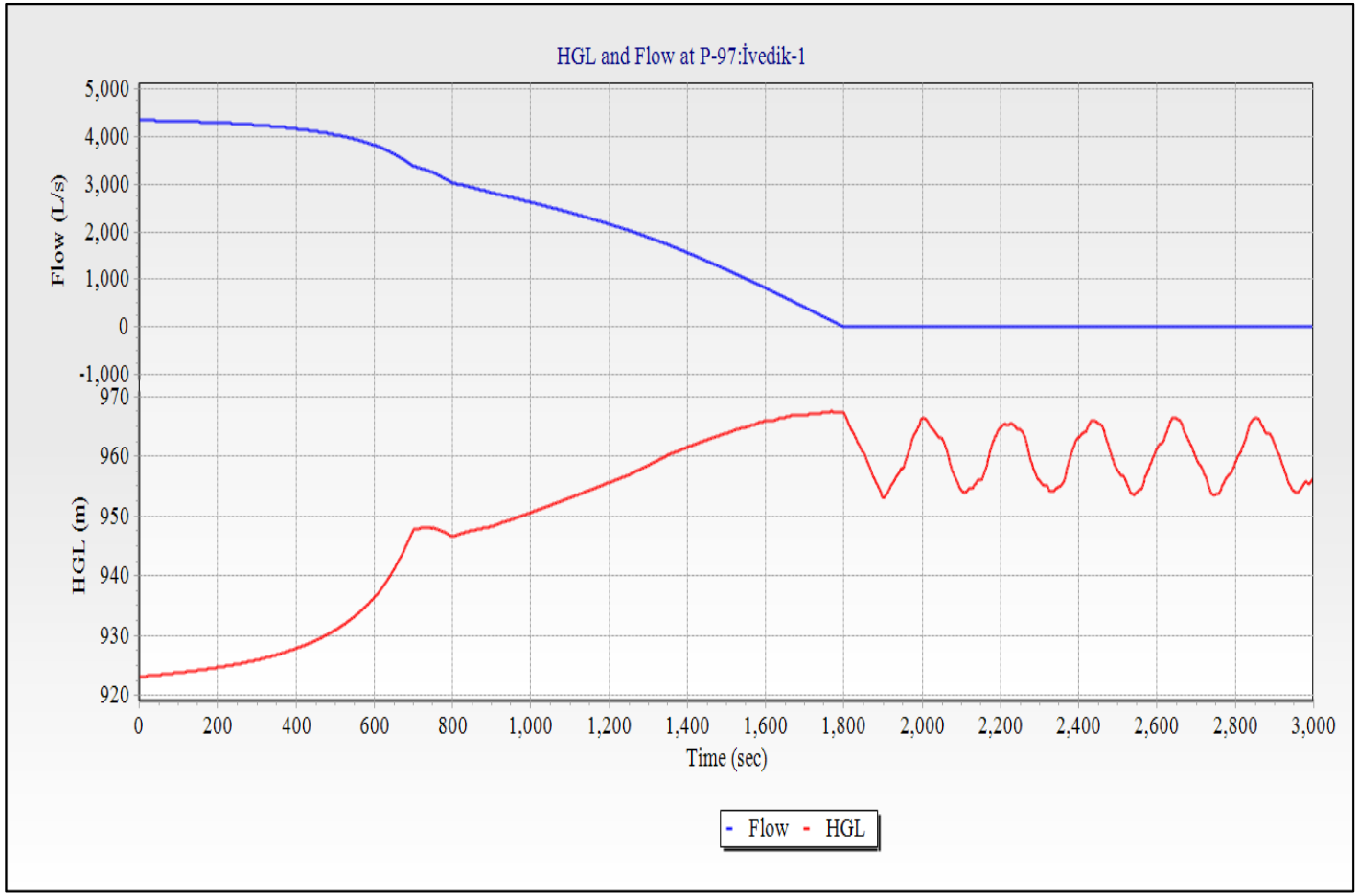

Figure 5.10 Variation of flow and HGL at IWTP entrance (Scn.: B4-30)

Analyses 11-20 are important in terms of observing peak HGL elevations at İvedik WTP since they illustrate the results of 45 minutes valve closure duration which is currently implemented by the operators work in IWTP. Governing valve closure principle for these scenarios is "VALVE45" which stands for 77.5% reduction in valve opening in 1,500 s and 2,700 s for total closure.

Contrary to expectations, peak HGL elevations computed are not lower than those of 30 minutes closure duration. Comparing the results of 30 and 45 minutes closure durations, the only difference is observed in terms of the value and time of the first peak HGL elevation obtained, since the first phase of closure is retarded (see Figure 5.11).

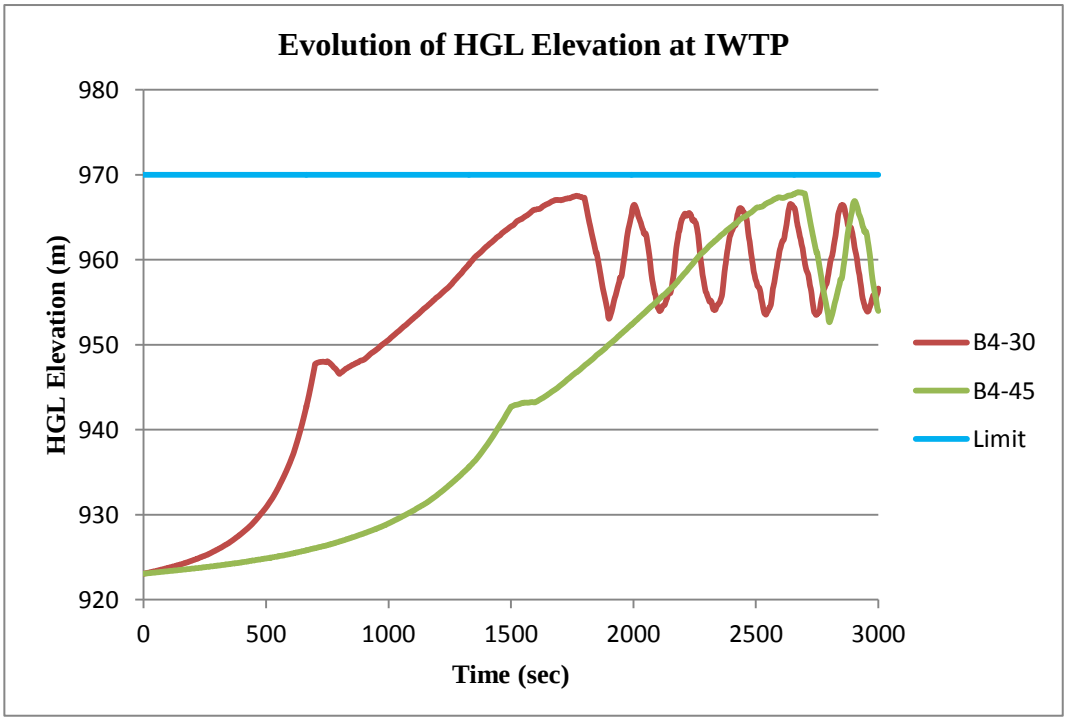

Figure 5.11 Comparison of HGL at IWTP under scenarios B4-30 and B4-45

The peak HGL elevations are computed as 965.73 m (ΔH=39.06 m) for single pipeline (B1-45), 966.94 m (ΔH=41.37 m) for double pipelines (B3-45) and 968.00 m (ΔH=44.41 m) for triple pipelines (B4-30).

The HGL elevations at İvedik WTP during closure are illustrated in Figure 5.12 for single, double and triple pipelines.

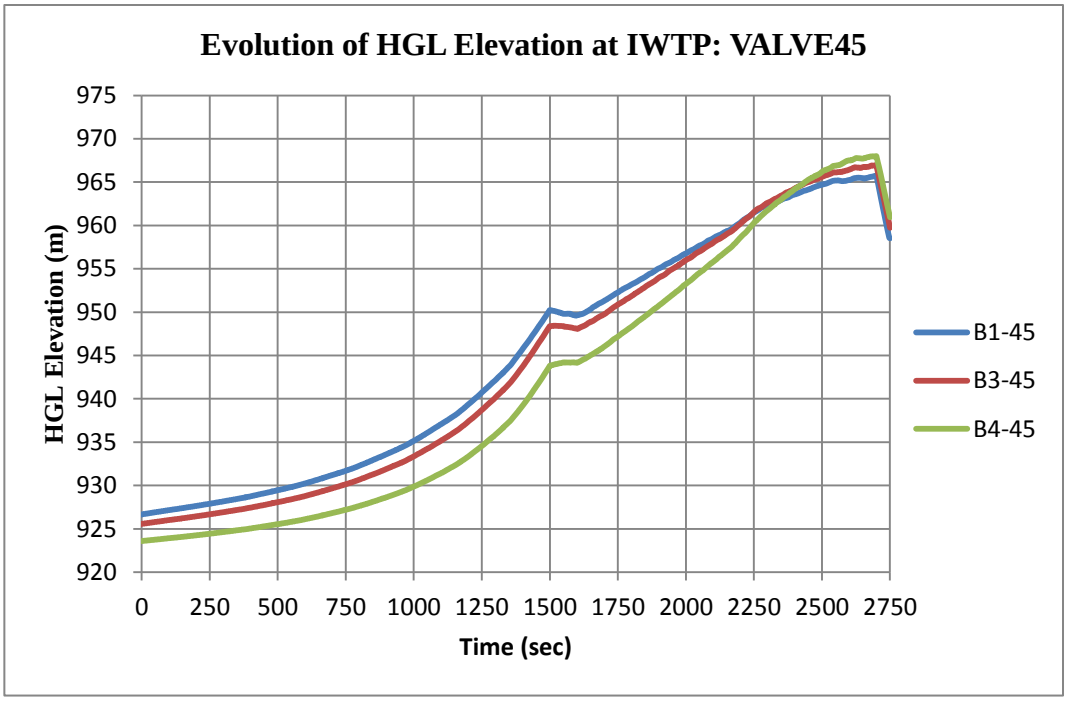

Figure 5.12 Comparison of HGL elevations for "VALVE45" closure

Obviously, maximum piezometric head value for these analyses is observed under scenario B4-45 (Triple pipelines) at the end of Çamlıdere 2 pipeline. Figure 5.13 shows the evolution of HGL elevations along Çamlıdere 2 profile due to 45 min. closure duration of LJ valves at IWTP. Also, Figure 5.14 illustrates the flow and HGL time – history of İvedik-2 node at the end of Çamlıdere 2 pipeline under scenario B4-45.

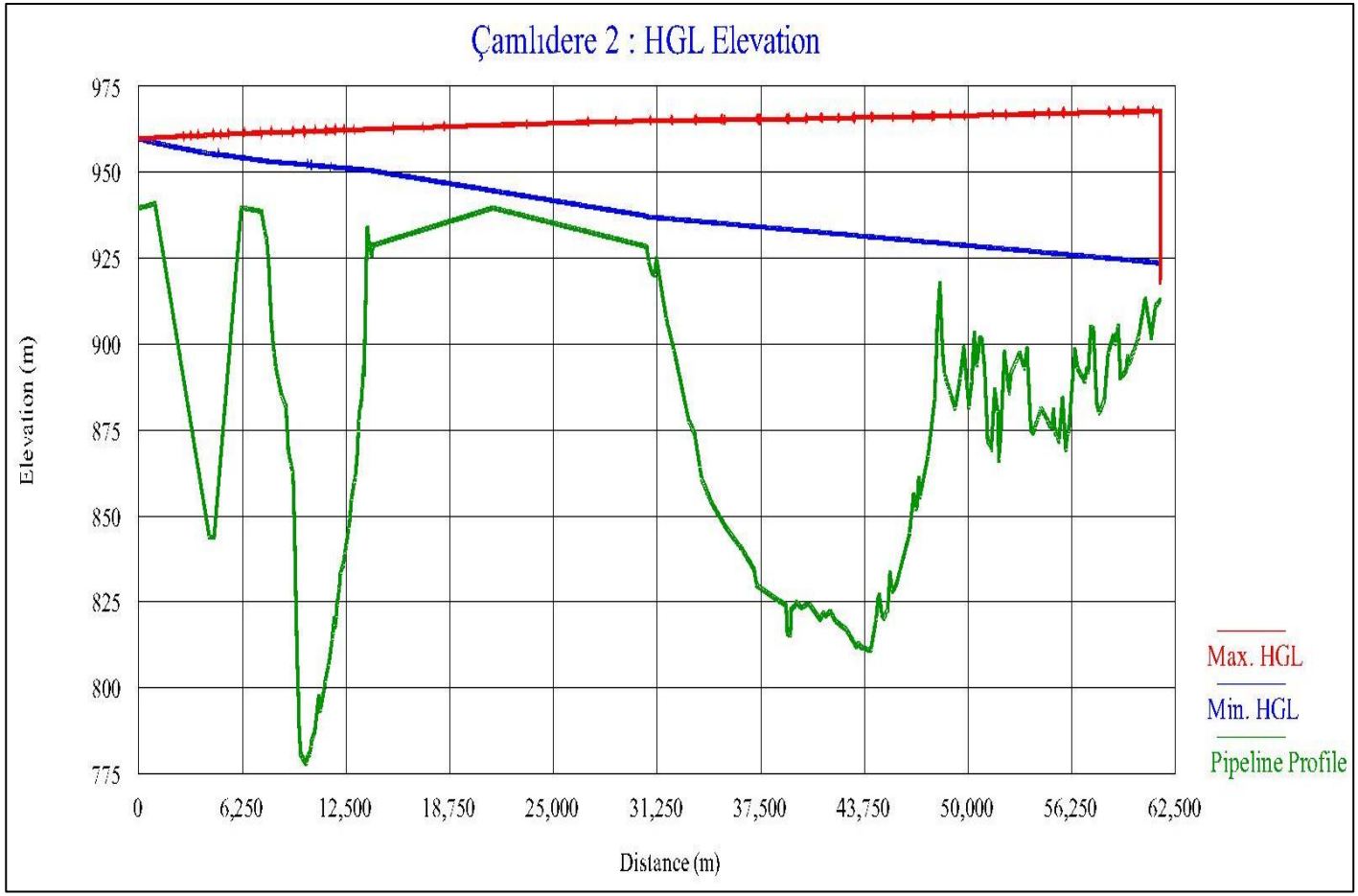

Figure 5.13 Max. and min. HGL envelopes of Çamlıdere 2 (Scn.: B4-45)

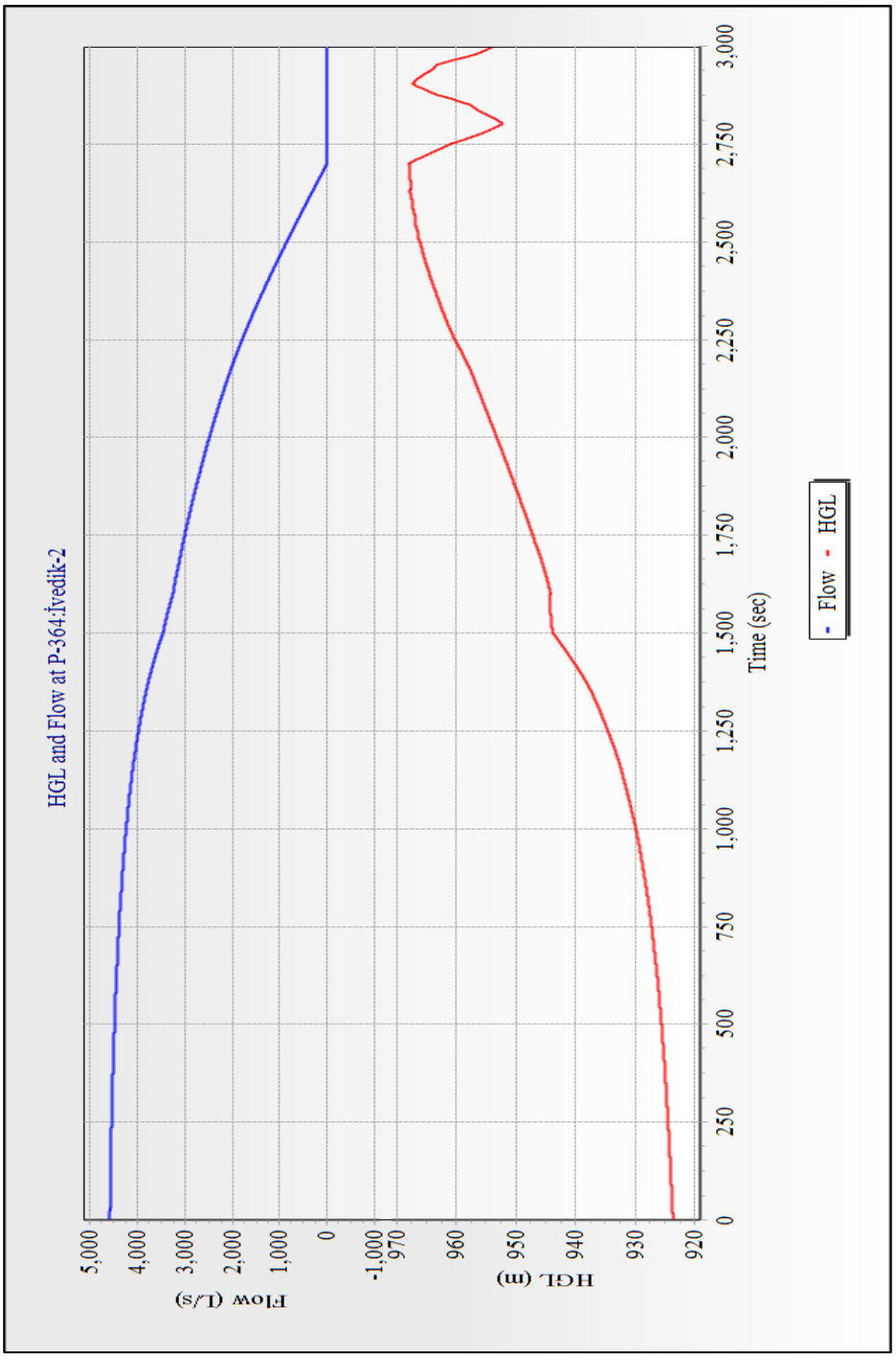

Figure 5.14 Variation of flow and HGL at IWTP entrance (Scn.: B4-45)

Analyses 21-30 stand for a fast closure of Larner-Johnson needle valves at İvedik WTP. It is important to perform a fast closure case in terms of the amount of pressure rises whether they are in an acceptable range. “VALVE6.5” represents the 6.5 minutes one-phase linear closure duration which is the minimum value for Larner-Johnson needle valves.

As it can be seen from the results given in Table 5.9, the case of an operational mistake causing a fast closure results in tremendous pressure rises across LJ valves. To illustrate, peak HGL elevation for single pipeline (B1-6.5) is 1,068.03 m (ΔH=140.36 m), 1,074.16 m (ΔH=149.35 m) for double pipelines (B3-6.5) and 1,068.40 m (ΔH=145.35 m) for triple pipelines (B4-6.5).

However, the highest HGL elevation is obtained in scenario B11-6.5 in which Çamlıdere 1+2+3 are in use between T2 and T3 tunnels and Çamlıdere 1+2 between T3 tunnel and İvedik WTP. The peak HGL elevation experienced by LJ valves is 1,074.18 m which corresponds to 149 m pressure head rise. Figure 5.15 shows the maximum and minimum HGL elevations experienced by Çamlıdere 1 pipeline.

System experiences negative pressures at T3 tunnel and some locations downstream of T3 tunnel as well as high pressure rises. Also, Figure 5.16 illustrates the HGL and flow time – history of LJ valve at the end of Çamlıdere 1 pipeline.

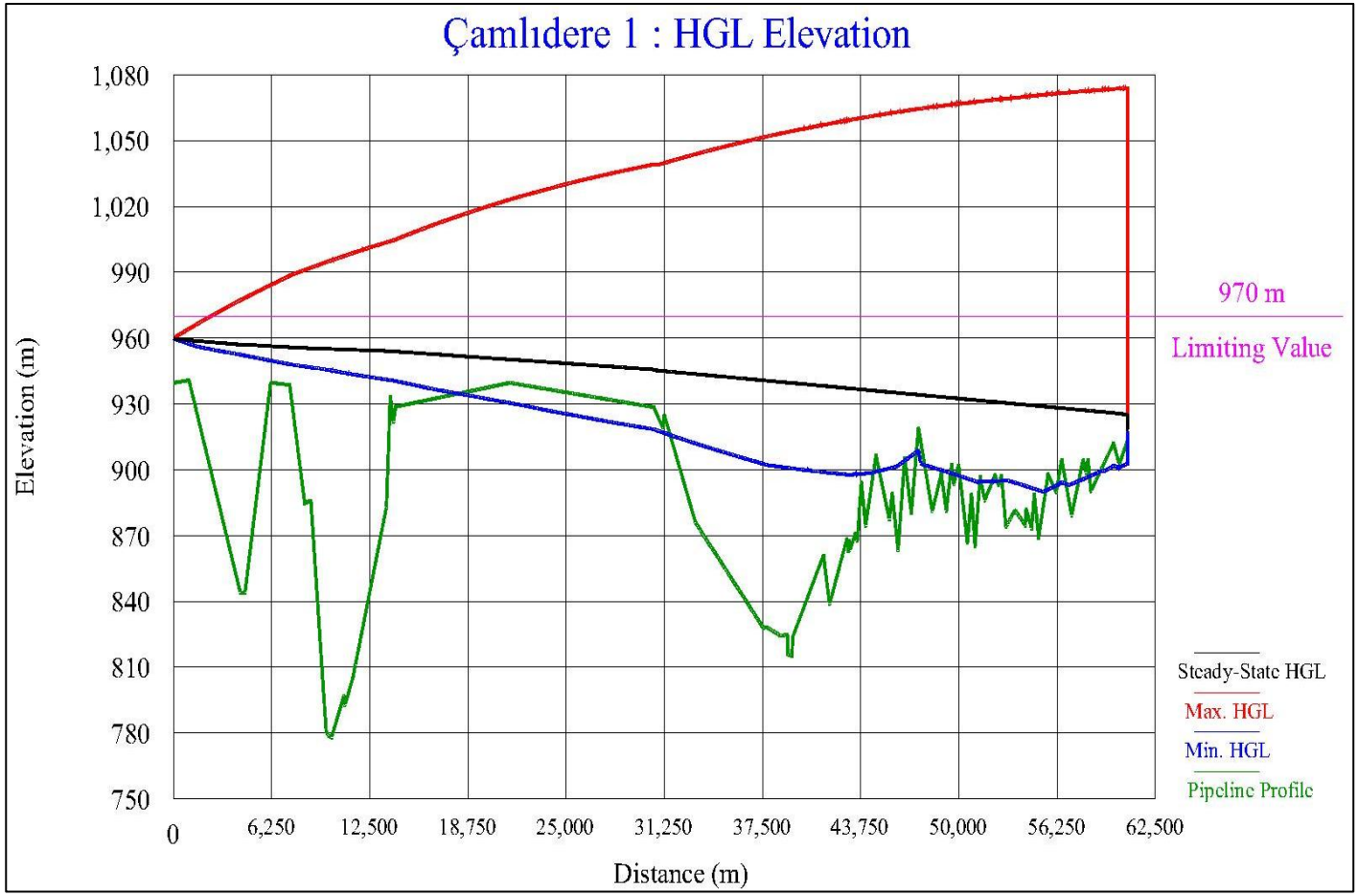

Figure 5.15 Max. and min. HGL envelopes of Çamlıdere 1 (Scn.: B11-6.5)

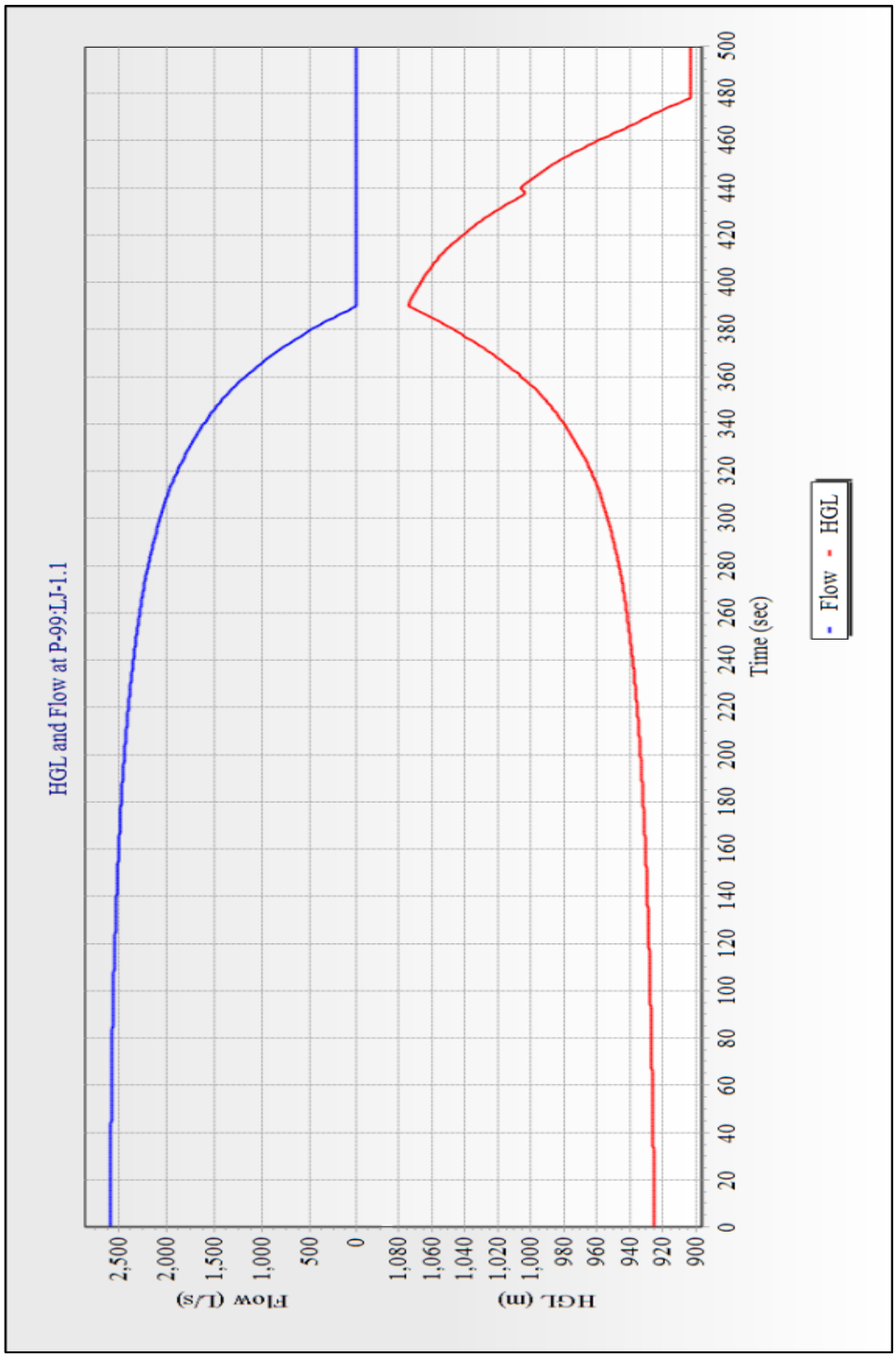

Figure 5.16 Variation of flow and HGL at IWTP entrance (Scn.: B11-6.5)

The case of a pipe fracture at downstream end of pipeline is investigated under analyses 31-60. Analyses denoted by "T3C" correspond to closure of PFSV's at the end of T3 tunnel in 30 minutes (see FAST3 closure principle in Appendix G) and results are given in Table 5.10. Thereby, comparing the common scenarios with Bozkuş's study, close results are obtained in terms of peak pressures.

Referring to the scenario U4-T3C in which the maximum piezometric head is obtained, Figure 5.17 shows maximum and minimum HGL elevations along Çamlıdere 1 pipeline, and flow and HGL time – history of end node of T3 tunnel is presented in Figure 5.18. For this scenario, the HGL elevation and discharge are computed as 931.25 m and 15.29 m^3/s respectively in steady – state condition and 964.89 m peak HGL elevation (ΔH=33.68 m) is obtained at the end of 30 minutes closure.

Similarly, the results of closure of PFSV's at the entrance of T3 tunnel denoted by "T3G" are given in Table 5.11. At this node, fortunately, transient analysis results are below 970 m limiting HGL. For instance, the maximum HGL elevation occurred in triple pipeline alternative as it is expected and it is 961.74 m corresponding to 13.93 m pressure rise since the steady – state HGL elevation is 947.91 m and discharge is 15.29 m^3/s. Figure 5.19 exhibits the hydraulic grade line along pipeline and pressure drop at the downstream of PFSV at the entrance of T3 tunnel can be observed easily. Also, evolution of the peak piezometric head is illustrated in Figure 5.20.

Finally, the result obtained at the exit of T2 tunnel denoted by "T2C" for all operation alternatives are below 970 m limiting HGL. Maximum piezometric head obtained under scenario U4-T2C is 960.95 m which is corresponding to 9.09 m pressure head rise at that point. Figures 5.21 and 5.22 exhibit the HGL along Çamlıdere 1 profile, and flow and HGL time – history at T2 tunnel exit respectively. Expected oscillation of the HGL elevation after complete closure of LJ valve at 1800^{th} second can be observed from Figure 5.22 easily.

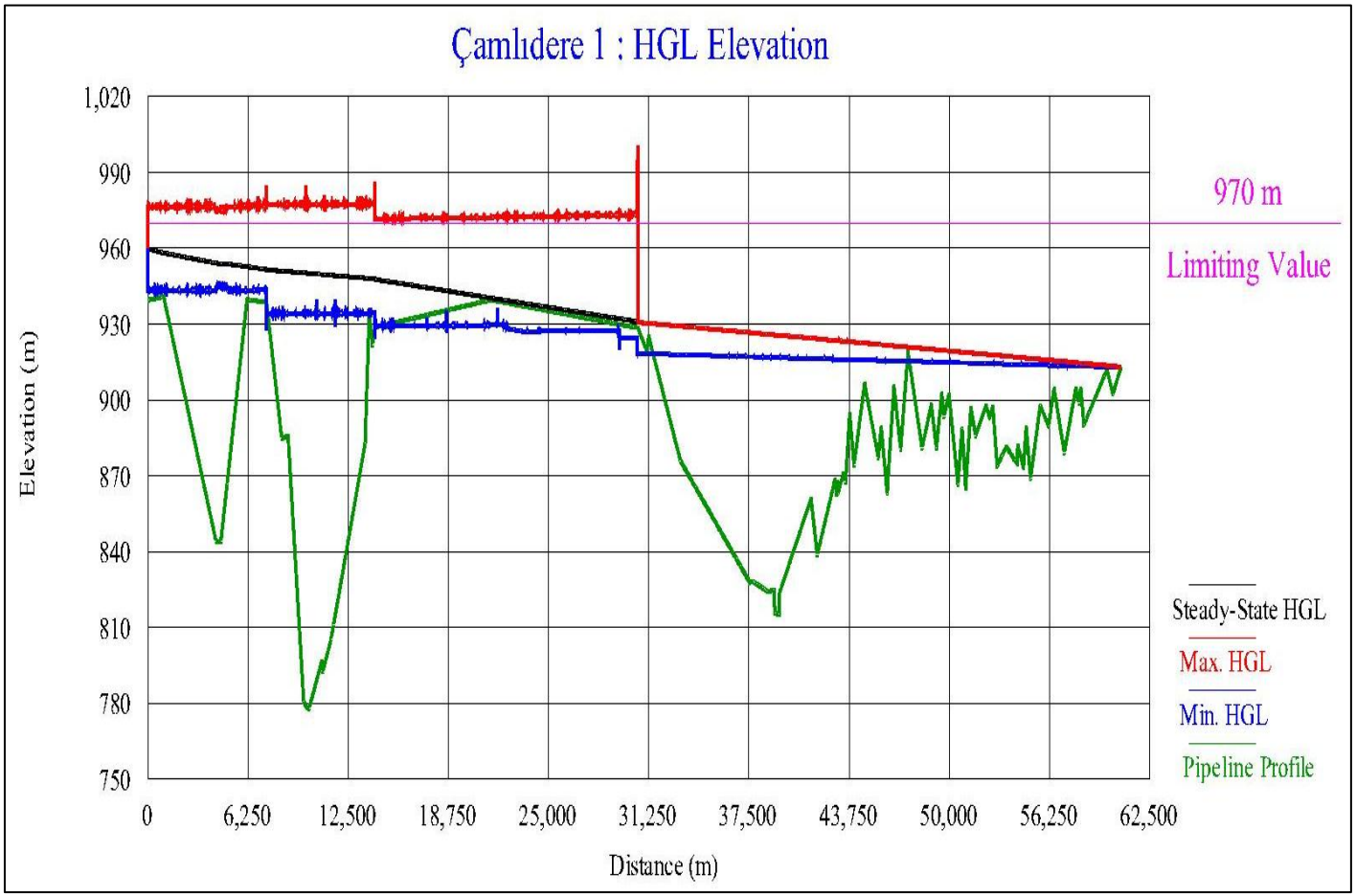

Figure 5.17 Max. and min. HGL envelopes of Çamlıdere 1 (Scn.: U4-T3C)

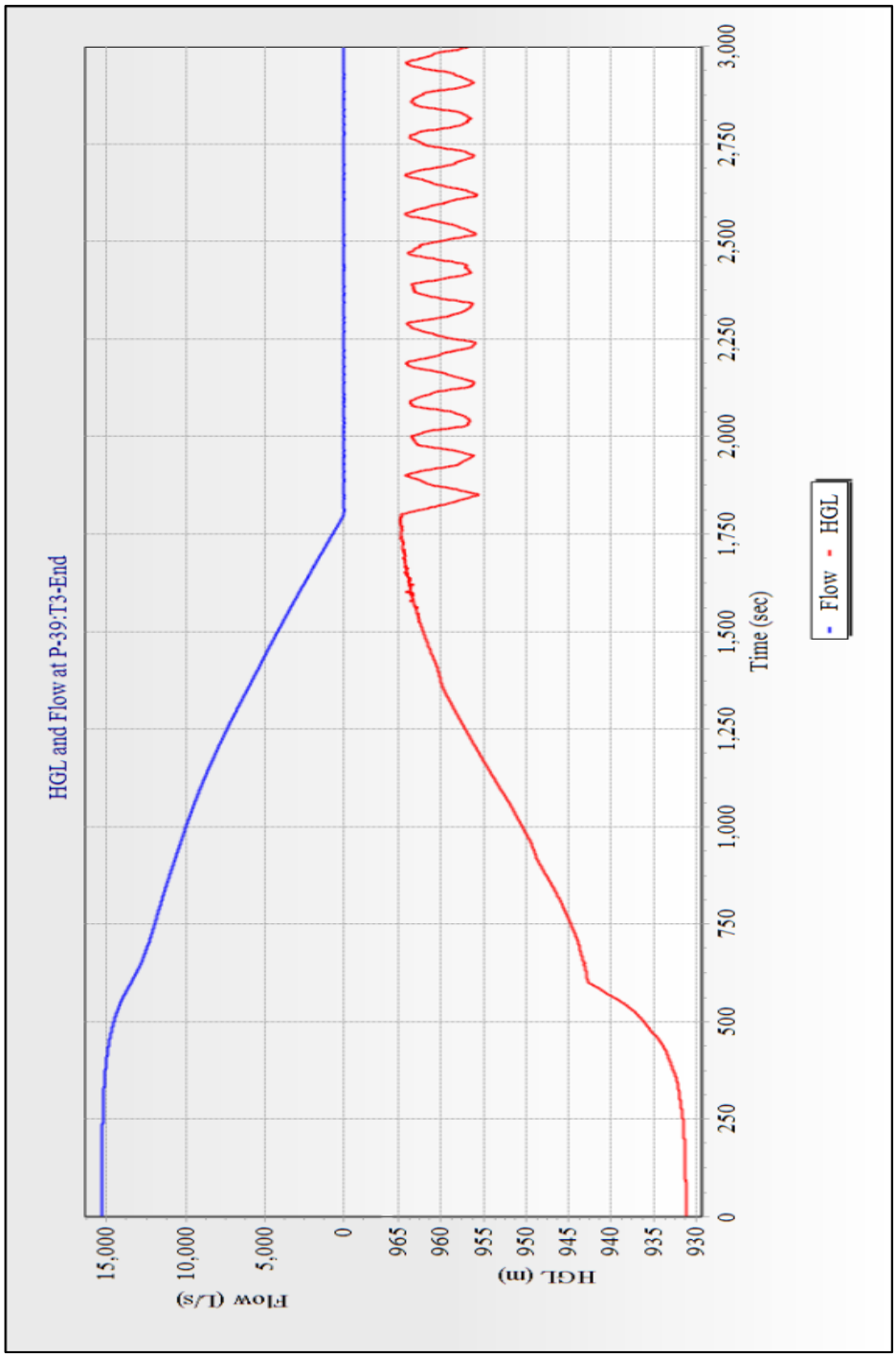

Figure 5.18 Variation of flow and HGL at T3 tunnel exit (Scn.: U4-T3C)

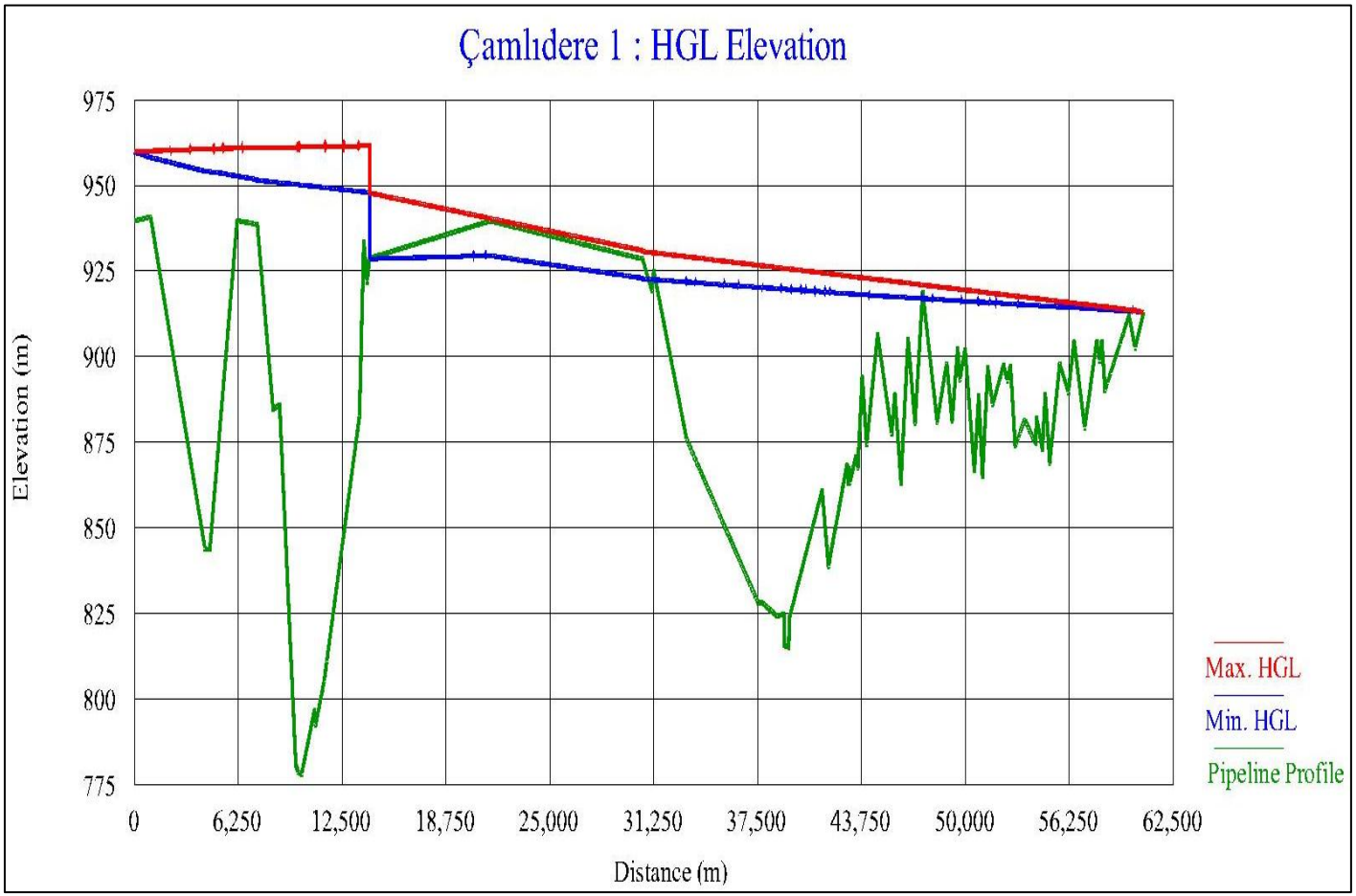

Figure 5.19 Max. and min. HGL envelopes of Çamlıdere 1 (Scn.: U4-T3G)

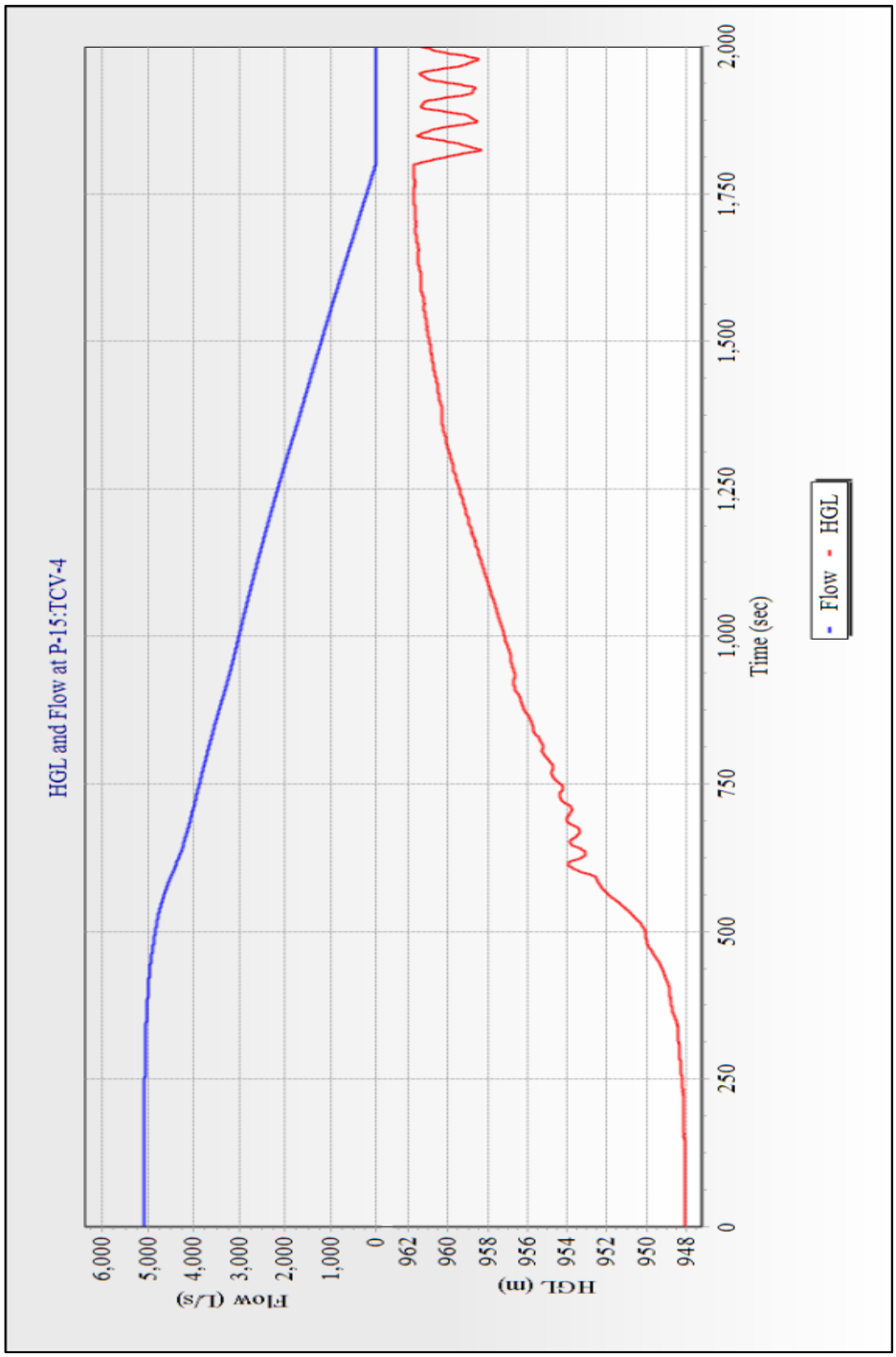

Figure 5.20 Variation of flow and HGL at T3 tunnel entrance (Scn.: U4-T3G)

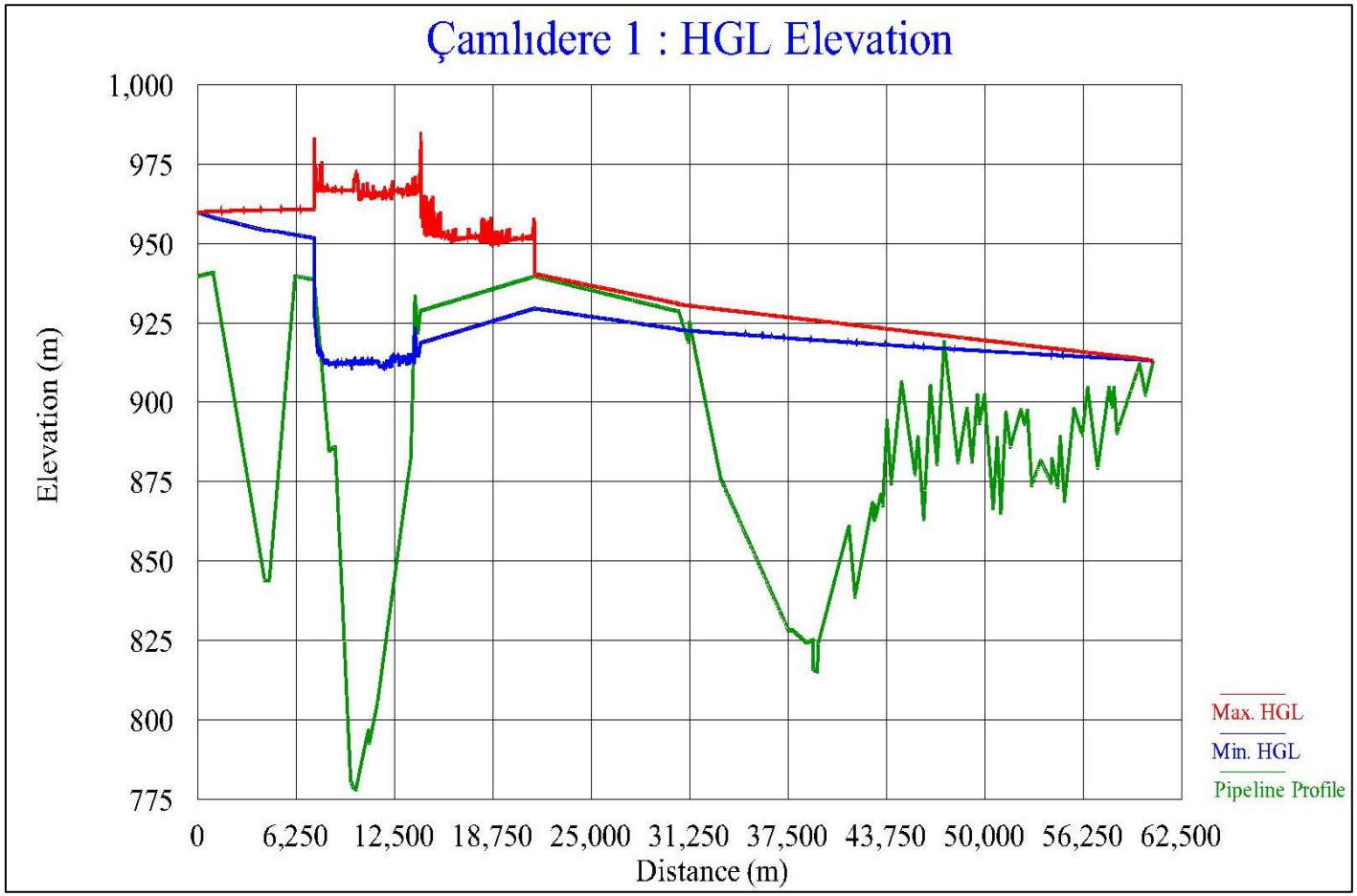

Figure 5.21 Max. and min. HGL envelopes of Çamlıdere 1 (Scn.: U4-T2C)

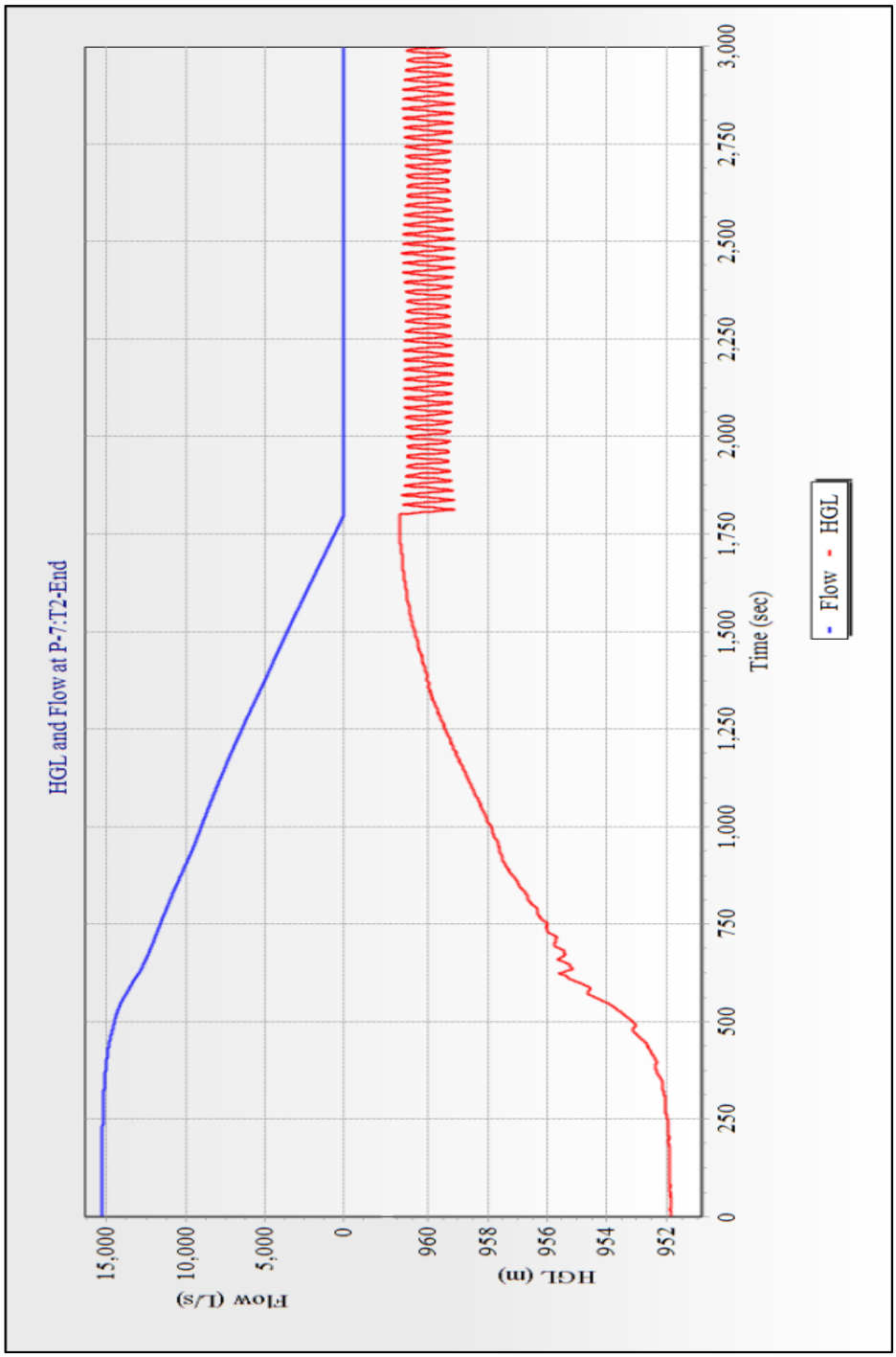

Figure 5.22 Variation of flow and HGL at T2 tunnel exit (Scn.: U4-T2C)

Analyses 61-64 are very important in terms of investigating pipeline system for 965 m water surface level at intake structure which is underlined as the maximum level for operation of system in a safe manner (Yüksel Proje Uluslararası A.Ş., 2004). For this reason, operation scenarios covering single, double and triple pipelines are performed for 45 minutes closure duration which is the recent operation strategy for LJ needle valves at İvedik WTP.

The results of analyses show that the 965 m WSE at intake structure is a critical value as it was underlined before by Yüksel Project (2004) considering the design strength of pipeline system which is 970 m piezometric head.

For single pipeline alternatives, the HGL elevations are 970.78 and 970.91 for Çamlıdere 1 and Çamlıdere 2 (or Çamlıdere 3) respectively. However, for double and triple pipeline alternatives piezometric head rises slightly above 970 m level. It is 972.17 m for double pipelines (ΔH=45.72 m) and 973.44 m for triple pipelines (ΔH=49.19 m).

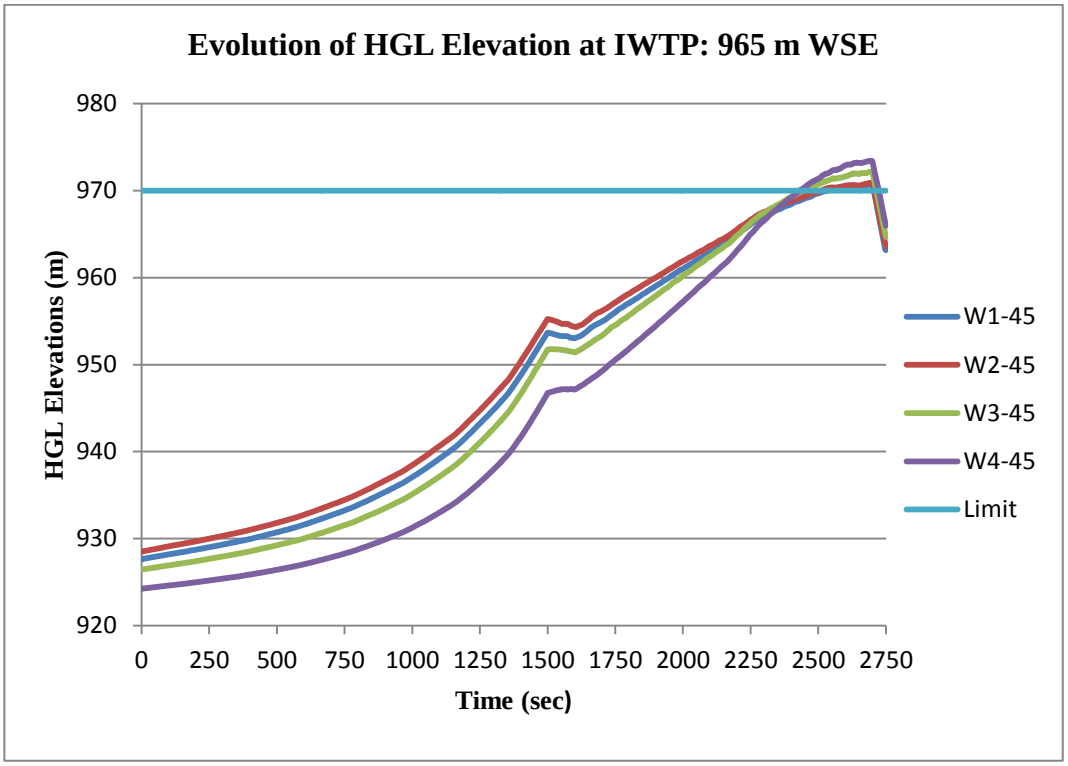

Figure 5.23 Evolution of HGL at IWTP for "W" scenarios

Evolution of excess pressure at İvedik WTP is illustrated in Figure 5.23 above for single, double and triple pipeline alternatives.

Also Figure 5.24 shows the evolution of HGL along Çamlıdere 2 (3) pipeline experiencing the maximum values under Scenario W4-45 which is the most critical. Fortunately, even if the hydraulic grade line rises above 970 m at İvedik WTP, it never rises above this limit at the end of T3 tunnel. This means lower risk for T3 tunnel and upstream parts of pipeline for WSE of 965 m at intake tower. The maximum piezometric head reached for this node is 969.58 m (see Figure 5.25) and this value corresponds to 29.71 m pressure head rise since the steady – state hydraulic grade line is at 939.87 m at the exit of T3 tunnel.

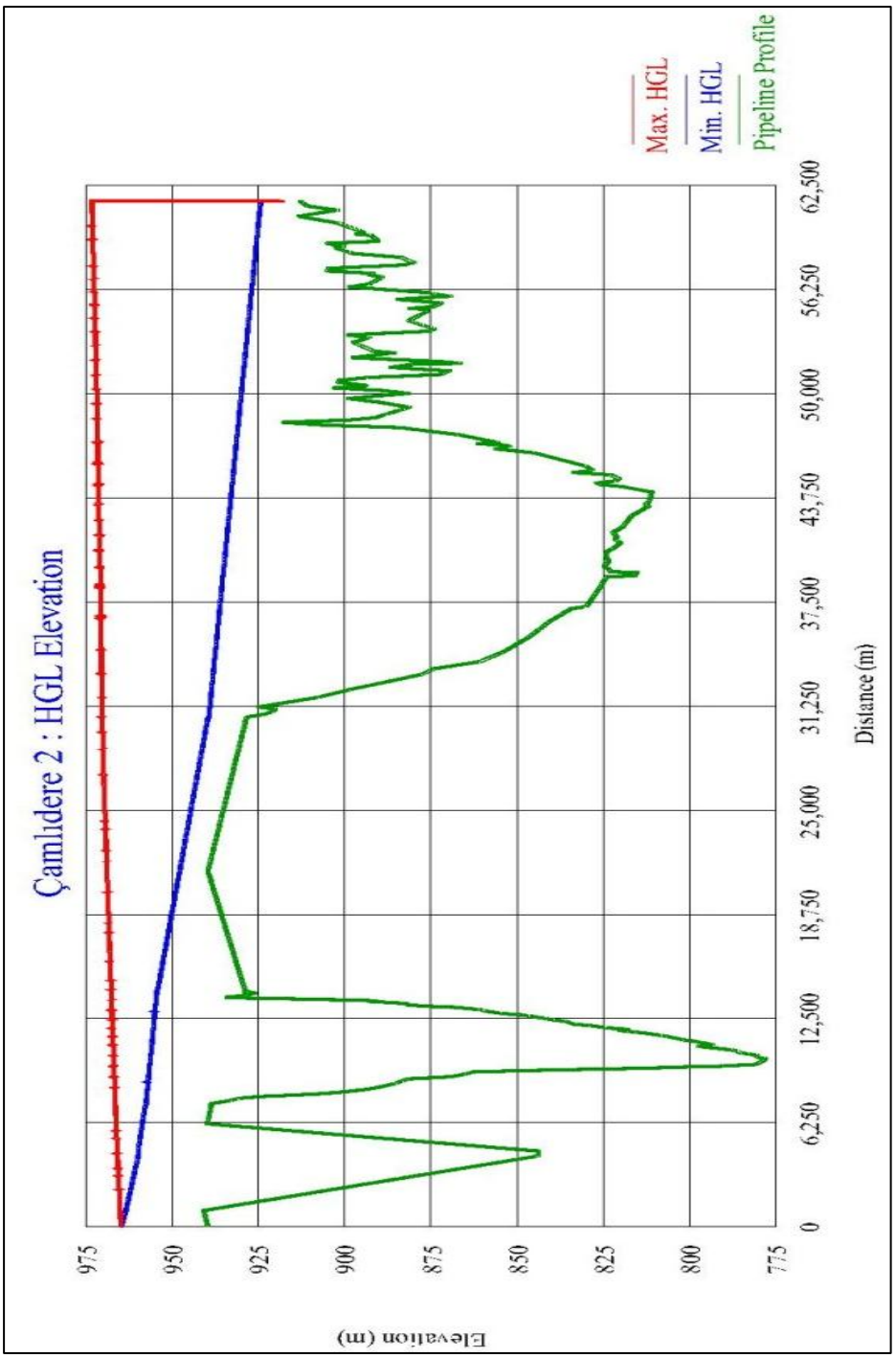

Figure 5.24 Max. and min. HGL envelopes of Çamlıdere 2 (Scn.: W4-45)

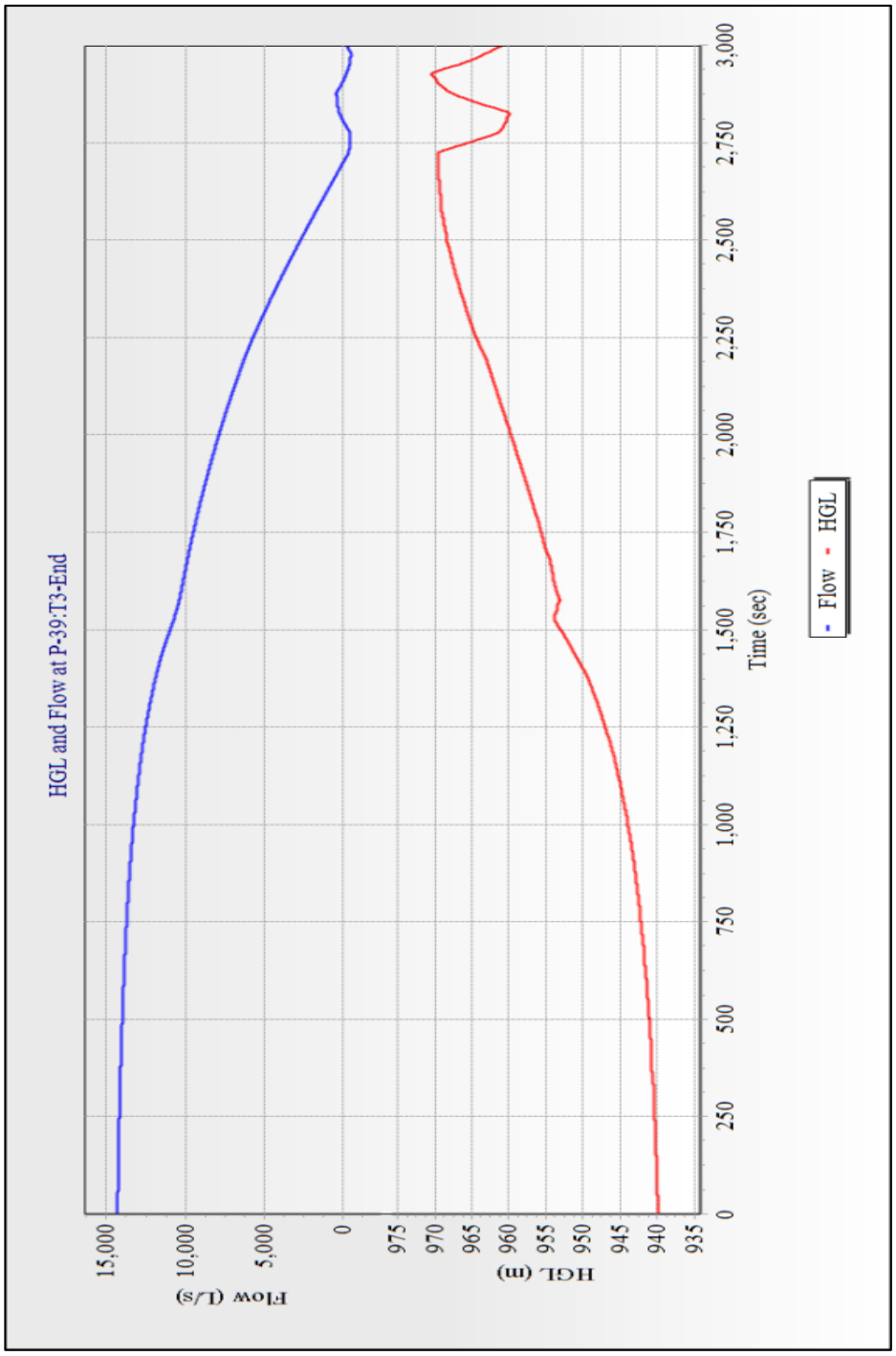

Figure 5.25 Variation of flow and HGL at T3tunnel exit (Scn.: W4-45)

Analyses 65-69 can be interesting in terms of investigating pipeline system for 970 m water surface level at intake structure which was performed by OPM in 1978 for single pipeline. Analysis No. 65 is performed to compare results with that of OPM (1978) computed for single pipeline. The main points here to take attention while comparing the results are the composition of Çamlıdere 1 pipeline and friction losses due to different roughness heights. OPM's study (1978) was performed considering the entire pipeline as concrete. Çamlıdere 1 pipeline was constructed and commissioned with Ø2200 mm concrete pipes. However, in passing years, pipeline section between T2 and T3 tunnels is replaced with Ø2200 mm steel pipes. Also, some disrupted sections between T3 tunnel and İvedik WTP were replaced with again Ø2200 mm steel pipes.

The result of Analysis No. 65 exhibits a slight difference in terms of discharge and peak HGL elevations due to 33 minutes closure. OPM (1978) came up with 7.35 m^3/s discharge and 976.21 m peak piezometric head at İvedik WTP. In spite of that, discharge of 6.35 m^3/s and peak piezometric head of 975.11 m are computed in this study. Even so, values are close to each other. This difference is thought to be resulted from the input data in terms of roughness height of pipes and replacement of some pipe sections with steel ones which affect friction losses along pipeline. Figure 5.26 exhibits the minimum and maximum HGL elevations of Çamlıdere 1 pipeline under 33 minutes closure duration at İvedik WTP computed by OPM in 1978 and Figure 5.27 shows that of in this study.

Thereby, computations with 45 minutes closure duration reveal peak piezometric head values above 970 m limiting HGL. Comparison of the HGL elevations at İvedik WTP for water surface elevations of 960 m, 965 m and 970 m at the intake structure is shown in Figure 5.28.

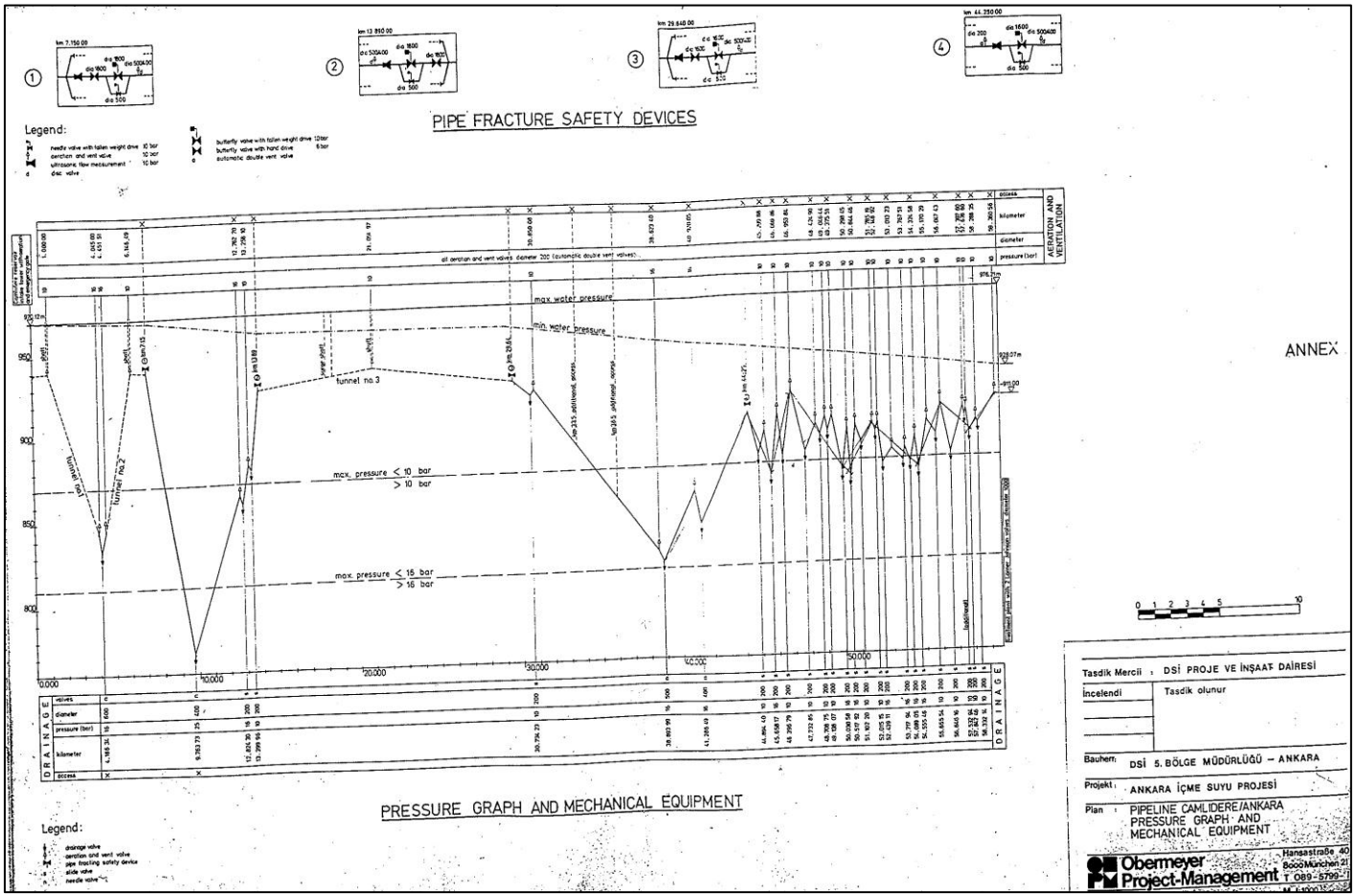

Figure 5.26 Max. and min. HGL elevations by OPM (1978) (Scn.: X1-33)

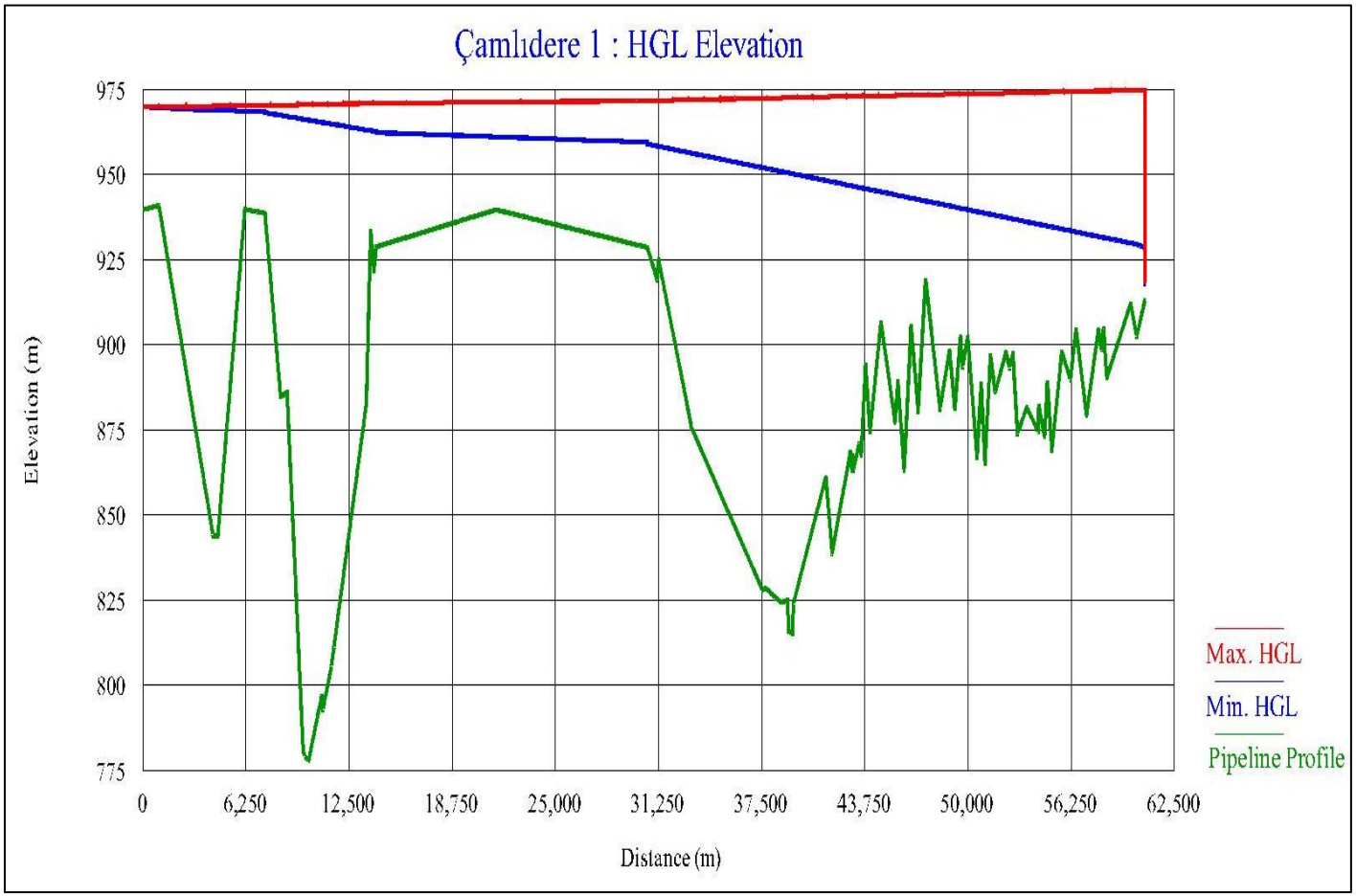

Figure 5.27 Max. and min. HGL elevations by HAMMER (Scn.: X1-33)

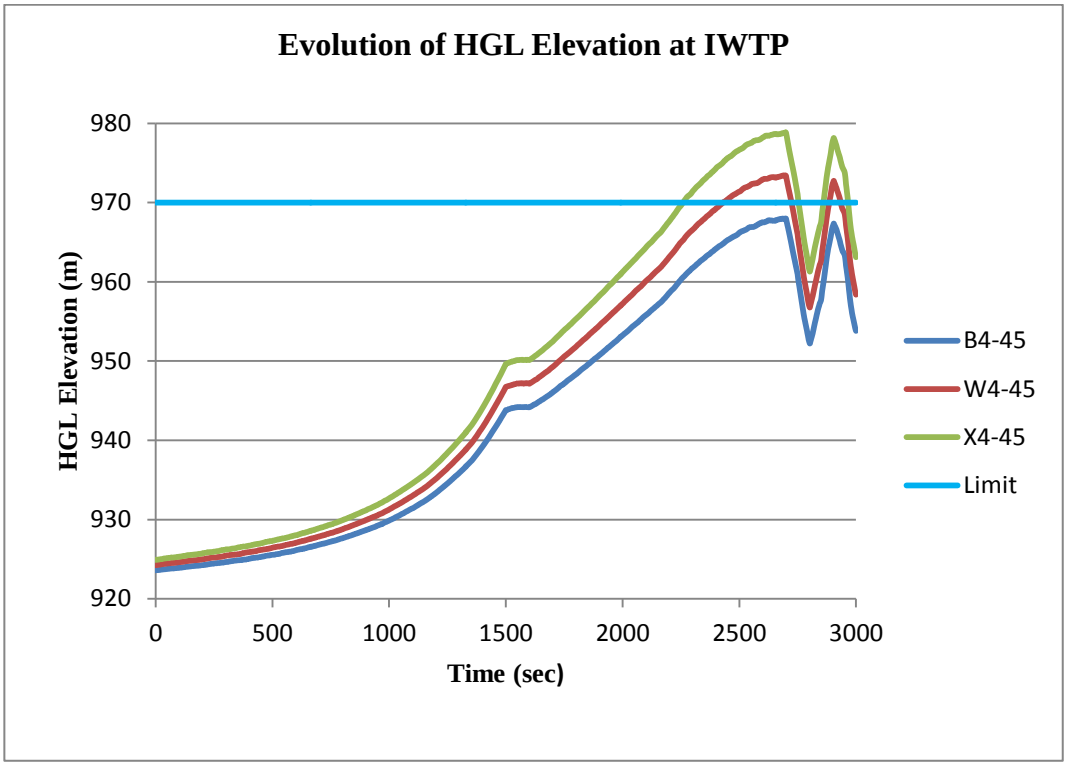

Figure 5.28 Comparison of HGL for 960 m, 965 m and 970 m WSE at intake

Analyses 70-73 denoted by "P_{45}" are performed to investigate the rising pressure heads in a single pipeline resulted from closure of the LJ valves at İvedik WTP from 45% partial opening under WSE of 960 m at intake structure which was defined as the maximum level that should not be exceeded for safe operation conditions.

The results of analyses show that the HGL elevations due to the complete closure of LJ valves at IWTP from 45% partial opening do not exceed the 970 m limiting HGL for tunnels and pipes. For instance, the maximum HGL elevation experienced at Çamlıdere 2 pipeline exit as 965.54 m. To illustrate, Figure 5.29 shows the evolution of HGL along Çamlıdere 2 (or 3) pipeline experiencing the maximum values under Scenario P_{45}2-27 which is the most critical. Also Figure 5.30 illustrates the HGL and flow time – history at Çamlıdere 2 pipeline exit.

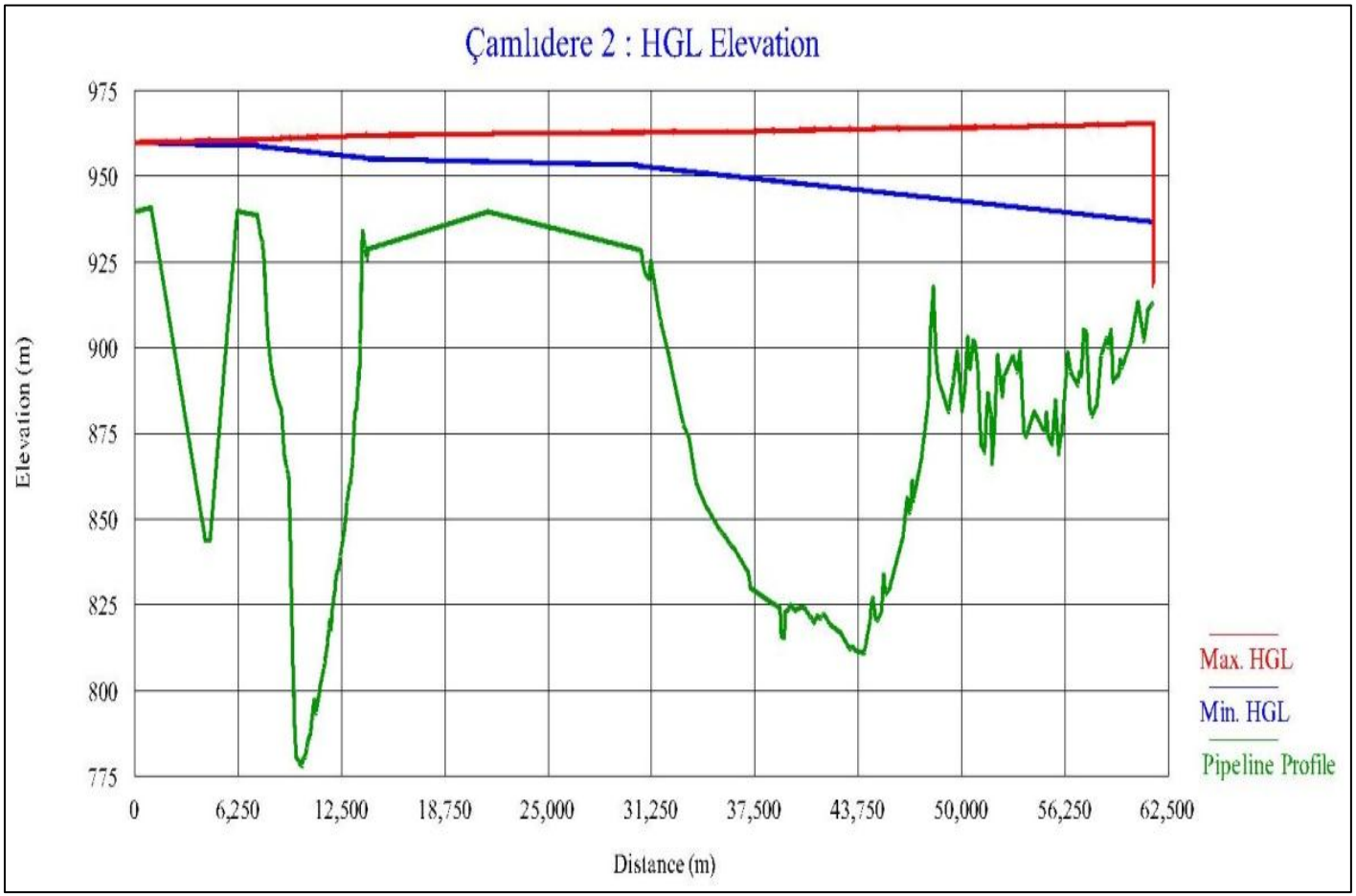

Figure 5.29 Max. and min. HGL envelopes of Çamlıdere 2 (Scn.: P_{45}2-27)

Figure 5.30 Variation of flow and HGL at IWTP entrance (Scn.: P_{45}2-27)

To sum up, all analyses in this study are performed disregarding the ventilation pipes and surge shaft located on T3 tunnel to simulate the worst case. Another point is that the surge shaft is located at the 18th km of 62 km long pipeline. Therefore the protective influence of the surge shaft due to its long distance from the WTP is minimal, thus its effect can be neglected. Doing so makes the results a little bit more conservative. Considering the design HGL of 970 m of pipeline system, piezometric heads at the location of the surge shaft and upstream of it are already below 970 m for all operation alternatives apart from the fast closure (VALVE6.5) of LJ valves at İvedik WTP. Contribution of the surge shaft had been discussed before by OPM (1978) and Bozkuş (2006) and the effect of the surge shaft was neglected in their computations as well.

Analyses results regarding WSE 960 m at intake structure show that the amount of pressure rises at İvedik WTP due to 30 min. long closure suggested by Yüksel Project (2004) and 45 min. long closure which is currently used in operation are in an acceptable range since the maximum level is defined as 970 m. However, fast closure (VALVE6.5) of LJ valves causes tremendous pressures which exceed the capability of pipelines. Considering the Joukowsky equation (Eqn. 5.12), maximum pressure rise expected in this system for rapid closure durations which is defined as durations less than or equal to $2L/a$ seconds can be calculated roughly as follows;

The wave speed along 62 km pipeline is approximately 1,200 m/s and velocity in downstream pipes is around 1.50 m/s. Therefore,

$$\Delta P = +\rho a \Delta V \tag{5.12}$$

$$\Delta P = (1{,}000\ \frac{kg}{m^3})(\ 1{,}200\ \frac{m}{s}\ )(1.50\frac{m}{s}) = 1{,}800{,}000\ Pa$$

$$\Delta H = \Delta P/\gamma = 1{,}800{,}000\ Pa\ /\ 9{,}810\ \frac{N}{m^3} = 183.5\ m$$

Even though 6.5 minutes (or 390 s) is a relatively fast closure duration compared to durations commonly used in practice, it is still considered as a slow closure in a transient analysis since closing time, T_C, is;

$$T_C = 390\ s > 2L/a = 2 \times 62000/1200 \cong 103\ s$$

Therefore, Joukowsky peak pressure rise is not observed. However, pressure rise for 390 s closure duration reaches almost 150 m, which cannot be ignored.

The results of analyses performed to investigate peak pressures at the valves located at the end of T2 tunnel and entrance and end of T3 tunnel as pipe fracture safety device are also below 970 m piezometric head. In these analyses, 30 minutes closure duration for PFSV's are verified under "FAST3" valve closure principle with those of Bozkuş's study (2006).

On the other hand, WSE of 965 m at intake structure pushes the limits of pipelines, even slightly goes beyond in case of double and triple pipeline alternatives under currently used 45 minutes closure duration for LJ valves at İvedik WTP. However, this is still not critical for tunnels due to the pressure values below 970 m in all cases. Nevertheless WSE of 970 m at intake structure causes an overloading in pipelines even for 45 minutes closure duration of LJ valves.

Transient analysis outputs of HAMMER for scenario B4-45 is given in Appendix H as an example.

CHAPTER 6

CONCLUSIONS AND RECOMMENDATIONS

Çamlıdere Dam – İvedik WTP pipeline system which extends over 60 km has an important role in terms of supplying potable water demand of Ankara. Therefore, investigation of safe operation conditions for the pipeline is a primary concern. Currently, two pipelines, Çamlıdere 1 and Çamlıdere 2, are in operation and a third steel pipeline parallel to Çamlıdere 2 is planned to be constructed for future projections. Until today, many studies have been conducted on pipelines in order to observe the behavior of pipeline under various conditions. In this thesis study, pipelines, including the third one, are defined again and updated in accordance with the recent data in order to observe system for water hammer problems due to valve operations.

These valve operations are simulated by computer software named HAMMER which uses the Method of Characteristics for solving non-linear differential equations of unsteady flow or water hammer and results obtained are compared with the ones performed within previous studies. Based on the discussion of scenarios, this study can be concluded as follows;

- Regarding the pressure rises for 960 m and 965 m water surface elevations at intake structure, it is obvious that the WSE never be allowed to exceed

960 m even if the reservoir elevation exceeds this level. Therefore, it is crucial to operate Gate 4 equipped inside the pressure reducing shaft of intake tower whenever required.

- OPM (1978) stated that, in order to prevent an overloading of the line, the HGL must not rise above 970 m and reservoir level above 970 m must be dissipated in the intake structure. WSE of 970 m at intake structure, on the other hand, seems unrealistic and unsafe in terms of resultant excess pressures. Analyses performed for WSE of 970 m exhibit the importance of pressure dissipation at intake structure clearly.

- Currently used, 45 minutes valve closure principle for Larner-Johnson needle valves located at İvedik WTP is an appropriate procedure in terms of handling excess pressures due to water hammer.

- Analyses simulating a pipe fracture illustrate that the 30 minutes closure duration for pipe fracture safety valves located along pipeline will be a safe operation strategy in terms of protecting the remaining system after a fracture. This closure principle was established considering the properties of Erhard Butterfly Valves (Bozkuş, 2006). Total closure must be completed in 2 phase. In first phase, 70% of the valve opening must be closed in 45-700 seconds and closure of remaining 30% must be completed in 140-2,000 seconds. In this study, 30 minutes valve closure principle (FAST3) established by Bozkuş (2006) is verified in which 70% of valve opening is closed in 600 seconds and remaining 30% is closed in 1200 seconds. This closure principle should be applied to PFSV's in case of a pipe fracture or maintenance purposes.

- Also, trial of a partial opening case of the LJ valves at IWTP entrance shows that the recent operating principle (45 min. closure duration) does not cause a problem along pipelines in terms of capability of tunnels and

pipes since the piezometric heads do not exceed the limiting value of 970 m.

Finally, as it was suggested by Bozkuş in 2006, valve operations at İvedik WTP must be implemented by experienced technicians and safe valve closure principles must be obeyed. Flow and pressure measurements must be carried out regularly and archived in computers. Thus, in the future, comparison of stored data with this thesis work will be a guideline for a better design and construction of Çamlıdere 3 pipeline.

REFERENCES

Bentley HAMMER V8i User's Guide. (2010). Bentley Systems, Incorporated.

Bentley HAMMER. (2011). (Bentley Systems, Incorporated) Retrieved November 26, 2011, from http://www.bentley.com/en-US/Products/HAMMER/

Basmacı, E. (1996). *Ankara Water Supply Project Hydraulic Calculation for Çamlıdere-İvedik Transmission Line.* Ankara: Su Yapı.

Bozkuş, Z. (1991). *The Hydrodynamics of an Individual Transient Slug in a Voided Line.* Ph.D Thesis, Michigan State University, Department of Civil and Environmental Engineering.

Bozkuş, Z. (1996). *Investigation of the Water Conveyance Line, and the Pressure Reduction Gate in the Intake Structure of the Çamlıdere Dam Under Various Hydraulic Conditions.* Final Report, Middle East Technical University, Civil Engineering Department, Hydromechanics Laboratory, Ankara.

Bozkuş, Z. (2006). *Çamlıdere Barajı-İvedik Arıtma Tesisleri İsale Hattında Çeşitli Hidrolik Koşullar Altında Su Koçu Analizleri.* Kesin Rapor, Orta Doğu Teknik Üniversitesi, İnşaat Mühendisliği Bölümü, Hidromekanik Laboratuvarı, Ankara.

Bozkuş, Z. (2008, Nisan). Çamlıdere - İvedik İsale Hattında Su Darbesi Analizleri. *TMMOB İnşaat Mühendisleir Odası Teknik Dergi, 19*(2), s. 4409-4422.

Bozkuş, Z. (2009). Fluid Transients in Closed Conduits, Lecture Notes.

Chaudhry, M. H. (1987). *Applied Hydraulic Transients* (2 ed.). New York: Van Nostrand Reinhold.

Ghidaoui, M. S., Zhao, M., Duncan, A. M., & Axworthy, D. H. (2005). A Review of Water Hammer Theory and Practice. *Transactions of the ASME: Applied Mechanics Reviews*(58).

Joukowsky, N. (1904). Waterhammer. *(v.24)*, 341-424. (O. Simin, Trans.) Proceedings AWWA.

KİSKA Komandit Şti. (1977). *Çamlıdere Ankara İçmesuyu İletim Hattı Hidrolik Danışmanlığı Ön raporu.*

Larock, B. E., Jeppson, R. W., & Watters, G. Z. (1999). *Hydraulics of Pipeline Systems.* United States of America: CRC Press LLC.

Obermeyer Project Management. (1978). *Drinking-Water Conveyance Line, Çamlıdere-Ankara, Hydraulic Consultancy, Final Report.* Technical University of Munich, Chair and Test Institute for Hydraulics and Hydrography, Munich.

Parmakian, J. (1955). *Waterhammer Analysis.* New York: Prentice-Hall.

Potter, M. C., & Wiggert, D. C. (2002). *Mechanics Of Fluids* (3. ed.). New York: Prentice Hall, Inc.

Thorley, D. (2004). *Fluid Transients in Pipeline Systems* (2. ed.). London, UK: Professional Engineering Publishing Limited.

Wylie, E. B., & Streeter, V. L. (1978). *Fluid Transients.* New York: McGraw-Hill International Book Co.

Yüksel Proje Uluslararası A.Ş. (2004). *Çamlıdere Barajı-İvedik Arıtma Tesisleri Arası İçmesuyu Sistemlerinin Etüdü ve İşletme Prensiplerinin Belirlenmesi İşi.* Kesin Rapor, Ankara.

APPENDIX A

IŞIKLI WATER SUPPLY PROJECT

Appendix A illustrates the Işıklı Water Supply Project planned for the future from Gerede Basin to Çamlıdere Dam. Recent studies on this project illustrates that the amount of this derivation will be around $230x10^6$ m^3 annually (Yüksel Proje Uluslararası A.Ş., 2004).

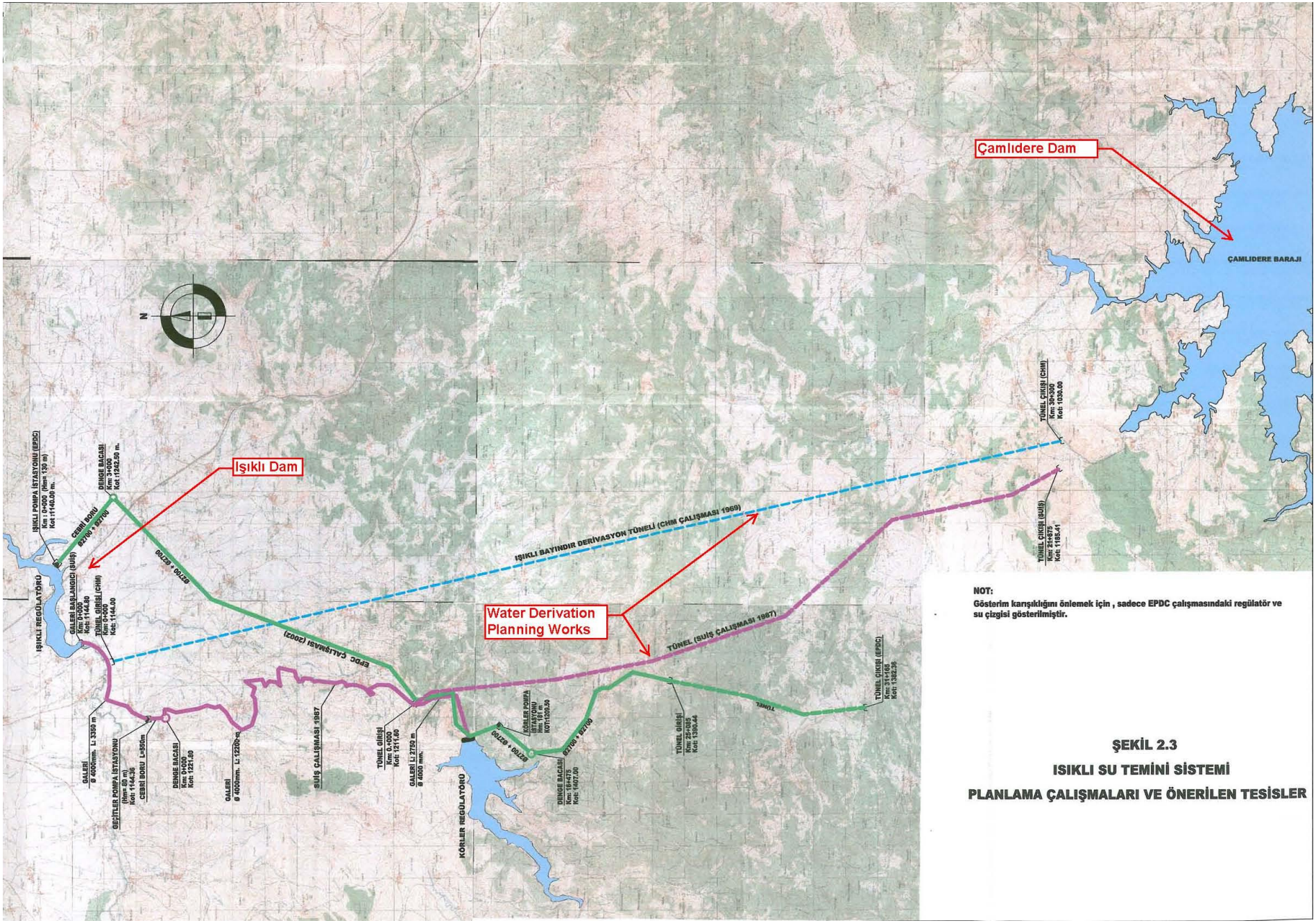

NOT:
Gösterim karışıklığını önlemek için , sadece EPDC çalışmasındaki regülatör ve su çizgisi gösterilmiştir.

ŞEKİL 2.3

ISIKLI SU TEMİNİ SİSTEMİ

PLANLAMA ÇALIŞMALARI VE ÖNERİLEN TESİSLER

APPENDIX B

WATER SUPPLY LAYOUT OF ANKARA

Çamlıdere Dam-İvedik WTP pipeline system plays an important role in terms of supplying the potable water demand of Ankara while it has been projected that 66% of the drinking water need for the city will be provided by Çamlıdere Dam in year 2027 (Bozkuş, 1996). Appendix B shows lay out of the dams and pipelines that supply potable water to the city of Ankara

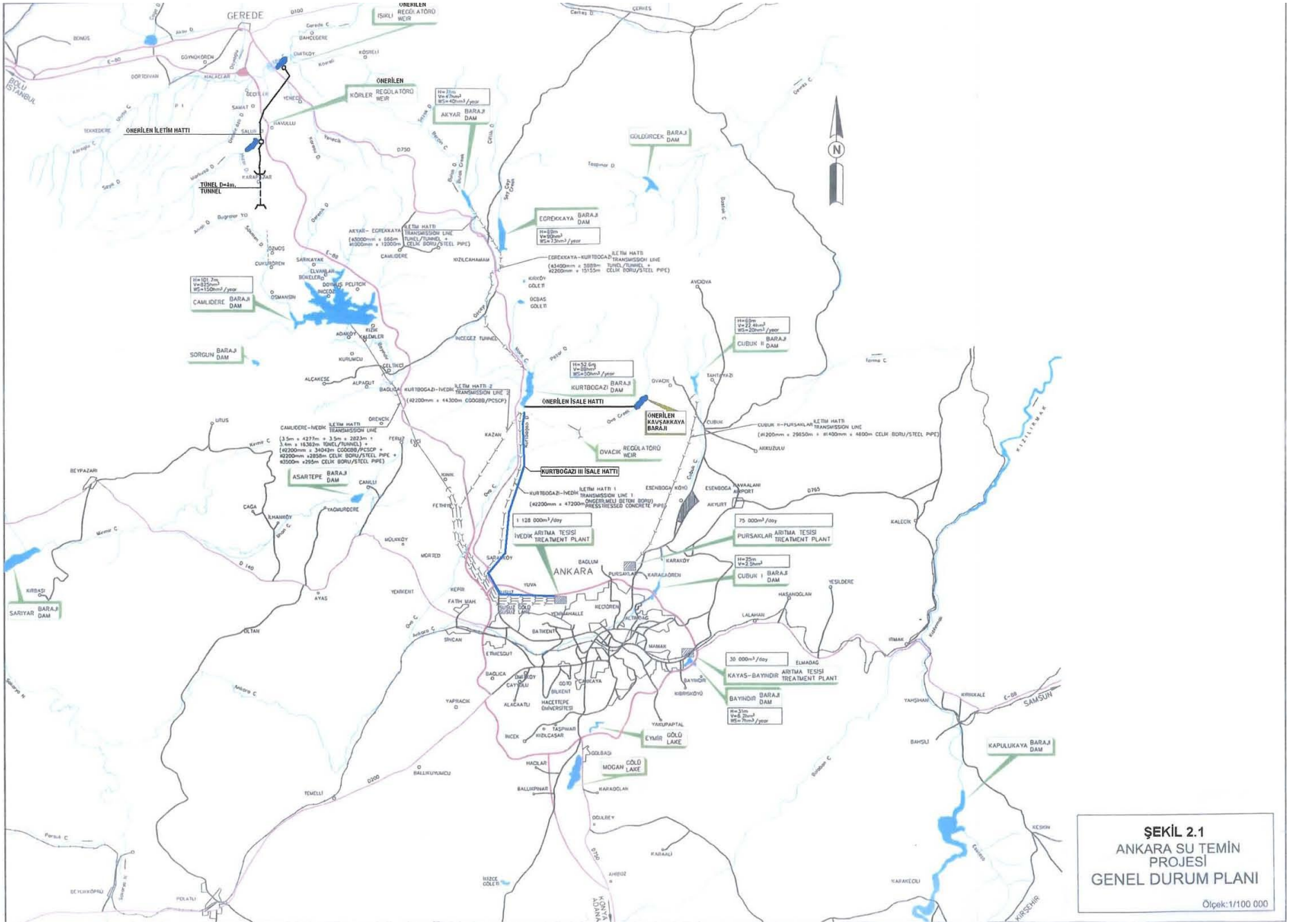

ŞEKİL 2.1
ANKARA SU TEMİN PROJESİ
GENEL DURUM PLANI
Ölçek:1/100 000

APPENDIX C

ÇAMLIDERE DAM INTAKE TOWER

The water intake of Çamlıdere Dam – İvedik WTP is a tower type structure including two independent vertical shafts. One of these shafts (Shaft A) is used to take water into pipeline and the other (Shaft B) is operated for pressure dissipation purposes and Appendix C is the drawing of intake tower.

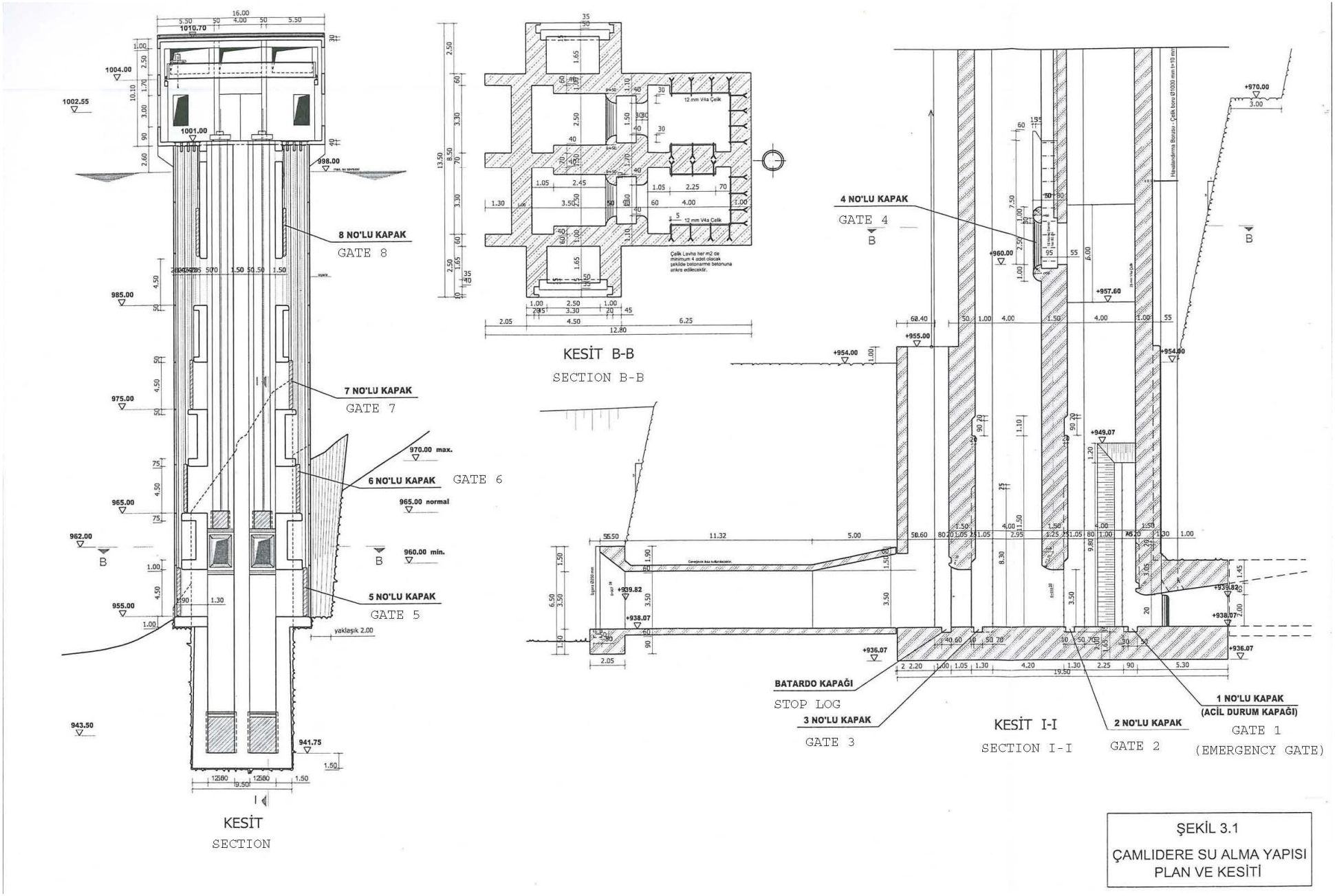

ŞEKİL 3.1

ÇAMLIDERE SU ALMA YAPISI
PLAN VE KESİTİ

APPENDIX D

ERHARD BUTTERFLY VALVES

ERHARD VALVES

50.. 9531
50.. 7231
DN 200 - DN 2600

ERHARD Butterfly Valves, DIN EN 593, PN 10-40

of ductile cast iron, with weight-loaded hydraulic actuator

Range of application	
Size	Pressure rating
DN 200 - 2600	PN 10 - 40

epoxy coating **EKB** epoxy coating

echtes email

DVGW

Materials/Equipment

Prod. No.	50.. 9531	50.. 7231
Corrosion protection of body components	**EKB** epoxy coating, blue, RAL 5015	Vitreous enamel Internal: ERHARD vitreous enamel cobalt blue External: **EKB** epoxy coating, blue, RAL 5015
Body	Ductile cast iron EN-JS 1030[1]	EN-JS1030[1]/ERHARD vitreous enamel
Body seat	Austenitic CrNi steel	ERHARD vitreous enamel
Valve disc (double offset) up to DN 1000	Ductile cast iron EN-JS1030[1] / **EKB**	Ductile cast iron EN-JS1030[1] / **EKB**
Clamping ring	Ductile cast iron EN-JS1030[1] or steel St 37 / **EKB**	Ductile cast iron EN-JS1030[1] or steel St 37 / **EKB**
Sealing ring	Elastomer: EPDM for water NBR for gas	Elastomer: EPDM for water NBR for gas
Valve shaft	Ferritic chrome steel	Ferritic chrome steel
Shaft bearing bushes (maintenance-free)	Steel/tin/PTFE	Steel/tin/PTFE
Sealing of shaft bore	Elastomer: EPDM for water NBR for gas	Elastomer: EPDM for water NBR for gas
Gearbox arrangement	To print 3/G19 Page 3 "Arrangement of Weight-loaded Hydraulic Actuators", Pattern 1-4	

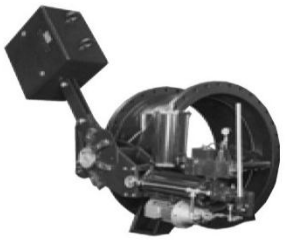

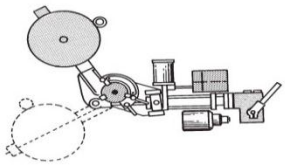

Note: Other materials, coatings and linings on request.

1) Corresponding to former DIN description 0.7040 (GGG-40).

Technical Data/Weight-loaded Hydraulic Actuator

Applications:
- main burst safety device
- combined pump discharge and non-return valve
- turbine inlet valve
- quick opening valve
- other services

With weight-loaded hydraulic actuator of compact design, with closed hydraulic system. All appliances required for hydraulic control as e.g. pumps and valves are rigidly fixed on the cylinder by using little tubing.

In order to reduce the flow rapidly, the first damping range (approx. 70% of the closing angle) is done quickly, the remaining part in a heavily throttled manner in order to keep dynamic pressure peaks on a low level.

Closing-time characteristic: 2-step.

Opening of the Valve:
For opening the Butterfly Valve the weight-loaded lever is lifted by switching-on the electro-hydraulic pump or by actuating the manual oil pump. The valve disc is hydraulically maintained in Open position.

ERHARD VALVES
ERHARD GmbH & Co. KG
Postfach 1280 · D-89502 Heidenheim · Phone (07321) 3200 · Fax (07321) 320525
http://www.erhard.de · E-Mail: export@erhard.de

APPENDIX E

İVEDİK WATER TREATMENT PLANT

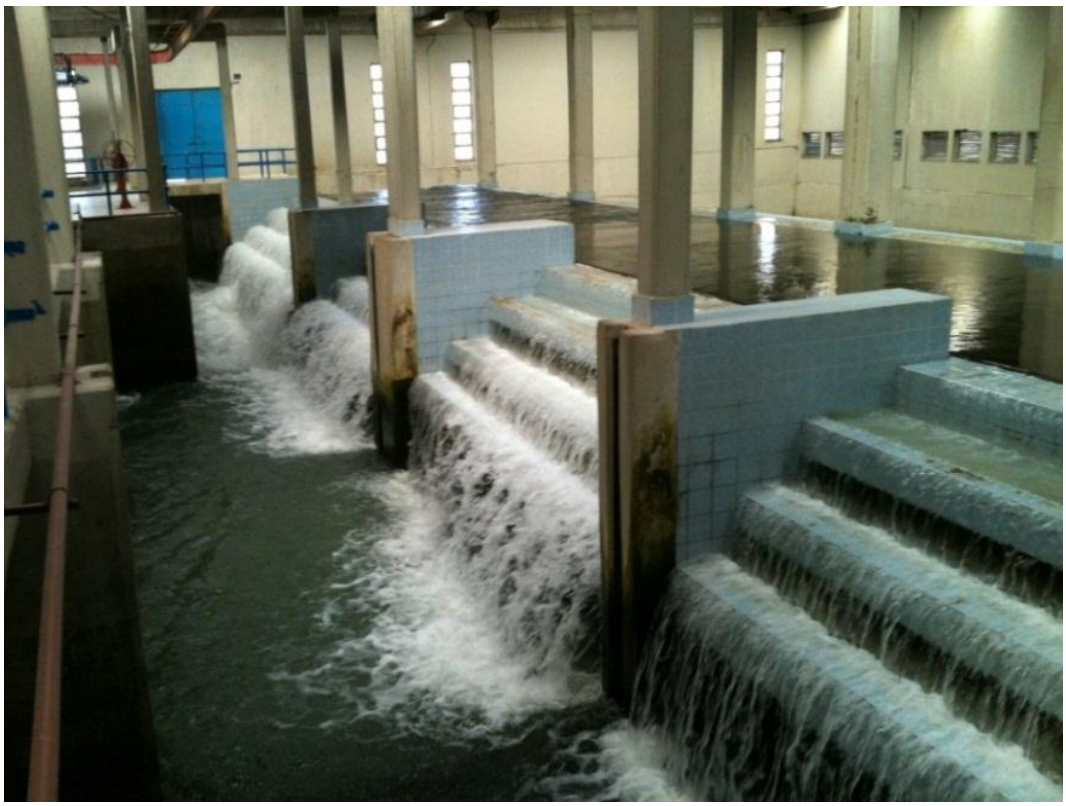

Figure E.1 Aeration pool and cascades

Figure E.2 Pipelines entering İvedik WTP

Figure E.3 Çamlıdere 1 pipeline entrance

APPENDIX F

HAMMER INPUTS OF PIPELINE SYSTEM

Table F.1 Pipe inputs of Hammer analysis model

Pipe Label	Zone	Start Node	Stop Node	Diameter (mm)	Length (m)	Material	ε (mm)	Minor Loss Coefficient, K	Wave Speed, a (m/s)
P-1	T1	Çamlıdere Dam	J-1	3,500	1,000.00	Concrete	7.42	6.059	1,230.0
P-2	T1	J-1	T1-End	3,500	3,277.10	Concrete	7.42	9.202	1,230.0
P-3	T2	T1-End	T2-Start	3,500	294.56	Steel	0.25	0	1,033.6
P-4	T2	T2-Start	J-4	3,500	391.50	Steel	0.25	0	1,033.6
P-5	T2	J-4	J-5	3,500	1,246.98	Concrete	7.42	0	1,230.0
P-6	T2	J-5	J-6	3,500	802.52	Concrete	7.42	0	1,230.0
P-7	T2	J-6	T2-End	3,500	382.01	Concrete	7.42	0	1,230.0
P-8	Ç-3.1	T2-End	TCV-1	1,600	18.01	Steel	0.25	0.072	1,076.3
P-9	Ç-1.1	T2-End	TCV-2	1,600	18.01	Steel	0.25	0.072	1,076.3
P-10	Ç-2.1	T2-End	TCV-3	1,600	18.01	Steel	0.25	0.072	1,076.3
P-11	Ç-1.1	J-8	J-29	2,200	951.00	Steel	0.25	0	1,198.0
P-12	Ç-2.1	J-9	J-11	2,200	192.00	Steel	0.25	0	1,198.0
P-13	Ç-3.1	J-10	J-12	2,200	192.00	Steel	0.25	0	1,198.0
P-14	T3	T3-Start	J-179	3,400	7,229.03	Concrete	7.42	0	1,240.0
P-15	Ç-1.1	J-175	TCV-4	1,600	6.70	Steel	0.25	0.056	1,076.3
P-16	Ç-2.1	J-176	TCV-5	1,600	6.70	Steel	0.25	0.056	1,076.3
P-17	Ç-3.1	J-177	TCV-6	1,600	6.70	Steel	0.25	0.056	1,076.3
P-18	Ç-1.1	J-62	J-65	2,200	214.00	Steel	0.25	0	1,198.0
P-19	Ç-1.1	J-65	J-80	2,200	781.67	Steel	0.25	0	1,198.0
P-20	Ç-1.1	J-97	J-152	2,200	1,975.88	Steel	0.25	0	1,198.0
P-21	Ç-1.1	J-29	J-34	2,200	392.18	Steel	0.25	0	1,198.0
P-22	Ç-1.1	J-34	J-39	2,200	280.44	Steel	0.25	0	1,198.0
P-23	Ç-1.1	J-39	J-52	2,200	557.68	Steel	0.25	0	1,198.0
P-24	Ç-1.1	J-52	J-57	2,200	137.84	Steel	0.25	0	1,198.0
P-25	Ç-1.1	J-57	J-62	2,200	129.50	Steel	0.25	0	1,198.0

Table F.1 cont.'d

Pipe Label	Zone	Start Node	Stop Node	Diameter (mm)	Length (m)	Material	ε (mm)	Minor Loss Coefficient, K	Wave Speed, a (m/s)
P-26	Ç-1.1	J-80	J-83	2,200	66.23	Steel	0.25	0	1,198.0
P-27	Ç-1.1	J-83	J-92	2,200	513.47	Steel	0.25	0	1,198.0
P-28	Ç-1.1	J-92	J-97	2,200	153.20	Steel	0.25	0	1,198.0
P-29	Ç-1.1	J-152	J-163	2,200	254.70	Steel	0.25	0	1,198.0
P-30	Ç-1.1	J-163	J-168	2,200	199.44	Steel	0.25	0	1,198.0
P-31	Ç-1.1	J-168	J-175	2,200	149.82	Steel	0.25	0	1,198.0
P-32	T3	J-179	J-180	3,400	8,594.87	Concrete	7.42	0	1,240.0
P-33	Ç-2.2	T3-End	TCV-7	1,600	18.01	Steel	0.25	0.350	1,076.3
P-34	Ç-3.2	T3-End	TCV-8	1,600	18.01	Steel	0.25	0.350	1,076.3
P-35	Ç-1.2	T3-End	TCV-9	1,600	18.01	Steel	0.25	0.350	1,076.3
P-36	Ç-2.2	J-182	J-185	2,200	109.29	Steel	0.25	0	1,198.0
P-37	Ç-1.2	J-183	J-191	2,200	583.96	Concrete	0.70	0	1,280.0
P-38	Ç-3.2	J-184	J-186	2,200	109.29	Steel	0.25	0	1,198.0
P-39	T3	J-180	T3-End	3,400	538.00	Concrete	7.42	0	1,240.0
P-40	Ç-1.2	J-191	J-194	2,200	99.32	Concrete	0.70	0	1,280.0
P-41	Ç-1.2	J-194	J-203	2,200	1,993.42	Concrete	0.70	0	1,280.0
P-42	Ç-1.2	J-203	J-218	2,200	4,296.06	Concrete	0.70	0	1,280.0
P-43	Ç-1.2	J-218	J-219	2,200	205.44	Concrete	0.70	0	1,280.0
P-44	Ç-1.2	J-219	J-222	2,200	932.65	Concrete	0.70	0	1,280.0
P-45	Ç-1.2	J-222	J-223	2,200	401.71	Concrete	0.70	0	1,280.0
P-46	Ç-1.2	J-223	J-226	2,200	36.32	Concrete	0.70	0	1,280.0
P-47	Ç-1.2	J-226	J-231	2,200	258.57	Steel	0.25	0	1,198.0
P-48	Ç-1.2	J-231	J-234	2,200	42.53	Concrete	0.70	0	1,280.0
P-49	Ç-1.2	J-234	J-249	2,200	1,961.68	Concrete	0.70	0	1,280.0
P-50	Ç-1.2	J-249	J-254	2,200	386.35	Concrete	0.70	0	1,280.0
P-51	Ç-1.2	J-254	J-259	2,200	1,106.98	Concrete	0.70	0	1,280.0
P-52	Ç-1.2	J-259	J-260	2,200	91.72	Concrete	0.70	0	1,280.0
P-53	Ç-1.2	J-260	J-261	2,200	40.44	Concrete	0.70	0	1,280.0
P-54	Ç-1.2	J-261	J-262	2,200	49.94	Concrete	0.70	0	1,280.0
P-55	Ç-1.2	J-262	J-265	2,200	346.73	Concrete	0.70	0	1,280.0
P-56	Ç-1.2	J-265	J-268	2,200	129.20	Concrete	0.70	0	1,280.0
P-57	Ç-1.2	J-268	J-271	2,200	263.29	Concrete	0.70	0	1,280.0
P-58	Ç-1.2	J-271	J-272	2,200	268.32	Concrete	0.70	0	1,280.0
P-59	Ç-1.2	J-272	J-281	2,200	660.11	Concrete	0.70	0	1,280.0
P-60	Ç-1.2	J-281	J-294	2,200	851.79	Concrete	0.70	0	1,280.0
P-61	Ç-1.2	J-294	J-297	2,200	183.09	Concrete	0.70	0	1,280.0

Table F.1 cont.'d

Pipe Label	Zone	Start Node	Stop Node	Diameter (mm)	Length (m)	Material	ε (mm)	Minor Loss Coefficient, K	Wave Speed, a (m/s)
P-62	Ç-1.2	J-297	J-298	2,200	371.36	Concrete	0.70	0	1,280.0
P-63	Ç-1.2	J-298	J-301	2,200	422.02	Concrete	0.70	0	1,280.0
P-64	Ç-1.2	J-301	J-306	2,200	421.51	Concrete	0.70	0	1,280.0
P-65	Ç-1.2	J-306	J-313	2,200	456.47	Concrete	0.70	0	1,280.0
P-66	Ç-1.2	J-313	J-320	2,200	876.08	Concrete	0.70	0	1,280.0
P-67	Ç-1.2	J-320	J-327	2,200	573.72	Concrete	0.70	0	1,280.0
P-68	Ç-1.2	J-327	J-328	2,200	321.33	Concrete	0.70	0	1,280.0
P-69	Ç-1.2	J-328	J-331	2,200	339.19	Concrete	0.70	0	1,280.0
P-70	Ç-1.2	J-331	J-334	2,200	129.36	Concrete	0.70	0	1,280.0
P-71	Ç-1.2	J-334	J-337	2,200	316.97	Concrete	0.70	0	1,280.0
P-72	Ç-1.2	J-337	J-346	2,200	555.99	Concrete	0.70	0	1,280.0
P-73	Ç-1.2	J-346	J-351	2,200	260.20	Concrete	0.70	0	1,280.0
P-74	Ç-1.2	J-351	J-354	2,200	228.00	Concrete	0.70	0	1,280.0
P-75	Ç-1.2	J-354	J-359	2,200	323.34	Concrete	0.70	0	1,280.0
P-76	Ç-1.2	J-359	J-362	2,200	290.13	Concrete	0.70	0	1,280.0
P-77	Ç-1.2	J-362	J-373	2,200	657.86	Concrete	0.70	0	1,280.0
P-78	Ç-1.2	J-373	J-374	2,200	223.59	Concrete	0.70	0	1,280.0
P-79	Ç-1.2	J-374	J-379	2,200	190.03	Concrete	0.70	0	1,280.0
P-80	Ç-1.2	J-379	J-380	2,200	281.76	Concrete	0.70	0	1,280.0
P-81	Ç-1.2	J-380	J-385	2,200	562.02	Concrete	0.70	0	1,280.0
P-82	Ç-1.2	J-385	J-392	2,200	674.47	Concrete	0.70	0	1,280.0
P-83	Ç-1.2	J-392	J-393	2,200	49.58	Concrete	0.70	0	1,280.0
P-84	Ç-1.2	J-393	J-396	2,200	351.64	Concrete	0.70	0	1,280.0
P-85	Ç-1.2	J-396	J-397	2,200	169.22	Concrete	0.70	0	1,280.0
P-86	Ç-1.2	J-397	J-400	2,200	274.27	Concrete	0.70	0	1,280.0
P-87	Ç-1.2	J-400	J-409	2,200	604.21	Concrete	0.70	0	1,280.0
P-88	Ç-1.2	J-409	J-418	2,200	515.47	Concrete	0.70	0	1,280.0
P-89	Ç-1.2	J-418	J-421	2,200	347.15	Concrete	0.70	0	1,280.0
P-90	Ç-1.2	J-421	J-428	2,200	635.71	Concrete	0.70	0	1,280.0
P-91	Ç-1.2	J-428	J-439	2,200	723.61	Concrete	0.70	0	1,280.0
P-92	Ç-1.2	J-439	J-442	2,200	183.52	Concrete	0.70	0	1,280.0
P-93	Ç-1.2	J-442	J-443	2,200	127.82	Concrete	0.70	0	1,280.0
P-94	Ç-1.2	J-443	J-446	2,200	189.04	Concrete	0.70	0	1,280.0
P-95	Ç-1.2	J-446	J-463	2,200	1,441.94	Concrete	0.70	0	1,280.0
P-96	Ç-1.2	J-463	J-464	2,200	370.06	Concrete	0.70	0	1,280.0
P-97	Ç-1.2	J-464	İvedik-1	2,200	504.69	Concrete	0.70	3.172	1,280.0

Table F.1 cont.'d

Pipe Label	Zone	Start Node	Stop Node	Diameter (mm)	Length (m)	Material	ε (mm)	Minor Loss Coefficient, K	Wave Speed, a (m/s)
P-98	IWTP-1	İvedik-1	LJ-1.2	1,600	24.71	Steel	0.25	0	1,076.3
P-99	IWTP-1	İvedik-1	LJ-1.1	1,600	24.71	Steel	0.25	0	1,076.3
P-100	Ç-2.1	J-11	J-13	2,200	120.00	Steel	0.25	0	1,198.0
P-101	Ç-2.1	J-13	J-15	2,200	108.00	Steel	0.25	0	1,198.0
P-102	Ç-2.1	J-15	J-17	2,200	96.00	Steel	0.25	0	1,198.0
P-103	Ç-2.1	J-17	J-19	2,200	60.00	Steel	0.25	0	1,198.0
P-104	Ç-2.1	J-19	J-21	2,200	36.00	Steel	0.25	0	1,198.0
P-105	Ç-2.1	J-21	J-23	2,200	60.00	Steel	0.25	0	1,198.0
P-106	Ç-2.1	J-23	J-25	2,200	96.00	Steel	0.25	0	1,198.0
P-107	Ç-2.1	J-25	J-27	2,200	96.00	Steel	0.25	0	1,198.0
P-108	Ç-2.1	J-27	J-30	2,200	144.00	Steel	0.25	0	1,198.0
P-109	Ç-2.1	J-30	J-32	2,200	214.48	Steel	0.25	0	1,198.0
P-110	Ç-2.1	J-32	J-35	2,200	255.61	Steel	0.25	0	1,198.0
P-111	Ç-2.1	J-35	J-37	2,200	139.97	Steel	0.25	0	1,198.0
P-112	Ç-2.1	J-37	J-40	2,200	144.39	Steel	0.25	0	1,198.0
P-113	Ç-2.1	J-40	J-42	2,200	29.00	Steel	0.25	0	1,198.0
P-114	Ç-2.1	J-42	J-44	2,200	108.47	Steel	0.25	0	1,198.0
P-115	Ç-2.1	J-44	J-46	2,200	86.14	Steel	0.25	0	1,198.0
P-116	Ç-2.1	J-46	J-48	2,200	138.50	Steel	0.25	0	1,198.0
P-117	Ç-2.1	J-48	J-50	2,200	13.43	Steel	0.25	0	1,198.0
P-118	Ç-2.1	J-50	J-53	2,200	87.78	Steel	0.25	0	1,198.0
P-119	Ç-2.1	J-53	J-55	2,200	30.24	Steel	0.25	0	1,198.0
P-120	Ç-2.1	J-55	J-58	2,200	100.35	Steel	0.25	0	1,198.0
P-121	Ç-2.1	J-58	J-60	2,200	63.34	Steel	0.25	0	1,198.0
P-122	Ç-2.1	J-60	J-63	2,200	101.18	Steel	0.25	0	1,198.0
P-123	Ç-2.1	J-63	J-66	2,200	183.97	Steel	0.25	0	1,198.0
P-124	Ç-2.1	J-66	J-68	2,200	64.11	Steel	0.25	0	1,198.0
P-125	Ç-2.1	J-68	J-70	2,200	65.56	Steel	0.25	0	1,198.0
P-126	Ç-2.1	J-70	J-72	2,200	62.63	Steel	0.25	0	1,198.0
P-127	Ç-2.1	J-72	J-74	2,200	84.62	Steel	0.25	0	1,198.0
P-128	Ç-2.1	J-74	J-76	2,200	56.91	Steel	0.25	0	1,198.0
P-129	Ç-2.1	J-76	J-78	2,200	180.33	Steel	0.25	0	1,198.0
P-130	Ç-2.1	J-78	J-81	2,200	230.58	Steel	0.25	0	1,198.0
P-131	Ç-2.1	J-81	J-84	2,200	71.66	Steel	0.25	0	1,198.0
P-132	Ç-2.1	J-84	J-86	2,200	26.40	Steel	0.25	0	1,198.0
P-133	Ç-2.1	J-86	J-88	2,200	242.51	Steel	0.25	0	1,198.0
P-134	Ç-2.1	J-88	J-90	2,200	35.60	Steel	0.25	0	1,198.0

Table F.1 cont.'d

Pipe Label	Zone	Start Node	Stop Node	Diameter (mm)	Length (m)	Material	ε (mm)	Minor Loss Coefficient, K	Wave Speed, a (m/s)
P-135	Ç-2.1	J-90	J-93	2,200	213.75	Steel	0.25	0	1,198.0
P-136	Ç-2.1	J-93	J-95	2,200	50.80	Steel	0.25	0	1,198.0
P-137	Ç-2.1	J-95	J-98	2,200	168.00	Steel	0.25	0	1,198.0
P-138	Ç-2.1	J-98	J-100	2,200	35.64	Steel	0.25	0	1,198.0
P-139	Ç-2.1	J-100	J-102	2,200	53.76	Steel	0.25	0	1,198.0
P-140	Ç-2.1	J-102	J-104	2,200	42.03	Steel	0.25	0	1,198.0
P-141	Ç-2.1	J-104	J-106	2,200	61.96	Steel	0.25	0	1,198.0
P-142	Ç-2.1	J-106	J-108	2,200	48.68	Steel	0.25	0	1,198.0
P-143	Ç-2.1	J-108	J-110	2,200	48.67	Steel	0.25	0	1,198.0
P-144	Ç-2.1	J-110	J-112	2,200	141.40	Steel	0.25	0	1,198.0
P-145	Ç-2.1	J-112	J-114	2,200	72.00	Steel	0.25	0	1,198.0
P-146	Ç-2.1	J-114	J-116	2,200	85.49	Steel	0.25	0	1,198.0
P-147	Ç-2.1	J-116	J-118	2,200	81.38	Steel	0.25	0	1,198.0
P-148	Ç-2.1	J-118	J-120	2,200	90.96	Steel	0.25	0	1,198.0
P-149	Ç-2.1	J-120	J-122	2,200	78.22	Steel	0.25	0	1,198.0
P-150	Ç-2.1	J-122	J-124	2,200	158.72	Steel	0.25	0	1,198.0
P-151	Ç-2.1	J-124	J-126	2,200	82.41	Steel	0.25	0	1,198.0
P-152	Ç-2.1	J-126	J-128	2,200	80.75	Steel	0.25	0	1,198.0
P-153	Ç-2.1	J-128	J-130	2,200	150.45	Steel	0.25	0	1,198.0
P-154	Ç-2.1	J-130	J-132	2,200	10.19	Steel	0.25	0	1,198.0
P-155	Ç-2.1	J-132	J-134	2,200	68.00	Steel	0.25	0	1,198.0
P-156	Ç-2.1	J-134	J-136	2,200	108.47	Steel	0.25	0	1,198.0
P-157	Ç-2.1	J-136	J-138	2,200	23.30	Steel	0.25	0	1,198.0
P-158	Ç-2.1	J-138	J-140	2,200	78.94	Steel	0.25	0	1,198.0
P-159	Ç-2.1	J-140	J-142	2,200	79.09	Steel	0.25	0	1,198.0
P-160	Ç-2.1	J-142	J-144	2,200	70.89	Steel	0.25	0	1,198.0
P-161	Ç-2.1	J-144	J-146	2,200	70.53	Steel	0.25	0	1,198.0
P-162	Ç-2.1	J-146	J-148	2,200	12.58	Steel	0.25	0	1,198.0
P-163	Ç-2.1	J-148	J-150	2,200	57.24	Steel	0.25	0	1,198.0
P-164	Ç-2.1	J-150	J-153	2,200	29.68	Steel	0.25	0	1,198.0
P-165	Ç-2.1	J-153	J-155	2,200	22.70	Steel	0.25	0	1,198.0
P-166	Ç-2.1	J-155	J-157	2,200	17.30	Steel	0.25	0	1,198.0
P-167	Ç-2.1	J-157	J-159	2,200	139.75	Steel	0.25	0	1,198.0
P-168	Ç-2.1	J-159	J-161	2,200	25.23	Steel	0.25	0	1,198.0
P-169	Ç-2.1	J-161	J-164	2,200	108.70	Steel	0.25	0	1,198.0
P-170	Ç-2.1	J-164	J-166	2,200	25.62	Steel	0.25	0	1,198.0
P-171	Ç-2.1	J-166	J-169	2,200	123.34	Steel	0.25	0	1,198.0

Table F.1 cont.'d

Pipe Label	Zone	Start Node	Stop Node	Diameter (mm)	Length (m)	Material	ε (mm)	Minor Loss Coefficient, K	Wave Speed, a (m/s)
P-172	Ç-2.1	J-169	J-171	2,200	8.30	Steel	0.25	0	1,198.0
P-173	Ç-2.1	J-171	J-173	2,200	45.83	Steel	0.25	0	1,198.0
P-174	Ç-2.1	J-173	J-176	2,200	5.00	Steel	0.25	0	1,198.0
P-175	Ç-3.1	J-12	J-14	2,200	120.00	Steel	0.25	0	1,198.0
P-176	Ç-3.1	J-14	J-16	2,200	108.00	Steel	0.25	0	1,198.0
P-177	Ç-3.1	J-16	J-18	2,200	96.00	Steel	0.25	0	1,198.0
P-178	Ç-3.1	J-18	J-20	2,200	60.00	Steel	0.25	0	1,198.0
P-179	Ç-3.1	J-20	J-22	2,200	36.00	Steel	0.25	0	1,198.0
P-180	Ç-3.1	J-22	J-24	2,200	60.00	Steel	0.25	0	1,198.0
P-181	Ç-3.1	J-24	J-26	2,200	96.00	Steel	0.25	0	1,198.0
P-182	Ç-3.1	J-26	J-28	2,200	96.00	Steel	0.25	0	1,198.0
P-183	Ç-3.1	J-28	J-31	2,200	144.00	Steel	0.25	0	1,198.0
P-184	Ç-3.1	J-31	J-33	2,200	214.48	Steel	0.25	0	1,198.0
P-185	Ç-3.1	J-33	J-36	2,200	255.61	Steel	0.25	0	1,198.0
P-186	Ç-3.1	J-36	J-38	2,200	139.97	Steel	0.25	0	1,198.0
P-187	Ç-3.1	J-38	J-41	2,200	144.39	Steel	0.25	0	1,198.0
P-188	Ç-3.1	J-41	J-43	2,200	29.00	Steel	0.25	0	1,198.0
P-189	Ç-3.1	J-43	J-45	2,200	108.47	Steel	0.25	0	1,198.0
P-190	Ç-3.1	J-45	J-47	2,200	86.14	Steel	0.25	0	1,198.0
P-191	Ç-3.1	J-47	J-49	2,200	138.50	Steel	0.25	0	1,198.0
P-192	Ç-3.1	J-49	J-51	2,200	13.43	Steel	0.25	0	1,198.0
P-193	Ç-3.1	J-51	J-54	2,200	87.78	Steel	0.25	0	1,198.0
P-194	Ç-3.1	J-54	J-56	2,200	30.24	Steel	0.25	0	1,198.0
P-195	Ç-3.1	J-56	J-59	2,200	100.35	Steel	0.25	0	1,198.0
P-196	Ç-3.1	J-59	J-61	2,200	63.34	Steel	0.25	0	1,198.0
P-197	Ç-3.1	J-61	J-64	2,200	101.18	Steel	0.25	0	1,198.0
P-198	Ç-3.1	J-64	J-67	2,200	183.97	Steel	0.25	0	1,198.0
P-199	Ç-3.1	J-67	J-69	2,200	64.11	Steel	0.25	0	1,198.0
P-200	Ç-3.1	J-69	J-71	2,200	65.56	Steel	0.25	0	1,198.0
P-201	Ç-3.1	J-71	J-73	2,200	62.63	Steel	0.25	0	1,198.0
P-202	Ç-3.1	J-73	J-75	2,200	84.62	Steel	0.25	0	1,198.0
P-203	Ç-3.1	J-75	J-77	2,200	56.91	Steel	0.25	0	1,198.0
P-204	Ç-3.1	J-77	J-79	2,200	180.33	Steel	0.25	0	1,198.0
P-205	Ç-3.1	J-79	J-82	2,200	230.58	Steel	0.25	0	1,198.0
P-206	Ç-3.1	J-82	J-85	2,200	71.66	Steel	0.25	0	1,198.0
P-207	Ç-3.1	J-85	J-87	2,200	26.40	Steel	0.25	0	1,198.0
P-208	Ç-3.1	J-87	J-89	2,200	242.51	Steel	0.25	0	1,198.0

Table F.1 cont.'d

Pipe Label	Zone	Start Node	Stop Node	Diameter (mm)	Length (m)	Material	ε (mm)	Minor Loss Coefficient, K	Wave Speed, a (m/s)
P-209	Ç-3.1	J-89	J-91	2,200	35.60	Steel	0.25	0	1,198.0
P-210	Ç-3.1	J-91	J-94	2,200	213.75	Steel	0.25	0	1,198.0
P-211	Ç-3.1	J-94	J-96	2,200	50.80	Steel	0.25	0	1,198.0
P-212	Ç-3.1	J-96	J-99	2,200	168.00	Steel	0.25	0	1,198.0
P-213	Ç-3.1	J-99	J-101	2,200	35.64	Steel	0.25	0	1,198.0
P-214	Ç-3.1	J-101	J-103	2,200	53.76	Steel	0.25	0	1,198.0
P-215	Ç-3.1	J-103	J-105	2,200	42.03	Steel	0.25	0	1,198.0
P-216	Ç-3.1	J-105	J-107	2,200	61.96	Steel	0.25	0	1,198.0
P-217	Ç-3.1	J-107	J-109	2,200	48.68	Steel	0.25	0	1,198.0
P-218	Ç-3.1	J-109	J-111	2,200	48.67	Steel	0.25	0	1,198.0
P-219	Ç-3.1	J-111	J-113	2,200	141.40	Steel	0.25	0	1,198.0
P-220	Ç-3.1	J-113	J-115	2,200	72.00	Steel	0.25	0	1,198.0
P-221	Ç-3.1	J-115	J-117	2,200	85.49	Steel	0.25	0	1,198.0
P-222	Ç-3.1	J-117	J-119	2,200	81.38	Steel	0.25	0	1,198.0
P-223	Ç-3.1	J-119	J-121	2,200	90.96	Steel	0.25	0	1,198.0
P-224	Ç-3.1	J-121	J-123	2,200	78.22	Steel	0.25	0	1,198.0
P-225	Ç-3.1	J-123	J-125	2,200	158.72	Steel	0.25	0	1,198.0
P-226	Ç-3.1	J-125	J-127	2,200	82.41	Steel	0.25	0	1,198.0
P-227	Ç-3.1	J-127	J-129	2,200	80.75	Steel	0.25	0	1,198.0
P-228	Ç-3.1	J-129	J-131	2,200	150.45	Steel	0.25	0	1,198.0
P-229	Ç-3.1	J-131	J-133	2,200	10.19	Steel	0.25	0	1,198.0
P-230	Ç-3.1	J-133	J-135	2,200	68.00	Steel	0.25	0	1,198.0
P-231	Ç-3.1	J-135	J-137	2,200	108.47	Steel	0.25	0	1,198.0
P-232	Ç-3.1	J-137	J-139	2,200	23.30	Steel	0.25	0	1,198.0
P-233	Ç-3.1	J-139	J-141	2,200	78.94	Steel	0.25	0	1,198.0
P-234	Ç-3.1	J-141	J-143	2,200	79.09	Steel	0.25	0	1,198.0
P-235	Ç-3.1	J-143	J-145	2,200	70.89	Steel	0.25	0	1,198.0
P-236	Ç-3.1	J-145	J-147	2,200	70.53	Steel	0.25	0	1,198.0
P-237	Ç-3.1	J-147	J-149	2,200	12.58	Steel	0.25	0	1,198.0
P-238	Ç-3.1	J-149	J-151	2,200	57.24	Steel	0.25	0	1,198.0
P-239	Ç-3.1	J-151	J-154	2,200	29.68	Steel	0.25	0	1,198.0
P-240	Ç-3.1	J-154	J-156	2,200	22.70	Steel	0.25	0	1,198.0
P-241	Ç-3.1	J-156	J-158	2,200	17.30	Steel	0.25	0	1,198.0
P-242	Ç-3.1	J-158	J-160	2,200	139.75	Steel	0.25	0	1,198.0
P-243	Ç-3.1	J-160	J-162	2,200	25.23	Steel	0.25	0	1,198.0
P-244	Ç-3.1	J-162	J-165	2,200	108.70	Steel	0.25	0	1,198.0
P-245	Ç-3.1	J-165	J-167	2,200	25.62	Steel	0.25	0	1,198.0

Table F.1 cont.'d

Pipe Label	Zone	Start Node	Stop Node	Diameter (mm)	Length (m)	Material	ε (mm)	Minor Loss Coefficient, K	Wave Speed, a (m/s)
P-246	Ç-3.1	J-167	J-170	2,200	123.34	Steel	0.25	0	1,198.0
P-247	Ç-3.1	J-170	J-172	2,200	8.30	Steel	0.25	0	1,198.0
P-248	Ç-3.1	J-172	J-174	2,200	45.83	Steel	0.25	0	1,198.0
P-249	Ç-3.1	J-174	J-177	2,200	5.00	Steel	0.25	0	1,198.0
P-250	Ç-2.2	J-185	J-187	2,200	131.40	Steel	0.25	0	1,198.0
P-251	Ç-2.2	J-187	J-189	2,200	159.69	Steel	0.25	0	1,198.0
P-252	Ç-2.2	J-189	J-192	2,200	187.05	Steel	0.25	0	1,198.0
P-253	Ç-2.2	J-192	J-195	2,200	113.63	Steel	0.25	0	1,198.0
P-254	Ç-2.2	J-195	J-197	2,200	586.59	Steel	0.25	0	1,198.0
P-255	Ç-2.2	J-197	J-199	2,200	471.11	Steel	0.25	0	1,198.0
P-256	Ç-2.2	J-199	J-201	2,200	902.76	Steel	0.25	0	1,198.0
P-257	Ç-2.2	J-201	J-204	2,200	346.82	Steel	0.25	0	1,198.0
P-258	Ç-2.2	J-204	J-206	2,200	418.65	Steel	0.25	0	1,198.0
P-259	Ç-2.2	J-206	J-208	2,200	547.76	Steel	0.25	0	1,198.0
P-260	Ç-2.2	J-208	J-210	2,200	847.94	Steel	0.25	0	1,198.0
P-261	Ç-2.2	J-210	J-212	2,200	1,065.92	Steel	0.25	0	1,198.0
P-262	Ç-2.2	J-212	J-214	2,200	697.32	Steel	0.25	0	1,198.0
P-263	Ç-2.2	J-214	J-216	2,200	144.19	Steel	0.25	0	1,198.0
P-264	Ç-2.2	J-216	J-220	2,200	1,075.59	Steel	0.25	0	1,198.0
P-265	Ç-2.2	J-220	J-224	2,200	709.00	Steel	0.25	0	1,198.0
P-266	Ç-2.2	J-224	J-227	2,200	65.96	Steel	0.25	0	1,198.0
P-267	Ç-2.2	J-227	J-229	2,200	192.40	Steel	0.25	0	1,198.0
P-268	Ç-2.2	J-229	J-232	2,200	54.35	Steel	0.25	0	1,198.0
P-269	Ç-2.2	J-232	J-235	2,200	169.65	Steel	0.25	0	1,198.0
P-270	Ç-2.2	J-235	J-237	2,200	147.24	Steel	0.25	0	1,198.0
P-271	Ç-2.2	J-237	J-239	2,200	288.01	Steel	0.25	0	1,198.0
P-272	Ç-2.2	J-239	J-241	2,200	381.84	Steel	0.25	0	1,198.0
P-273	Ç-2.2	J-241	J-243	2,200	156.00	Steel	0.25	0	1,198.0
P-274	Ç-2.2	J-243	J-245	2,200	597.21	Steel	0.25	0	1,198.0
P-275	Ç-2.2	J-245	J-247	2,200	191.67	Steel	0.25	0	1,198.0
P-276	Ç-2.2	J-247	J-250	2,200	156.00	Steel	0.25	0	1,198.0
P-277	Ç-2.2	J-250	J-252	2,200	254.07	Steel	0.25	0	1,198.0
P-278	Ç-2.2	J-252	J-255	2,200	330.97	Steel	0.25	0	1,198.0
P-279	Ç-2.2	J-255	J-257	2,200	666.68	Steel	0.25	0	1,198.0
P-280	Ç-2.2	J-257	J-263	2,200	578.29	Steel	0.25	0	1,198.0
P-281	Ç-2.2	J-263	J-266	2,200	123.21	Steel	0.25	0	1,198.0
P-282	Ç-2.2	J-266	J-269	2,200	146.25	Steel	0.25	0	1,198.0

Table F.1 cont.'d

Label	Zone	Start Node	Stop Node	Diameter (mm)	Length (m)	Material	ε (mm)	Minor Loss Coefficient, K	Wave Speed, a (m/s)
P-283	Ç-2.2	J-269	J-273	2,200	592.11	Steel	0.25	0	1,198.0
P-284	Ç-2.2	J-273	J-275	2,200	332.67	Steel	0.25	0	1,198.0
P-285	Ç-2.2	J-275	J-277	2,200	120.00	Steel	0.25	0	1,198.0
P-286	Ç-2.2	J-277	J-279	2,200	72.00	Steel	0.25	0	1,198.0
P-287	Ç-2.2	J-279	J-282	2,200	146.10	Steel	0.25	0	1,198.0
P-288	Ç-2.2	J-282	J-284	2,200	127.77	Steel	0.25	0	1,198.0
P-289	Ç-2.2	J-284	J-286	2,200	234.79	Steel	0.25	0	1,198.0
P-290	Ç-2.2	J-286	J-288	2,200	140.90	Steel	0.25	0	1,198.0
P-291	Ç-2.2	J-288	J-290	2,200	83.30	Steel	0.25	0	1,198.0
P-292	Ç-2.2	J-290	J-292	2,200	69.66	Steel	0.25	0	1,198.0
P-293	Ç-2.2	J-292	J-295	2,200	217.32	Steel	0.25	0	1,198.0
P-294	Ç-2.2	J-295	J-299	2,200	801.24	Steel	0.25	0	1,198.0
P-295	Ç-2.2	J-299	J-302	2,200	244.88	Steel	0.25	0	1,198.0
P-296	Ç-2.2	J-302	J-304	2,200	147.87	Steel	0.25	0	1,198.0
P-297	Ç-2.2	J-304	J-307	2,200	72.19	Steel	0.25	0	1,198.0
P-298	Ç-2.2	J-307	J-309	2,200	89.31	Steel	0.25	0	1,198.0
P-299	Ç-2.2	J-309	J-311	2,200	71.34	Steel	0.25	0	1,198.0
P-300	Ç-2.2	J-311	J-314	2,200	480.23	Steel	0.25	0	1,198.0
P-301	Ç-2.2	J-314	J-316	2,200	417.18	Steel	0.25	0	1,198.0
P-302	Ç-2.2	J-316	J-318	2,200	147.72	Steel	0.25	0	1,198.0
P-303	Ç-2.2	J-318	J-321	2,200	161.53	Steel	0.25	0	1,198.0
P-304	Ç-2.2	J-321	J-323	2,200	146.05	Steel	0.25	0	1,198.0
P-305	Ç-2.2	J-323	J-325	2,200	132.00	Steel	0.25	0	1,198.0
P-306	Ç-2.2	J-325	J-329	2,200	638.66	Steel	0.25	0	1,198.0
P-307	Ç-2.2	J-329	J-332	2,200	293.31	Steel	0.25	0	1,198.0
P-308	Ç-2.2	J-332	J-335	2,200	230.60	Steel	0.25	0	1,198.0
P-309	Ç-2.2	J-335	J-338	2,200	301.40	Steel	0.25	0	1,198.0
P-310	Ç-2.2	J-338	J-340	2,200	172.82	Steel	0.25	0	1,198.0
P-311	Ç-2.2	J-340	J-342	2,200	159.30	Steel	0.25	0	1,198.0
P-312	Ç-2.2	J-342	J-344	2,200	105.23	Steel	0.25	0	1,198.0
P-313	Ç-2.2	J-344	J-347	2,200	50.67	Steel	0.25	0	1,198.0
P-314	Ç-2.2	J-347	J-349	2,200	182.62	Steel	0.25	0	1,198.0
P-315	Ç-2.2	J-349	J-352	2,200	112.27	Steel	0.25	0	1,198.0
P-316	Ç-2.2	J-352	J-355	2,200	166.25	Steel	0.25	0	1,198.0
P-317	Ç-2.2	J-355	J-357	2,200	186.67	Steel	0.25	0	1,198.0
P-318	Ç-2.2	J-357	J-360	2,200	215.92	Steel	0.25	0	1,198.0
P-319	Ç-2.2	J-360	J-363	2,200	210.60	Steel	0.25	0	1,198.0
P-320	Ç-2.2	J-363	J-365	2,200	181.87	Steel	0.25	0	1,198.0

Table F.1 cont.'d

Label	Zone	Start Node	Stop Node	Diameter (mm)	Length (m)	Material	ε (mm)	Minor Loss Coefficient, K	Wave Speed, a (m/s)
P-321	Ç-2.2	J-365	J-367	2,200	60.85	Steel	0.25	0	1,198.0
P-322	Ç-2.2	J-367	J-369	2,200	110.55	Steel	0.25	0	1,198.0
P-323	Ç-2.2	J-369	J-371	2,200	228.00	Steel	0.25	0	1,198.0
P-324	Ç-2.2	J-371	J-375	2,200	288.00	Steel	0.25	0	1,198.0
P-325	Ç-2.2	J-375	J-377	2,200	108.00	Steel	0.25	0	1,198.0
P-326	Ç-2.2	J-377	J-381	2,200	530.45	Steel	0.25	0	1,198.0
P-327	Ç-2.2	J-381	J-383	2,200	266.35	Steel	0.25	0	1,198.0
P-328	Ç-2.2	J-383	J-386	2,200	170.75	Steel	0.25	0	1,198.0
P-329	Ç-2.2	J-386	J-388	2,200	229.30	Steel	0.25	0	1,198.0
P-330	Ç-2.2	J-388	J-390	2,200	132.00	Steel	0.25	0	1,198.0
P-331	Ç-2.2	J-390	J-394	2,200	495.50	Steel	0.25	0	1,198.0
P-332	Ç-2.2	J-394	J-398	2,200	540.00	Steel	0.25	0	1,198.0
P-333	Ç-2.2	J-398	J-401	2,200	144.00	Steel	0.25	0	1,198.0
P-334	Ç-2.2	J-401	J-403	2,200	48.00	Steel	0.25	0	1,198.0
P-335	Ç-2.2	J-403	J-405	2,200	108.00	Steel	0.25	0	1,198.0
P-336	Ç-2.2	J-405	J-407	2,200	228.00	Steel	0.25	0	1,198.0
P-337	Ç-2.2	J-407	J-410	2,200	216.00	Steel	0.25	0	1,198.0
P-338	Ç-2.2	J-410	J-412	2,200	192.00	Steel	0.25	0	1,198.0
P-339	Ç-2.2	J-412	J-414	2,200	108.00	Steel	0.25	0	1,198.0
P-340	Ç-2.2	J-414	J-416	2,200	84.00	Steel	0.25	0	1,198.0
P-341	Ç-2.2	J-416	J-419	2,200	358.05	Steel	0.25	0	1,198.0
P-342	Ç-2.2	J-419	J-422	2,200	173.48	Steel	0.25	0	1,198.0
P-343	Ç-2.2	J-422	J-424	2,200	43.87	Steel	0.25	0	1,198.0
P-344	Ç-2.2	J-424	J-426	2,200	376.79	Steel	0.25	0	1,198.0
P-345	Ç-2.2	J-426	J-429	2,200	132.00	Steel	0.25	0	1,198.0
P-346	Ç-2.2	J-429	J-431	2,200	88.06	Steel	0.25	0	1,198.0
P-347	Ç-2.2	J-431	J-433	2,200	153.56	Steel	0.25	0	1,198.0
P-348	Ç-2.2	J-433	J-435	2,200	151.19	Steel	0.25	0	1,198.0
P-349	Ç-2.2	J-435	J-437	2,200	197.83	Steel	0.25	0	1,198.0
P-350	Ç-2.2	J-437	J-440	2,200	147.62	Steel	0.25	0	1,198.0
P-351	Ç-2.2	J-440	J-444	2,200	313.97	Steel	0.25	0	1,198.0
P-352	Ç-2.2	J-444	J-447	2,200	232.79	Steel	0.25	0	1,198.0
P-353	Ç-2.2	J-447	J-449	2,200	326.25	Steel	0.25	0	1,198.0
P-354	Ç-2.2	J-449	J-451	2,200	108.00	Steel	0.25	0	1,198.0
P-355	Ç-2.2	J-451	J-453	2,200	170.30	Steel	0.25	0	1,198.0
P-356	Ç-2.2	J-453	J-455	2,200	129.20	Steel	0.25	0	1,198.0
P-357	Ç-2.2	J-455	J-457	2,200	350.80	Steel	0.25	0	1,198.0
P-358	Ç-2.2	J-457	J-459	2,200	84.00	Steel	0.25	0	1,198.0

Table F.1 cont.'d

Label	Zone	Start Node	Stop Node	Diameter (mm)	Length (m)	Material	ε (mm)	Minor Loss Coefficient, K	Wave Speed, a (m/s)
P-359	Ç-2.2	J-459	J-461	2,200	110.45	Steel	0.25	0	1,198.0
P-360	Ç-2.2	J-461	J-465	2,200	540.00	Steel	0.25	0	1,198.0
P-361	Ç-2.2	J-465	J-467	2,200	410.45	Steel	0.25	0	1,198.0
P-362	Ç-2.2	J-467	J-469	2,200	372.00	Steel	0.25	0	1,198.0
P-363	Ç-2.2	J-469	J-471	2,200	248.50	Steel	0.25	0	1,198.0
P-364	Ç-2.2	J-471	İvedik-2	2,200	297.94	Steel	0.25	3.172	1,198.0
P-365	IWTP-2	İvedik-2	LJ-2.2	1,600	24.71	Steel	0.25	0	1,076.3
P-366	IWTP-2	İvedik-2	LJ-2.1	1,600	24.71	Steel	0.25	0	1,076.3
P-367	Ç-3.2	J-186	J-188	2,200	131.40	Steel	0.25	0	1,198.0
P-368	Ç-3.2	J-188	J-190	2,200	159.69	Steel	0.25	0	1,198.0
P-369	Ç-3.2	J-190	J-193	2,200	187.05	Steel	0.25	0	1,198.0
P-370	Ç-3.2	J-193	J-196	2,200	113.63	Steel	0.25	0	1,198.0
P-371	Ç-3.2	J-196	J-198	2,200	586.59	Steel	0.25	0	1,198.0
P-372	Ç-3.2	J-198	J-200	2,200	471.11	Steel	0.25	0	1,198.0
P-373	Ç-3.2	J-200	J-202	2,200	902.76	Steel	0.25	0	1,198.0
P-374	Ç-3.2	J-202	J-205	2,200	346.82	Steel	0.25	0	1,198.0
P-375	Ç-3.2	J-205	J-207	2,200	418.65	Steel	0.25	0	1,198.0
P-376	Ç-3.2	J-207	J-209	2,200	547.76	Steel	0.25	0	1,198.0
P-377	Ç-3.2	J-209	J-211	2,200	847.94	Steel	0.25	0	1,198.0
P-378	Ç-3.2	J-211	J-213	2,200	1,065.92	Steel	0.25	0	1,198.0
P-379	Ç-3.2	J-213	J-215	2,200	697.32	Steel	0.25	0	1,198.0
P-380	Ç-3.2	J-215	J-217	2,200	144.19	Steel	0.25	0	1,198.0
P-381	Ç-3.2	J-217	J-221	2,200	1,075.59	Steel	0.25	0	1,198.0
P-382	Ç-3.2	J-221	J-225	2,200	709.00	Steel	0.25	0	1,198.0
P-383	Ç-3.2	J-225	J-228	2,200	65.96	Steel	0.25	0	1,198.0
P-384	Ç-3.2	J-228	J-230	2,200	192.40	Steel	0.25	0	1,198.0
P-385	Ç-3.2	J-230	J-233	2,200	54.35	Steel	0.25	0	1,198.0
P-386	Ç-3.2	J-233	J-236	2,200	169.65	Steel	0.25	0	1,198.0
P-387	Ç-3.2	J-236	J-238	2,200	147.24	Steel	0.25	0	1,198.0
P-388	Ç-3.2	J-238	J-240	2,200	288.01	Steel	0.25	0	1,198.0
P-389	Ç-3.2	J-240	J-242	2,200	381.84	Steel	0.25	0	1,198.0
P-390	Ç-3.2	J-242	J-244	2,200	156.00	Steel	0.25	0	1,198.0
P-391	Ç-3.2	J-244	J-246	2,200	597.21	Steel	0.25	0	1,198.0
P-392	Ç-3.2	J-246	J-248	2,200	191.67	Steel	0.25	0	1,198.0
P-393	Ç-3.2	J-248	J-251	2,200	156.00	Steel	0.25	0	1,198.0
P-394	Ç-3.2	J-251	J-253	2,200	254.07	Steel	0.25	0	1,198.0
P-395	Ç-3.2	J-253	J-256	2,200	330.97	Steel	0.25	0	1,198.0
P-396	Ç-3.2	J-256	J-258	2,200	666.68	Steel	0.25	0	1,198.0

Table F.1 cont.'d

Label	Zone	Start Node	Stop Node	Diameter (mm)	Length (m)	Material	ε (mm)	Minor Loss Coefficient, K	Wave Speed, a (m/s)
P-397	Ç-3.2	J-258	J-264	2,200	578.29	Steel	0.25	0	1,198.0
P-398	Ç-3.2	J-264	J-267	2,200	123.21	Steel	0.25	0	1,198.0
P-399	Ç-3.2	J-267	J-270	2,200	146.25	Steel	0.25	0	1,198.0
P-400	Ç-3.2	J-270	J-274	2,200	592.11	Steel	0.25	0	1,198.0
P-401	Ç-3.2	J-274	J-276	2,200	332.67	Steel	0.25	0	1,198.0
P-402	Ç-3.2	J-276	J-278	2,200	120.00	Steel	0.25	0	1,198.0
P-403	Ç-3.2	J-278	J-280	2,200	72.00	Steel	0.25	0	1,198.0
P-404	Ç-3.2	J-280	J-283	2,200	146.10	Steel	0.25	0	1,198.0
P-405	Ç-3.2	J-283	J-285	2,200	127.77	Steel	0.25	0	1,198.0
P-406	Ç-3.2	J-285	J-287	2,200	234.79	Steel	0.25	0	1,198.0
P-407	Ç-3.2	J-287	J-289	2,200	140.90	Steel	0.25	0	1,198.0
P-408	Ç-3.2	J-289	J-291	2,200	83.30	Steel	0.25	0	1,198.0
P-409	Ç-3.2	J-291	J-293	2,200	69.66	Steel	0.25	0	1,198.0
P-410	Ç-3.2	J-293	J-296	2,200	217.32	Steel	0.25	0	1,198.0
P-411	Ç-3.2	J-296	J-300	2,200	801.24	Steel	0.25	0	1,198.0
P-412	Ç-3.2	J-300	J-303	2,200	244.88	Steel	0.25	0	1,198.0
P-413	Ç-3.2	J-303	J-305	2,200	147.87	Steel	0.25	0	1,198.0
P-414	Ç-3.2	J-305	J-308	2,200	72.19	Steel	0.25	0	1,198.0
P-415	Ç-3.2	J-308	J-310	2,200	89.31	Steel	0.25	0	1,198.0
P-416	Ç-3.2	J-310	J-312	2,200	71.34	Steel	0.25	0	1,198.0
P-417	Ç-3.2	J-312	J-315	2,200	480.23	Steel	0.25	0	1,198.0
P-418	Ç-3.2	J-315	J-317	2,200	417.18	Steel	0.25	0	1,198.0
P-419	Ç-3.2	J-317	J-319	2,200	147.72	Steel	0.25	0	1,198.0
P-420	Ç-3.2	J-319	J-322	2,200	161.53	Steel	0.25	0	1,198.0
P-421	Ç-3.2	J-322	J-324	2,200	146.05	Steel	0.25	0	1,198.0
P-422	Ç-3.2	J-324	J-326	2,200	132.00	Steel	0.25	0	1,198.0
P-423	Ç-3.2	J-326	J-330	2,200	638.66	Steel	0.25	0	1,198.0
P-424	Ç-3.2	J-330	J-333	2,200	293.31	Steel	0.25	0	1,198.0
P-425	Ç-3.2	J-333	J-336	2,200	230.60	Steel	0.25	0	1,198.0
P-426	Ç-3.2	J-336	J-339	2,200	301.40	Steel	0.25	0	1,198.0
P-427	Ç-3.2	J-339	J-341	2,200	172.82	Steel	0.25	0	1,198.0
P-428	Ç-3.2	J-341	J-343	2,200	159.30	Steel	0.25	0	1,198.0
P-429	Ç-3.2	J-343	J-345	2,200	105.23	Steel	0.25	0	1,198.0
P-430	Ç-3.2	J-345	J-348	2,200	50.67	Steel	0.25	0	1,198.0
P-431	Ç-3.2	J-348	J-350	2,200	182.62	Steel	0.25	0	1,198.0
P-432	Ç-3.2	J-350	J-353	2,200	112.27	Steel	0.25	0	1,198.0
P-433	Ç-3.2	J-353	J-356	2,200	166.25	Steel	0.25	0	1,198.0
P-434	Ç-3.2	J-356	J-358	2,200	186.67	Steel	0.25	0	1,198.0

Table F.1 cont.'d

Label	Zone	Start Node	Stop Node	Diameter (mm)	Length (m)	Material	ε (mm)	Minor Loss Coefficient, K	Wave Speed, a (m/s)
P-435	Ç-3.2	J-358	J-361	2,200	215.92	Steel	0.25	0	1,198.0
P-436	Ç-3.2	J-361	J-364	2,200	210.60	Steel	0.25	0	1,198.0
P-437	Ç-2.2	J-364	J-366	2,200	181.87	Steel	0.25	0	1,198.0
P-438	Ç-3.2	J-366	J-368	2,200	60.85	Steel	0.25	0	1,198.0
P-439	Ç-3.2	J-368	J-370	2,200	110.55	Steel	0.25	0	1,198.0
P-440	Ç-3.2	J-370	J-372	2,200	228.00	Steel	0.25	0	1,198.0
P-441	Ç-3.2	J-372	J-376	2,200	288.00	Steel	0.25	0	1,198.0
P-442	Ç-3.2	J-376	J-378	2,200	108.00	Steel	0.25	0	1,198.0
P-443	Ç-3.2	J-378	J-382	2,200	530.45	Steel	0.25	0	1,198.0
P-444	Ç-3.2	J-382	J-384	2,200	266.35	Steel	0.25	0	1,198.0
P-445	Ç-3.2	J-384	J-387	2,200	170.75	Steel	0.25	0	1,198.0
P-446	Ç-3.2	J-387	J-389	2,200	229.30	Steel	0.25	0	1,198.0
P-447	Ç-3.2	J-389	J-391	2,200	132.00	Steel	0.25	0	1,198.0
P-448	Ç-3.2	J-391	J-395	2,200	495.50	Steel	0.25	0	1,198.0
P-449	Ç-3.2	J-395	J-399	2,200	540.00	Steel	0.25	0	1,198.0
P-450	Ç-3.2	J-399	J-402	2,200	144.00	Steel	0.25	0	1,198.0
P-451	Ç-3.2	J-402	J-404	2,200	48.00	Steel	0.25	0	1,198.0
P-452	Ç-3.2	J-404	J-406	2,200	108.00	Steel	0.25	0	1,198.0
P-453	Ç-3.2	J-406	J-408	2,200	228.00	Steel	0.25	0	1,198.0
P-454	Ç-3.2	J-408	J-411	2,200	216.00	Steel	0.25	0	1,198.0
P-455	Ç-3.2	J-411	J-413	2,200	192.00	Steel	0.25	0	1,198.0
P-456	Ç-3.2	J-413	J-415	2,200	108.00	Steel	0.25	0	1,198.0
P-457	Ç-3.2	J-415	J-417	2,200	84.00	Steel	0.25	0	1,198.0
P-458	Ç-3.2	J-417	J-420	2,200	358.05	Steel	0.25	0	1,198.0
P-459	Ç-3.2	J-420	J-423	2,200	173.48	Steel	0.25	0	1,198.0
P-460	Ç-3.2	J-423	J-425	2,200	43.87	Steel	0.25	0	1,198.0
P-461	Ç-3.2	J-425	J-427	2,200	376.79	Steel	0.25	0	1,198.0
P-462	Ç-3.2	J-427	J-430	2,200	132.00	Steel	0.25	0	1,198.0
P-463	Ç-3.2	J-430	J-432	2,200	88.06	Steel	0.25	0	1,198.0
P-464	Ç-3.2	J-432	J-434	2,200	153.56	Steel	0.25	0	1,198.0
P-465	Ç-3.2	J-434	J-436	2,200	151.19	Steel	0.25	0	1,198.0
P-466	Ç-3.2	J-436	J-438	2,200	197.83	Steel	0.25	0	1,198.0
P-467	Ç-3.2	J-438	J-441	2,200	147.62	Steel	0.25	0	1,198.0
P-468	Ç-3.2	J-441	J-445	2,200	313.97	Steel	0.25	0	1,198.0
P-469	Ç-3.2	J-445	J-448	2,200	232.79	Steel	0.25	0	1,198.0
P-470	Ç-3.2	J-448	J-450	2,200	326.25	Steel	0.25	0	1,198.0
P-471	Ç-3.2	J-450	J-452	2,200	108.00	Steel	0.25	0	1,198.0

Table F.1 cont.'d

Label	Zone	Start Node	Stop Node	Diameter (mm)	Length (m)	Material	ε (mm)	Minor Loss Coefficient, K	Wave Speed, a (m/s)
P-472	Ç-3.2	J-452	J-454	2,200	170.30	Steel	0.25	0	1,198.0
P-473	Ç-3.2	J-454	J-456	2,200	129.20	Steel	0.25	0	1,198.0
P-474	Ç-3.2	J-456	J-458	2,200	350.80	Steel	0.25	0	1,198.0
P-475	Ç-3.2	J-458	J-460	2,200	84.00	Steel	0.25	0	1,198.0
P-476	Ç-3.2	J-460	J-462	2,200	110.45	Steel	0.25	0	1,198.0
P-477	Ç-3.2	J-462	J-466	2,200	540.00	Steel	0.25	0	1,198.0
P-478	Ç-3.2	J-466	J-468	2,200	410.45	Steel	0.25	0	1,198.0
P-479	Ç-3.2	J-468	J-470	2,200	372.00	Steel	0.25	0	1,198.0
P-480	Ç-3.2	J-470	J-472	2,200	248.50	Steel	0.25	0	1,198.0
P-481	Ç-3.2	J-472	İvedik-3	2,200	297.94	Steel	0.25	3.172	1,198.0
P-482	IWTP-3	İvedik-3	LJ-3.2	1,600	24.71	Steel	0.25	0	1,076.3
P-483	IWTP-3	İvedik-3	LJ-3.1	1,600	24.71	Steel	0.25	0	1,076.3
P-484	IWTP-1	LJ-1.1	R-1.1	1,600	10.00	Steel	0.25	0.219	1,076.3
P-485	IWTP-1	LJ-1.2	R-1.2	1,600	10.00	Steel	0.25	0.219	1,076.3
P-486	IWTP-2	LJ-2.1	R-2.1	1,600	10.00	Steel	0.25	0.219	1,076.3
P-487	IWTP-2	LJ-2.2	R-2.2	1,600	10.00	Steel	0.25	0.219	1,076.3
P-488	IWTP-3	LJ-3.1	R-3.1	1,600	10.00	Steel	0.25	0.219	1,076.3
P-489	IWTP-3	LJ-3.2	R-3.2	1,600	10.00	Steel	0.25	0.219	1,076.3
P-490	Ç-1.1	TCV-2	J-8	1,600	6.70	Steel	0.25	0.042	1,076.3
P-491	Ç-2.1	TCV-3	J-9	1,600	6.70	Steel	0.25	0.042	1,076.3
P-492	Ç-3.1	TCV-1	J-10	1,600	6.70	Steel	0.25	0.042	1,076.3
P-493	Ç-1.1	TCV-4	T3-Start	1,600	18.01	Steel	0.25	0.085	1,076.3
P-494	Ç-2.1	TCV-5	T3-Start	1,600	18.01	Steel	0.25	0.085	1,076.3
P-495	Ç-3.1	TCV-6	T3-Start	1,600	18.01	Steel	0.25	0.085	1,076.3
P-496	Ç-1.2	TCV-9	J-183	1,600	6.70	Steel	0.25	0.200	1,076.3
P-497	Ç-2.2	TCV-7	J-182	1,600	6.70	Steel	0.25	0.200	1,076.3
P-498	Ç-3.2	TCV-8	J-184	1,600	6.70	Steel	0.25	0.200	1,076.3

Table F.2 Junction inputs of Hammer analysis model

Junction Label	Position (m)	Elevation (m)
J-1	1.000,00	941,00
T1-End	***4.277,10***	***844,02***
T2-Start	***4.571,66***	***844,02***
J-4	4.963,16	866,93
J-5	6.210,14	939,92
J-6	7.012,66	939,17
T2-End	***7.394,67***	***938,80***
J-8	7.419,38	938,80
J-9	7.419,38	938,80
J-10	7.419,38	938,80
J-11	7.611,38	933,00
J-12	7.611,38	933,00
J-13	7.731,38	930,90
J-14	7.731,38	930,90
J-15	7.839,38	924,87
J-16	7.839,38	924,87
J-17	7.935,38	914,84
J-18	7.935,38	914,84
J-19	7.995,38	908,12
J-20	7.995,38	908,12
J-21	8.031,38	905,90
J-22	8.031,38	905,90
J-23	8.091,38	901,88
J-24	8.091,38	901,88
J-25	8.187,38	897,54
J-26	8.187,38	897,54
J-27	8.283,38	893,45
J-28	8.283,38	893,45
J-29	8.370,38	884,81
J-30	8.427,38	889,69

Junction Label	Position (m)	Elevation (m)
J-31	8.427,38	889,69
J-32	8.641,86	885,10
J-33	8.641,86	885,10
J-34	8.762,56	886,11
J-35	8.897,47	881,80
J-36	8.897,47	881,80
J-37	9.037,44	869,25
J-38	9.037,44	869,25
J-39	9.043,00	855,84
J-40	9.181,83	865,38
J-41	9.181,83	865,38
J-42	9.210,83	864,73
J-43	9.210,83	864,73
J-44	9.319,30	862,95
J-45	9.319,30	862,95
J-46	9.405,44	847,70
J-47	9.405,44	847,70
J-48	9.543,94	814,44
J-49	9.543,94	814,44
J-50	9.557,37	811,65
J-51	9.557,37	811,65
J-52	9.600,68	795,65
J-53	9.645,15	797,45
J-54	9.645,15	797,45
J-55	9.675,39	789,95
J-56	9.675,39	789,95
J-57	9.738,52	780,77
J-58	9.775,74	780,93
J-59	9.775,74	780,93
J-60	9.839,08	780,29

Table F.2 cont.'d

Junction Label	Position (m)	Elevation (m)
J-61	9,839.08	780.29
J-62	9,868.02	779.04
J-63	9,940.26	779.21
J-64	9,940.26	779.21
J-65	10,082.02	778.12
J-66	10,124.23	778.16
J-67	10,124.23	778.16
J-68	10,188.34	780.08
J-69	10,188.34	780.08
J-70	10,253.90	780.68
J-71	10,253.90	780.68
J-72	10,316.53	780.53
J-73	10,316.53	780.53
J-74	10,401.15	782.94
J-75	10,401.15	782.94
J-76	10,458.06	784.90
J-77	10,458.06	784.90
J-78	10,638.39	787.55
J-79	10,638.39	787.55
J-80	10,863.69	796.87
J-81	10,868.97	797.57
J-82	10,868.97	797.57
J-83	10,929.92	792.74
J-84	10,940.63	793.97
J-85	10,940.63	793.97
J-86	10,967.03	793.62
J-87	10,967.03	793.62
J-88	11,209.54	800.02
J-89	11,209.54	800.02
J-90	11,245.14	801.83

Junction Label	Position (m)	Elevation (m)
J-91	11,245.14	801.83
J-92	11,443.39	805.32
J-93	11,458.89	806.66
J-94	11,458.89	806.66
J-95	11,509.69	808.13
J-96	11,509.69	808.13
J-97	11,596.59	810.90
J-98	11,677.69	813.99
J-99	11,677.69	813.99
J-100	11,713.33	815.74
J-101	11,713.33	815.74
J-102	11,767.09	818.19
J-103	11,767.09	818.19
J-104	11,809.12	820.43
J-105	11,809.12	820.43
J-106	11,871.08	818.12
J-107	11,871.08	818.12
J-108	11,919.76	820.37
J-109	11,919.76	820.37
J-110	11,968.43	824.16
J-111	11,968.43	824.16
J-112	12,109.83	828.89
J-113	12,109.83	828.89
J-114	12,181.83	833.39
J-115	12,181.83	833.39
J-116	12,267.32	834.97
J-117	12,267.32	834.97
J-118	12,348.70	835.68
J-119	12,348.70	835.68
J-120	12,439.66	839.08

Table F.2 cont.'d

Junction Label	Position (m)	Elevation (m)
J-121	12,439.66	839.08
J-122	12,517.88	841.56
J-123	12,517.88	841.56
J-124	12,676.60	846.38
J-125	12,676.60	846.38
J-126	12,759.01	849.61
J-127	12,759.01	849.61
J-128	12,839.76	854.71
J-129	12,839.76	854.71
J-130	12,990.21	859.62
J-131	12,990.21	859.62
J-132	13,000.40	859.79
J-133	13,000.40	859.79
J-134	13,068.40	860.97
J-135	13,068.40	860.97
J-136	13,176.87	866.62
J-137	13,176.87	866.62
J-138	13,200.17	868.33
J-139	13,200.17	868.33
J-140	13,279.11	877.46
J-141	13,279.11	877.46
J-142	13,358.20	881.76
J-143	13,358.20	881.76
J-144	13,429.09	882.36
J-145	13,429.09	882.36
J-146	13,499.62	887.39
J-147	13,499.62	887.39
J-148	13,512.20	888.53
J-149	13,512.20	888.53
J-150	13,569.44	893.41

Junction Label	Position (m)	Elevation (m)
J-151	13,569.44	893.41
J-152	13,572.47	882.82
J-153	13,599.12	891.32
J-154	13,599.12	891.32
J-155	13,621.82	895.28
J-156	13,621.82	895.28
J-157	13,639.12	898.04
J-158	13,639.12	898.04
J-159	13,778.87	932.24
J-160	13,778.87	932.24
J-161	13,804.10	934.08
J-162	13,804.10	934.08
J-163	13,827.17	933.57
J-164	13,912.80	929.27
J-165	13,912.80	929.27
J-166	13,938.42	928.61
J-167	13,938.42	928.61
J-168	14,026.61	921.93
J-169	14,061.76	925.96
J-170	14,061.76	925.96
J-171	14,070.06	926.14
J-172	14,070.06	926.14
J-173	14,115.89	927.98
J-174	14,115.89	927.98
J-175	14,176.43	928.95
J-176	14,176.43	928.95
J-177	14,176.43	928.95
T3-Start	***14,201.14***	***928.95***
J-179	21,430.17	939.80
J-180	30,025.04	929.40

Table F.2 cont.'d

Junction Label	Position (m)	Elevation (m)
T3-End	***30,563.04***	***928.76***
J-182	30,587.75	928.76
J-183	30,587.75	928.76
J-184	30,587.75	928.76
J-185	30,697.04	928.25
J-186	30,697.04	928.25
J-187	30,828.44	923.92
J-188	30,828.44	923.92
J-189	30,988.13	921.17
J-190	30,988.13	921.17
J-191	31,171.71	919.21
J-192	31,175.18	920.19
J-193	31,175.18	920.19
J-194	31,271.03	925.10
J-195	31,288.81	925.08
J-196	31,288.81	925.08
J-197	31,875.40	907.61
J-198	31,875.40	907.61
J-199	32,346.51	898.34
J-200	32,346.51	898.34
J-201	33,249.27	877.57
J-202	33,249.27	877.57
J-203	33,264.45	875.74
J-204	33,596.09	873.77
J-205	33,596.09	873.77
J-206	34,014.74	860.81
J-207	34,014.74	860.81
J-208	34,562.50	854.37
J-209	34,562.50	854.37
J-210	35,410.44	847.32

Junction Label	Position (m)	Elevation (m)
J-211	35,410.44	847.32
J-212	36,476.36	840.27
J-213	36,476.36	840.27
J-214	37,173.68	834.57
J-215	37,173.68	834.57
J-216	37,317.87	830.03
J-217	37,317.87	830.03
J-218	37,560.51	828.08
J-219	37,765.95	828.49
J-220	38,393.46	826.37
J-221	38,393.46	826.37
J-222	38,698.60	824.39
J-223	39,100.31	825.18
J-224	39,102.46	824.20
J-225	39,102.46	824.20
J-226	39,136.63	815.95
J-227	39,168.42	816.03
J-228	39,168.42	816.03
J-229	39,360.82	815.55
J-230	39,360.82	815.55
J-231	39,395.20	815.33
J-232	39,415.17	823.09
J-233	39,415.17	823.09
J-234	39,437.73	823.89
J-235	39,584.82	823.68
J-236	39,584.82	823.68
J-237	39,732.06	824.97
J-238	39,732.06	824.97
J-239	40,020.07	823.52
J-240	40,020.07	823.52

Table F.2 cont.'d

Junction Label	Position (m)	Elevation (m)
J-241	40,401.91	824.50
J-242	40,401.91	824.50
J-243	40,557.91	824.23
J-244	40,557.91	824.23
J-245	41,155.12	820.05
J-246	41,155.12	820.05
J-247	41,346.79	821.86
J-248	41,346.79	821.86
J-249	41,399.41	861.12
J-250	41,502.79	821.12
J-251	41,502.79	821.12
J-252	41,756.86	822.44
J-253	41,756.86	822.44
J-254	41,785.76	838.85
J-255	42,087.83	819.55
J-256	42,087.83	819.55
J-257	42,754.51	817.01
J-258	42,754.51	817.01
J-259	42,892.74	868.60
J-260	42,984.46	863.10
J-261	43,024.90	867.60
J-262	43,074.84	863.29
J-263	43,332.80	812.11
J-264	43,332.80	812.11
J-265	43,421.57	871.00
J-266	43,456.01	813.00
J-267	43,456.01	813.00
J-268	43,550.77	867.62
J-269	43,602.26	811.99
J-270	43,602.26	811.99

Junction Label	Position (m)	Elevation (m)
J-271	43,814.06	894.33
J-272	44,082.38	874.38
J-273	44,194.37	811.00
J-274	44,194.37	811.00
J-275	44,527.04	819.94
J-276	44,527.04	819.94
J-277	44,647.04	825.97
J-278	44,647.04	825.97
J-279	44,719.04	827.21
J-280	44,719.04	827.21
J-281	44,742.49	906.63
J-282	44,865.14	821.41
J-283	44,865.14	821.41
J-284	44,992.91	820.52
J-285	44,992.91	820.52
J-286	45,227.70	822.94
J-287	45,227.70	822.94
J-288	45,368.60	833.71
J-289	45,368.60	833.71
J-290	45,451.90	829.25
J-291	45,451.90	829.25
J-292	45,521.56	828.38
J-293	45,521.56	828.38
J-294	45,594.28	877.43
J-295	45,738.88	830.09
J-296	45,738.88	830.09
J-297	45,777.37	889.22
J-298	46,148.73	863.34
J-299	46,540.12	844.99
J-300	46,540.12	844.99

Table F.2 cont.'d

Junction Label	Position (m)	Elevation (m)
J-301	46,570.75	905.39
J-302	46,785.00	856.18
J-303	46,785.00	856.18
J-304	46,932.87	852.14
J-305	46,932.87	852.14
J-306	46,992.26	880.53
J-307	47,005.06	853.37
J-308	47,005.06	853.37
J-309	47,094.37	861.35
J-310	47,094.37	861.35
J-311	47,165.71	855.72
J-312	47,165.71	855.72
J-313	47,448.73	919.07
J-314	47,645.94	867.37
J-315	47,645.94	867.37
J-316	48,063.12	884.16
J-317	48,063.12	884.16
J-318	48,210.84	905.82
J-319	48,210.84	905.82
J-320	48,324.81	881.10
J-321	48,372.37	917.85
J-322	48,372.37	917.85
J-323	48,518.42	898.69
J-324	48,518.42	898.69
J-325	48,650.42	891.28
J-326	48,650.42	891.28
J-327	48,898.53	898.20
J-328	49,219.86	881.27
J-329	49,289.08	881.36
J-330	49,289.08	881.36

Junction Label	Position (m)	Elevation (m)
J-331	49,559.05	902.51
J-332	49,582.39	890.01
J-333	49,582.39	890.01
J-334	49,688.41	893.41
J-335	49,812.99	899.07
J-336	49,812.99	899.07
J-337	50,005.38	902.33
J-338	50,114.39	881.79
J-339	50,114.39	881.79
J-340	50,287.21	889.06
J-341	50,287.21	889.06
J-342	50,446.51	903.28
J-343	50,446.51	903.28
J-344	50,551.74	894.37
J-345	50,551.74	894.37
J-346	50,561.37	866.85
J-347	50,602.41	894.03
J-348	50,602.41	894.03
J-349	50,785.03	902.11
J-350	50,785.03	902.11
J-351	50,821.57	888.79
J-352	50,897.30	901.60
J-353	50,897.30	901.60
J-354	51,049.57	865.24
J-355	51,063.55	893.52
J-356	51,063.55	893.52
J-357	51,250.22	872.17
J-358	51,250.22	872.17
J-359	51,372.91	896.96
J-360	51,466.14	869.64

Table F.2 cont.'d

Junction Label	Position (m)	Elevation (m)
J-361	51,466.14	869.64
J-362	51,663.04	886.09
J-363	51,676.74	886.75
J-364	51,676.74	886.75
J-365	51,858.61	880.38
J-366	51,858.61	880.38
J-367	51,919.46	866.49
J-368	51,919.46	866.49
J-369	52,030.01	872.79
J-370	52,030.01	872.79
J-371	52,258.01	897.84
J-372	52,258.01	897.84
J-373	52,320.90	897.79
J-374	52,544.49	893.09
J-375	52,546.01	885.90
J-376	52,546.01	885.90
J-377	52,654.01	891.71
J-378	52,654.01	891.71
J-379	52,734.52	897.50
J-380	53,016.28	874.02
J-381	53,184.46	897.66
J-382	53,184.46	897.66
J-383	53,450.81	893.07
J-384	53,450.81	893.07
J-385	53,578.30	881.61
J-386	53,621.56	898.89
J-387	53,621.56	898.89
J-388	53,850.86	875.40
J-389	53,850.86	875.40
J-390	53,982.86	874.15

Junction Label	Position (m)	Elevation (m)
J-391	53,982.86	874.15
J-392	54,252.77	874.72
J-393	54,302.35	882.23
J-394	54,478.36	881.50
J-395	54,478.36	881.50
J-396	54,653.99	873.20
J-397	54,823.21	889.07
J-398	55,018.36	876.26
J-399	55,018.36	876.26
J-400	55,097.48	869.14
J-401	55,162.36	876.07
J-402	55,162.36	876.07
J-403	55,210.36	881.20
J-404	55,210.36	881.20
J-405	55,318.36	874.39
J-406	55,318.36	874.39
J-407	55,546.36	871.97
J-408	55,546.36	871.97
J-409	55,701.69	898.09
J-410	55,762.36	884.62
J-411	55,762.36	884.62
J-412	55,954.36	869.26
J-413	55,954.36	869.26
J-414	56,062.36	873.79
J-415	56,062.36	873.79
J-416	56,146.36	874.98
J-417	56,146.36	874.98
J-418	56,217.16	889.70
J-419	56,504.41	898.66
J-420	56,504.41	898.66

Table F.2 cont.'d

Junction Label	Position (m)	Elevation (m)
J-421	56,564.31	904.60
J-422	56,677.89	892.97
J-423	56,677.89	892.97
J-424	56,721.76	892.59
J-425	56,721.76	892.59
J-426	57,098.55	889.18
J-427	57,098.55	889.18
J-428	57,200.02	879.29
J-429	57,230.55	893.03
J-430	57,230.55	893.03
J-431	57,318.61	892.03
J-432	57,318.61	892.03
J-433	57,472.17	905.15
J-434	57,472.17	905.15
J-435	57,623.36	904.70
J-436	57,623.36	904.70
J-437	57,821.19	882.99
J-438	57,821.19	882.99
J-439	57,923.63	904.61
J-440	57,968.81	880.12
J-441	57,968.81	880.12
J-442	58,107.15	898.67
J-443	58,234.97	904.69
J-444	58,282.78	883.71
J-445	58,282.78	883.71
J-446	58,424.01	890.32
J-447	58,515.57	897.60
J-448	58,515.57	897.60
J-449	58,841.82	902.81
J-450	58,841.82	902.81

Junction Label	Position (m)	Elevation (m)
J-451	58,949.82	900.32
J-452	58,949.82	900.32
J-453	59,120.12	905.29
J-454	59,120.12	905.29
J-455	59,249.32	890.37
J-456	59,249.32	890.37
J-457	59,600.12	892.40
J-458	59,600.12	892.40
J-459	59,684.12	896.57
J-460	59,684.12	896.57
J-461	59,794.57	894.52
J-462	59,794.57	894.52
J-463	59,865.95	912.15
J-464	60,236.01	902.50
J-465	60,334.57	901.90
J-466	60,334.57	901.90
J-467	60,745.02	913.51
J-468	60,745.02	913.51
J-469	61,117.02	902.21
J-470	61,117.02	902.21
J-471	61,365.52	911.14
J-472	61,365.52	911.14
İvedik-1	***61,662.96***	***913.10***
İvedik-2	***61,663.46***	***913.10***
İvedik-3	***61,663.46***	***913.10***

APPENDIX G

VALVE CLOSURE PRINCIPLES

Pattern Detailed Report: VALVE30
Licensed for Academic Use Only

Element Details			
ID	1195	Notes	
Label	VALVE30		

<Pattern Summary>			
Start Time	00:00:00	Pattern Category Type	Operational (Transient, Valve)
Starting Relative Closure	0.00 %	Pattern Format	Continuous

Transient Valve Curve

Time from Start (sec)	Relative Closure (%)
100.0	11.40
200.0	22.86
300.0	34.29
400.0	45.72
500.0	57.15
600.0	68.58
700.0	80.00
800.0	81.83
900.0	83.65
1,000.0	85.47
1,100.0	87.29
1,200.0	89.11
1,300.0	90.93
1,400.0	92.75
1,500.0	94.57
1,600.0	96.39
1,700.0	98.21
1,800.0	100.00

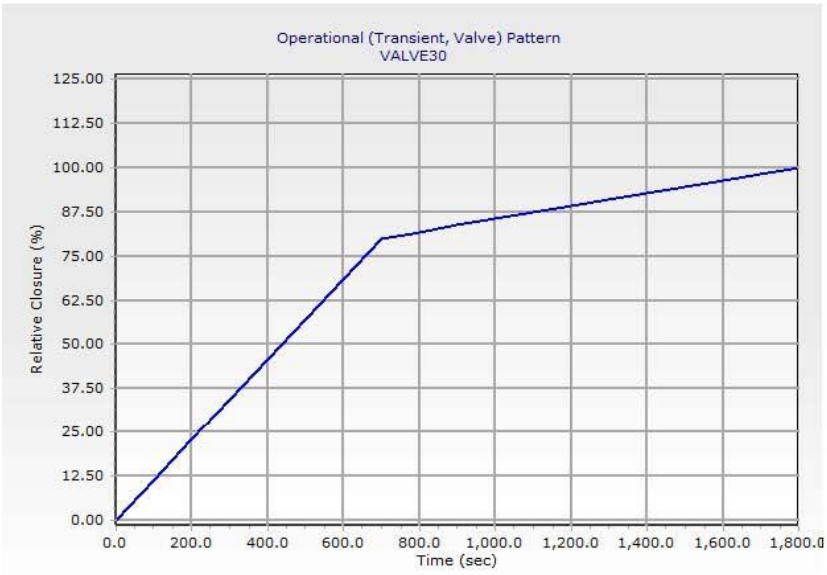

Figure G.1 VALVE30 closure principle

Pattern Detailed Report: VALVE45
Licensed for Academic Use Only

Element Details			
ID	1308	Notes	
Label	VALVE45		

<Pattern Summary>			
Start Time	00:00:00	Pattern Category Type	Operational (Transient, Valve)
Starting Relative Closure	0.00 %	Pattern Format	Continuous

Transient Valve Curve

Time from Start (sec)	Relative Closure (%)
1,500.0	77.50
2,700.0	100.00

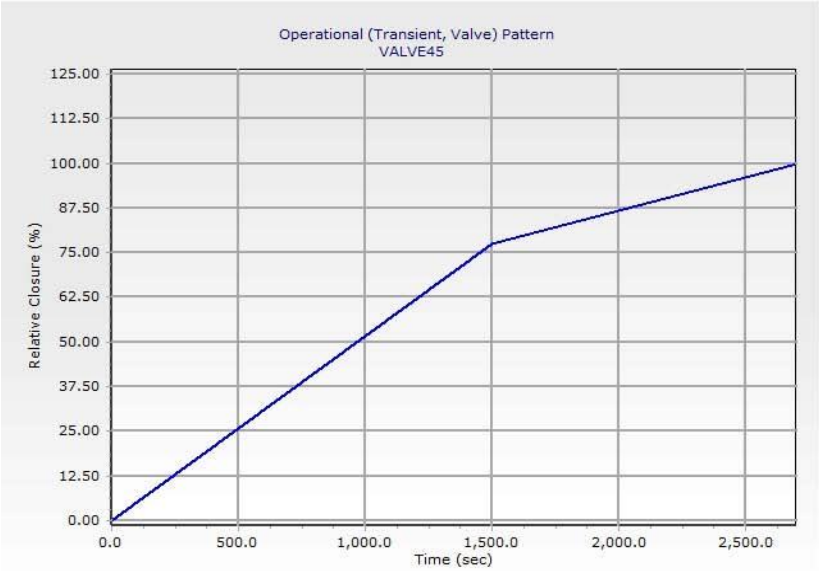

Figure G.2 VALVE45 closure principle

Pattern Detailed Report: VALVE6.5
Licensed for Academic Use Only

Element Details			
ID	1319	Notes	
Label	VALVE6.5		

<Pattern Summary>			
Start Time	00:00:00	Pattern Category Type	Operational (Transient, Valve)
Starting Relative Closure	0.00 %	Pattern Format	Continuous

Transient Valve Curve

Time from Start (sec)	Relative Closure (%)
390.0	100.00

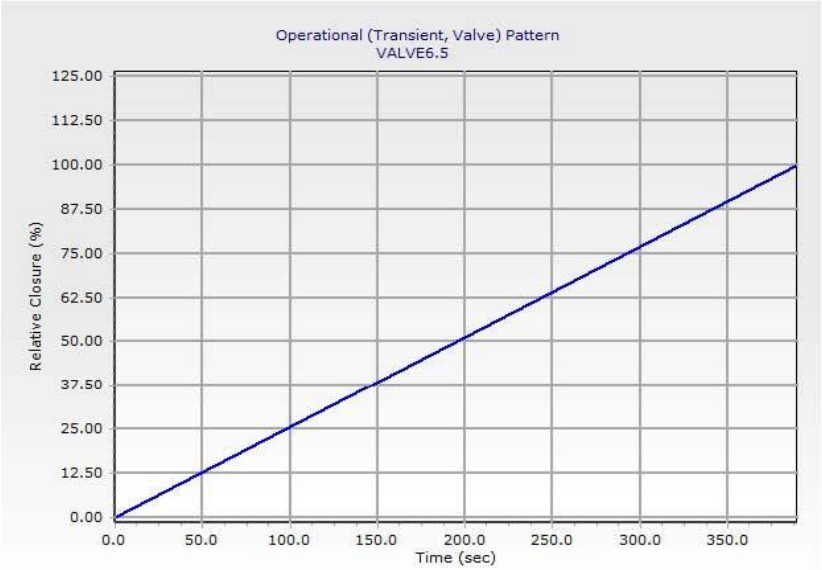

Figure G.3 VALVE6.5 closure principle

Pattern Detailed Report: FAST3
Licensed for Academic Use Only

Element Details			
ID	1210	Notes	
Label	FAST3		

<Pattern Summary>			
Start Time	00:00:00	Pattern Category Type	Operational (Transient, Valve)
Starting Relative Closure	0.00 %	Pattern Format	Continuous

Transient Valve Curve

Time from Start (sec)	Relative Closure (%)
30.0	3.50
60.0	7.00
90.0	10.50
120.0	14.00
150.0	17.50
180.0	21.00
210.0	24.50
240.0	28.00
270.0	31.50
300.0	35.00
330.0	38.50
360.0	42.00
390.0	45.50
420.0	49.00
450.0	52.50
480.0	56.00
510.0	59.50
540.0	63.00
570.0	66.50
600.0	70.00
630.0	70.75
660.0	71.50
690.0	72.25
720.0	73.00
750.0	73.75
780.0	74.50
810.0	75.25
840.0	76.00
870.0	76.75
900.0	77.50
930.0	78.25
960.0	79.00
990.0	79.75
1,020.0	80.50
1,050.0	81.25
1,080.0	82.00
1,110.0	82.75
1,140.0	83.50
1,170.0	84.25
1,200.0	85.00
1,230.0	85.75
1,260.0	86.50
1,290.0	87.25
1,320.0	88.00
1,350.0	88.75
1,380.0	89.50
1,410.0	90.25
1,440.0	91.00
1,470.0	91.75
1,500.0	92.50
1,530.0	93.25

Figure G.4 FAST3 closure principle

Pattern Detailed Report: FAST3
Licensed for Academic Use Only

Transient Valve Curve

Time from Start (sec)	Relative Closure (%)
1,560.0	94.00
1,590.0	94.75
1,620.0	95.50
1,650.0	96.25
1,680.0	97.00
1,710.0	97.75
1,740.0	98.50
1,770.0	99.25
1,800.0	100.00

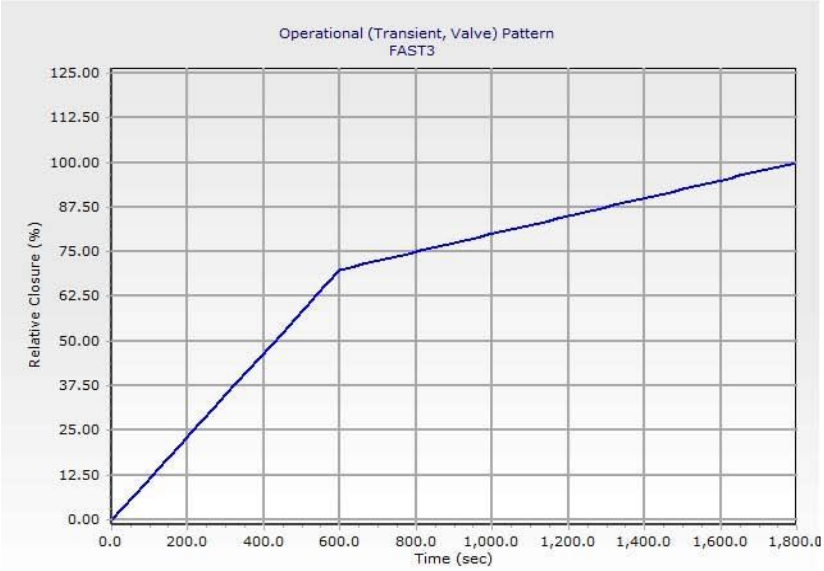

Figure G.4 FAST3 closure principle cont.'d

Pattern Detailed Report: VALVE33
Licensed for Academic Use Only

Element Details			
ID	1318	Notes	
Label	VALVE33		

<Pattern Summary>			
Start Time	00:00:00	Pattern Category Type	Operational (Transient, Valve)
Starting Relative Closure	0.00 %	Pattern Format	Continuous

Transient Valve Curve

Time from Start (sec)	Relative Closure (%)
720.0	80.00
1,980.0	100.00

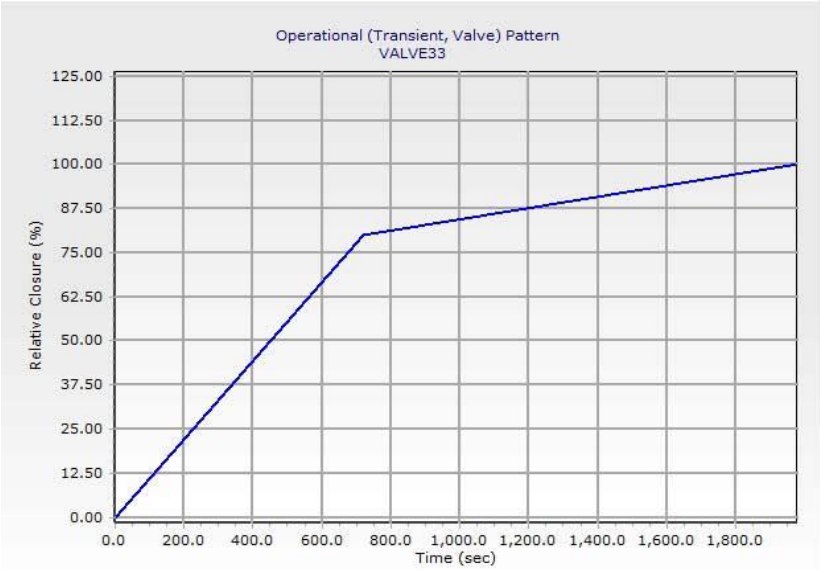

Figure G.5 VALVE33 closure principle

Pattern Detailed Report: VALVE27
Licensed for Academic Use Only

Element Details			
ID	1318	Notes	
Label	VALVE27		

<Pattern Summary>			
Start Time	00:00:00	Pattern Category Type	Operational (Transient, Valve)
Starting Relative Closure	55.00 %	Pattern Format	Continuous

Transient Valve Curve

Time from Start (sec)	Relative Closure (%)
435.0	77.50
1,635.0	100.00

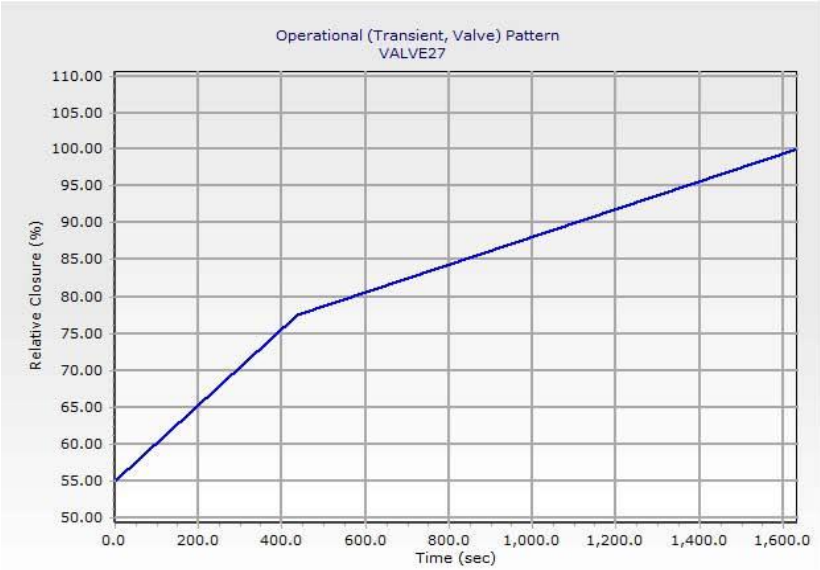

Figure G.6 VALVE27 closure principle

APPENDIX H

RESULTS OF THE SCENARIO: B4-45

Transient Calculation Summary: Base

Licensed for Academic Use Only

Transient Calculation Summary			
Time Step	0.005 sec	Specific Gravity	0.998
Number of Time Steps	600001	Wave Speed (Global)	1,000.00 m/s
Total Simulated Time	3,000.0 sec	Vapor Pressure	-10.1 m H2O
Number of Nodes	497	Number of Report Paths	6
Number of Pipes	498		

Transient Initial Conditions Summary

Label	Start Node	Head (Initial at Start Node, Transient) (m)	Stop Node	Head (Initial at Stop Node, Transient) (m)
P-1	Çamlıdere Dam	960.00	J-1	958.70
P-2	J-1	958.70	T1-End	955.50
P-4	T2-Start	955.50	J-4	955.30
P-3	T1-End	955.60	T2-Start	955.50
P-5	J-4	955.30	J-5	954.50
P-6	J-5	954.50	J-6	953.90
P-7	J-6	953.90	T2-End	953.70
P-18	J-62	952.50	J-65	952.40
P-11	J-8	953.50	J-29	953.10
P-21	J-29	953.10	J-34	953.00
P-22	J-34	953.00	J-39	952.90
P-23	J-39	952.90	J-52	952.60
P-24	J-52	952.60	J-57	952.60
P-25	J-57	952.60	J-62	952.50
P-26	J-80	952.10	J-83	952.10
P-27	J-83	952.10	J-92	951.80
P-28	J-92	951.80	J-97	951.80
P-20	J-97	951.80	J-152	951.00
P-29	J-152	951.00	J-163	950.90
P-30	J-163	950.90	J-168	950.80
P-31	J-168	950.80	J-175	950.70
P-40	J-191	937.10	J-194	937.00
P-41	J-194	937.00	J-203	936.10
P-43	J-218	934.10	J-219	934.00
P-44	J-219	934.00	J-222	933.50
P-45	J-222	933.50	J-223	933.40
P-46	J-223	933.40	J-226	933.30
P-47	J-226	933.30	J-231	933.20
P-48	J-231	933.20	J-234	933.20
P-49	J-234	933.20	J-249	932.30
P-50	J-249	932.30	J-254	932.10
P-51	J-254	932.10	J-259	931.60
P-52	J-259	931.60	J-260	931.60
P-53	J-260	931.60	J-261	931.50
P-54	J-261	931.50	J-262	931.50
P-55	J-262	931.50	J-265	931.40
P-56	J-265	931.40	J-268	931.30
P-57	J-268	931.30	J-271	931.20
P-58	J-271	931.20	J-272	931.00
P-59	J-272	931.00	J-281	930.70
P-60	J-281	930.70	J-294	930.30
P-61	J-294	930.30	J-297	930.30
P-62	J-297	930.30	J-298	930.10
P-63	J-298	930.10	J-301	929.90
P-64	J-301	929.90	J-306	929.70
P-65	J-306	929.70	J-313	929.50
P-66	J-313	929.50	J-320	929.10
P-67	J-320	929.10	J-327	928.80
P-68	J-327	928.80	J-328	928.60
P-69	J-328	928.60	J-331	928.50
P-70	J-331	928.50	J-334	928.40
P-71	J-334	928.40	J-337	928.30

Transient Initial Conditions Summary

Label	Start Node	Head (Initial at Start Node, Transient) (m)	Stop Node	Head (Initial at Stop Node, Transient) (m)
P-72	J-337	928.30	J-346	928.00
P-73	J-346	928.00	J-351	927.90
P-74	J-351	927.90	J-354	927.80
P-75	J-354	927.80	J-359	927.60
P-76	J-359	927.60	J-362	927.50
P-77	J-362	927.50	J-373	927.20
P-78	J-373	927.20	J-374	927.10
P-79	J-374	927.10	J-379	927.00
P-80	J-379	927.00	J-380	926.90
P-81	J-380	926.90	J-385	926.60
P-82	J-385	926.60	J-392	926.30
P-83	J-392	926.30	J-393	926.30
P-84	J-393	926.30	J-396	926.10
P-85	J-396	926.10	J-397	926.00
P-86	J-397	926.00	J-400	925.90
P-87	J-400	925.90	J-409	925.60
P-88	J-409	925.60	J-418	925.40
P-89	J-418	925.40	J-421	925.20
P-90	J-421	925.20	J-428	924.90
P-91	J-428	924.90	J-439	924.60
P-92	J-439	924.60	J-442	924.50
P-93	J-442	924.50	J-443	924.40
P-94	J-443	924.40	J-446	924.30
P-95	J-446	924.30	J-463	923.70
P-96	J-463	923.70	J-464	923.50
P-97	J-464	923.50	İvedik-1	923.00
P-32	J-179	944.80	J-180	938.00
P-39	J-180	938.00	T3-End	937.60
P-12	J-9	953.50	J-11	953.40
P-100	J-11	953.40	J-13	953.40
P-101	J-13	953.40	J-15	953.40
P-102	J-15	953.40	J-17	953.30
P-103	J-17	953.30	J-19	953.30
P-104	J-19	953.30	J-21	953.30
P-105	J-21	953.30	J-23	953.20
P-106	J-23	953.20	J-25	953.20
P-107	J-25	953.20	J-27	953.20
P-108	J-27	953.20	J-30	953.10
P-109	J-30	953.10	J-32	953.00
P-110	J-32	953.00	J-35	952.90
P-111	J-35	952.90	J-37	952.80
P-112	J-37	952.80	J-40	952.80
P-113	J-40	952.80	J-42	952.80
P-114	J-42	952.80	J-44	952.70
P-115	J-44	952.70	J-46	952.70
P-116	J-46	952.70	J-48	952.60
P-117	J-48	952.60	J-50	952.60
P-118	J-50	952.60	J-53	952.60
P-119	J-53	952.60	J-55	952.60
P-120	J-55	952.60	J-58	952.50
P-121	J-58	952.50	J-60	952.50
P-122	J-60	952.50	J-63	952.50
P-123	J-63	952.50	J-66	952.40
P-124	J-66	952.40	J-68	952.40
P-125	J-68	952.40	J-70	952.30
P-126	J-70	952.30	J-72	952.30
P-127	J-72	952.30	J-74	952.30
P-128	J-74	952.30	J-76	952.30
P-129	J-76	952.30	J-78	952.20

Transient Initial Conditions Summary

Label	Start Node	Head (Initial at Start Node, Transient) (m)	Stop Node	Head (Initial at Stop Node, Transient) (m)
P-130	J-78	952.20	J-81	952.10
P-131	J-81	952.10	J-84	952.00
P-132	J-84	952.00	J-86	952.00
P-133	J-86	952.00	J-88	951.90
P-134	J-88	951.90	J-90	951.90
P-135	J-90	951.90	J-93	951.80
P-136	J-93	951.80	J-95	951.80
P-137	J-95	951.80	J-98	951.70
P-138	J-98	951.70	J-100	951.70
P-139	J-100	951.70	J-102	951.70
P-140	J-102	951.70	J-104	951.70
P-141	J-104	951.70	J-106	951.70
P-142	J-106	951.70	J-108	951.60
P-143	J-108	951.60	J-110	951.60
P-144	J-110	951.60	J-112	951.60
P-145	J-112	951.60	J-114	951.50
P-146	J-114	951.50	J-116	951.50
P-147	J-116	951.50	J-118	951.50
P-148	J-118	951.50	J-120	951.40
P-149	J-120	951.40	J-122	951.40
P-150	J-122	951.40	J-124	951.30
P-151	J-124	951.30	J-126	951.30
P-152	J-126	951.30	J-128	951.20
P-153	J-128	951.20	J-130	951.20
P-154	J-130	951.20	J-132	951.20
P-155	J-132	951.20	J-134	951.20
P-156	J-134	951.20	J-136	951.10
P-157	J-136	951.10	J-138	951.10
P-158	J-138	951.10	J-140	951.10
P-159	J-140	951.10	J-142	951.00
P-160	J-142	951.00	J-144	951.00
P-161	J-144	951.00	J-146	951.00
P-162	J-146	951.00	J-148	951.00
P-163	J-148	951.00	J-150	950.90
P-164	J-150	950.90	J-153	950.90
P-165	J-153	950.90	J-155	950.90
P-166	J-155	950.90	J-157	950.90
P-167	J-157	950.90	J-159	950.90
P-168	J-159	950.90	J-161	950.80
P-169	J-161	950.80	J-164	950.80
P-170	J-164	950.80	J-166	950.80
P-171	J-166	950.80	J-169	950.70
P-172	J-169	950.70	J-171	950.70
P-173	J-171	950.70	J-173	950.70
P-174	J-173	950.70	J-176	950.70
P-13	J-10	953.50	J-12	953.40
P-175	J-12	953.40	J-14	953.40
P-176	J-14	953.40	J-16	953.40
P-177	J-16	953.40	J-18	953.30
P-178	J-18	953.30	J-20	953.30
P-179	J-20	953.30	J-22	953.30
P-180	J-22	953.30	J-24	953.20
P-181	J-24	953.20	J-26	953.20
P-182	J-26	953.20	J-28	953.20
P-183	J-28	953.20	J-31	953.10
P-184	J-31	953.10	J-33	953.00
P-185	J-33	953.00	J-36	952.90
P-186	J-36	952.90	J-38	952.80
P-187	J-38	952.80	J-41	952.80

Transient Initial Conditions Summary

Label	Start Node	Head (Initial at Start Node, Transient) (m)	Stop Node	Head (Initial at Stop Node, Transient) (m)
P-188	J-41	952.80	J-43	952.80
P-189	J-43	952.80	J-45	952.70
P-190	J-45	952.70	J-47	952.70
P-191	J-47	952.70	J-49	952.60
P-192	J-49	952.60	J-51	952.60
P-193	J-51	952.60	J-54	952.60
P-194	J-54	952.60	J-56	952.60
P-195	J-56	952.60	J-59	952.50
P-196	J-59	952.50	J-61	952.50
P-197	J-61	952.50	J-64	952.50
P-198	J-64	952.50	J-67	952.40
P-199	J-67	952.40	J-69	952.40
P-200	J-69	952.40	J-71	952.30
P-201	J-71	952.30	J-73	952.30
P-202	J-73	952.30	J-75	952.30
P-203	J-75	952.30	J-77	952.30
P-204	J-77	952.30	J-79	952.20
P-205	J-79	952.20	J-82	952.10
P-206	J-82	952.10	J-85	952.00
P-207	J-85	952.00	J-87	952.00
P-208	J-87	952.00	J-89	951.90
P-209	J-89	951.90	J-91	951.90
P-210	J-91	951.90	J-94	951.80
P-211	J-94	951.80	J-96	951.80
P-212	J-96	951.80	J-99	951.70
P-213	J-99	951.70	J-101	951.70
P-214	J-101	951.70	J-103	951.70
P-215	J-103	951.70	J-105	951.70
P-216	J-105	951.70	J-107	951.70
P-217	J-107	951.70	J-109	951.60
P-218	J-109	951.60	J-111	951.60
P-219	J-111	951.60	J-113	951.60
P-220	J-113	951.60	J-115	951.50
P-221	J-115	951.50	J-117	951.50
P-222	J-117	951.50	J-119	951.50
P-223	J-119	951.50	J-121	951.40
P-224	J-121	951.40	J-123	951.40
P-225	J-123	951.40	J-125	951.30
P-226	J-125	951.30	J-127	951.30
P-227	J-127	951.30	J-129	951.20
P-228	J-129	951.20	J-131	951.20
P-229	J-131	951.20	J-133	951.20
P-230	J-133	951.20	J-135	951.20
P-231	J-135	951.20	J-137	951.10
P-232	J-137	951.10	J-139	951.10
P-233	J-139	951.10	J-141	951.10
P-234	J-141	951.10	J-143	951.00
P-235	J-143	951.00	J-145	951.00
P-236	J-145	951.00	J-147	951.00
P-237	J-147	951.00	J-149	951.00
P-238	J-149	951.00	J-151	950.90
P-239	J-151	950.90	J-154	950.90
P-240	J-154	950.90	J-156	950.90
P-241	J-156	950.90	J-158	950.90
P-242	J-158	950.90	J-160	950.90
P-243	J-160	950.90	J-162	950.80
P-244	J-162	950.80	J-165	950.80
P-245	J-165	950.80	J-167	950.80
P-246	J-167	950.80	J-170	950.70

Transient Initial Conditions Summary

Label	Start Node	Head (Initial at Start Node, Transient) (m)	Stop Node	Head (Initial at Stop Node, Transient) (m)
P-247	J-170	950.70	J-172	950.70
P-248	J-172	950.70	J-174	950.70
P-249	J-174	950.70	J-177	950.70
P-36	J-182	937.30	J-185	937.30
P-250	J-185	937.30	J-187	937.20
P-251	J-187	937.20	J-189	937.10
P-252	J-189	937.10	J-192	937.10
P-253	J-192	937.10	J-195	937.00
P-254	J-195	937.00	J-197	936.80
P-255	J-197	936.80	J-199	936.50
P-256	J-199	936.50	J-201	936.20
P-257	J-201	936.20	J-204	936.00
P-258	J-204	936.00	J-206	935.80
P-259	J-206	935.80	J-208	935.60
P-260	J-208	935.60	J-210	935.20
P-261	J-210	935.20	J-212	934.80
P-262	J-212	934.80	J-214	934.50
P-263	J-214	934.50	J-216	934.40
P-264	J-216	934.40	J-220	933.90
P-265	J-220	933.90	J-224	933.60
P-266	J-224	933.60	J-227	933.60
P-267	J-227	933.60	J-229	933.50
P-268	J-229	933.50	J-232	933.50
P-269	J-232	933.50	J-235	933.40
P-270	J-235	933.40	J-237	933.30
P-271	J-237	933.30	J-239	933.20
P-272	J-239	933.20	J-241	933.10
P-273	J-241	933.10	J-243	933.00
P-274	J-243	933.00	J-245	932.70
P-275	J-245	932.70	J-247	932.60
P-276	J-247	932.60	J-250	932.60
P-277	J-250	932.60	J-252	932.50
P-278	J-252	932.50	J-255	932.30
P-279	J-255	932.30	J-257	932.00
P-280	J-257	932.00	J-263	931.80
P-281	J-263	931.80	J-266	931.70
P-282	J-266	931.70	J-269	931.70
P-283	J-269	931.70	J-273	931.40
P-284	J-273	931.40	J-275	931.30
P-285	J-275	931.30	J-277	931.20
P-286	J-277	931.20	J-279	931.20
P-287	J-279	931.20	J-282	931.10
P-288	J-282	931.10	J-284	931.10
P-289	J-284	931.10	J-286	931.00
P-290	J-286	931.00	J-288	930.90
P-291	J-288	930.90	J-290	930.90
P-292	J-290	930.90	J-292	930.80
P-293	J-292	930.80	J-295	930.70
P-294	J-295	930.70	J-299	930.40
P-295	J-299	930.40	J-302	930.30
P-296	J-302	930.30	J-304	930.20
P-297	J-304	930.20	J-307	930.20
P-298	J-307	930.20	J-309	930.10
P-299	J-309	930.10	J-311	930.10
P-300	J-311	930.10	J-314	929.90
P-301	J-314	929.90	J-316	929.70
P-302	J-316	929.70	J-318	929.70
P-303	J-318	929.70	J-321	929.60
P-304	J-321	929.60	J-323	929.50

Transient Initial Conditions Summary

Label	Start Node	Head (Initial at Start Node, Transient) (m)	Stop Node	Head (Initial at Stop Node, Transient) (m)
P-305	J-323	929.50	J-325	929.50
P-306	J-325	929.50	J-329	929.20
P-307	J-329	929.20	J-332	929.10
P-308	J-332	929.10	J-335	929.00
P-309	J-335	929.00	J-338	928.80
P-310	J-338	928.80	J-340	928.80
P-311	J-340	928.80	J-342	928.70
P-312	J-342	928.70	J-344	928.60
P-313	J-344	928.60	J-347	928.60
P-314	J-347	928.60	J-349	928.50
P-315	J-349	928.50	J-352	928.50
P-316	J-352	928.50	J-355	928.40
P-317	J-355	928.40	J-357	928.30
P-318	J-357	928.30	J-360	928.20
P-319	J-360	928.20	J-363	928.20
P-320	J-363	928.20	J-365	928.10
P-321	J-365	928.10	J-367	928.10
P-322	J-367	928.10	J-369	928.00
P-323	J-369	928.00	J-371	927.90
P-324	J-371	927.90	J-375	927.80
P-325	J-375	927.80	J-377	927.70
P-326	J-377	927.70	J-381	927.50
P-327	J-381	927.50	J-383	927.40
P-328	J-383	927.40	J-386	927.30
P-329	J-386	927.30	J-388	927.20
P-330	J-388	927.20	J-390	927.20
P-331	J-390	927.20	J-394	926.90
P-332	J-394	926.90	J-398	926.70
P-333	J-398	926.70	J-401	926.60
P-334	J-401	926.60	J-403	926.60
P-335	J-403	926.60	J-405	926.60
P-336	J-405	926.60	J-407	926.50
P-337	J-407	926.50	J-410	926.40
P-338	J-410	926.40	J-412	926.30
P-339	J-412	926.30	J-414	926.30
P-340	J-414	926.30	J-416	926.20
P-341	J-416	926.20	J-419	926.10
P-342	J-419	926.10	J-422	926.00
P-343	J-422	926.00	J-424	926.00
P-344	J-424	926.00	J-426	925.80
P-345	J-426	925.80	J-429	925.70
P-346	J-429	925.70	J-431	925.70
P-347	J-431	925.70	J-433	925.60
P-348	J-433	925.60	J-435	925.60
P-349	J-435	925.60	J-437	925.50
P-350	J-437	925.50	J-440	925.40
P-351	J-440	925.40	J-444	925.30
P-352	J-444	925.30	J-447	925.20
P-353	J-447	925.20	J-449	925.00
P-354	J-449	925.00	J-451	925.00
P-355	J-451	925.00	J-453	924.90
P-356	J-453	924.90	J-455	924.90
P-357	J-455	924.90	J-457	924.70
P-358	J-457	924.70	J-459	924.70
P-359	J-459	924.70	J-461	924.60
P-360	J-461	924.60	J-465	924.40
P-361	J-465	924.40	J-467	924.20
P-362	J-467	924.20	J-469	924.10
P-363	J-469	924.10	J-471	924.00

Transient Initial Conditions Summary

Label	Start Node	Head (Initial at Start Node, Transient) (m)	Stop Node	Head (Initial at Stop Node, Transient) (m)
P-364	J-471	924.00	İvedik-2	923.60
P-38	J-184	937.30	J-186	937.30
P-367	J-186	937.30	J-188	937.20
P-368	J-188	937.20	J-190	937.10
P-369	J-190	937.10	J-193	937.10
P-370	J-193	937.10	J-196	937.00
P-371	J-196	937.00	J-198	936.80
P-372	J-198	936.80	J-200	936.50
P-373	J-200	936.50	J-202	936.20
P-374	J-202	936.20	J-205	936.00
P-375	J-205	936.00	J-207	935.80
P-376	J-207	935.80	J-209	935.60
P-377	J-209	935.60	J-211	935.20
P-378	J-211	935.20	J-213	934.80
P-379	J-213	934.80	J-215	934.50
P-380	J-215	934.50	J-217	934.40
P-381	J-217	934.40	J-221	933.90
P-382	J-221	933.90	J-225	933.60
P-383	J-225	933.60	J-228	933.60
P-384	J-228	933.60	J-230	933.50
P-385	J-230	933.50	J-233	933.50
P-386	J-233	933.50	J-236	933.40
P-387	J-236	933.40	J-238	933.30
P-388	J-238	933.30	J-240	933.20
P-389	J-240	933.20	J-242	933.10
P-390	J-242	933.10	J-244	933.00
P-391	J-244	933.00	J-246	932.70
P-392	J-246	932.70	J-248	932.60
P-393	J-248	932.60	J-251	932.60
P-394	J-251	932.60	J-253	932.50
P-395	J-253	932.50	J-256	932.30
P-396	J-256	932.30	J-258	932.00
P-397	J-258	932.00	J-264	931.80
P-398	J-264	931.80	J-267	931.70
P-399	J-267	931.70	J-270	931.70
P-400	J-270	931.70	J-274	931.40
P-401	J-274	931.40	J-276	931.30
P-402	J-276	931.30	J-278	931.20
P-403	J-278	931.20	J-280	931.20
P-404	J-280	931.20	J-283	931.10
P-405	J-283	931.10	J-285	931.10
P-406	J-285	931.10	J-287	931.00
P-407	J-287	931.00	J-289	930.90
P-408	J-289	930.90	J-291	930.90
P-409	J-291	930.90	J-293	930.80
P-410	J-293	930.80	J-296	930.70
P-411	J-296	930.70	J-300	930.40
P-412	J-300	930.40	J-303	930.30
P-413	J-303	930.30	J-305	930.20
P-414	J-305	930.20	J-308	930.20
P-415	J-308	930.20	J-310	930.10
P-416	J-310	930.10	J-312	930.10
P-417	J-312	930.10	J-315	929.90
P-418	J-315	929.90	J-317	929.70
P-419	J-317	929.70	J-319	929.70
P-420	J-319	929.70	J-322	929.60
P-421	J-322	929.60	J-324	929.50
P-422	J-324	929.50	J-326	929.50
P-423	J-326	929.50	J-330	929.20

Transient Initial Conditions Summary

Label	Start Node	Head (Initial at Start Node, Transient) (m)	Stop Node	Head (Initial at Stop Node, Transient) (m)
P-424	J-330	929.20	J-333	929.10
P-425	J-333	929.10	J-336	929.00
P-426	J-336	929.00	J-339	928.80
P-427	J-339	928.80	J-341	928.80
P-428	J-341	928.80	J-343	928.70
P-429	J-343	928.70	J-345	928.60
P-430	J-345	928.60	J-348	928.60
P-431	J-348	928.60	J-350	928.50
P-432	J-350	928.50	J-353	928.50
P-433	J-353	928.50	J-356	928.40
P-434	J-356	928.40	J-358	928.30
P-435	J-358	928.30	J-361	928.20
P-436	J-361	928.20	J-364	928.20
P-437	J-364	928.20	J-366	928.10
P-438	J-366	928.10	J-368	928.10
P-439	J-368	928.10	J-370	928.00
P-440	J-370	928.00	J-372	927.90
P-441	J-372	927.90	J-376	927.80
P-442	J-376	927.80	J-378	927.70
P-443	J-378	927.70	J-382	927.50
P-444	J-382	927.50	J-384	927.40
P-445	J-384	927.40	J-387	927.30
P-446	J-387	927.30	J-389	927.20
P-447	J-389	927.20	J-391	927.20
P-448	J-391	927.20	J-395	926.90
P-449	J-395	926.90	J-399	926.70
P-450	J-399	926.70	J-402	926.60
P-451	J-402	926.60	J-404	926.60
P-452	J-404	926.60	J-406	926.60
P-453	J-406	926.60	J-408	926.50
P-454	J-408	926.50	J-411	926.40
P-455	J-411	926.40	J-413	926.30
P-456	J-413	926.30	J-415	926.30
P-457	J-415	926.30	J-417	926.20
P-458	J-417	926.20	J-420	926.10
P-459	J-420	926.10	J-423	926.00
P-460	J-423	926.00	J-425	926.00
P-461	J-425	926.00	J-427	925.80
P-462	J-427	925.80	J-430	925.70
P-463	J-430	925.70	J-432	925.70
P-464	J-432	925.70	J-434	925.60
P-465	J-434	925.60	J-436	925.60
P-466	J-436	925.60	J-438	925.50
P-467	J-438	925.50	J-441	925.40
P-468	J-441	925.40	J-445	925.30
P-469	J-445	925.30	J-448	925.20
P-470	J-448	925.20	J-450	925.00
P-471	J-450	925.00	J-452	925.00
P-472	J-452	925.00	J-454	924.90
P-473	J-454	924.90	J-456	924.90
P-474	J-456	924.90	J-458	924.70
P-475	J-458	924.70	J-460	924.70
P-476	J-460	924.70	J-462	924.60
P-477	J-462	924.60	J-466	924.40
P-478	J-466	924.40	J-468	924.20
P-479	J-468	924.20	J-470	924.10
P-480	J-470	924.10	J-472	924.00
P-481	J-472	924.00	İvedik-3	923.60
P-9	T2-End	953.70	TCV-2	953.60

Transient Calculation Summary: Base

Licensed for Academic Use Only

Transient Initial Conditions Summary

Label	Start Node	Head (Initial at Start Node, Transient) (m)	Stop Node	Head (Initial at Stop Node, Transient) (m)
P-490	TCV-2	953.60	J-8	953.50
P-10	T2-End	953.70	TCV-3	953.60
P-491	TCV-3	953.60	J-9	953.50
P-8	T2-End	953.70	TCV-1	953.60
P-492	TCV-1	953.60	J-10	953.50
P-15	J-175	950.70	TCV-4	950.70
P-493	TCV-4	950.60	T3-Start	950.60
P-16	J-176	950.70	TCV-5	950.70
P-494	TCV-5	950.60	T3-Start	950.60
P-17	J-177	950.70	TCV-6	950.70
P-495	TCV-6	950.60	T3-Start	950.60
P-35	T3-End	937.60	TCV-9	937.40
P-496	TCV-9	937.40	J-183	937.30
P-33	T3-End	937.60	TCV-7	937.40
P-497	TCV-7	937.40	J-182	937.30
P-34	T3-End	937.60	TCV-8	937.40
P-498	TCV-8	937.40	J-184	937.30
P-99	İvedik-1	923.00	LJ-1.1	923.00
P-98	İvedik-1	923.00	LJ-1.2	923.00
P-366	İvedik-2	923.60	LJ-2.1	923.60
P-365	İvedik-2	923.60	LJ-2.2	923.60
P-483	İvedik-3	923.60	LJ-3.1	923.60
P-482	İvedik-3	923.60	LJ-3.2	923.60
P-484	LJ-1.1	918.10	R-1.1	918.10
P-485	LJ-1.2	918.10	R-1.2	918.10
P-486	LJ-2.1	918.10	R-2.1	918.10
P-487	LJ-2.2	918.10	R-2.2	918.10
P-488	LJ-3.1	918.10	R-3.1	918.10
P-489	LJ-3.2	918.10	R-3.2	918.10
P-42	J-203	936.10	J-218	934.10
P-19	J-65	952.40	J-80	952.10
P-37	J-183	937.30	J-191	937.10
P-14	T3-Start	950.60	J-179	944.80

Extreme Pressures and Heads

End Point	Upsurge Ratio	Max. Pressure (m H2O)	Min. Pressure (m H2O)	Max. Head (m)	Min. Head (m)
P-1:Çamlıdere Dam	1.000	20.2	20.2	960.00	960.00
P-1:J-1	1.090	19.2	17.7	960.25	958.70
P-2:J-1	1.090	19.2	17.7	960.25	958.70
P-2:T1-End	1.050	116.7	111.3	961.00	955.53
P-4:T2-Start	1.050	116.8	111.2	961.06	955.43
P-4:J-4	1.070	94.0	88.2	961.15	955.29
P-3:T1-End	1.050	116.7	111.3	961.00	955.53
P-3:T2-Start	1.050	116.8	111.2	961.06	955.43
P-5:J-4	1.070	94.0	88.2	961.15	955.29
P-5:J-5	1.480	21.4	14.5	961.41	954.44
P-6:J-5	1.480	21.4	14.5	961.41	954.44
P-6:J-6	1.520	22.4	14.7	961.57	953.90
P-7:J-6	1.520	22.4	14.7	961.57	953.90
P-7:T2-End	1.540	22.8	14.8	961.64	953.64
P-18:J-62	1.050	182.6	173.1	962.03	952.49
P-18:J-65	1.060	183.6	173.9	962.06	952.40
P-11:J-8	1.550	22.8	14.7	961.66	953.50
P-11:J-29	1.130	76.8	68.2	961.81	953.11
P-21:J-29	1.130	76.8	68.2	961.81	953.11
P-21:J-34	1.130	75.6	66.7	961.86	952.95

Transient Calculation Summary: Base

Extreme Pressures and Heads

End Point	Upsurge Ratio	Max. Pressure (m H2O)	Min. Pressure (m H2O)	Max. Head (m)	Min. Head (m)
P-22:J-34	1.130	75.6	66.7	961.86	952.95
P-22:J-39	1.090	105.9	96.8	961.91	952.83
P-23:J-39	1.090	105.9	96.8	961.91	952.83
P-23:J-52	1.060	166.0	156.6	961.98	952.60
P-24:J-52	1.060	166.0	156.6	961.98	952.60
P-24:J-57	1.060	180.9	171.4	962.01	952.54
P-25:J-57	1.060	180.9	171.4	962.01	952.54
P-25:J-62	1.050	182.6	173.1	962.03	952.49
P-26:J-80	1.060	165.0	154.9	962.17	952.08
P-26:J-83	1.060	169.1	159.0	962.18	952.05
P-27:J-83	1.060	169.1	159.0	962.18	952.05
P-27:J-92	1.070	156.6	146.2	962.26	951.84
P-28:J-92	1.070	156.6	146.2	962.26	951.84
P-28:J-97	1.070	151.1	140.6	962.29	951.77
P-20:J-97	1.070	151.1	140.6	962.29	951.77
P-20:J-152	1.170	79.7	68.0	962.64	950.94
P-29:J-152	1.170	79.7	68.0	962.64	950.94
P-29:J-163	1.680	29.0	17.2	962.67	950.83
P-30:J-163	1.680	29.0	17.2	962.67	950.83
P-30:J-168	1.410	40.7	28.8	962.70	950.74
P-31:J-168	1.410	40.7	28.8	962.70	950.74
P-31:J-175	1.550	33.7	21.7	962.73	950.68
P-40:J-191	2.570	45.8	17.8	965.14	937.06
P-40:J-194	3.360	40.0	11.9	965.14	937.02
P-41:J-194	3.360	40.0	11.9	965.14	937.02
P-41:J-203	1.480	89.2	60.2	965.14	936.08
P-43:J-218	1.300	137.1	105.8	965.44	934.08
P-43:J-219	1.300	136.7	105.3	965.46	933.98
P-44:J-219	1.300	136.7	105.3	965.46	933.98
P-44:J-222	1.290	140.9	108.9	965.56	933.54
P-45:J-222	1.290	140.9	108.9	965.56	933.54
P-45:J-223	1.300	140.1	108.0	965.60	933.36
P-46:J-223	1.300	140.1	108.0	965.60	933.36
P-46:J-226	1.270	149.3	117.2	965.60	933.34
P-47:J-226	1.270	149.3	117.2	965.60	933.34
P-47:J-231	1.270	150.0	117.7	965.61	933.24
P-48:J-231	1.270	150.0	117.7	965.61	933.24
P-48:J-234	1.300	141.4	109.1	965.62	933.22
P-49:J-234	1.300	141.4	109.1	965.62	933.22
P-49:J-249	1.470	104.4	71.0	965.76	932.30
P-50:J-249	1.470	104.4	71.0	965.76	932.30
P-50:J-254	1.360	126.7	93.1	965.78	932.12
P-51:J-254	1.360	126.7	93.1	965.78	932.12
P-51:J-259	1.540	97.1	62.9	965.85	931.60
P-52:J-259	1.540	97.1	62.9	965.85	931.60
P-52:J-260	1.500	102.6	68.3	965.86	931.56
P-53:J-260	1.500	102.6	68.3	965.86	931.56
P-53:J-261	1.540	98.1	63.8	965.86	931.54
P-54:J-261	1.540	98.1	63.8	965.86	931.54
P-54:J-262	1.500	102.4	68.1	965.87	931.52
P-55:J-262	1.500	102.4	68.1	965.87	931.52
P-55:J-265	1.570	94.7	60.2	965.89	931.35
P-56:J-265	1.570	94.7	60.2	965.89	931.35
P-56:J-268	1.540	98.1	63.5	965.90	931.29
P-57:J-268	1.540	98.1	63.5	965.90	931.29
P-57:J-271	1.940	71.4	36.8	965.92	931.17
P-58:J-271	1.940	71.4	36.8	965.92	931.17
P-58:J-272	1.620	91.4	56.6	965.94	931.05
P-59:J-272	1.620	91.4	56.6	965.94	931.05
P-59:J-281	2.460	59.3	24.1	966.03	930.74
P-60:J-281	2.460	59.3	24.1	966.03	930.74

Transient Calculation Summary: Base

Extreme Pressures and Heads

End Point	Upsurge Ratio	Max. Pressure (m H2O)	Min. Pressure (m H2O)	Max. Head (m)	Min. Head (m)
P-60:J-294	1.680	88.5	52.8	966.13	930.34
P-61:J-294	1.680	88.5	52.8	966.13	930.34
P-61:J-297	1.880	76.8	41.0	966.16	930.25
P-62:J-297	1.880	76.8	41.0	966.16	930.25
P-62:J-298	1.540	102.7	66.6	966.20	930.08
P-63:J-298	1.540	102.7	66.6	966.20	930.08
P-63:J-301	2.480	60.7	24.4	966.25	929.88
P-64:J-301	2.490	60.7	24.4	966.25	929.88
P-64:J-306	1.750	85.6	49.1	966.31	929.68
P-65:J-306	1.750	85.6	49.1	966.31	929.68
P-65:J-313	4.550	47.2	10.4	966.36	929.47
P-66:J-313	4.550	47.2	10.4	966.36	929.47
P-66:J-320	1.780	85.2	47.9	966.47	929.06
P-67:J-320	1.780	85.2	47.9	966.47	929.06
P-67:J-327	2.230	68.2	30.5	966.55	928.79
P-68:J-327	2.230	68.2	30.5	966.55	928.79
P-68:J-328	1.800	85.1	47.3	966.58	928.64
P-69:J-328	1.800	85.1	47.3	966.58	928.64
P-69:J-331	2.470	64.0	25.9	966.63	928.48
P-70:J-331	2.470	64.0	25.9	966.63	928.48
P-70:J-334	2.090	73.1	34.9	966.64	928.42
P-71:J-334	2.090	73.1	34.9	966.64	928.42
P-71:J-337	2.480	64.2	25.9	966.68	928.28
P-72:J-337	2.480	64.2	25.9	966.68	928.28
P-72:J-346	1.630	99.7	61.0	966.75	928.02
P-73:J-346	1.630	99.7	61.0	966.75	928.02
P-73:J-351	1.990	77.8	39.0	966.79	927.89
P-74:J-351	1.990	77.8	39.0	966.79	927.89
P-74:J-354	1.620	101.4	62.4	966.81	927.79
P-75:J-354	1.620	101.4	62.4	966.81	927.79
P-75:J-359	2.280	69.8	30.6	966.85	927.64
P-76:J-359	2.280	69.8	30.6	966.85	927.64
P-76:J-362	1.950	80.6	41.3	966.89	927.50
P-77:J-362	1.950	80.6	41.3	966.89	927.50
P-77:J-373	2.350	69.0	29.3	966.96	927.19
P-78:J-373	2.350	69.0	29.3	966.96	927.19
P-78:J-374	2.170	73.8	33.9	966.99	927.09
P-79:J-374	2.170	73.8	33.9	966.99	927.09
P-79:J-379	2.360	69.4	29.4	967.01	927.00
P-80:J-379	2.360	69.4	29.4	967.01	927.00
P-80:J-380	1.760	92.8	52.7	967.04	926.87
P-81:J-380	1.760	92.8	52.7	967.04	926.87
P-81:J-385	1.900	85.3	44.9	967.11	926.61
P-82:J-385	1.900	85.3	44.9	967.11	926.61
P-82:J-392	1.790	92.3	51.5	967.19	926.29
P-83:J-392	1.790	92.3	51.5	967.19	926.29
P-83:J-393	1.930	84.8	43.9	967.19	926.27
P-84:J-393	1.930	84.8	43.9	967.19	926.27
P-84:J-396	1.780	93.8	52.8	967.24	926.10
P-85:J-396	1.780	93.8	52.8	967.24	926.10
P-85:J-397	2.120	78.0	36.9	967.25	926.02
P-86:J-397	2.120	78.0	36.9	967.25	926.02
P-86:J-400	1.730	97.9	56.6	967.28	925.89
P-87:J-400	1.730	97.9	56.6	967.28	925.89
P-87:J-409	2.520	69.1	27.5	967.36	925.61
P-88:J-409	2.520	69.1	27.5	967.36	925.61
P-88:J-418	2.180	77.6	35.6	967.43	925.37
P-89:J-418	2.180	77.6	35.6	967.43	925.37
P-89:J-421	3.050	62.7	20.6	967.47	925.21
P-90:J-421	3.050	62.7	20.6	967.47	925.21
P-90:J-428	1.930	88.1	45.5	967.54	924.91

Transient Calculation Summary: Base

Extreme Pressures and Heads

End Point	Upsurge Ratio	Max. Pressure (m H2O)	Min. Pressure (m H2O)	Max. Head (m)	Min. Head (m)
P-91:J-428	1.930	88.1	45.5	967.54	924.91
P-91:J-439	3.160	62.9	19.9	967.64	924.57
P-92:J-439	3.160	62.9	19.9	967.64	924.57
P-92:J-442	2.670	68.8	25.8	967.66	924.49
P-93:J-442	2.670	68.8	25.8	967.66	924.49
P-93:J-443	3.190	62.9	19.7	967.67	924.43
P-94:J-443	3.190	62.9	19.7	967.67	924.43
P-94:J-446	2.270	77.2	34.0	967.70	924.34
P-95:J-446	2.270	77.2	34.0	967.70	924.34
P-95:J-463	4.840	55.6	11.5	967.87	923.66
P-96:J-463	4.840	55.6	11.5	967.87	923.66
P-96:J-464	3.120	65.3	20.9	967.91	923.49
P-97:J-464	3.120	65.3	20.9	967.91	923.49
P-97:İvedik-1	5.520	54.8	9.9	967.97	923.04
P-32:J-179	4.790	24.0	5.0	963.87	944.81
P-32:J-180	4.140	35.6	8.6	965.07	937.99
P-39:J-180	4.150	35.6	8.6	965.07	937.99
P-39:T3-End	4.130	36.3	8.8	965.12	937.56
P-12:J-9	1.550	22.8	14.7	961.65	953.50
P-12:J-11	1.400	28.6	20.4	961.68	953.42
P-100:J-11	1.400	28.6	20.4	961.68	953.42
P-100:J-13	1.370	30.7	22.4	961.70	953.37
P-101:J-13	1.370	30.7	22.4	961.70	953.37
P-101:J-15	1.290	36.8	28.4	961.72	953.33
P-102:J-15	1.290	36.8	28.4	961.72	953.33
P-102:J-17	1.220	46.8	38.4	961.74	953.28
P-103:J-17	1.220	46.8	38.4	961.74	953.28
P-103:J-19	1.190	53.5	45.0	961.74	953.26
P-104:J-19	1.190	53.5	45.0	961.74	953.26
P-104:J-21	1.180	55.7	47.3	961.75	953.25
P-105:J-21	1.180	55.7	47.3	961.75	953.25
P-105:J-23	1.170	59.8	51.2	961.76	953.22
P-106:J-23	1.170	59.8	51.2	961.76	953.22
P-106:J-25	1.150	64.1	55.5	961.78	953.18
P-107:J-25	1.150	64.1	55.5	961.78	953.18
P-107:J-27	1.140	68.2	59.6	961.79	953.14
P-108:J-27	1.140	68.2	59.6	961.79	953.14
P-108:J-30	1.140	72.0	63.3	961.82	953.08
P-109:J-30	1.140	72.0	63.3	961.82	953.08
P-109:J-32	1.130	76.6	67.8	961.84	952.99
P-110:J-32	1.130	76.6	67.8	961.84	952.99
P-110:J-35	1.130	79.9	70.9	961.88	952.88
P-111:J-35	1.130	79.9	70.9	961.88	952.88
P-111:J-37	1.110	92.5	83.4	961.91	952.82
P-112:J-37	1.110	92.5	83.4	961.91	952.82
P-112:J-40	1.100	96.4	87.2	961.92	952.76
P-113:J-40	1.100	96.4	87.2	961.92	952.76
P-113:J-42	1.100	97.0	87.8	961.93	952.75
P-114:J-42	1.100	97.0	87.8	961.93	952.75
P-114:J-44	1.100	98.8	89.6	961.95	952.70
P-115:J-44	1.100	98.8	89.6	961.95	952.70
P-115:J-46	1.090	114.0	104.8	961.97	952.67
P-116:J-46	1.090	114.0	104.8	961.97	952.67
P-116:J-48	1.070	147.2	137.9	961.98	952.61
P-117:J-48	1.070	147.2	137.9	961.98	952.61
P-117:J-50	1.070	150.0	140.7	961.98	952.61
P-118:J-50	1.070	150.0	140.7	961.98	952.61
P-118:J-53	1.060	164.2	154.8	962.00	952.58
P-119:J-53	1.060	164.2	154.8	962.00	952.58
P-119:J-55	1.060	171.7	162.3	962.00	952.56
P-120:J-55	1.060	171.7	162.3	962.00	952.56

Transient Calculation Summary: Base

Extreme Pressures and Heads

End Point	Upsurge Ratio	Max. Pressure (m H2O)	Min. Pressure (m H2O)	Max. Head (m)	Min. Head (m)
P-120:J-58	1.060	180.7	171.2	962.01	952.52
P-121:J-58	1.060	180.7	171.2	962.01	952.52
P-121:J-60	1.060	181.4	171.9	962.02	952.49
P-122:J-60	1.060	181.4	171.9	962.02	952.49
P-122:J-63	1.060	182.5	172.9	962.04	952.45
P-123:J-63	1.060	182.5	172.9	962.04	952.45
P-123:J-66	1.060	183.5	173.9	962.06	952.37
P-124:J-66	1.060	183.5	173.9	962.06	952.37
P-124:J-68	1.060	181.6	171.9	962.08	952.35
P-125:J-68	1.060	181.6	171.9	962.08	952.35
P-125:J-70	1.060	181.0	171.3	962.08	952.32
P-126:J-70	1.060	181.0	171.3	962.08	952.32
P-126:J-72	1.060	181.2	171.4	962.10	952.29
P-127:J-72	1.060	181.2	171.4	962.10	952.29
P-127:J-74	1.060	178.8	169.0	962.11	952.26
P-128:J-74	1.060	178.8	169.0	962.11	952.26
P-128:J-76	1.060	176.9	167.0	962.12	952.23
P-129:J-76	1.060	176.9	167.0	962.12	952.23
P-129:J-78	1.060	174.3	164.3	962.15	952.16
P-130:J-78	1.060	174.3	164.3	962.15	952.16
P-130:J-81	1.070	164.3	154.2	962.18	952.06
P-131:J-81	1.070	164.3	154.2	962.18	952.06
P-131:J-84	1.060	167.9	157.7	962.20	952.03
P-132:J-84	1.060	167.9	157.7	962.20	952.03
P-132:J-86	1.060	168.2	158.1	962.19	952.02
P-133:J-86	1.060	168.2	158.1	962.19	952.02
P-133:J-88	1.070	161.9	151.6	962.23	951.92
P-134:J-88	1.070	161.9	151.6	962.23	951.92
P-134:J-90	1.070	160.1	149.8	962.24	951.90
P-135:J-90	1.070	160.1	149.8	962.24	951.90
P-135:J-93	1.070	155.3	144.9	962.28	951.82
P-136:J-93	1.070	155.3	144.9	962.28	951.82
P-136:J-95	1.070	153.8	143.4	962.27	951.78
P-137:J-95	1.070	153.8	143.4	962.27	951.78
P-137:J-98	1.080	148.0	137.4	962.32	951.71
P-138:J-98	1.080	148.0	137.4	962.32	951.71
P-138:J-100	1.080	146.3	135.7	962.31	951.70
P-139:J-100	1.080	146.3	135.7	962.31	951.70
P-139:J-102	1.080	143.9	133.2	962.34	951.67
P-140:J-102	1.080	143.9	133.2	962.34	951.67
P-140:J-104	1.080	141.6	131.0	962.34	951.66
P-141:J-104	1.080	141.6	131.0	962.34	951.66
P-141:J-106	1.080	143.9	133.2	962.34	951.63
P-142:J-106	1.080	143.9	133.2	962.34	951.63
P-142:J-108	1.080	141.7	131.0	962.36	951.61
P-143:J-108	1.080	141.7	131.0	962.36	951.61
P-143:J-110	1.080	137.9	127.2	962.37	951.59
P-144:J-110	1.080	137.9	127.2	962.37	951.59
P-144:J-112	1.090	133.2	122.4	962.39	951.53
P-145:J-112	1.090	133.2	122.4	962.39	951.53
P-145:J-114	1.090	128.8	117.9	962.40	951.50
P-146:J-114	1.090	128.8	117.9	962.40	951.50
P-146:J-116	1.090	127.2	116.3	962.43	951.46
P-147:J-116	1.090	127.2	116.3	962.43	951.46
P-147:J-118	1.090	126.5	115.5	962.44	951.43
P-148:J-118	1.090	126.5	115.5	962.44	951.43
P-148:J-120	1.100	123.1	112.1	962.45	951.39
P-149:J-120	1.100	123.1	112.1	962.45	951.39
P-149:J-122	1.100	120.7	109.6	962.47	951.36
P-150:J-122	1.100	120.7	109.6	962.47	951.36
P-150:J-124	1.110	115.9	104.7	962.49	951.29

Transient Calculation Summary: Base

Extreme Pressures and Heads

End Point	Upsurge Ratio	Max. Pressure (m H2O)	Min. Pressure (m H2O)	Max. Head (m)	Min. Head (m)
P-151:J-124	1.110	115.9	104.7	962.49	951.29
P-151:J-126	1.110	112.7	101.4	962.50	951.26
P-152:J-126	1.110	112.7	101.4	962.50	951.26
P-152:J-128	1.120	107.6	96.3	962.52	951.22
P-153:J-128	1.120	107.6	96.3	962.52	951.22
P-153:J-130	1.120	102.7	91.4	962.54	951.16
P-154:J-130	1.120	102.7	91.4	962.54	951.16
P-154:J-132	1.120	102.6	91.2	962.55	951.16
P-155:J-132	1.120	102.6	91.2	962.55	951.16
P-155:J-134	1.130	101.4	90.0	962.56	951.13
P-156:J-134	1.130	101.4	90.0	962.56	951.13
P-156:J-136	1.140	95.8	84.3	962.57	951.08
P-157:J-136	1.140	95.8	84.3	962.57	951.08
P-157:J-138	1.140	94.1	82.6	962.59	951.07
P-158:J-138	1.140	94.1	82.6	962.59	951.07
P-158:J-140	1.160	85.0	73.4	962.59	951.04
P-159:J-140	1.160	85.0	73.4	962.59	951.04
P-159:J-142	1.170	80.7	69.1	962.61	951.01
P-160:J-142	1.170	80.7	69.1	962.61	951.01
P-160:J-144	1.170	80.1	68.5	962.61	950.98
P-161:J-144	1.170	80.1	68.5	962.61	950.98
P-161:J-146	1.180	75.1	63.4	962.63	950.95
P-162:J-146	1.180	75.1	63.4	962.63	950.95
P-162:J-148	1.190	74.0	62.3	962.63	950.94
P-163:J-148	1.190	74.0	62.3	962.63	950.94
P-163:J-150	1.200	69.1	57.4	962.64	950.92
P-164:J-150	1.200	69.1	57.4	962.64	950.92
P-164:J-153	1.200	71.2	59.5	962.64	950.91
P-165:J-153	1.200	71.2	59.5	962.64	950.91
P-165:J-155	1.210	67.2	55.5	962.65	950.89
P-166:J-155	1.210	67.2	55.5	962.65	950.89
P-166:J-157	1.220	64.5	52.7	962.66	950.89
P-167:J-157	1.220	64.5	52.7	962.66	950.89
P-167:J-159	1.640	30.4	18.5	962.68	950.82
P-168:J-159	1.640	30.4	18.5	962.68	950.82
P-168:J-161	1.710	28.5	16.7	962.68	950.81
P-169:J-161	1.710	28.5	16.7	962.68	950.81
P-169:J-164	1.550	33.4	21.5	962.70	950.77
P-170:J-164	1.550	33.4	21.5	962.70	950.77
P-170:J-166	1.540	34.0	22.1	962.70	950.76
P-171:J-166	1.540	34.0	22.1	962.70	950.76
P-171:J-169	1.480	36.7	24.7	962.72	950.71
P-172:J-169	1.480	36.7	24.7	962.72	950.71
P-172:J-171	1.490	36.5	24.5	962.72	950.70
P-173:J-171	1.490	36.5	24.5	962.72	950.70
P-173:J-173	1.530	34.7	22.7	962.73	950.68
P-174:J-173	1.530	34.7	22.7	962.73	950.68
P-174:J-176	1.550	33.7	21.7	962.73	950.68
P-13:J-10	1.550	22.8	14.7	961.65	953.50
P-13:J-12	1.400	28.6	20.4	961.68	953.42
P-175:J-12	1.400	28.6	20.4	961.68	953.42
P-175:J-14	1.370	30.7	22.4	961.70	953.37
P-176:J-14	1.370	30.7	22.4	961.70	953.37
P-176:J-16	1.290	36.8	28.4	961.72	953.33
P-177:J-16	1.290	36.8	28.4	961.72	953.33
P-177:J-18	1.220	46.8	38.4	961.74	953.28
P-178:J-18	1.220	46.8	38.4	961.74	953.28
P-178:J-20	1.190	53.5	45.0	961.74	953.26
P-179:J-20	1.190	53.5	45.0	961.74	953.26
P-179:J-22	1.180	55.7	47.3	961.75	953.25
P-180:J-22	1.180	55.7	47.3	961.75	953.25

Transient Calculation Summary: Base

Extreme Pressures and Heads

End Point	Upsurge Ratio	Max. Pressure (m H2O)	Min. Pressure (m H2O)	Max. Head (m)	Min. Head (m)
P-180:J-24	1.170	59.8	51.2	961.76	953.22
P-181:J-24	1.170	59.8	51.2	961.76	953.22
P-181:J-26	1.150	64.1	55.5	961.78	953.18
P-182:J-26	1.150	64.1	55.5	961.78	953.18
P-182:J-28	1.140	68.2	59.6	961.79	953.14
P-183:J-28	1.140	68.2	59.6	961.79	953.14
P-183:J-31	1.140	72.0	63.3	961.82	953.08
P-184:J-31	1.140	72.0	63.3	961.82	953.08
P-184:J-33	1.130	76.6	67.8	961.84	952.99
P-185:J-33	1.130	76.6	67.8	961.84	952.99
P-185:J-36	1.130	79.9	70.9	961.88	952.88
P-186:J-36	1.130	79.9	70.9	961.88	952.88
P-186:J-38	1.110	92.5	83.4	961.91	952.82
P-187:J-38	1.110	92.5	83.4	961.91	952.82
P-187:J-41	1.100	96.4	87.2	961.92	952.76
P-188:J-41	1.100	96.4	87.2	961.92	952.76
P-188:J-43	1.100	97.0	87.8	961.93	952.75
P-189:J-43	1.100	97.0	87.8	961.93	952.75
P-189:J-45	1.100	98.8	89.6	961.95	952.70
P-190:J-45	1.100	98.8	89.6	961.95	952.70
P-190:J-47	1.090	114.0	104.8	961.97	952.67
P-191:J-47	1.090	114.0	104.8	961.97	952.67
P-191:J-49	1.070	147.2	137.9	961.98	952.61
P-192:J-49	1.070	147.2	137.9	961.98	952.61
P-192:J-51	1.070	150.0	140.7	961.98	952.61
P-193:J-51	1.070	150.0	140.7	961.98	952.61
P-193:J-54	1.060	164.2	154.8	962.00	952.58
P-194:J-54	1.060	164.2	154.8	962.00	952.58
P-194:J-56	1.060	171.7	162.3	962.00	952.56
P-195:J-56	1.060	171.7	162.3	962.00	952.56
P-195:J-59	1.060	180.7	171.2	962.01	952.52
P-196:J-59	1.060	180.7	171.2	962.01	952.52
P-196:J-61	1.060	181.4	171.9	962.02	952.49
P-197:J-61	1.060	181.4	171.9	962.02	952.49
P-197:J-64	1.060	182.5	172.9	962.04	952.45
P-198:J-64	1.060	182.5	172.9	962.04	952.45
P-198:J-67	1.060	183.5	173.9	962.06	952.37
P-199:J-67	1.060	183.5	173.9	962.06	952.37
P-199:J-69	1.060	181.6	171.9	962.08	952.35
P-200:J-69	1.060	181.6	171.9	962.08	952.35
P-200:J-71	1.060	181.0	171.3	962.08	952.32
P-201:J-71	1.060	181.0	171.3	962.08	952.32
P-201:J-73	1.060	181.2	171.4	962.10	952.29
P-202:J-73	1.060	181.2	171.4	962.10	952.29
P-202:J-75	1.060	178.8	169.0	962.11	952.26
P-203:J-75	1.060	178.8	169.0	962.11	952.26
P-203:J-77	1.060	176.9	167.0	962.12	952.23
P-204:J-77	1.060	176.9	167.0	962.12	952.23
P-204:J-79	1.060	174.3	164.3	962.15	952.16
P-205:J-79	1.060	174.3	164.3	962.15	952.16
P-205:J-82	1.070	164.3	154.2	962.18	952.06
P-206:J-82	1.070	164.3	154.2	962.18	952.06
P-206:J-85	1.060	167.9	157.7	962.20	952.03
P-207:J-85	1.060	167.9	157.7	962.20	952.03
P-207:J-87	1.060	168.2	158.1	962.19	952.02
P-208:J-87	1.060	168.2	158.1	962.19	952.02
P-208:J-89	1.070	161.9	151.6	962.23	951.92
P-209:J-89	1.070	161.9	151.6	962.23	951.92
P-209:J-91	1.070	160.1	149.8	962.24	951.90
P-210:J-91	1.070	160.1	149.8	962.24	951.90
P-210:J-94	1.070	155.3	144.9	962.28	951.82

Transient Calculation Summary: Base

Extreme Pressures and Heads

End Point	Upsurge Ratio	Max. Pressure (m H2O)	Min. Pressure (m H2O)	Max. Head (m)	Min. Head (m)
P-211:J-94	1.070	155.3	144.9	962.28	951.82
P-211:J-96	1.070	153.8	143.4	962.27	951.78
P-212:J-96	1.070	153.8	143.4	962.27	951.78
P-212:J-99	1.080	148.0	137.4	962.32	951.71
P-213:J-99	1.080	148.0	137.4	962.32	951.71
P-213:J-101	1.080	146.3	135.7	962.31	951.70
P-214:J-101	1.080	146.3	135.7	962.31	951.70
P-214:J-103	1.080	143.9	133.2	962.34	951.67
P-215:J-103	1.080	143.9	133.2	962.34	951.67
P-215:J-105	1.080	141.6	131.0	962.34	951.66
P-216:J-105	1.080	141.6	131.0	962.34	951.66
P-216:J-107	1.080	143.9	133.2	962.34	951.63
P-217:J-107	1.080	143.9	133.2	962.34	951.63
P-217:J-109	1.080	141.7	131.0	962.36	951.61
P-218:J-109	1.080	141.7	131.0	962.36	951.61
P-218:J-111	1.080	137.9	127.2	962.37	951.59
P-219:J-111	1.080	137.9	127.2	962.37	951.59
P-219:J-113	1.090	133.2	122.4	962.39	951.53
P-220:J-113	1.090	133.2	122.4	962.39	951.53
P-220:J-115	1.090	128.8	117.9	962.40	951.50
P-221:J-115	1.090	128.8	117.9	962.40	951.50
P-221:J-117	1.090	127.2	116.3	962.43	951.46
P-222:J-117	1.090	127.2	116.3	962.43	951.46
P-222:J-119	1.090	126.5	115.5	962.44	951.43
P-223:J-119	1.090	126.5	115.5	962.44	951.43
P-223:J-121	1.100	123.1	112.1	962.45	951.39
P-224:J-121	1.100	123.1	112.1	962.45	951.39
P-224:J-123	1.100	120.7	109.6	962.47	951.36
P-225:J-123	1.100	120.7	109.6	962.47	951.36
P-225:J-125	1.110	115.9	104.7	962.49	951.29
P-226:J-125	1.110	115.9	104.7	962.49	951.29
P-226:J-127	1.110	112.7	101.4	962.50	951.26
P-227:J-127	1.110	112.7	101.4	962.50	951.26
P-227:J-129	1.120	107.6	96.3	962.52	951.22
P-228:J-129	1.120	107.6	96.3	962.52	951.22
P-228:J-131	1.120	102.7	91.4	962.54	951.16
P-229:J-131	1.120	102.7	91.4	962.54	951.16
P-229:J-133	1.120	102.6	91.2	962.55	951.16
P-230:J-133	1.120	102.6	91.2	962.55	951.16
P-230:J-135	1.130	101.4	90.0	962.56	951.13
P-231:J-135	1.130	101.4	90.0	962.56	951.13
P-231:J-137	1.140	95.8	84.3	962.57	951.08
P-232:J-137	1.140	95.8	84.3	962.57	951.08
P-232:J-139	1.140	94.1	82.6	962.59	951.07
P-233:J-139	1.140	94.1	82.6	962.59	951.07
P-233:J-141	1.160	85.0	73.4	962.59	951.04
P-234:J-141	1.160	85.0	73.4	962.59	951.04
P-234:J-143	1.170	80.7	69.1	962.61	951.01
P-235:J-143	1.170	80.7	69.1	962.61	951.01
P-235:J-145	1.170	80.1	68.5	962.61	950.98
P-236:J-145	1.170	80.1	68.5	962.61	950.98
P-236:J-147	1.180	75.1	63.4	962.63	950.95
P-237:J-147	1.180	75.1	63.4	962.63	950.95
P-237:J-149	1.190	74.0	62.3	962.63	950.94
P-238:J-149	1.190	74.0	62.3	962.63	950.94
P-238:J-151	1.200	69.1	57.4	962.64	950.92
P-239:J-151	1.200	69.1	57.4	962.64	950.92
P-239:J-154	1.200	71.2	59.5	962.64	950.91
P-240:J-154	1.200	71.2	59.5	962.64	950.91
P-240:J-156	1.210	67.2	55.5	962.65	950.89
P-241:J-156	1.210	67.2	55.5	962.65	950.89

Transient Calculation Summary: Base

Extreme Pressures and Heads

End Point	Upsurge Ratio	Max. Pressure (m H2O)	Min. Pressure (m H2O)	Max. Head (m)	Min. Head (m)
P-241:J-158	1.220	64.5	52.7	962.66	950.89
P-242:J-158	1.220	64.5	52.7	962.66	950.89
P-242:J-160	1.640	30.4	18.5	962.68	950.82
P-243:J-160	1.640	30.4	18.5	962.68	950.82
P-243:J-162	1.710	28.5	16.7	962.68	950.81
P-244:J-162	1.710	28.5	16.7	962.68	950.81
P-244:J-165	1.550	33.4	21.5	962.70	950.77
P-245:J-165	1.550	33.4	21.5	962.70	950.77
P-245:J-167	1.540	34.0	22.1	962.70	950.76
P-246:J-167	1.540	34.0	22.1	962.70	950.76
P-246:J-170	1.480	36.7	24.7	962.72	950.71
P-247:J-170	1.480	36.7	24.7	962.72	950.71
P-247:J-172	1.490	36.5	24.5	962.72	950.70
P-248:J-172	1.490	36.5	24.5	962.72	950.70
P-248:J-174	1.530	34.7	22.7	962.73	950.68
P-249:J-174	1.530	34.7	22.7	962.73	950.68
P-249:J-177	1.550	33.7	21.7	962.73	950.68
P-36:J-182	4.250	36.3	8.5	965.13	937.31
P-36:J-185	4.090	36.8	9.0	965.13	937.26
P-250:J-185	4.090	36.8	9.0	965.13	937.26
P-250:J-187	3.100	41.1	13.3	965.14	937.21
P-251:J-187	3.100	41.1	13.3	965.14	937.21
P-251:J-189	2.750	43.9	15.9	965.15	937.14
P-252:J-189	2.750	43.9	15.9	965.15	937.14
P-252:J-192	2.670	44.9	16.8	965.17	937.06
P-253:J-192	2.670	44.9	16.8	965.17	937.06
P-253:J-195	3.360	40.0	11.9	965.19	937.01
P-254:J-195	3.360	40.0	11.9	965.19	937.01
P-254:J-197	1.980	57.5	29.1	965.23	936.75
P-255:J-197	1.980	57.5	29.1	965.23	936.75
P-255:J-199	1.750	66.8	38.1	965.26	936.55
P-256:J-199	1.750	66.8	38.1	965.26	936.55
P-256:J-201	1.500	87.6	58.5	965.32	936.16
P-257:J-201	1.500	87.6	58.5	965.32	936.16
P-257:J-204	1.470	91.4	62.1	965.34	936.01
P-258:J-204	1.470	91.4	62.1	965.34	936.01
P-258:J-206	1.390	104.4	74.9	965.38	935.82
P-259:J-206	1.390	104.4	74.9	965.38	935.82
P-259:J-208	1.370	110.8	81.1	965.41	935.59
P-260:J-208	1.370	110.8	81.1	965.41	935.59
P-260:J-210	1.340	117.9	87.7	965.45	935.22
P-261:J-210	1.340	117.9	87.7	965.45	935.22
P-261:J-212	1.330	125.0	94.3	965.50	934.76
P-262:J-212	1.330	125.0	94.3	965.50	934.76
P-262:J-214	1.310	130.7	99.7	965.53	934.45
P-263:J-214	1.310	130.7	99.7	965.53	934.45
P-263:J-216	1.300	135.2	104.2	965.54	934.39
P-264:J-216	1.300	135.2	104.2	965.54	934.39
P-264:J-220	1.290	139.0	107.3	965.61	933.92
P-265:J-220	1.290	139.0	107.3	965.61	933.92
P-265:J-224	1.290	141.2	109.2	965.64	933.62
P-266:J-224	1.290	141.2	109.2	965.64	933.62
P-266:J-227	1.270	149.3	117.3	965.65	933.59
P-267:J-227	1.270	149.3	117.3	965.65	933.59
P-267:J-229	1.270	149.8	117.7	965.66	933.50
P-268:J-229	1.270	149.8	117.7	965.66	933.50
P-268:J-232	1.290	142.3	110.2	965.68	933.48
P-269:J-232	1.290	142.3	110.2	965.68	933.48
P-269:J-235	1.290	141.7	109.5	965.69	933.41
P-270:J-235	1.290	141.7	109.5	965.69	933.41
P-270:J-237	1.300	140.5	108.2	965.70	933.34

Transient Calculation Summary: Base

Extreme Pressures and Heads

End Point	Upsurge Ratio	Max. Pressure (m H2O)	Min. Pressure (m H2O)	Max. Head (m)	Min. Head (m)
P-271:J-237	1.300	140.5	108.2	965.70	933.34
P-271:J-239	1.300	141.9	109.5	965.72	933.22
P-272:J-239	1.300	141.9	109.5	965.72	933.22
P-272:J-241	1.300	141.0	108.3	965.76	933.05
P-273:J-241	1.300	141.0	108.3	965.76	933.05
P-273:J-243	1.300	141.3	108.5	965.77	932.98
P-274:J-243	1.300	141.3	108.5	965.77	932.98
P-274:J-245	1.290	145.5	112.4	965.84	932.72
P-275:J-245	1.290	145.5	112.4	965.84	932.72
P-275:J-247	1.300	143.7	110.6	965.87	932.64
P-276:J-247	1.300	143.7	110.6	965.87	932.64
P-276:J-250	1.300	144.5	111.2	965.89	932.57
P-277:J-250	1.300	144.5	111.2	965.89	932.57
P-277:J-252	1.300	143.2	109.8	965.91	932.46
P-278:J-252	1.300	143.2	109.8	965.91	932.46
P-278:J-255	1.300	146.1	112.5	965.94	932.32
P-279:J-255	1.300	146.1	112.5	965.94	932.32
P-279:J-257	1.300	148.7	114.8	966.01	932.03
P-280:J-257	1.300	148.7	114.8	966.01	932.03
P-280:J-263	1.290	153.6	119.4	966.06	931.78
P-281:J-263	1.290	153.6	119.4	966.06	931.78
P-281:J-266	1.290	152.8	118.5	966.07	931.73
P-282:J-266	1.290	152.8	118.5	966.07	931.73
P-282:J-269	1.290	153.8	119.4	966.08	931.66
P-283:J-269	1.290	153.8	119.4	966.08	931.66
P-283:J-273	1.290	154.8	120.2	966.15	931.41
P-284:J-273	1.290	154.8	120.2	966.15	931.41
P-284:J-275	1.310	145.9	111.1	966.17	931.26
P-285:J-275	1.310	145.9	111.1	966.17	931.26
P-285:J-277	1.330	139.9	105.0	966.18	931.21
P-286:J-277	1.330	139.9	105.0	966.18	931.21
P-286:J-279	1.340	138.7	103.8	966.19	931.18
P-287:J-279	1.340	138.7	103.8	966.19	931.18
P-287:J-282	1.320	144.5	109.5	966.19	931.11
P-288:J-282	1.320	144.5	109.5	966.19	931.11
P-288:J-284	1.320	145.4	110.3	966.20	931.06
P-289:J-284	1.320	145.4	110.3	966.20	931.06
P-289:J-286	1.330	143.0	107.8	966.23	930.96
P-290:J-286	1.330	143.0	107.8	966.23	930.96
P-290:J-288	1.360	132.3	97.0	966.24	930.90
P-291:J-288	1.360	132.3	97.0	966.24	930.90
P-291:J-290	1.350	136.7	101.4	966.24	930.86
P-292:J-290	1.350	136.7	101.4	966.24	930.86
P-292:J-292	1.350	137.6	102.2	966.25	930.83
P-293:J-292	1.350	137.6	102.2	966.25	930.83
P-293:J-295	1.350	135.9	100.4	966.26	930.74
P-294:J-295	1.350	135.9	100.4	966.26	930.74
P-294:J-299	1.420	121.1	85.2	966.34	930.39
P-295:J-299	1.420	121.1	85.2	966.34	930.39
P-295:J-302	1.490	110.0	74.0	966.36	930.28
P-296:J-302	1.490	110.0	74.0	966.36	930.28
P-296:J-304	1.460	114.0	77.9	966.37	930.22
P-297:J-304	1.460	114.0	77.9	966.37	930.22
P-297:J-307	1.470	112.8	76.7	966.37	930.19
P-298:J-307	1.470	112.8	76.7	966.37	930.19
P-298:J-309	1.530	104.8	68.7	966.37	930.15
P-299:J-309	1.530	104.8	68.7	966.37	930.15
P-299:J-311	1.490	110.4	74.2	966.38	930.12
P-300:J-311	1.490	110.4	74.2	966.38	930.12
P-300:J-314	1.580	98.9	62.4	966.42	929.91
P-301:J-314	1.580	98.9	62.4	966.42	929.91

Transient Calculation Summary: Base

Extreme Pressures and Heads

End Point	Upsurge Ratio	Max. Pressure (m H2O)	Min. Pressure (m H2O)	Max. Head (m)	Min. Head (m)
P-301:J-316	1.810	82.1	45.5	966.46	929.73
P-302:J-316	1.810	82.1	45.5	966.46	929.73
P-302:J-318	2.540	60.5	23.8	966.47	929.66
P-303:J-318	2.540	60.5	23.8	966.47	929.66
P-303:J-321	4.140	48.5	11.7	966.48	929.59
P-304:J-321	4.140	48.5	11.7	966.48	929.59
P-304:J-323	2.200	67.7	30.8	966.50	929.53
P-305:J-323	2.200	67.7	30.8	966.50	929.53
P-305:J-325	1.970	75.1	38.1	966.50	929.47
P-306:J-325	1.970	75.1	38.1	966.50	929.47
P-306:J-329	1.780	85.0	47.7	966.58	929.19
P-307:J-329	1.780	85.0	47.7	966.58	929.19
P-307:J-332	1.960	76.5	39.0	966.62	929.07
P-308:J-332	1.960	76.5	39.0	966.62	929.07
P-308:J-335	2.260	67.4	29.8	966.65	928.96
P-309:J-335	2.260	67.4	29.8	966.65	928.96
P-309:J-338	1.800	84.7	47.0	966.68	928.84
P-310:J-338	1.800	84.7	47.0	966.68	928.84
P-310:J-340	1.960	77.5	39.6	966.70	928.76
P-311:J-340	1.960	77.5	39.6	966.70	928.76
P-311:J-342	2.500	63.3	25.4	966.73	928.69
P-312:J-342	2.500	63.3	25.4	966.73	928.69
P-312:J-344	2.110	72.2	34.2	966.74	928.65
P-313:J-344	2.110	72.2	34.2	966.74	928.65
P-313:J-347	2.100	72.6	34.5	966.74	928.62
P-314:J-347	2.100	72.6	34.5	966.74	928.62
P-314:J-349	2.450	64.5	26.4	966.76	928.55
P-315:J-349	2.450	64.5	26.4	966.76	928.55
P-315:J-352	2.420	65.0	26.8	966.78	928.50
P-316:J-352	2.420	65.0	26.8	966.78	928.50
P-316:J-355	2.100	73.1	34.8	966.80	928.42
P-317:J-355	2.100	73.1	34.8	966.80	928.42
P-317:J-357	1.680	94.5	56.1	966.82	928.34
P-318:J-357	1.680	94.5	56.1	966.82	928.34
P-318:J-360	1.660	97.0	58.5	966.85	928.25
P-319:J-360	1.660	97.0	58.5	966.85	928.25
P-319:J-363	1.930	80.0	41.3	966.87	928.16
P-320:J-363	1.930	80.0	41.3	966.87	928.16
P-320:J-365	1.810	86.3	47.6	966.90	928.08
P-321:J-365	1.810	86.3	47.6	966.90	928.08
P-321:J-367	1.630	100.2	61.4	966.90	928.05
P-322:J-367	1.630	100.2	61.4	966.90	928.05
P-322:J-369	1.700	93.9	55.1	966.91	928.01
P-323:J-369	1.700	93.9	55.1	966.91	928.01
P-323:J-371	2.300	69.0	30.0	966.94	927.91
P-324:J-371	2.300	69.0	30.0	966.94	927.91
P-324:J-375	1.940	80.9	41.8	966.98	927.78
P-325:J-375	1.940	80.9	41.8	966.98	927.78
P-325:J-377	2.090	75.1	36.0	966.99	927.73
P-326:J-377	2.090	75.1	36.0	966.99	927.73
P-326:J-381	2.330	69.3	29.8	967.05	927.50
P-327:J-381	2.330	69.3	29.8	967.05	927.50
P-327:J-383	2.160	73.9	34.2	967.08	927.39
P-328:J-383	2.160	73.9	34.2	967.08	927.39
P-328:J-386	2.400	68.1	28.4	967.10	927.31
P-329:J-386	2.400	68.1	28.4	967.10	927.31
P-329:J-388	1.770	91.5	51.7	967.13	927.21
P-330:J-388	1.770	91.5	51.7	967.13	927.21
P-330:J-390	1.750	92.8	52.9	967.14	927.16
P-331:J-390	1.750	92.8	52.9	967.14	927.16
P-331:J-394	1.890	85.5	45.4	967.20	926.94

Transient Calculation Summary: Base

Extreme Pressures and Heads

End Point	Upsurge Ratio	Max. Pressure (m H2O)	Min. Pressure (m H2O)	Max. Head (m)	Min. Head (m)
P-332:J-394	1.890	85.5	45.4	967.20	926.94
P-332:J-398	1.800	90.8	50.3	967.26	926.71
P-333:J-398	1.800	90.8	50.3	967.26	926.71
P-333:J-401	1.800	91.0	50.5	967.27	926.65
P-334:J-401	1.800	91.0	50.5	967.27	926.65
P-334:J-403	1.900	85.9	45.3	967.28	926.62
P-335:J-403	1.900	85.9	45.3	967.28	926.62
P-335:J-405	1.780	92.7	52.1	967.30	926.58
P-336:J-405	1.780	92.7	52.1	967.30	926.58
P-336:J-407	1.750	95.2	54.4	967.33	926.48
P-337:J-407	1.750	95.2	54.4	967.33	926.48
P-337:J-410	1.980	82.6	41.7	967.34	926.39
P-338:J-410	1.980	82.6	41.7	967.34	926.39
P-338:J-412	1.720	97.9	56.9	967.37	926.30
P-339:J-412	1.720	97.9	56.9	967.37	926.30
P-339:J-414	1.780	93.4	52.4	967.38	926.25
P-340:J-414	1.780	93.4	52.4	967.38	926.25
P-340:J-416	1.800	92.2	51.1	967.39	926.22
P-341:J-416	1.800	92.2	51.1	967.39	926.22
P-341:J-419	2.510	68.6	27.3	967.43	926.06
P-342:J-419	2.510	68.6	27.3	967.43	926.06
P-342:J-422	2.260	74.3	33.0	967.45	925.99
P-343:J-422	2.260	74.3	33.0	967.45	925.99
P-343:J-424	2.240	74.7	33.3	967.45	925.97
P-344:J-424	2.240	74.7	33.3	967.45	925.97
P-344:J-426	2.140	78.2	36.6	967.50	925.81
P-345:J-426	2.140	78.2	36.6	967.50	925.81
P-345:J-429	2.280	74.3	32.7	967.51	925.75
P-346:J-429	2.280	74.3	32.7	967.51	925.75
P-346:J-431	2.240	75.3	33.6	967.51	925.71
P-347:J-431	2.240	75.3	33.6	967.51	925.71
P-347:J-433	3.040	62.3	20.5	967.53	925.64
P-348:J-433	3.040	62.3	20.5	967.53	925.64
P-348:J-435	3.010	62.7	20.8	967.55	925.58
P-349:J-435	3.010	62.7	20.8	967.55	925.58
P-349:J-437	1.990	84.4	42.4	967.57	925.49
P-350:J-437	1.990	84.4	42.4	967.57	925.49
P-350:J-440	1.930	87.3	45.2	967.59	925.43
P-351:J-440	1.930	87.3	45.2	967.59	925.43
P-351:J-444	2.020	83.7	41.5	967.62	925.29
P-352:J-444	2.020	83.7	41.5	967.62	925.29
P-352:J-447	2.540	69.9	27.5	967.64	925.19
P-353:J-447	2.540	69.9	27.5	967.64	925.19
P-353:J-449	2.920	64.7	22.2	967.68	925.05
P-354:J-449	2.920	64.7	22.2	967.68	925.05
P-354:J-451	2.730	67.2	24.6	967.69	925.00
P-355:J-451	2.730	67.2	24.6	967.69	925.00
P-355:J-453	3.180	62.3	19.6	967.71	924.93
P-356:J-453	3.180	62.3	19.6	967.71	924.93
P-356:J-455	2.240	77.2	34.4	967.72	924.87
P-357:J-455	2.240	77.2	34.4	967.72	924.87
P-357:J-457	2.330	75.2	32.3	967.77	924.72
P-358:J-457	2.330	75.2	32.3	967.77	924.72
P-358:J-459	2.530	71.1	28.1	967.77	924.68
P-359:J-459	2.530	71.1	28.1	967.77	924.68
P-359:J-461	2.430	73.1	30.1	967.79	924.64
P-360:J-461	2.430	73.1	30.1	967.79	924.64
P-360:J-465	2.930	65.8	22.5	967.85	924.40
P-361:J-465	2.930	65.8	22.5	967.85	924.40
P-361:J-467	5.080	54.3	10.7	967.89	924.22
P-362:J-467	5.080	54.3	10.7	967.89	924.22

Transient Calculation Summary: Base

Extreme Pressures and Heads

End Point	Upsurge Ratio	Max. Pressure (m H2O)	Min. Pressure (m H2O)	Max. Head (m)	Min. Head (m)
P-362:J-469	3.010	65.6	21.8	967.94	924.06
P-363:J-469	3.010	65.6	21.8	967.94	924.06
P-363:J-471	4.430	56.7	12.8	967.97	923.95
P-364:J-471	4.430	56.7	12.8	967.97	923.95
P-364:İvedik-2	5.230	54.8	10.5	968.00	923.59
P-38:J-184	4.250	36.3	8.5	965.13	937.31
P-38:J-186	4.090	36.8	9.0	965.13	937.26
P-367:J-186	4.090	36.8	9.0	965.13	937.26
P-367:J-188	3.100	41.1	13.3	965.14	937.21
P-368:J-188	3.100	41.1	13.3	965.14	937.21
P-368:J-190	2.750	43.9	15.9	965.15	937.14
P-369:J-190	2.750	43.9	15.9	965.15	937.14
P-369:J-193	2.670	44.9	16.8	965.17	937.06
P-370:J-193	2.670	44.9	16.8	965.17	937.06
P-370:J-196	3.360	40.0	11.9	965.19	937.01
P-371:J-196	3.360	40.0	11.9	965.19	937.01
P-371:J-198	1.980	57.5	29.1	965.23	936.75
P-372:J-198	1.980	57.5	29.1	965.23	936.75
P-372:J-200	1.750	66.8	38.1	965.26	936.55
P-373:J-200	1.750	66.8	38.1	965.26	936.55
P-373:J-202	1.500	87.6	58.5	965.32	936.16
P-374:J-202	1.500	87.6	58.5	965.32	936.16
P-374:J-205	1.470	91.4	62.1	965.34	936.01
P-375:J-205	1.470	91.4	62.1	965.34	936.01
P-375:J-207	1.390	104.4	74.9	965.38	935.82
P-376:J-207	1.390	104.4	74.9	965.38	935.82
P-376:J-209	1.370	110.8	81.1	965.41	935.59
P-377:J-209	1.370	110.8	81.1	965.41	935.59
P-377:J-211	1.340	117.9	87.7	965.45	935.22
P-378:J-211	1.340	117.9	87.7	965.45	935.22
P-378:J-213	1.330	125.0	94.3	965.50	934.76
P-379:J-213	1.330	125.0	94.3	965.50	934.76
P-379:J-215	1.310	130.7	99.7	965.53	934.45
P-380:J-215	1.310	130.7	99.7	965.53	934.45
P-380:J-217	1.300	135.2	104.2	965.54	934.39
P-381:J-217	1.300	135.2	104.2	965.54	934.39
P-381:J-221	1.290	139.0	107.3	965.61	933.92
P-382:J-221	1.290	139.0	107.3	965.61	933.92
P-382:J-225	1.290	141.2	109.2	965.64	933.62
P-383:J-225	1.290	141.2	109.2	965.64	933.62
P-383:J-228	1.270	149.3	117.3	965.65	933.59
P-384:J-228	1.270	149.3	117.3	965.65	933.59
P-384:J-230	1.270	149.8	117.7	965.66	933.50
P-385:J-230	1.270	149.8	117.7	965.66	933.50
P-385:J-233	1.290	142.3	110.2	965.68	933.48
P-386:J-233	1.290	142.3	110.2	965.68	933.48
P-386:J-236	1.290	141.7	109.5	965.69	933.41
P-387:J-236	1.290	141.7	109.5	965.69	933.41
P-387:J-238	1.300	140.5	108.2	965.70	933.34
P-388:J-238	1.300	140.5	108.2	965.70	933.34
P-388:J-240	1.300	141.9	109.5	965.72	933.22
P-389:J-240	1.300	141.9	109.5	965.72	933.22
P-389:J-242	1.300	141.0	108.3	965.76	933.05
P-390:J-242	1.300	141.0	108.3	965.76	933.05
P-390:J-244	1.300	141.3	108.5	965.77	932.98
P-391:J-244	1.300	141.3	108.5	965.77	932.98
P-391:J-246	1.290	145.5	112.4	965.84	932.72
P-392:J-246	1.290	145.5	112.4	965.84	932.72
P-392:J-248	1.300	143.7	110.6	965.87	932.64
P-393:J-248	1.300	143.7	110.6	965.87	932.64
P-393:J-251	1.300	144.5	111.2	965.89	932.57

Transient Calculation Summary: Base

Extreme Pressures and Heads

End Point	Upsurge Ratio	Max. Pressure (m H2O)	Min. Pressure (m H2O)	Max. Head (m)	Min. Head (m)
P-394:J-251	1.300	144.5	111.2	965.89	932.57
P-394:J-253	1.300	143.2	109.8	965.91	932.46
P-395:J-253	1.300	143.2	109.8	965.91	932.46
P-395:J-256	1.300	146.1	112.5	965.94	932.32
P-396:J-256	1.300	146.1	112.5	965.94	932.32
P-396:J-258	1.300	148.7	114.8	966.01	932.03
P-397:J-258	1.300	148.7	114.8	966.01	932.03
P-397:J-264	1.290	153.6	119.4	966.06	931.78
P-398:J-264	1.290	153.6	119.4	966.06	931.78
P-398:J-267	1.290	152.8	118.5	966.07	931.73
P-399:J-267	1.290	152.8	118.5	966.07	931.73
P-399:J-270	1.290	153.8	119.4	966.08	931.66
P-400:J-270	1.290	153.8	119.4	966.08	931.66
P-400:J-274	1.290	154.8	120.2	966.15	931.41
P-401:J-274	1.290	154.8	120.2	966.15	931.41
P-401:J-276	1.310	145.9	111.1	966.17	931.26
P-402:J-276	1.310	145.9	111.1	966.17	931.26
P-402:J-278	1.330	139.9	105.0	966.18	931.21
P-403:J-278	1.330	139.9	105.0	966.18	931.21
P-403:J-280	1.340	138.7	103.8	966.19	931.18
P-404:J-280	1.340	138.7	103.8	966.19	931.18
P-404:J-283	1.320	144.5	109.5	966.19	931.11
P-405:J-283	1.320	144.5	109.5	966.19	931.11
P-405:J-285	1.320	145.4	110.3	966.20	931.06
P-406:J-285	1.320	145.4	110.3	966.20	931.06
P-406:J-287	1.330	143.0	107.8	966.23	930.96
P-407:J-287	1.330	143.0	107.8	966.23	930.96
P-407:J-289	1.360	132.3	97.0	966.24	930.90
P-408:J-289	1.360	132.3	97.0	966.24	930.90
P-408:J-291	1.350	136.7	101.4	966.24	930.86
P-409:J-291	1.350	136.7	101.4	966.24	930.86
P-409:J-293	1.350	137.6	102.2	966.25	930.83
P-410:J-293	1.350	137.6	102.2	966.25	930.83
P-410:J-296	1.350	135.9	100.4	966.26	930.74
P-411:J-296	1.350	135.9	100.4	966.26	930.74
P-411:J-300	1.420	121.1	85.2	966.34	930.39
P-412:J-300	1.420	121.1	85.2	966.34	930.39
P-412:J-303	1.490	110.0	74.0	966.36	930.28
P-413:J-303	1.490	110.0	74.0	966.36	930.28
P-413:J-305	1.460	114.0	77.9	966.37	930.22
P-414:J-305	1.460	114.0	77.9	966.37	930.22
P-414:J-308	1.470	112.8	76.7	966.37	930.19
P-415:J-308	1.470	112.8	76.7	966.37	930.19
P-415:J-310	1.530	104.8	68.7	966.37	930.15
P-416:J-310	1.530	104.8	68.7	966.37	930.15
P-416:J-312	1.490	110.4	74.2	966.38	930.12
P-417:J-312	1.490	110.4	74.2	966.38	930.12
P-417:J-315	1.580	98.9	62.4	966.42	929.91
P-418:J-315	1.580	98.9	62.4	966.42	929.91
P-418:J-317	1.810	82.1	45.5	966.46	929.73
P-419:J-317	1.810	82.1	45.5	966.46	929.73
P-419:J-319	2.540	60.5	23.8	966.47	929.66
P-420:J-319	2.540	60.5	23.8	966.47	929.66
P-420:J-322	4.140	48.5	11.7	966.48	929.59
P-421:J-322	4.140	48.5	11.7	966.48	929.59
P-421:J-324	2.200	67.7	30.8	966.50	929.53
P-422:J-324	2.200	67.7	30.8	966.50	929.53
P-422:J-326	1.970	75.1	38.1	966.50	929.47
P-423:J-326	1.970	75.1	38.1	966.50	929.47
P-423:J-330	1.780	85.0	47.7	966.58	929.19
P-424:J-330	1.780	85.0	47.7	966.58	929.19

Transient Calculation Summary: Base

Extreme Pressures and Heads

End Point	Upsurge Ratio	Max. Pressure (m H2O)	Min. Pressure (m H2O)	Max. Head (m)	Min. Head (m)
P-424:J-333	1.960	76.5	39.0	966.62	929.07
P-425:J-333	1.960	76.5	39.0	966.62	929.07
P-425:J-336	2.260	67.4	29.8	966.65	928.96
P-426:J-336	2.260	67.4	29.8	966.65	928.96
P-426:J-339	1.800	84.7	47.0	966.68	928.84
P-427:J-339	1.800	84.7	47.0	966.68	928.84
P-427:J-341	1.960	77.5	39.6	966.70	928.76
P-428:J-341	1.960	77.5	39.6	966.70	928.76
P-428:J-343	2.500	63.3	25.4	966.73	928.69
P-429:J-343	2.500	63.3	25.4	966.73	928.69
P-429:J-345	2.110	72.2	34.2	966.74	928.65
P-430:J-345	2.110	72.2	34.2	966.74	928.65
P-430:J-348	2.100	72.6	34.5	966.74	928.62
P-431:J-348	2.100	72.6	34.5	966.74	928.62
P-431:J-350	2.450	64.5	26.4	966.76	928.55
P-432:J-350	2.450	64.5	26.4	966.76	928.55
P-432:J-353	2.420	65.0	26.8	966.78	928.50
P-433:J-353	2.420	65.0	26.8	966.78	928.50
P-433:J-356	2.100	73.1	34.8	966.80	928.42
P-434:J-356	2.100	73.1	34.8	966.80	928.42
P-434:J-358	1.680	94.5	56.1	966.82	928.34
P-435:J-358	1.680	94.5	56.1	966.82	928.34
P-435:J-361	1.660	97.0	58.5	966.85	928.25
P-436:J-361	1.660	97.0	58.5	966.85	928.25
P-436:J-364	1.930	80.0	41.3	966.87	928.16
P-437:J-364	1.930	80.0	41.3	966.87	928.16
P-437:J-366	1.810	86.3	47.6	966.90	928.08
P-438:J-366	1.810	86.3	47.6	966.90	928.08
P-438:J-368	1.630	100.2	61.4	966.90	928.05
P-439:J-368	1.630	100.2	61.4	966.90	928.05
P-439:J-370	1.700	93.9	55.1	966.91	928.01
P-440:J-370	1.700	93.9	55.1	966.91	928.01
P-440:J-372	2.300	69.0	30.0	966.94	927.91
P-441:J-372	2.300	69.0	30.0	966.94	927.91
P-441:J-376	1.940	80.9	41.8	966.98	927.78
P-442:J-376	1.940	80.9	41.8	966.98	927.78
P-442:J-378	2.090	75.1	36.0	966.99	927.73
P-443:J-378	2.090	75.1	36.0	966.99	927.73
P-443:J-382	2.330	69.3	29.8	967.05	927.50
P-444:J-382	2.330	69.3	29.8	967.05	927.50
P-444:J-384	2.160	73.9	34.2	967.08	927.39
P-445:J-384	2.160	73.9	34.2	967.08	927.39
P-445:J-387	2.400	68.1	28.4	967.10	927.31
P-446:J-387	2.400	68.1	28.4	967.10	927.31
P-446:J-389	1.770	91.5	51.7	967.13	927.21
P-447:J-389	1.770	91.5	51.7	967.13	927.21
P-447:J-391	1.750	92.8	52.9	967.14	927.16
P-448:J-391	1.750	92.8	52.9	967.14	927.16
P-448:J-395	1.890	85.5	45.4	967.20	926.94
P-449:J-395	1.890	85.5	45.4	967.20	926.94
P-449:J-399	1.800	90.8	50.3	967.26	926.71
P-450:J-399	1.800	90.8	50.3	967.26	926.71
P-450:J-402	1.800	91.0	50.5	967.27	926.65
P-451:J-402	1.800	91.0	50.5	967.27	926.65
P-451:J-404	1.900	85.9	45.3	967.28	926.62
P-452:J-404	1.900	85.9	45.3	967.28	926.62
P-452:J-406	1.780	92.7	52.1	967.30	926.58
P-453:J-406	1.780	92.7	52.1	967.30	926.58
P-453:J-408	1.750	95.2	54.4	967.33	926.48
P-454:J-408	1.750	95.2	54.4	967.33	926.48
P-454:J-411	1.980	82.6	41.7	967.34	926.39

Transient Calculation Summary: Base

Extreme Pressures and Heads

End Point	Upsurge Ratio	Max. Pressure (m H2O)	Min. Pressure (m H2O)	Max. Head (m)	Min. Head (m)
P-455:J-411	1.980	82.6	41.7	967.34	926.39
P-455:J-413	1.720	97.9	56.9	967.37	926.30
P-456:J-413	1.720	97.9	56.9	967.37	926.30
P-456:J-415	1.780	93.4	52.4	967.38	926.25
P-457:J-415	1.780	93.4	52.4	967.38	926.25
P-457:J-417	1.800	92.2	51.1	967.39	926.22
P-458:J-417	1.800	92.2	51.1	967.39	926.22
P-458:J-420	2.510	68.6	27.3	967.43	926.06
P-459:J-420	2.510	68.6	27.3	967.43	926.06
P-459:J-423	2.260	74.3	33.0	967.45	925.99
P-460:J-423	2.260	74.3	33.0	967.45	925.99
P-460:J-425	2.240	74.7	33.3	967.45	925.97
P-461:J-425	2.240	74.7	33.3	967.45	925.97
P-461:J-427	2.140	78.2	36.6	967.50	925.81
P-462:J-427	2.140	78.2	36.6	967.50	925.81
P-462:J-430	2.280	74.3	32.7	967.51	925.75
P-463:J-430	2.280	74.3	32.7	967.51	925.75
P-463:J-432	2.240	75.3	33.6	967.51	925.71
P-464:J-432	2.240	75.3	33.6	967.51	925.71
P-464:J-434	3.040	62.3	20.5	967.53	925.64
P-465:J-434	3.040	62.3	20.5	967.53	925.64
P-465:J-436	3.010	62.7	20.8	967.55	925.58
P-466:J-436	3.010	62.7	20.8	967.55	925.58
P-466:J-438	1.990	84.4	42.4	967.57	925.49
P-467:J-438	1.990	84.4	42.4	967.57	925.49
P-467:J-441	1.930	87.3	45.2	967.59	925.43
P-468:J-441	1.930	87.3	45.2	967.59	925.43
P-468:J-445	2.020	83.7	41.5	967.62	925.29
P-469:J-445	2.020	83.7	41.5	967.62	925.29
P-469:J-448	2.540	69.9	27.5	967.64	925.19
P-470:J-448	2.540	69.9	27.5	967.64	925.19
P-470:J-450	2.920	64.7	22.2	967.68	925.05
P-471:J-450	2.920	64.7	22.2	967.68	925.05
P-471:J-452	2.730	67.2	24.6	967.69	925.00
P-472:J-452	2.730	67.2	24.6	967.69	925.00
P-472:J-454	3.180	62.3	19.6	967.71	924.93
P-473:J-454	3.180	62.3	19.6	967.71	924.93
P-473:J-456	2.240	77.2	34.4	967.72	924.87
P-474:J-456	2.240	77.2	34.4	967.72	924.87
P-474:J-458	2.330	75.2	32.3	967.77	924.72
P-475:J-458	2.330	75.2	32.3	967.77	924.72
P-475:J-460	2.530	71.1	28.1	967.77	924.68
P-476:J-460	2.530	71.1	28.1	967.77	924.68
P-476:J-462	2.430	73.1	30.1	967.79	924.64
P-477:J-462	2.430	73.1	30.1	967.79	924.64
P-477:J-466	2.930	65.8	22.5	967.85	924.40
P-478:J-466	2.930	65.8	22.5	967.85	924.40
P-478:J-468	5.080	54.3	10.7	967.89	924.22
P-479:J-468	5.080	54.3	10.7	967.89	924.22
P-479:J-470	3.010	65.6	21.8	967.94	924.06
P-480:J-470	3.010	65.6	21.8	967.94	924.06
P-480:J-472	4.430	56.7	12.8	967.97	923.95
P-481:J-472	4.430	56.7	12.8	967.97	923.95
P-481:Ïvedik-3	5.230	54.8	10.5	968.00	923.59
P-9:T2-End	1.540	22.8	14.8	961.64	953.64
P-9:TCV-2	1.540	22.8	14.8	961.66	953.58
P-490:TCV-2	1.550	22.8	14.7	961.66	953.52
P-490:J-8	1.550	22.8	14.7	961.66	953.50
P-10:T2-End	1.540	22.8	14.8	961.64	953.64
P-10:TCV-3	1.540	22.8	14.8	961.65	953.58
P-491:TCV-3	1.550	22.8	14.7	961.65	953.52

Transient Calculation Summary: Base

Licensed for Academic Use Only

Extreme Pressures and Heads

End Point	Upsurge Ratio	Max. Pressure (m H2O)	Min. Pressure (m H2O)	Max. Head (m)	Min. Head (m)
P-491:J-9	1.550	22.8	14.7	961.65	953.50
P-8:T2-End	1.540	22.8	14.8	961.64	953.64
P-8:TCV-1	1.540	22.8	14.8	961.65	953.58
P-492:TCV-1	1.550	22.8	14.7	961.65	953.52
P-492:J-10	1.550	22.8	14.7	961.65	953.50
P-15:J-175	1.550	33.7	21.7	962.73	950.68
P-15:TCV-4	1.550	33.7	21.7	962.74	950.66
P-493:TCV-4	1.560	33.7	21.6	962.74	950.59
P-493:T3-Start	1.560	33.7	21.6	962.74	950.54
P-16:J-176	1.550	33.7	21.7	962.73	950.68
P-16:TCV-5	1.550	33.7	21.7	962.74	950.66
P-494:TCV-5	1.560	33.7	21.6	962.74	950.59
P-494:T3-Start	1.560	33.7	21.6	962.74	950.54
P-17:J-177	1.550	33.7	21.7	962.73	950.68
P-17:TCV-6	1.550	33.7	21.7	962.74	950.66
P-495:TCV-6	1.560	33.7	21.6	962.74	950.59
P-495:T3-Start	1.560	33.7	21.6	962.74	950.54
P-35:T3-End	4.130	36.3	8.8	965.12	937.56
P-35:TCV-9	4.190	36.3	8.7	965.13	937.44
P-496:TCV-9	4.210	36.3	8.6	965.13	937.38
P-496:J-183	4.240	36.3	8.6	965.13	937.34
P-33:T3-End	4.130	36.3	8.8	965.12	937.56
P-33:TCV-7	4.190	36.3	8.7	965.13	937.43
P-497:TCV-7	4.220	36.3	8.6	965.13	937.36
P-497:J-182	4.250	36.3	8.5	965.13	937.31
P-34:T3-End	4.130	36.3	8.8	965.12	937.56
P-34:TCV-8	4.190	36.3	8.7	965.13	937.43
P-498:TCV-8	4.220	36.3	8.6	965.13	937.36
P-498:J-184	4.250	36.3	8.5	965.13	937.31
P-99:İvedik-1	5.520	54.8	9.9	967.97	923.04
P-99:LJ-1.1	5.530	54.8	9.9	967.98	923.03
P-98:İvedik-1	5.520	54.8	9.9	967.97	923.04
P-98:LJ-1.2	5.530	54.8	9.9	967.98	923.03
P-366:İvedik-2	5.230	54.8	10.5	968.00	923.59
P-366:LJ-2.1	5.240	54.8	10.5	968.01	923.58
P-365:İvedik-2	5.230	54.8	10.5	968.00	923.59
P-365:LJ-2.2	5.240	54.8	10.5	968.01	923.58
P-483:İvedik-3	5.230	54.8	10.5	968.00	923.59
P-483:LJ-3.1	5.240	54.8	10.5	968.01	923.58
P-482:İvedik-3	5.230	54.8	10.5	968.00	923.59
P-482:LJ-3.2	5.240	54.8	10.5	968.01	923.58
P-484:LJ-1.1	1.000	5.0	5.0	918.15	918.11
P-484:R-1.1	1.000	5.0	5.0	918.12	918.12
P-485:LJ-1.2	1.000	5.0	5.0	918.15	918.11
P-485:R-1.2	1.000	5.0	5.0	918.12	918.12
P-486:LJ-2.1	1.000	5.0	5.0	918.14	918.11
P-486:R-2.1	1.000	5.0	5.0	918.12	918.12
P-487:LJ-2.2	1.000	5.0	5.0	918.14	918.11
P-487:R-2.2	1.000	5.0	5.0	918.12	918.12
P-488:LJ-3.1	1.000	5.0	5.0	918.14	918.11
P-488:R-3.1	1.000	5.0	5.0	918.12	918.12
P-489:LJ-3.2	1.000	5.0	5.0	918.14	918.11
P-489:R-3.2	1.000	5.0	5.0	918.12	918.12
P-42:J-203	1.480	89.2	60.2	965.14	936.08
P-42:J-218	1.300	137.1	105.8	965.44	934.08
P-19:J-65	1.060	183.6	173.9	962.06	952.40
P-19:J-80	1.060	165.0	154.9	962.17	952.08
P-37:J-183	4.240	36.3	8.6	965.13	937.34
P-37:J-191	2.570	45.8	17.8	965.14	937.06
P-14:T3-Start	1.560	33.7	21.6	962.74	950.54
P-14:J-179	4.770	24.0	5.0	963.87	944.81